Vascular Endothelial Growth Factor-Inhibitors in the Treatment of Abnormal Angiogenesis

Submitted in accordance with the requirements for the degree of

Doctor of Philosophy

The University of Leeds

Faculty of Biological Sciences

School Of Molecular and Cellular Biology

&

Astbury Centre for Structural Molecular Biology

August 2021

INTELLECTUAL PROPERTY STATEMENT

The candidate confirms that the work submitted is her own and that appropriate credit has been given where reference has been made to the work of others.

ACKNOWLEDGEMENTS

First of all, I would very much like to thank Dr. Vas Ponnambalam for being such a wonderful support to me both inside and outside of the lab. He is not only very kind but his passion for science inspires me so much. I always love having a chat with him and I will always be grateful for all of his help. Thank you to Ty too for being such a fun little guy! I would also like to thank Dr. Darren Tomlinson for being so kind and patient with me by welcoming me into his lab, I really enjoyed getting to learn new molecular techniques. I appreciated being able to learn more about Affimers from him and the other members of the BSTG lab during the lab meetings. I would also very much like to thank Dr. Mike Harrison who has also been a great role model for me in the lab and has also shown me so much kindness. I enjoyed the demonstrating classes with him too! I would also sincerely like to thank Dr. Christian Tiede and Anna Tang from the BSTG lab. They were always an immense help to me which I really appreciated as a new PhD student. I learnt a lot from them, and I will always be so grateful. Thank you also to the assessors of my final viva, Professor Paul Millner and Professor Nick Brindle, whose kindness and feedback have helped to improve this final thesis. I would also like to thank the BHF for funding this project and allowing me to have such a wonderful experience which has been a great start to my scientific career.

I cannot of course forget Ponnambalam *et al.,* the best lab group that I could ever have had the pleasure to be in. Not only have they all helped me professionally, but I feel lucky to call them my friends. I would like to thank Faheem who has been an incredible support and friend ever since I started my PhD (and thanks for the great recommendations from Café on Campus). Thank you to Will for always being so helpful in the lab and always great to chat to – I will miss trying to get HUVECs with you! Thank you to Gary for your kindness and always being a laugh, I cannot listen to Ed Sheeran the same way again! I also want to thank both of your adorable families' too for always making me smile. Thank you to Barney and Sophie (the *al* to our group) for being such great supports both in and outside the lab and for the fun times, especially in kimonos! I cannot forget Areej, Queen and Hala who are all so kind and lovely, I am so glad we have a shared love of desserts too! There are so many great people I would like to thank from the labs both past and present who have helped me get to where I am today, so here are just a few: Izma, Andrew, Jon, Reema, Maali, Hala, Sandie, Ghaadeer, Catherine, Connie, Phillipa, Simon, Claudia and many more. Special thanks to Kiran as well for aiding me in the FUCCI experiments and to Oleg and Gina for their contributions to the

Affimer project. I would also like to pay a special tribute to Anthony Chan, the *et* to our lab group and who was one of the first friends that I made in Leeds. His chattiness, love of musicals and talk of unicorns always made him fun to hang out with and he was also so kind. not only. I would like to dedicate this work to him, we all miss him a lot.

Thank you also to my friends from home for supporting me through the PhD as well, I cannot write enough about how grateful I am to have you all in my life. Thank you to Liesl for our amazing geeky chats and woodland walks and to Anna Cranston for our long chats from across the world. Thank you to my school crew Dami, Esther and Humayal for the amazing support and deep convos as well as laughs. Thank you very “mutch” to Sarah-Emily for always being like a big sister to me and for providing fun London times in between the PhD! Thank you to my other sister from another mister, Karen for the great virtual tea chats and to Emma for hyping me up so much and for being so kind (and thanks to both of you for pet pictures). They are of course part of the epic Aberdeen squad (where there are also more pet pictures): Kyle, Kathryn, Linda, the two Andrews, Anna, Jayne, Janet, and Craig. Thank you all so much for the best virtual and in person games nights and for always being in my corner, I feel so lucky to have you all as friends.

A major thank you also has to go to my parents who have shown me so much support and love. Thank you to my mum whose support I could not do without (especially during thesis writing in my pink chair) and to my dad who always has always been so interested to hear about my work and Affimers. They are the kindest people and I am not biased in saying that! Thank you so much to all of the Hendersons as well, who have welcomed me into their family and been such a wonderful support to me too (especially when it comes to the flat). Last, but definitely not least, I have to say a massive thanks to my partner Jamie. He has been my rock over the past 8 years and especially during the PhD. I am so lucky to have someone who has not only supported me professionally but who can always make me laugh, especially at the stupidest things. Hanging out with him and our hamster, Lyra definitely helped me write this thesis too.

ABSTRACT

Angiogenesis is defined as the development of blood vessels from a pre-existing vasculature and has a major role in both normal physiology and pathological functions. Vascular endothelial growth factor-A (VEGF-A) is a key pro-angiogenic factor which binds to the receptor tyrosine kinases, VEGFR1 and VEGFR2. VEGFR2 is the main pro-angiogenic receptor whilst VEGFR1 is thought to be indirectly anti-angiogenic. Specifically targeting VEGFR1 or VEGFR2 could provide benefits for various disease states involving angiogenesis, for instance, increasing its activity in repairing arterial damage or in decreasing blood vessel growth to tumours. This study uses novel affinity reagents called Affimers, which are synthetic antibody-mimetic proteins. The Affimers were selected against VEGFR1 and VEGFR2 *via* phage display and expressed using the IPTG-induced *E.coli* expression system. Dose-dependence studies of VEGFR-specific Affimers on proangiogenic responses within human umbilical vein endothelial cells (HUVECs) were carried out in the presence of VEGF ligands. Live cell imaging of an A431 epithelial cell line, stably transfected with the fluorescence ubiquitin cell cycle indicator (FUCCI) system, was also used to assess the effects of VEGFR Affimers on cancer cell cycle progression in the presence of VEGF and placental growth factor (PlGF). VEGFR1-specific Affimers were useful immunofluorescence tools and also promoted angiogenic responses, cell viability, proliferation, migration and endothelial tube formation. Additionally, VEGFR2-inhibitory Affimers promoted endothelial cell viability, whilst decreasing proangiogenic responses: migration. VEGFR1- and -2 specific Affimers, had differential, dosage dependent, effects on the pattern of cell growth, thereby altering the G1 and S phases cell cycle. These *in vitro* studies show that inhibiting VEGFR1 could stimulate angiogenesis to promote cardiovascular recovery. In contrast, VEGFR2-inhibitory Affimers show promise as useful anti-angiogenic tools. Live-cell imaging demonstrated that VEGFR Affimers are also valuable tools in assessing both endothelial and epithelial cell function. This study suggests that Affimers may provide a viable alternative for the usage of antibodies in therapeutic and diagnostic procedures as part of the treatment for both heart disease and cancer.

TABLE OF CONTENTS

LIST OF TABLES

LIST OF FIGURES

LIST OF ABBREVIATIONS

Abbreviation	Definition
A431	Human squamous carcinoma cell line
AKT	Protein kinase B
ALT	Alanine aminotransferase
AMD	Age-related macular degeneration
AST	Aspartate aminotransferase
BAM	Bead assisted mass spectrometry
BCA	Bichinchonic acid
BCL-2	B-cell lymphoma-2
BRDU	Bromodeoxyuridine
CD	Cytoplasmic domain
CEA	Carcinoembryonic antigen
COA	Coronary artery disease
COPD	Chronic obstructive pulmonary disease
CRC	Colorectal cancer
CVD	Cardiovascular disease
DAG	Diacylglycerol
DAPI	4'.6-diamidino-2-phenylindole
DDM	Dodecyl maltoside
DMEM	Dulbecco's Modified Eagle Medium
ECD	Extracellular domain
ECGM	Endothelial cell growth medium
ECL	Enhanced chemiluminescence
ECM	Extracellular matrix
eNOS	Endothelial nitric oxide synthase
ER	Endoplasmic reticulum
ERK1/2	Extracellular signal-regulated kinase 1/2 (p42/44)
FBS	Foetal bovine serum
FGF	Fibroblast growth factor
FGFR	Fibroblast growth factor receptor
FLK-1	Fetal liver kinase 1
FLT-1	Fms-like tyrosine kinase 1
FUCCI	Fluorescent ubiquitination-based cell cycle indicator
HAE	Hereditary angioedema
HER	Human epidermal growth factor
HIF	Hypoxia inducible factor
HR	Hazard ratio
HRE	Hypoxia-responsive elements
HUVEC	Human umbilical vein endothelial cells

ICK	Inhibitor cystine-knots
IP	Immunoprecipitation
IPTG	Isopropylthio-β-galactoside
JNK	c-Jun N-terminal kinase
KDR	Kinase inserts domain receptor
LB	Lennox broth
MAPK	Mitogen-activated protein kinase
MCDB131	Serum-free medium
MEK	Mitogen-activated protein kinase
MI	Myocardial infarction
MMP	Matrix metalloproteinases
MTT	3-(4,5-Dimethylthiazol-2-yl)-2,5-Diphenyltetrazolium Bromide)
MVB	Endosomal multivesicular bodies
NDS	Normal donkey serum
Ni-NTA	Nickel-Nitrolotriacetic acid
NF-κB	Nuclear factor kappa B
NHDF	Normal human dermal fibroblasts
NOS	Nitric oxide synthase
NRP	Neuropilin
PECAM-1	Platelet endothelial cell adhesion molecule 1
PFA	Paraformaldehyde
PFS	Progression-free survival
PHD	Prolyl hydroxylases
PI3-K	Phosphoinositide 3-kinases
PIP2	Phosphatidylinositol 4,5-bisphosphate
PlGF-1	Placental growth factor 1
PMSF	Phenylmethylsulfonyl fluoride
PPI	Protein-protein interactions
PSG	Pig skin gelatin
PTB	Protein tyrosine binding
RFP	Red Fluorescent Protein
RR	Relative risk
RTK	Receptor tyrosine kinase
SEM	Standard error of the mean
SOC	Super Optimal Broth
sRAGE	Soluble receptor for advanced glycation end products
SUMO	Small ubiquitin modifier
TCEP	Tris(2-carboxyethyl) phosphine
TK	Tyrosine kinase
TKI	Tyrosine kinase inhibitor
TMB	3,3',5,5'-Tetramethylbenzidine
TMD	Transmembrane domain

TNF	Tumour necrosis factor
TSAd	T cell specific adapter
TTP	Thrombotic thrombocytopenic purpura
UPS	Ubiquitin-proteasome system
V_HH	Variable heavy domain
VEGF	Vascular endothelial growth factor
VEGFR	Vascular endothelial growth factor receptor
VWF	Von Willebrand factor

CHAPTER 1

INTRODUCTION

1.1 History of Cardiovascular Medicine

1.1.1 Ancient Greece

A lot of our basic knowledge of the human heart and vascular system has deep roots in many ancient civilizations. Greece was the home of Hippocrates of Kos (460-377 BCE), one of the key figures in the history of medicine. He is credited as being the father of modern medicine and has had a major influence on the diagnostic and ethical procedures of medical professionals right up to the present day.

Hippocrates believed that the human body was a combination of four fluids or 'humors,' these being blood, phlegm, black bile and yellow bile. He further theorized that in the case of a healthy human there existed a state of equilibrium between all of these 'humors,' and that any extant disease within a body was therefore caused a projected imbalance within their respective levels (Yapijakis, 2009).

Two other key figures of note around this time were Herophilus of Chalcedon (330-260BC) and Erasistratus Ceos (330-255BC). Herophilus, considered the founder of human anatomy, was the first to identify differences between veins and arteries, whilst Erasistratus, considered the first physiologist, established that the heart was the origin of these veins and arteries. Erasistratus is also considered to be one of the first people to identify capillaries and to state that the heart is a pump containing four valves which direct fluid flow. These early physicians, however, also lived at a time when influential Greek Philosophers caused many people to believe that a substance known as 'pneuma' (spirit), permeated the body. This commonly held belief left many physicians of this era, and of later time periods, to feel a necessity to try to explain several important biological phenomena with reference to the perceived underlying physiological presence of 'pneuma'. Erasistratus, for example, believed that the veins he described carried blood from the right side of the heart, but that the arteries

carried ‘pneuma’, which he, because of his underlying philosophical belief system, felt was supported by dissections which demonstrated blood draining from arteries into veins after death (Adler, 2004). His false conclusion, incorrectly drawn from a potentially sound process of experimentation, well illustrates the necessity for even modern scientists to try to set aside personally strongly held beliefs when attempting to interpret the data from their experiments, and to always rely on cold hard logic. Asclepiades of Bithynia (124-40 BCE), known as the father of molecular medicine, suggested that the human body was made of molecules made of atoms and void spaces, leading to a more scientific-driven theory of disease, as opposed to a belief in a more philosophically based theory. An example of such a theory being that discussed above in which ‘changes in elemental fluid states,’ are perceived as being responsible for specific disease presentations. Asclepiades was also believed to have been one of the first physicians to discover that there are both acute and chronic forms of disease, and also advocated that a healthy diet, accompanied by an exercise regimen, was a pathway to improve a patient’s health (Yapijakis, 2009).

1.1.2 Ancient Egypt and Rome

The medical practices of Ancient Egypt were well-documented in the text of number of surviving papyri. Each of these important papyri dealt with a specific medical specialty. One of this number is the Ebers Papyrus (1500 BCE), which focused on human anatomy and the cardiovascular system. The heart was thought to be the physiological ‘epicenter’ of the body and was also thought to be the key to a patient’s general health. The papyrus, for instance, details that ‘*mtw,’* which loosely translates as being the ‘vessels originating from the heart’, a very important physiological discovery for the benefit of potential patients at the time and focuses on the importance of the pulse in diagnosis. The papyri may also contain one of the oldest descriptions of varicose veins and arterial aneurysms (Barr, 2014).

Queen Cleopatra VII (69-30 BC) is also known to have been interested in learning about medical matters. In fact, the whole of the Ptolemaic family had a great passion for science. She is believed to have had a great interest in gynecology and pharmacology, leading to her being credited as the author of a script called ‘Cosmetics.’ This script gave guidance on how to prepare treatments for several ailments, such as the use of antiseptics (Tsoucalas *et al.*, 2014). Cleopatra’s treatise would be used as medical guidance by many students of human physiology in the future, including o*ne* of the most well-known figures in the study of the cardiovascular system, Galen of Pergamon (130-200 AD), a great Roman anatomist (Tsoucalas *et al.*, 2014).

The study of human anatomy by 150 BC was made nearly impossible due to the influence of Christianity on Romans. For instance, the vivisection of corpses was highly disapproved practice, being proscribed as a Paganist activity. Even the revered Galen could only work on ‘legally available bodies’ which included pigs, and he was reduced to proposing that Barbary apes were a good model for the human body as means of continuing his work. His experiments included carefully tying off arteries in these animals and inserting a fine tube into the wall of the left ventricle to show blood flow from the heart through these vessels. However, Galen still included the theory of ‘pneuma’ in formulating his theories, which led to his supposing that there were invisible pores which allowed blood to flow from the left to the right ventricles, and that ‘pneuma’ would therefore, as a matter of course, flow from the right to left. From there, the left ventricle would charge the blood with this ‘pneuma’ and ‘innate heat,’ to be carried thereby around the body. It was further assumed, that the present state of ‘pneuma’ circulating around the body was changed depending upon where it was flowing; its presence in blood flow to the brain converted it into a ‘psychic’ form, whilst its progress through the liver, then thought to produce blood via digested food, would change it to a ‘vegetative’ state in order to allow it to nourish the vena cava and therefore the whole human body. Galen’s conclusion was that the arteries carried the ‘pneuma’ and the ‘innate heat’, that the veins carried ‘vegetative pneuma,’ and that the nerves carried the ‘psychic pneuma’

(Fig. 1.1). These conclusions would be combined with the Hippocratic four humor theory, in order to help with the final diagnosis of any medical condition. These theories created a system called Galenism, which was a gold standard for many physicians and anatomists alike well up until at least the middle ages (Adler, 2004; Aird, 2011).

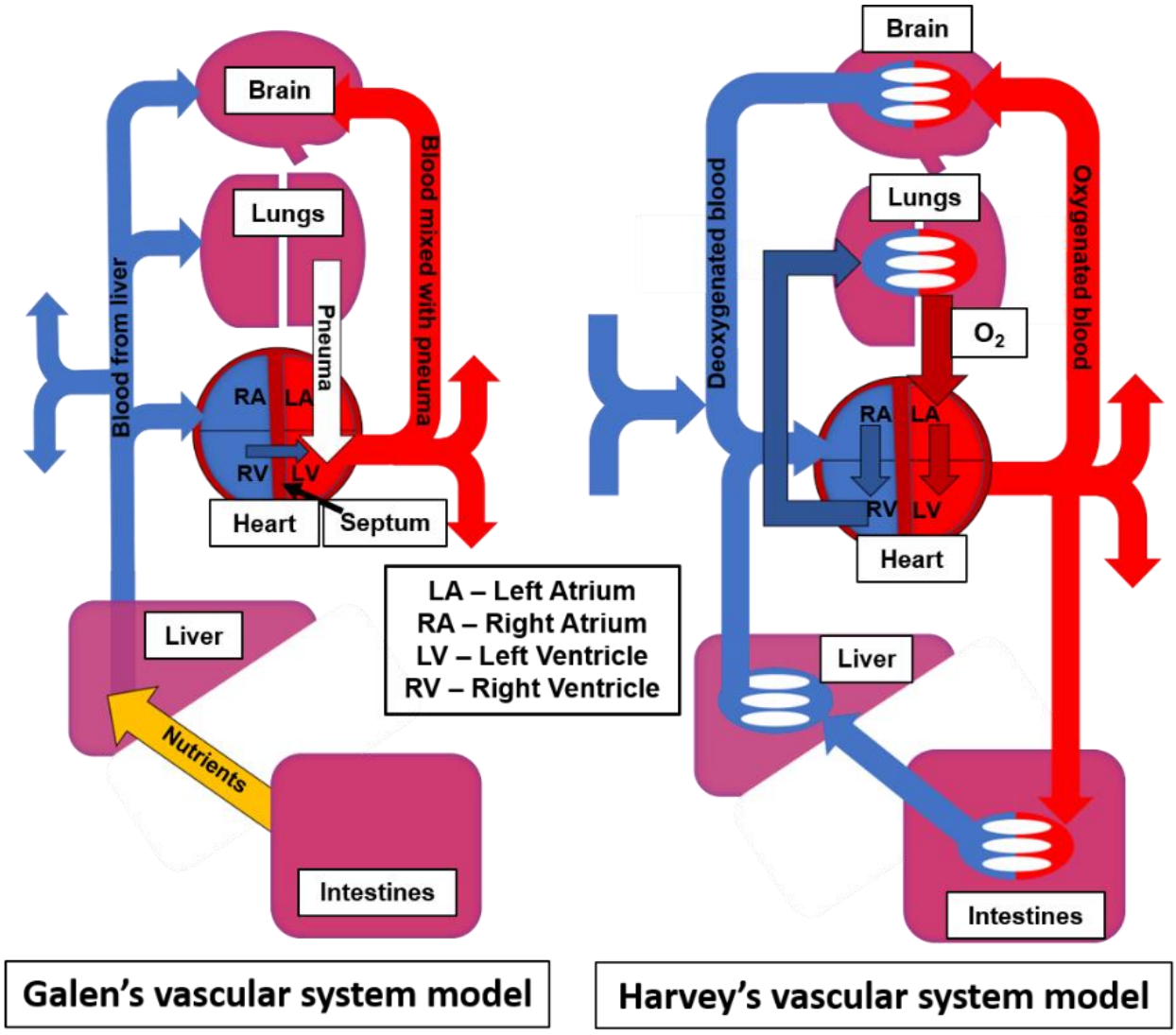

Figure 1.1. Historical cardiovascular system models. Cartoon representations of models as put forward by Galen and Harvey. **(A)** Galen's model of an open-ended vascular system where blood was produced by the liver and transported to organs including the heart through veins. Galen's theory included small holes in the septum of the heart which would allow blood to flow from the right to left ventricle of the heart The blood would be charged with 'pneuma' or 'spirit' from the lungs, which would then be transported to the rest of the body through the arteries. **(B)** Harvey's model shows a closed circulatory system in which the heart as an active pump of recycled blood carrying oxygen. The model involves the pulmonary circulation, where blood flowing through veins and to the heart is oxygenated by the lungs, and the systemic circulation, where the resulting oxygenated blood flows to the rest of the body through arteries. This description is the closest to our current understanding of the heart. Image adapted from (Aird, 2011)

1.1.3 The Middle Ages

One person, however, who questioned the beliefs of Galen and Hippocrates, was the Islamic physician and surgeon Ibn al-Nafis (approximately 1213-1288 AD). He wanted to be able to test out theories with first-hand experimentation instead of relying upon belief-systems held by others, and furthermore systems hampered by the fact that vivisections were heavily frowned upon at the time. He seemed to find ways around this problem and identified the septum in the heart as having a thick wall with no invisible pores, as previously described by Galen, and therefore concluded blood did not pass from the right to left ventricle. The first person, therefore, attributed with discovering and describing the pulmonary circulation is Ibn al-Nafis. This discovery was in fact made hundreds of years earlier than later, now found to be, 're-discoveries' of the system, made by people previously such as Michael Servetus (1511-1553 AD) (West, 2008).

One revolutionary book on anatomy was "De Humani Corporis Fabrica," (On the Fabric of the Human body) written by the Italian Andreas Vesalius (1514-1564 AD) in 1543 AD. Andreas, although he was originally taught to be a Galenist, would later go on to be the first to accurately describe both the structure and functions of the human body. Using the bodies of recently executed Parisian criminals, he found over two hundred inconsistencies between animal and human anatomy which would disprove most, but not all, of Galen's previous errors. This included the lack of invisible pores within the septum as previously described (Adler, 2004; Mesquita *et al.,* 2015) .

A key figure in cardiovascular research was William Harvey (1578-1657 AD), an English anatomist and physician. Unlike his peers at the time, Harvey did not wish to blindly follow Galenism without being able to come to his own conclusions through experimentation. To find out the relationship between a heartbeat and the pulsing of arteries, Harvey experimented on the slower beating hearts of cold-blooded animals. His observation of heart contractions allowed a conclusion that the heart is a muscle and actively pumping blood, the pressure from which would create a pulse. Harvey also identified the specific roles of the pulmonic, aortic, mitral and tricuspid valves

and the systemic blood circulation as a whole, using animal dissections and a rudimentary version of our modern blood pressure tests in humans. He would use cords to compress the upper arm to alter blood pressure to show blood flow being cut off in veins alone or in both the veins and arteries. Harvey was also one of the first researcher to quantify his data to back up his observations; he was able to calculate the volume of blood that the human heart could expel during each contraction. This led to his conclusion that blood flow was actually in a loop and not in fact produced by the liver (Fig. 1.1). Harvey's 1628 book "*De Motu Cordis*" was a controversial one having been criticized by those who still followed Galenism. However, he was, and still is, an inspiration for scientists today to develop and to test their own theories through their own experimentation, not relying solely, or chiefly on prior scientific dogma, and to further, back these experiments up with rigorous quantitative analysis. To quote Harvey: "I profess both to learn and to teach anatomy not from books but from dissections; not from the positions of philosophers but from the very fabric of nature" (Adler, 2004; Bolli, 2019).

The field of cardiovascular research has been replete with towering figures, creating, and testing theories based upon ancient and modern paradigms, which shifted the ground of research over the millennia, but which still relies upon discoveries made thousands of years ago. The parameters of proper analysis and experimentation were always at its core, even if at times, philosophical ideas which are now left as interesting footnotes in history, served to blight its true implementation and to curb and to slow down the natural curve of the development of scientific enquiry which might have otherwise developed. Medical research has been an evolution of ideas from its beginning, its true aim has always been to benefit society by improving the general health of humanity. Our understanding of the cardiovascular system on both a molecular and physiological basis is ever increasing, which is essential in designing and developing therapeutics to target it.

1.2 Vasculogenesis and Angiogenesis

The cardiovascular system is of upmost importance to the successful development and maintenance of the human body from birth until death. The *de novo* formation of blood vessels is a key process that happens during the development of the embryonic circulatory system. Such a process is termed vasculogenesis, where the mesoderm is induced to form haemangioblasts, stem cells which direct the formation of new blood vessels (Risau, 1997; Huppertz and Peeters, 2005). Such blood vessels are dependent on specific cell types collectively known as the endothelium, which lines all blood vessels, forming a cell monolayer and barrier between the blood and the vessel wall. The endothelium has a variety of important functions throughout the body: maintaining a barrier between blood and tissue, platelet adherence, thrombosis regulation, vascular tone and blood flow (Galley and Webster, 2004). The endothelium is also important for another important process in vascular physiology: angiogenesis (Hsieh *et al.*, 2006). Angiogenesis is defined as the sprouting of new blood vessels from an existing vascular network. This phenomenon is important for normal health but can be subverted in many disease states including cancer, heart disease and forms of blindness.

For example, angiogenesis after myocardial infarction (MI), is essential for the repair of the ischaemic myocardium and to prevent the apoptosis of cardiomyocytes (Nagaya *et al.*, 2004). Cardiomyocytes have a close interface with the endothelium due to an intricate anatomical arrangement in the capillary network, highlighting the importance of their interaction in cardiac repair (Hsieh *et al.*, 2006). Cardiomyocytes may go through two types of cell death after a myocardial infarction; necrosis, which is random, inflammatory and not physiologically normal, or apoptosis, which is controlled by many signalling pathways as well as having a physiological purpose (Pulkki, 1997). Apoptosis is defined as organised cell death which acts in response to either intra- or extracellular signals to maintain homeostasis within the body. It is characterised by chromatin condensation, protein lysis and phagocytosis of single cells

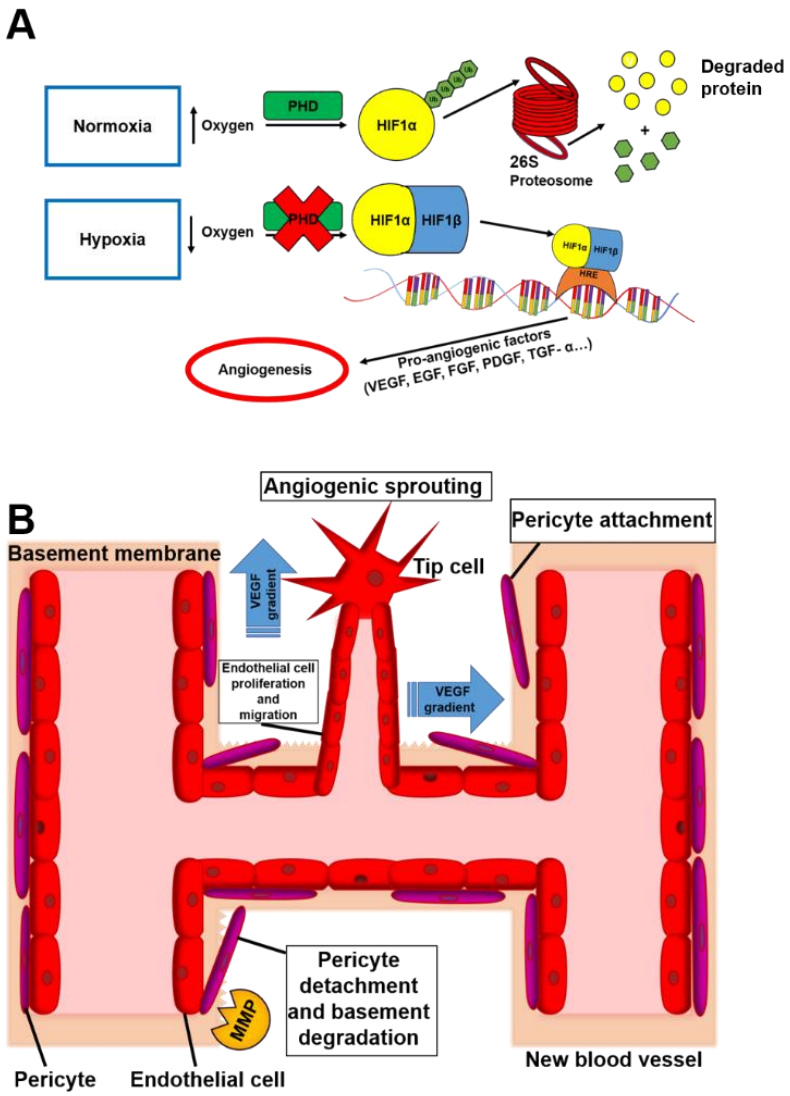

Figure 1.2. The angiogenic process. Cartoon representation of the molecular and physiological aspects of angiogenesis of blood vessels. **(A)** Prolyl hydroxylases (PHD) promote the ubiquitination and degradation of hypoxia-inducible factors (HIF-1α) via a proteosome. In hypoxic conditions, PHD is not active and therefore allows the binding of HIF-1α to HIF-1β. This complex binds to hypoxia response elements (HRE) in genes which release growth factors to promote angiogenesis. Image adapted from (Zhou *et al.*, 2019). **(B)** Endothelial cells respond to increased growth factors, mainly VEGF during hypoxia. Hypoxic conditions also promote the degradation of the basement membrane and detachment of supporting cells, and pericytes by matrix metalloproteinases (MMPs) to allow space for the formation of a new vessel. Endothelial tip cells from the pre-existing vessel proliferate and migrate along a VEGF gradient to form a new blood vessel network. Image adapted from (Raza, Franklin and Dudek, 2010).

The concentrations of several apoptotic cytokines, such as tumour necrosis factor-α (TNF-α) and Fas have shown to be increased in the blood of chronic heart failure patients (Levine *et al.,* 1990; Nishigaki *et al.*, 1997). This proinflammatory pathway, however, may in fact induce a cardioprotective effect in the long-term. Apoptotic cardiomyocytes may release these cytokines after cardiac injury to attract endothelial cells in order to aid recovery, such as leukocyte β-integrins which promote adhesion, through aiding cell proliferation or promoting the differentiation of cardiac stem cells to promote repair (Nian *et al.*, 2004; Hsieh *et al.*, 2006). This highlights the potential of the endothelium in repair, in which they contribute to this process by aiding blood vessel branching. The chain of events started by cytokine signalling induces increases of many pro-angiogenic factors. Endothelial cells also have protein-based oxygen sensory mechanisms which involve hypoxia-inducible factors (HIFs) controlling gene transcription. This process regulates angiogenesis and vascular physiology during hypoxia or inflammation. This chain of events includes the elevated expression of pro-angiogenic factors such as vascular endothelial growth factor-A (VEGF-A) (Carmeliet and Jain, 2011).

Hypoxia induces an upregulation in the expression of VEGF-A *via* the action of hypoxia inducible factor (HIF), which binds to hypoxia-responsive elements (HREs) within the *VEGFA* promoter (Fig. 1.2A). In normoxia (3-5% oxygen), prolyl hydroxylases (PHDs) target the HIF-1α subunit for hydroxylation (leading to ubiquitination and proteolysis), but these enzymes have an oxygen requirement. Therefore, when conditions are hypoxic (<1% oxygen), PHD action is blocked, allowing the HIF-1α subunit to form a complex with the HIF-1β subunit (Fig. 1.2A). This HIF-1 heterodimer translocates into the nucleus to bind to HREs within many hypoxia-inducible genes and triggers the transcription of many genes involved in angiogenesis, including the expression and secretion of VEGF-A (Tammela *et al.*, 2005). VEGF-A is also important in several other events within this process, including endothelial cell permeability, extracellular matrix (ECM) secretion, and new blood vessel guidance (Carmeliet and Jain, 2011) (Fig. 1.2B).

1.3.1 Vascular endothelial growth factors (VEGFs)

Vascular endothelial growth factors (VEGFs) are a family of ligands that are upregulated during normal physiological processes involved in organ development, tissue regeneration and wound healing (Leung *et al.*, 1989; Ferrara, 1999). These factors are also implicated in various disease states such as neovascular age-related macular degeneration (AMD), diabetic retinopathy and rheumatoid arthritis. VEGF-stimulated signal transduction in different cells and tissues is also implicated in certain types of cancer. The development of such diseases involves an abnormal level of angiogenesis, in which it can be targeted by cancerous cells in order to provide a blood supply for tumours. This could be linked to VEGF-A, which is often overexpressed in solid tumours and is associated with poorer survival outcomes (Jain, 2005; Zhao *et al.*, 2011). Blocking VEGF signalling is therefore a well-established route towards targeting pathological angiogenesis in disease states.

The metazoan VEGF family consists of: VEGF-A, VEGF-B, VEGF-C, VEGF-D, the viral VEGF-E, the snake-venom derived VEGF-F, and placental growth factor (PIGF) (Iyer and Acharya, 2011). All VEGFs have 8 highly conserved cysteine residues containing a combination of intra- and intermolecular disulphide bonds and a cystine-knot domain. The combination of this cystine-knot structure and loops formed by the disulphide bonds allows binding to vascular endothelial growth receptors (VEGFRs) (Holmes and Zachary, 2005; Shibuya, 2011). This, however, does not mean that there are not differences between these isoforms. For example, VEGF-C and VEGF-D have N- and C-terminal propeptide extensions on either side of the central cystine-knot regions. Processing of the premature forms of these VEGFs occurs by cleaving the propeptide regions with proteases, increasing their binding affinities for receptors such as VEGFR2 (Holmes and Zachary, 2005; Shibuya, 2011; Schwarz, 2017). VEGFs can even differ within the same group, such as the alternative splicing seen with VEGF-A to form isoforms of different amino acid lengths such as 121, 145, 165, and 183. These can all have different properties, such as VEGF-A_{121} being secreted whilst VEGF-A_{183} is sequestered in the

extracellular matrix, and then only released via cleavage. VEGF-A_{165} is arguably the most biologically important and abundant of these isoforms due to its role in several physiological processes, such as angiogenesis. These isoforms can also differ in their ability to interact with co-receptors which usually aid binding of VEGFs to the VEGFRs, known as neuropilins (Holmes and Zachary, 2005). Neuropilin-1 (NRP1) and neuropilin-2 (NRP2) are transmembrane glycoproteins within the endothelium which act as co-receptors for VEGF and are often over-expressed in areas of both physiological and pathological angiogenesis (Staton *et al.*, 2007). The presence of NRP1, for instance, has been seen to enhance VEGF-A_{165} binding to the mouse form of VEGF receptor 2 (VEGFR2), KDR, by about 4- to 6-fold in endothelial cells. In addition, blocking the ability of VEGF-A_{165} to bind to NRP1 also prevented VEGF-A_{165} binding to KDR (Soker *et al.*, 1998). It should also be noted that VEGF-A_{165} can bind to NRP2, unlike the VEGF-A_{145} isoform, which binds to NRP2 and not NRP1 (Holmes and Zachary, 2005). These relationships may partly explain why VEGF-A_{165} is so potent as a growth factor.

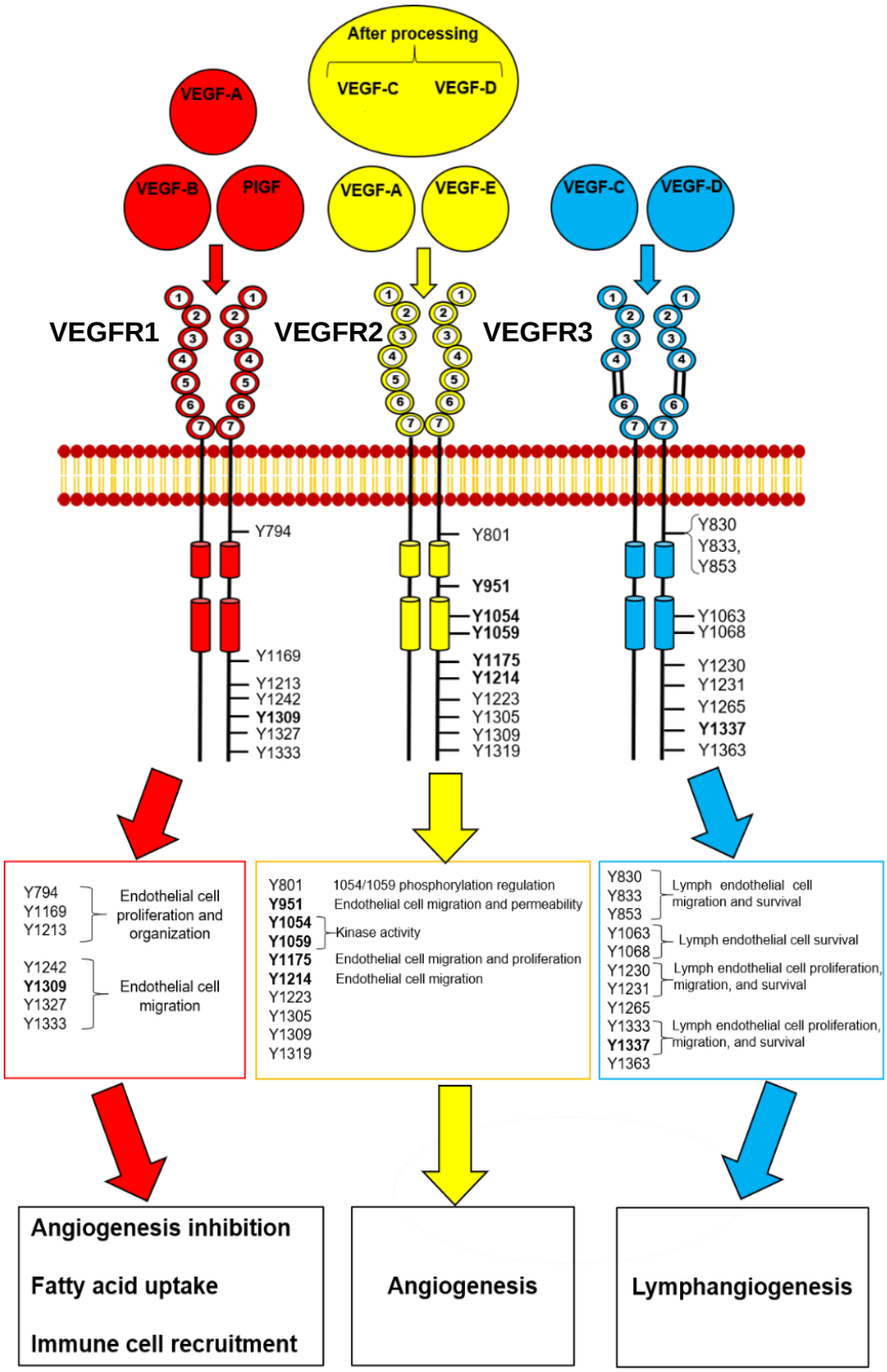

Figure 1.3. VEGF-VEGFR signalling. Vascular endothelial growth factor receptors (VEGFRs) all contain 7 immunoglobulin-like domains apart from VEGFR3, where the 5th domain is replaced by disulfide bonds. The VEGF family includes several members which can bind to multiple receptors, such as VEGF-A to VEGFR1 and VEGFR2. VEGF-C and –D both have to be proteolytically processed before they can bind to VEGFR2. The cytoplasmic domains of each receptor each contain multiple tyrosine kinase sites which can be phosphorylated to induce certain biological functions. Image adapted from (Lugano *et al.,* 2018)

1.3.2 Vascular endothelial growth factor receptors (VEGFRs)

There are also three *VEGFR* gene loci that encode related receptor tyrosine kinases (RTKs) that comprise an RTK subfamily: VEGFR1 (Flt1), VEGFR2 (KDR/Flk1) and VEGFR3 (Flt4) (Fig. 1.3). These VEGFRs contain an extracellular domain consisting of seven immunoglobulin-like (Ig) domains, which enable VEGF recognition, a transmembrane region, a cytoplasmic or juxtamembrane region adjacent to the lipid bilayer, a tyrosine kinase domain, and a flexible carboxy-terminal tail region (Fig. 1.3). These VEGFRs follow a general model for RTK activation and signal transduction (Lemmon and Schlessinger, 2010; Karpov *et al.*, 2015). VEGF ligand binding induces VEGFR dimerisation followed by a conformational change in the intracellular cytoplasmic domain, allowing opening and increased solvent accessibility to the ATP-binding site within the tyrosine kinase domain (Koch *et al.*, 2011). The exchange of ADP for ATP stimulates tyrosine kinase activity and trans-autophosphorylation of key tyrosine residues within the cytoplasmic domain; RTK activation also triggers phosphorylation of downstream effectors and enzymes within different signalling pathways (Koch *et al.*, 2011).

VEGFR1 and VEGFR2 are both membrane receptors that bind VEGF-A. Although they are thought to function in signalling as homodimers, VEGFR1 can form a heterodimer with VEGFR2 (Koch *et al.*, 2011). One idea is that VEGFR1 acts as a decoy receptor (a 'VEGF-A trap') to regulate the angiogenic activity of VEGFR2 (Smith *et al.*, 2015). VEGFR1 also binds VEGF-A with a greater affinity compared to VEGFR2 (K_d values of~15 pM vs. ~750 pM respectively) (Koch *et al.*, 2011). The VEGFR1 tyrosine kinase (TK) activity is relatively weak (compared to VEGFR2) when activated by specific VEGF ligands. This could be due to a repressor sequence in the VEGFR1 juxtamembrane region or some underlying structural difference in the activation loop within the TK domain. By contrast, VEGFR2 is known to induce a wide spectrum of endothelial responses including cell proliferation, migration and angiogenesis. VEGFR2 receptor is a focus of current therapies targeting pathological angiogenesis in diseases such as cancer and macular degeneration.

1.4. Signal Transduction

1.4.1. VEGFR1 (Flt-1)

Signal transduction through each VEGFR is complex. VEGFR1, for example, can bind VEGF-A but also has VEGFR1-specific ligands i.e., VEGF-B and PlGF. The phosphorylation of specific cytoplasmic tyrosine residues depends on the VEGF ligand e.g. PlGF binding to VEGFR1 causes activation (phosphorylation) of Y1309 whilst VEGF-A does not (Koch *et al.*, 2011). Specific tyrosine residues can have certain effects, such as VEGFR1-pY794 being involved in phospholipase Cγ1 (PLCγ1) recruitment activation, thus causing PIP2 hydrolysis to diacylglycerol (DAG) and inositol 1,4,5-trisphosphate (IP3): binding of IP3 to IP3 receptors on the ER stimulates cytosolic calcium ion rise and flux (Koch *et al.*, 2011). Another epitope, VEGFR1-pY1169 also enables recruitment of PLCγ1 to the plasma membrane; this is also linked to activation of the canonical mitogen-activated protein kinase (MAPK) pathway which controls cell proliferation (Shibuya and Claesson-Welsh, 2006). It is also interesting to note that the autophosphorylation patterns of VEGFR1 caused by either VEGF-A or PlGF are different, indicating different conformational changes in VEGFR1 caused by binding of either of the VEGF ligands (Autiero *et al.*, 2003). The consensus view is that VEGFR1 has distinct molecular properties that impact on distinct aspects of cell function; notably it is also more widely expressed in many cells and tissues suggesting it has essential function(s) outside of the vascular system.

1.4.2. VEGFR2 (KDR, Flk-1)

The interaction between VEGF-A and VEGFR2 is one of the central regulatory aspects in angiogenesis in health and disease. This signalling cascade includes activation of phosphatidylinositol 3-kinase (PI3-K), protein kinase B (Akt), PLCγ1, and extracellular signal-regulated kinase (ERK). All of these contribute to several angiogenic functions including cell survival and proliferation. The other functions such as cell migration, blood vessel guidance, and formation depend on neuropilin receptors (Shibuya and Claesson-Welsh, 2006). The activation of VEGFR2 will activate the autophosphorylation of several tyrosine residues with many different effects, such as Y951. This allows phosphorylation of the T cell specific adapter (TSAd) which contains Src Homology 2 (SH2) and protein tyrosine binding (PTB) domains to promote bind the tyrosine kinase Src; these interactions regulate actin dynamics and endothelial cell migration (Shibuya and Claesson-Welsh, 2006).

1.4.3. VEGFR3 (Flt-4)

VEGFR3 can be activated by the binding of VEGF-C or VEGF-D (Fig. 1.3). The activated VEGFR3 shows phosphorylation of Y1063 which allows recruitment of the adaptor protein CRK I/II (C10 regulator of kinase) which in turn activates the c-Jun N-terminal kinase (JNK) pathway. Such interactions promote cell survival. VEGFR3 regulates lymphangiogenesis, which requires the activation of the PI3K/Akt pathway. PI3K regulates lympho-endothelial migration to help develop lymphatics (Koch *et al.*, 2011). VEGF-C can also promote the formation of VEGFR2/VEGFR3 heterodimers, which can inhibit the phosphorylation of specific tyrosine residues such as Y1337 and Y1363 (Shibuya and Claesson-Welsh, 2006).

1.5. Ubiquitination, Membrane Trafficking and Proteolysis

Membrane trafficking is important in the regulation of RTK signalling. One protein modification which is important in this process is the attachment of ubiquitin, a protein tag which is conjugated to protein substrates via ε-amino side chains of lysine residues (Hjerpe *et al.*, 2009) (Fig. 1.4). Ubiquitination is important for marking proteins to be degraded, redistributed to a new location or to modify target protein activity. Not much is known about the ubiquitination of VEGFR1 and VEGFR2, but we do know that it can occur through pathways either dependent or independent of VEGF-A binding to these RTKs (Ewan *et al.*, 2006; Smith *et al.*, 2017). For instance, VEGF-A can activate VEGFR2 proteolysis upon binding as regulated by E3 ubiquitin ligases such as c-Cbl (a proto-oncogene) (Smith *et al.*, 2017). Alternatively, the synthesis of VEGFR2 may be regulated in the secretory pathway *via* RNF121, another E3 ubiquitin ligase; this in turn can inhibit other VEGF-A mediated processes such as angiogenesis (Maghsoudlou *et al.*, 2016). In contrast to this E3 ligase-mitigated ubiquitination, VEGFR2 may also undergo this same process through a regulatory VEGF-A independent pathway *via* the E1 ubiquitin ligase, UBA1; this in turn has been shown to promote *in vitro* angiogenesis (tubulogenesis) (Smith *et al.*, 2017).

VEGFR internalisation occurs through clathrin-dependent endocytosis, in which the receptor is either targeted for recycling or degradation. VEGF-A binding to VEGFRs triggers this process via causing receptor dimerisation and tyrosine phosphorylation. The result is the recruitment of the activated VEGFR to clathrin-coated pits. These pits bud off from the membrane and form clathrin-coated vesicles containing the receptor cargo, where they either fuse with endosomes for degradation or migrate back to the membrane for recycling (Horowitz and Seerapu, 2012) (Fig. 1.5).

Neuropilin aids in this procedure by aiding the binding of VEGFR2 to myosin VI via synectin, thus increasing movement and trafficking to the endosomes (Fig. 1.5). VEGFR2 is moved to recycling endosomes, the plasma membrane, or to lysosomes, via Rab4, Rab11 or Rab7 respectively (Horowitz and Seerapu, 2012) (Fig 1.5.

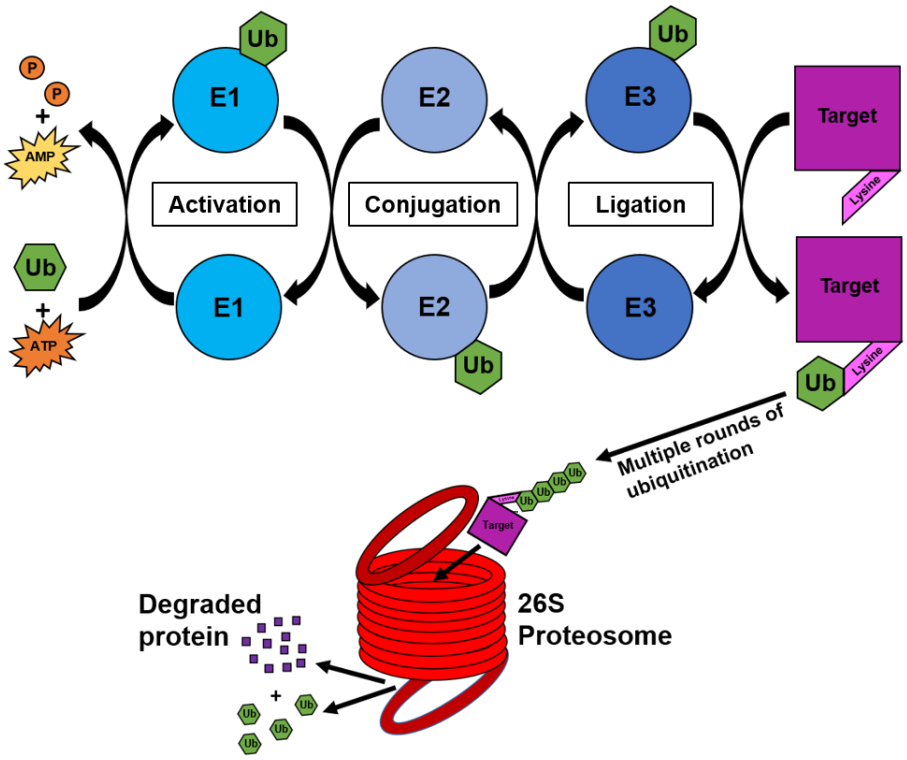

Figure 1.4. The ubiquitin-proteasome system (UPS). Cell homeostasis is regulated by the attachment of ubiquitin (Ub) to a protein targeted for degradation. This is facilitated by the sequential activation of enzymes within the UPS: E1, E2 and E3. Ubiquitin is attached to the E1 ubiquitin-activating enzyme in an ATP-dependent manner. The E2 conjugating enzyme allows ubiquitin to be passed from the E1 to the E3 ligase enzyme. The E3 enzyme ligates ubiquitin to its substrate protein via lysine residues which mark the target protein for degradation by the 26S proteosome. Other events may be induced depending on whether a single molecule of ubiquitin or a chain (poly-ubiquitin) is attached to its substrate protein. For instance, a protein may not be degraded but instead redistributed to a new cellular location depending on the linkage types or length of the attached poly-ubiquitin chain. Ubiquitin attachment can also change protein activity or functionality without affecting degradation or location. Image adapted from (Leestemaker and Ovaa, 2017).

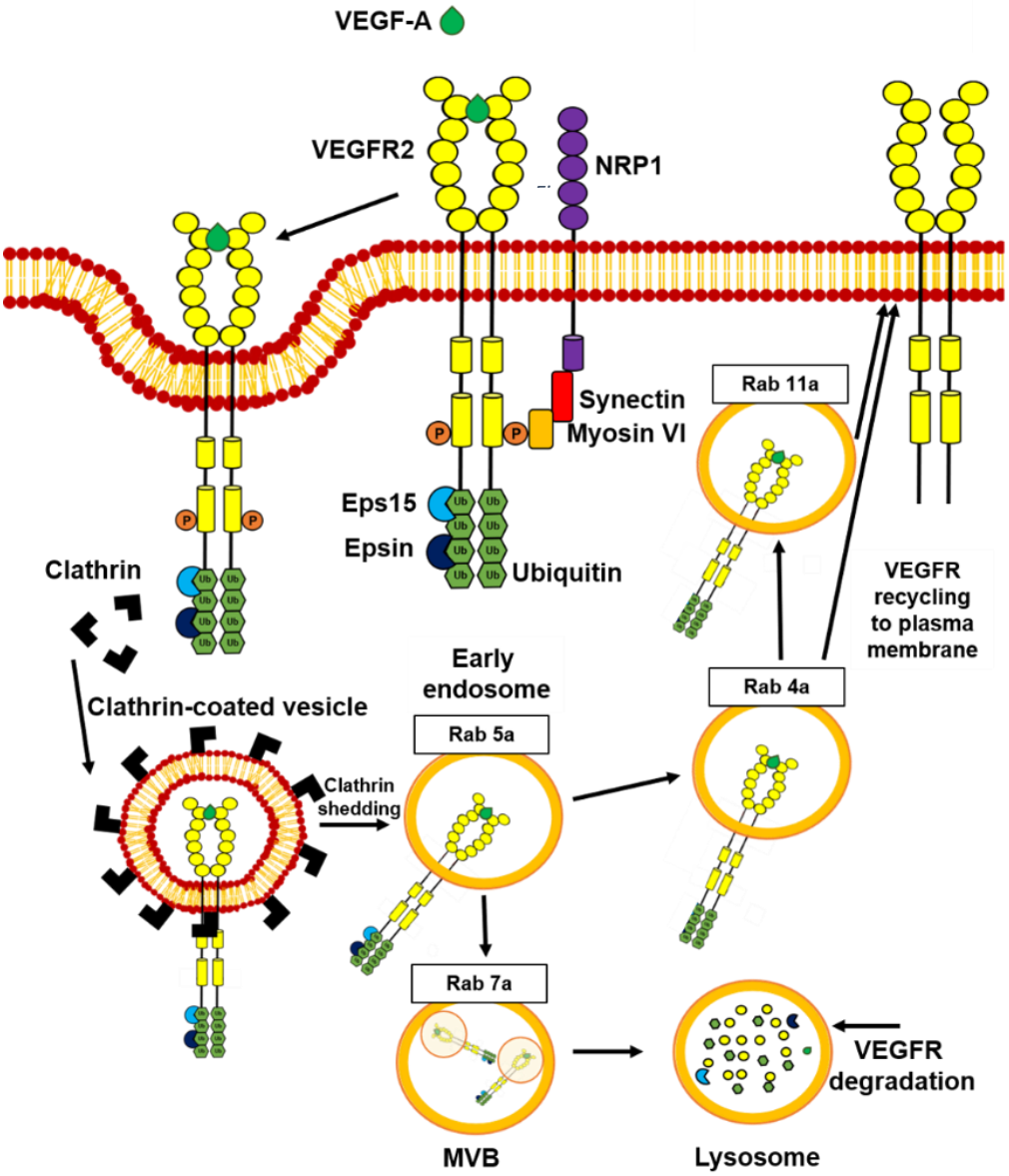

Figure 1.5. Clathrin-dependent VEGFR recycling and degradation. VEGFRs can either undergo degradation or be recycled to the plasma membrane to inhibit or promote angiogenesis respectively. Movement throughout the cell is aided by the VEGFR co-receptor, neuropilin (NRP1) via its connection to myosin VI through binding to synectin. VEGF-A binding to the receptor promotes its internalization into the cell through clathrin-mediated endocytosis. VEGFRs fuse to a sorting endosome, mediated by the small GTPase Rab5a, after clathrin shedding. A VEGFR may be tagged by ubiquitin(s) which are recognized by epsins; this allows Rab7a-mediated degradation of the receptor through endosomal multivesicular bodies (MVBs) and lysosomes. The alternative is recycling of the VEGFR to the plasma membrane via Rab4a- or Rab11a-dependent routes (Horowitz and Seerapu, 2012). Image adapted from (Shi *et al.*, 2017).

One important form of VEGFR regulation is proteolysis, the degradation of large proteins into their truncated forms. Proteolytic cleavage of VEGF-C and VEGF-D, for example, allows them to not only bind to VEGFR3, but also to VEGFR2. This is also accompanied by an increase in affinity for the two receptors (Koch *et al.*, 2011) VEGFR2 itself may be targeted for proteasomal degradation by ubiquitination induced by E3 ligases. VEGFR1 is also targeted for proteolysis by ubiquitination, but this is much lower compared to that of VEGFR2. VEGFR2 may, therefore, be the main target for ubiquitination following VEGF-A stimulation (Bruns *et al.*, 2010). VEGFR2 proteolytic cleavage can also occur after it has passed through early endosomes on the way to final degradation in lysosomes, with these fragments producing transmembrane and ectoplasmic domains (Horowitz and Seerapu, 2012). All of these processes are, therefore, important in maintaining the homeostasis of each of the receptors.

1.6 VEGF-associated therapeutics

There is an ever-growing number of therapeutics which target several pathways mediated by VEGF-A in order to treat pathological angiogenesis. The largest and most commonly used of these are humanized antibodies (Fig. 1.6) and small molecule inhibitors, where their modalities can include directly binding to VEGF-A or inhibiting its receptors, such as VEGFR2. Their proposed efficacy and safety have led to several being approved by the FDA including: bevacizumab (Avastin), ramucirumab (Cyramza), suntinib malate (Sutent, SU11248) and sorafenib (Nexavar, BAY 43-9006). The majority of this list are humanised antibodies while the latter two, sunitinib and sorafenib, are small molecule tyrosine kinase inhibitors (TKIs) (Zirlik and Duyster, 2018). A more detailed examination of these inhibitors along with the emerging therapeutics, nanobodies, will be detailed below.

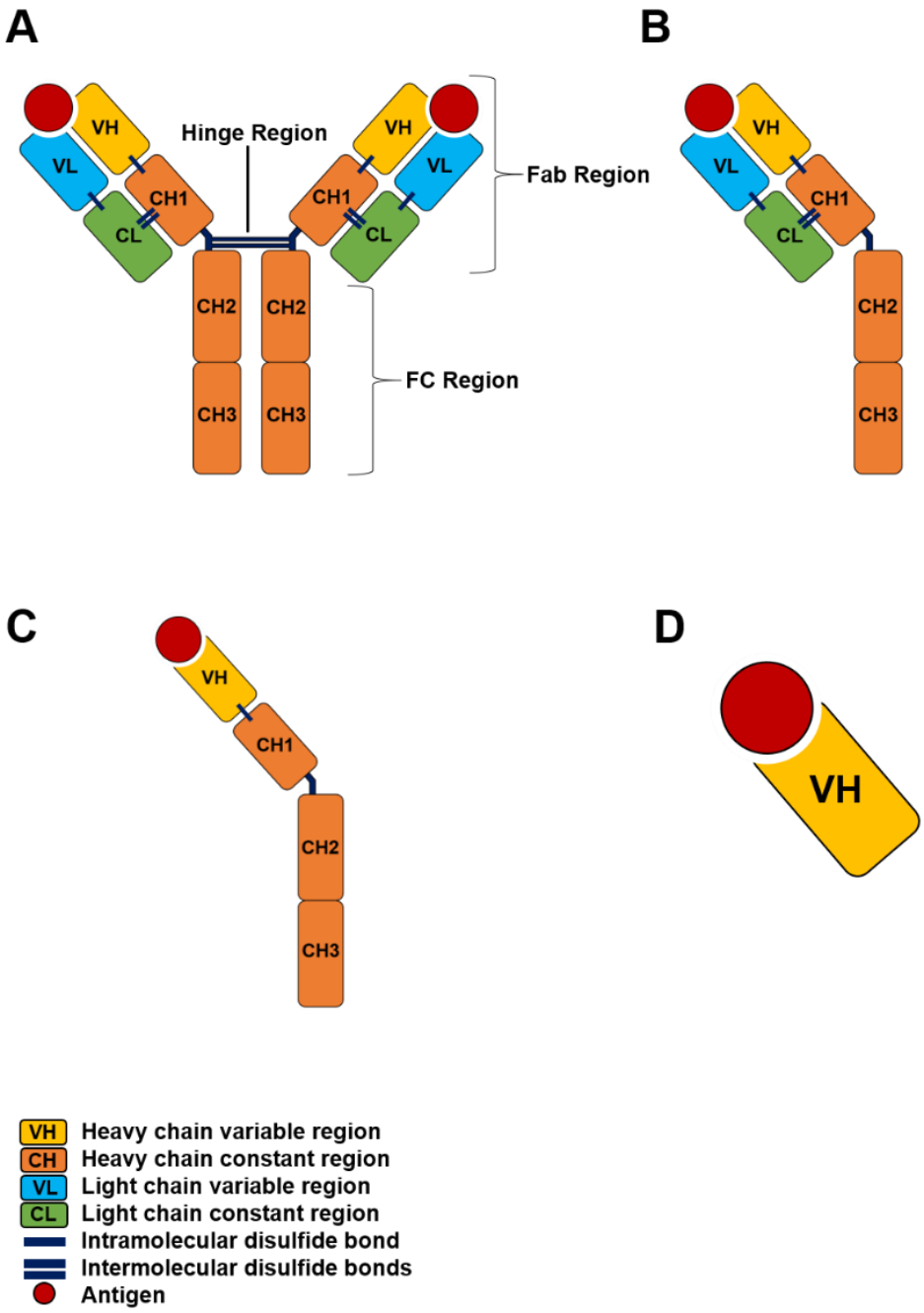

Figure 1.6. Different antibody structures. The represented antibody structures all contain a variable domain (Fab region), but with some differences. (A) Divalent antibody, has two sets of light and heavy chains, can bind two antigens. (B) Monovalent antibody, has one set of light and heavy chains, can only bind one antigen. (C) Camelid antibody, which only contains a heavy chain. (D) Nanobody-based on camelid antibodies, only contains a heavy chain variable region. Image adapted from (Alfaleh *et al.*, 2020).

1.6.1 Bevacizumab

One therapy which has proven to be effective in the treatment of several diseases is a humanized monoclonal antibody called bevacizumab (Avastin). Its action is mediated by specifically binding to VEGF-A, which ultimately inhibits angiogenesis (Ahmadizar *et al.*, 2015) (Fig. 1.7A). Bevacizumab had previously been shown to be effective in combination with current chemotherapy drugs, such as Paclitaxel, to treat HER2-negative metastatic breast cancer. In this particular study, it was found to increase progression-free survival (PFS), the time it takes for the disease to progress or for toxic effects to appear in patients, compared to when paclitaxel was used alone (11.8 vs 5.9 months) (Miller *et al.*, 2007). This drug combination was later approved for the treatment of HER2-negative metastatic breast cancer by the FDA in 2008. This, however, was later retracted in 2011 due to the results of three phase III trials (AVADO, RIBBON-1, and RIBBON-2), where there was still an extension of PFS but no effect on overall survival (OS). This has not, however, affected its FDA status with regards to use in treatment of colon, lung, kidney and brain cancers (US Food and Drug Administration, 2011a; Zirlik and Duyster, 2018).

There has also been an increased usage of this drug in the past few years to treat neovascular age-related macular degeneration (AMD) where intravitreal injections of it and another VEGF inhibitor, ranibizumab, have helped improve the vision of many patients. However, one population study has shown that a combination of these drugs increased the risk of myocardial infarction (MI) by 2.3-2.5 times more in patients with AMD as compared to the control group (95% CI, 1.3-4.9) (Kemp *et al.*, 2013). This could have of course been due to several factors, but there have been several reports of bevacizumab having adverse effects on the cardiovascular system. These have included the most frequent adverse effect hypertension as well as gastrointestinal tract perforations, arterial thromboses and even heart failure (Mourad *et al.,* 2008; Nalluri *et al.,* 2008, Perren *et al.,* 2011; Ahmadizar *et al.,* 2015). This was also observed in the study of bevacizumab which led to its approval by the FDA for use in HER2-

negative cancer, as patients were frequently reported to experience hypertension, headaches and cerebrovascular ischaemia (Miller *et al.,* 2007).

1.6.2 Ramucirumab

Antibodies of course not only can target growth factors but the receptors to which they bind to. Ramucirumab is an example of a monoclonal antibody which specifically binds to VEGFR2 (Abdel-Rahman and ElHalawani, 2016) (Fig. 1.7B). Ramucirumab was first approved for use by the FDA in 2014 for use in patients with gastric cancer either as a single or combination therapy, but it has also been approved for several other types of cancer such as non-small cell lung cancer (US Food and Drug Administration, 2020). Like bevacizumab, ramucirumab has also been associated with adverse effects on the cardiovascular system. For instance, in a meta-analysis of several studies totalling 3103 patients involving the use of ramucirumab, the RR of high-grade hypertension was 3.73 (95% CI 2.82-4.93; $p<0.0001$), although there was no statistical significance between using it as a monotherapy vs as a combination with other drugs. There was also a non-significant increase in bleeding with an RR of 1.08 (95% CI 0.78-1.5; $p = 0.64$), but this increase could maybe be explained by hypertension. Interestingly, the meta-analysis did not show an increase in arterial and venous thrombotic events. It is not clarified as to why this was the case, but it is theorised that it could be either due to the criteria for inclusion may have left out patients with atherosclerosis or due to different anti-angiogenic mechanisms (Abdel-Rahman and ElHalawani, 2016). If it is due to the anti-angiogenic mechanisms, this could imply that directly blocking the VEGFR receptors may be safer than blocking their signalling molecules.

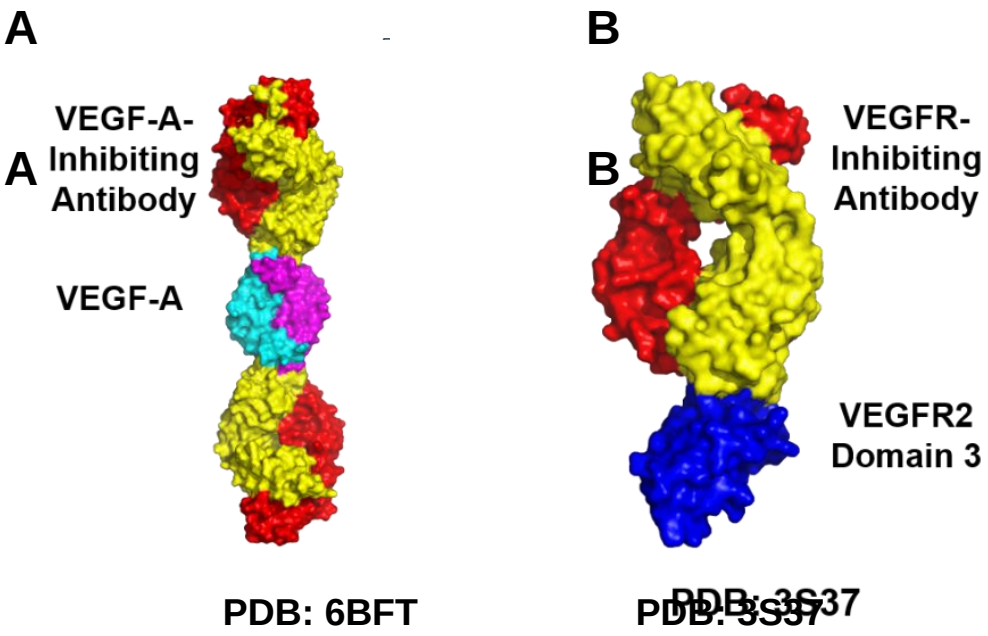

Figure 1.7. Binding of antibodies specific to the VEGF-signalling pathway. Figure depicts examples of antibodies which target diseases such as cancer by either inhibiting VEGF-A or VEGFR2. (A) The VEGF-A binding antibody, bevacizumab, in complex with a VEGF-A dimer (purple and cyan). (PDB ID: **6BFT**) (B) The VEGFR2-binding antibody, ramucirumab in complex with the third domain of VEGFR2 (blue). (PDB ID: **3S37**). Antibody light and heavy chains are depicted as yellow and red respectively. Images were obtained using the PyMOL program.

1.6.3 Sorafenib and Sunitinib

Rather than targeting extracellular ligands or domains, VEGFR signalling can be blocked by targeting the cytoplasmic TK activity using small molecule inhibitors that can permeate through the plasma membrane. Sorafenib (Nexavar) and sunitinib (Sutent), for example, are small molecule tyrosine kinase inhibitors of VEGFR2 (Hsu and Wakelee, 2009; Zirlik and Duyster, 2018), which inhibit signalling via the canonical Raf/MEK/ERK pathway (Pölcher *et al.*, 2010). Sorafenib and sunitinib have been used as cancer treatment adjuvants for a relatively long time, with them being granted FDA approval in 2005 and 2006 respectively (US Food and Drug Administration, 2011, 2018c). Their use as adjuvants to established monoclonal antibody therapies such as interferons and bevacizumab have shown statistically significant effects on progression-free survival and tumour size has been

seen in as many as 888 studies (including eight clinical trials) on patients with advanced and/or metastatic renal cell carcinoma (RCC) (Thompson Coon *et al.*, 2010).

Sunitinib malate has been shown in clinical trials to show reduced metastasis, as seen by increased cancer progression times of 28.9 weeks in patients taking this drug compared to 7 weeks for placebo cases (RR = 0.28; P<0.001) (Adams, 2007). This, however, does not mean that there are no toxic side-effects. Sunitinib has recently been associated with an increase in hepatotoxicity, which can be seen in clinical trials such as the ones which allowed sunitinib to be approved by the FDA. In this study, the response of gastrointestinal stromal tumours (GIST) to sunitinib treatment was tested; in addition to hypertension and left ventricular dysfunction, there were also increased levels of liver enzymes which are often associated with liver disease. This can be seen in all grades of GIST, where 39% of patients experienced higher aspartate aminotransferase(AST)/alanine aminotransferase (ALT) vs 23% in the control, and total bilirubin was 32% vs 8% (Goodman *et al.*, 2007). This could potentially be related to decreased clearance of sunitinib from the livers of mice (Zhao Q, *et al.,* 2019).

In the case of sorafenib, a phase I study was carried out where 39 cancer patients took daily oral doses of sorafenib combined with a gradually increasing intravenous dose of bevacizumab (every 2 weeks). There was, however, an unexpectedly large degree of toxicity observed during this study due to the combination of these drugs, with proteinuria, thrombocytopenia and hypertension being seen in a lot of the patients. The toxicity was so great that neither of the drugs could be used at their maximum/recommended dose compared to when they were used alone. 74% of the patients needed to have their sorafenib dose reduced from two daily doses of 200 mg to just one at this dosage (Azad *et al.*, 2008).

Despite this, it should be noted that there is a theory that hypertension may be a good indication of successful VEGF-signalling inhibition, which can be seen in studies of both sunitinib and sorafenib. In a study of sunitinib treatment for metastatic renal cell carcinoma (mRCC), a longer PFS was seen in hypertensive patients with a hazard ratio (HR) of 0.36 (95% CI 0.27-0.50, P<0.001) and OS was significantly improved as seen by a HR of 0.36 (95% CI, 0.27-0.50, P<0.001) (Donskov, *et al.,* 2015). Meanwhile, a study on sorafenib treatment showed 58% of hepatocellular carcinoma patients developed hypertension within 2 weeks, but this correlated with a significant increased cancer progression time of 153 days vs 50.5 days in the control group (P<0.017). This was also seen with OS, which was 1329 days compared to the control of 302 days (P<0.004) (Akutsu *et al.,* 2015).

Therapeutics, therefore, which target the VEGFR receptors could theoretically still be viable even if they produce a side-effect like hypertension. Hypertension may be managed with proper diet and exercise alongside antihypertensive drugs. The four classes of these antihypertensive drugs are: diuretics, beta blockers, renin-angiotensin system (RAS) blockers and calcium antagonists. Angiotensin-converting enzyme (ACE) inhibitors, part of the RAS blocker class, are some of the most commonly prescribed antihypertensives. However, they can induce side-effects such as nausea or a persistent dry cough, which is why it is beneficial that there are alternative reagents which target other systems for reducing hypertension and thus tailor it to the patient (Burnier *et al.,* 2020). Therefore, managing hypertension could accrue an additional benefit of potentially increasing the effectiveness of the treatments targeting the VEGFR-axis.

1.6.4 Nanobodies

Nanobodies were first described nearly 30 years ago after studies on the immunogenic response using camel serum showed a mixture of standard IgG_1 antibodies, having both light and heavy chains, as well as two new IgGs containing only heavy chains and lacked the CH1 region. These would later be classified as camelid antibodies due their presence in animals within the C*amelidae* family (Hamer-Casterman, Atarchouch, T *et al.*, 1993). Further analysis into their structures identified a single variable V_HH domain as the binding site of antigens at a molecular mass of ~15 kDa (Fig. 1.6D). This meant that this was the smallest functioning antibody fragment found so far to be useful, thereby creating a new classification of potential therapeutics to explore called nanobodies (Cortez-Retamozo *et al.*, 2004).

Caplacizumab (Ablynx) is a nanobody which is a dimerized version of an antibody that targets Von Willebrand factor (VWF), a key component in the pathogenesis of thrombotic thrombocytopenic purpura (TTP). TTP is disease, often fatal, characterised by the presentation of thrombi and haemolytic anaemia within the capillaries (microangiopathy) as well as thrombocytopenia. TTP is an autoimmune disorder caused by the production of antibodies against the ADAMTS13, a disintegrin and metalloproteinase which regulates platelet activity by regulating VWF activity (Hanlon and Metjian, 2020). It does this by either proteolytic cleavage of VWF multimers or inhibiting their formation by preventing disulfide bond formation (Zheng, 2015). If uninhibited, VWF can promote abnormally high platelet aggregation and activation followed by the formation of microthrombi and tissue ischaemia. Tissue ischaemia causes an increase in the consumption of platelets which ultimately decreases their population, hence the occurrence of thrombocytopenia. Caplacizumab binds to the A1 domain of VWF which prevents binding to the glycoprotein-Ib receptor of platelets (Hanlon and Metjian, 2020). The phase II TITAN and HERCULES trials both showed the promise of caplacizumab, with patients showing faster platelet count normalization, reduced relapses of TTP and thromboembolic events. Although there was increased bleeding in some of the patients taking caplacizumab, the drug was ultimately deemed safe. This

led to the FDA formally approving this as a therapy for TTP in combination with plasma exchange and immunosuppressants in 2019 (Peyvandi *et al.*, 2016; Scully *et al.*, 2019; US Food and Drug Administration, 2019c).

Despite the many benefits of camelid-based antibodies, there are a few disadvantages which should be noted. For example, antigen binding is heavily reliant on the small, single V_HH domain. The lack of a variable domain (VL) has led to evolutionary compensation within these antibodies, such as somatic hypermutation and extended CDR1 and CDR3 domains (Muyldermans, 2013). These changes are of course beneficial adaptations to animals within the *Camelidae* family, especially since they also have IgG antibodies within their systems. Trying, however, to adapt the V_HH antibodies to humans could potentially prove difficult due to these changes. Mutating residues outside of the antigen-binding loops for total humanization have in fact previously reduced the expression yield, binding affinity and stability of the resultant V_HH antibodies. There is also currently a heavy reliance on the use of direct camelid immunizations to generate new V_HH antibodies against specific proteins. There have, however, been studies where specific camelid antibodies have been generated using synthetic or semi-synthetic libraries (Arbabi-Ghahroudi, 2017). This evidence, when added to that provided by other work in this field, highlights the potential benefits of generating new therapeutics using the emerging synthetic technologies. The products resulting from these technologies are often referred to as antibody-mimetics, which have often been found to work in the same manner as conventional antibodies, whilst aiming to reduce their potential drawbacks.

1.7. Synthetic Proteins as Targeted Therapies

The use of antibodies as therapeutics has been well-established for decades. This, however, does not mean that there cannot be improvements made as to their functionality. As stated above, even current therapeutics can have adverse reactions, meaning that their mechanisms of action can be better tailored to fit into their intended domain of activity. The production of antibodies is, also, often time-consuming and requiring the use of

animals. Using animals is not only expensive, but also raises ethical concerns with regards to their welfare within research. There are, of course, many protocols with regards to ensuring the general welfare of animals used in testing, but of course an ideal solution would be to move to other sources for research materials in the production of therapeutics. This is where synthetic antibody mimetics may prove to be of central importance. Synthetic antibody mimetics come in many different forms (Fig. 1.8; Table 1.1) yet are often expressed using the *E.coli* bacterium, which not only eliminates the need for animals but also allows increased production and reduced batch variability. This can be seen when comparing some other expression systems available to a researcher, such as with mammalian and insect cells. These eukaryotic systems do allow the chance to produce functional proteins due to the ability to add modifications which mimic wild-type post-translational modifications (PTMs) such as glycosylation. However, this additional procedure can make these particular expression systems very costly and also add extra complications to the culture conditions needed. In contrast, bacterial expression systems can offer higher yields of protein at grams/litre with lower costs and less complicated culture conditions. There are still some challenges, however, with using an *E.coli* based system, such as the lack of ability to reproduce some mammalian proteins due to the inability to replicate PTMs (ThermoFisher Scientific, 2015).

There is also a potential risk that codon bias may occur in *E.coli* which can reduce protein yield. Codon bias occurs when a ribosome comes across mRNA coding which is different to that of the bacterium, resulting in the detachment of the target protein codon, stopping translation and therefore reduce its expression. Some bacterial strains have been adapted to reduce this effect and thus increase translation, but this can cause the protein to become insoluble (Rosano and Ceccarelli, 2009). However, these challenges do not mean that protein expression using bacteria is not viable, as there is an abundance of optimisation strategies that can be used. One of the most popular of these strategies is the T7 promoter system which are within pET vectors, where the target gene is cloned behind the promotor

which recognises T7 RNA polymerase; this highly prolific enzyme allows protein production to be induced by lactose or isopropyl β-D-1-thiogalactopyranoside (IPTG), which are effective yet tight regulators of this system (Rosano and Ceccarelli, 2014). Using different *E.coli* strains depending on your target protein can also provide effective results. For instance, one of the benefits of the BL21 strain is that the cells lack the Lon protease, which knocks down foreign proteins i.e., the target of interest. The BL21 (DE3) version also has the λDE3 prophage within its chromosome, therefore providing it the gene for the highly effective T7 RNA polymerase (Rosano and Ceccarelli, 2014). One other benefit is the ability to explore sequence space using *E.coli* due to its ability to be altered without eliminating protein activity. This can be seen with one study on the *E.*coli diacylglycerol kinase, where three-quarters of its sequence can tolerate changes such as the addition of large numbers of side-chains to the transmembrane domain residues and the conversion of polar to non-polar residues (Wen *et al.*, 1996). These are just a few of the reasons as to why the use of *E.coli* is very popular in the manufacture of synthetic proteins.

Antibody mimetics can be raised to meet a variety of cellular targets, increasing their potential on the market. Synthetically producing these proteins also allows a potential for modifications to both improve binding kinetics and safety. Table 1.1 illustrates a few of the antibody mimetics currently being researched which target signalling pathways involved in the cardiovascular system and cancer. A few examples of antibody mimetics have been approved by the FDA and those currently undergoing clinical trials will be detailed below (Table 1.1).

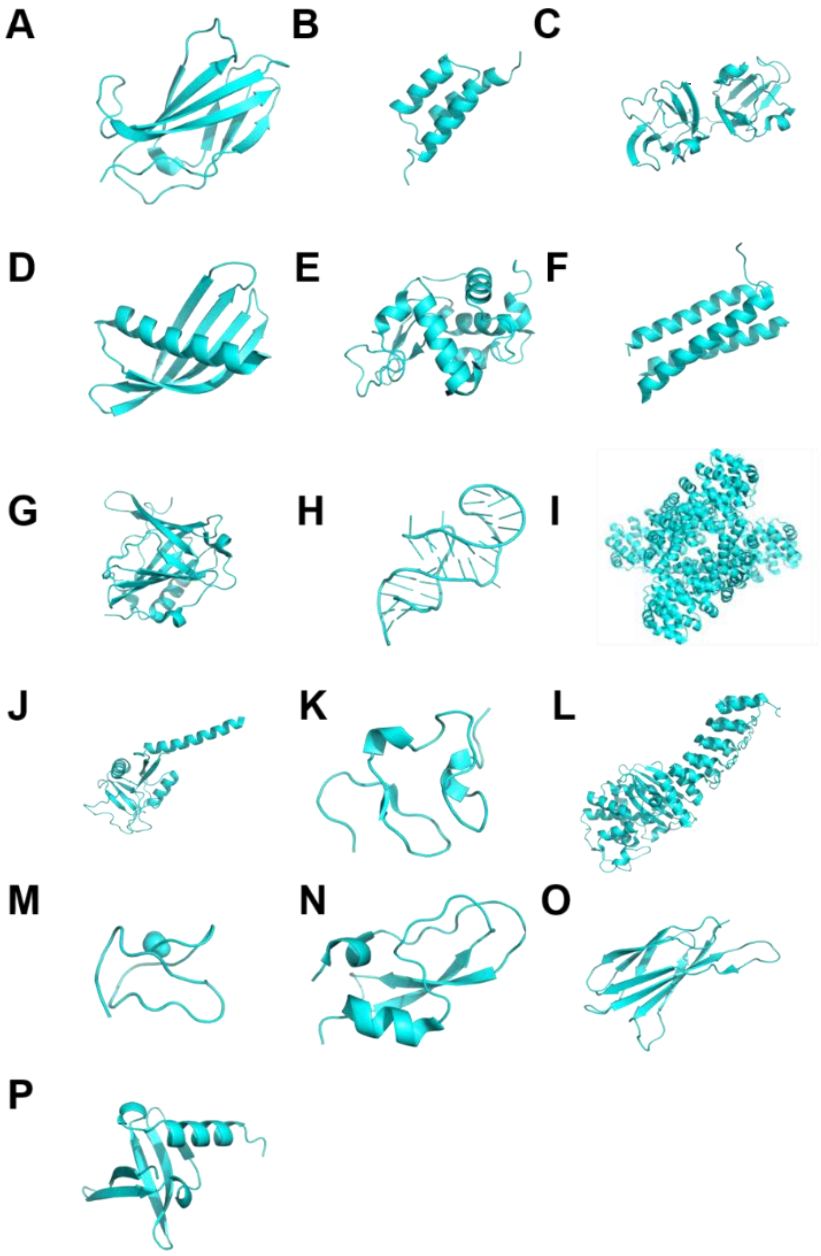

Figure 1.8. Synthetic antibody-mimetic scaffolds. Examples of synthetic antibody-mimetic scaffolds showing the differences in their structures. Protein Database (PDB) codes are shown in brackets. These include **(A)** Adnectin (4OV6), **(B)** Affibody (1H0T), **(C)** Affilin (2JDG), **(D)** Affimer (4N6T), **(E)** Affitin (4CJ2), **(F)** Alphabody (5MJ3), **(G)** Anticalin (6S8V), **(H)** Aptamer (2AU4), **(I)** Armadillo Repeat Proteins (4V3O), **(J)** Atrimer (1HTN), **(K)** Avimer (1AJJ), **(L)** DARPin (5AQA), **(M)** Knottin (1OMG), **(N)** Kunitz Domain Peptides (1KTH), **(O)** Monobody (5MTJ), and **(P)** Nanofitin (1AZP). Images were obtained from PDB using PyMOL software.

Antibody Mimetics or Synthetic Protein Scaffolds	Example References
Adnectins	(Mamluk *et al.*, 2010; Tolcher *et al.*, 2011; Lipovšek *et al.*, 2018)
Affibodies	(Löfblom, J. *et al.,* 2010; Barozzi *et al.,* 2020; Altunay *et al.,* 2021)
Affilins	(Ebersbach *et al.,* 2007); Mirecka *et al.,* 2009; Settele *et al.,* 2018)
Affimers	(Hughes *et al.*, 2017; Tiede *et al.*, 2017; Carrington *et al.,*2019)
Affitins	(Béhar *et al.*, 2014; Kalichuk *et al.*, 2020; Loussouarn *et al.*, 2020)
Alphabodies	(Desmet *et al.*, 2014; Škrlec, Štrukelj and Berlec, 2015; Pannecoucke *et al.*, 2021)
Anticalins	(Skerra, 2001; Gebauer and Skerra, 2012; Mross *et al.*, 2013)
Aptamers	(Martins and Ulrich, 2007; Kurt *et al.*, 2011; Nimjee *et al.*, 2017)
Armadillo repeat protein-based scaffolds	(Parmeggiani *et al.*, 2008; Reichen *et al.*, 2016; Hansen *et al.*, 2018)
Atrimers	(Allen *et al.*, 2012; Weidle *et al.*, 2013)
Avimers	(Silverman *et al.*, 2005; Smith *et al.*, 2013; Baghban Kohnehrouz *et al.*, 2018)
DARPins	(Stahl *et al.*, 2013a; Agarwal *et al.*, 2015; Sokolova *et al.*, 2016; Moisseiev and Loewenstein, 2020)
Fynomers	(Schlatter *et al.*, 2012; Silacci *et al.*, 2014; Simeon and Chen, 2018)
Knottins	(Moore *et al*., 2012; Postic *et al.*, 2018; Lee *et al.*, 2019)
Kunitz domain peptides	(Ding *et al.*, 2015; Bendre *et al.,* 2018; Mishra, 2020)
Monobodies	(Nicholes *et al.*, 2015; Zorba *et al.*, 2019; Kondo *et al.*, 2020)
Nanofittins	(Dammicco *et al.*, 2017; Goux *et al.*, 2017; Marcion *et al.*, 2021)

Table 1.1. A list of common antibody mimetics. Examples of common antibody mimetics which have been shown to target signalling pathways involved in the cardiovascular system and cancer

1.7.1 Synthetic protein therapies

Synthetic protein technology is an ever-growing industry. The aim of using such molecules as therapeutics is to have the benefits which antibodies provide but with both improved efficacy and reduced adverse effects. A number of these antibody-like mimetics are much smaller than conventional antibodies, often being <20 kDa, allowing them to not only bind to cell-surface receptors but also penetrate the cell membranes and large protein structures to target previously inaccessible epitopes. The use of methods such as phage display also not only enables increased protein expression and production, but also increases the chance to manipulate synthetic protein structure to allow the better recognition of their targets. Synthetic proteins can also be prepared without an Fc region, which means that they can bind to a variety of immune-linked receptors. This not only reduces the lifetime of these reagents, therefore reducing potential toxicity build-up, but also prevents them accidentally triggering the immune response (Ta and Mcnaughton, 2017). Although there is a broad spectrum of antibody mimetics currently available for a multitude of targets and disease, there are still a relatively low number that are currently approved by the FDA. Aflibercept, also known as VEGF-trap eye is one such example; it is a soluble receptor for VEGF produced by a combination of the second binding domain of VEGFR1 and third domain of VEGFR2 (Singh *et al.*, 2017).

There are two variations currently approved by the FDA for use in ocular disorders: Eylea (approved in 2011) and Zaltrap (approved in 2012). Interestingly, these variations were approved for different diseases involving the vascular system, Zaltrap for metastatic colorectal cancer (mCRC) and Eylea for ocular disorders such as neovascular (wet age-related macular degeneration (AMD) and diabetic retinopathy (US Food and Drug Administration, 2012, 2019b). Treatments for ocular disorders have other success stories which have received FDA approval, such as Pegaptanib sodium, known as Macugen. Macugen is an anti-VEGF RNA aptamer which has been selected to VEGF 165. It was in fact the first aptamer to be approved by the FDA in 2004 along with being the first anti-angiogenic drug

to be used for treating neovascular AMD (Ng *et al.*, 2006; US Food and Drug Administration, 2011b).

Another set of synthetic therapies are kunitz domain inhibitors. These are a class of protease inhibitors with irregular secondary structures containing 60 amino acids, three disulfide bonds and three loops which can be mutated (Hosse, 2006). Ecallantide, also known as Kalbitor, is a plasma kallikrein enzyme inhibitor. Plasma kallikrein produces the vasodilator bradykinin., which when upregulated increases vascular permeability, inflammation and pain (Lehmann, 2008). Plasma kallikrein is usually inhibited by the protein C1 esterase inhibitor, but this is depleted in the disease hereditary angioedema (HAE), which involves increases in edema and therefore swelling and pain (MacGinnitie *et al.*, 2012). Kalbitor was therefore approved by the FDA for use in treating HAE in 2009 (US Food and Drug Administration, 2014). Inhibitor cystine-knots (ICKs) are highly stable miniproteins of ~30-50 amino acids in length. They are often known as knottins due to this being the largest of the groups in the ICK family. The knottin group is characterized by three disulfides bonds forming a tight knot due to the cystines they are between and constrained loops. This structure enables high thermostability and proteolytic resistance along with sequence diversity between members of the knottin family due to the loops (Moore, 2012; Postic *et al.,* 2018). One of the best known of these knottins is Ziconotide, an synthetic form of ω-conotoxin MVIIa, which is produced by the venomous *Conus* magus snail (McGivern, 2007). Ziconotide is an analgesic N-type calcium channel antagonist which is used for the treatment of severe chronic pain in the nervous system and was approved for use by the FDA in 2004 (US Food and Drug Administration, 2011d).

One of the most recent approvals of synthetic proteins made by the FDA was in 2019, that of brolucizumab, also known as Beovu (Novartis). Brolucizumab is the first single-chain antibody fragment that has been humanized and deemed safe as a therapeutic (Sharma *et al.,* 2020). It is VEGF-A inhibitor, binding to VEGF-A_{110}, VEGF-A_{121} and VEGF-A_{165} and has been approved for use as an anti-angiogenic for the treatment of

neovascular AMD (US Food and Drug Administration, 2019a). Brolucizumab was also compared to the other FDA approved synthetic VEGF-A antagonist, Aflibercept in the HAWK and HARRIER phase III clinical trials. These trials both showed that both of these drugs improved best-corrected visual acuity (BCVA) to almost the same degree, as well as safety. In addition, brolucizumab showed improved anatomic retinal fluid outcomes. Patients taking brolucizumab had, also, less disease activity in their eyes by week 16 when compared to aflibercept patients at the same dosage of 6 mg. These results were replicated in both the HAWK (24% vs 34.5%; P = 0.001) and HARRIER trials (22.7% vs. 32.2%; P = 0.002) (Dugel *et al.*, 2020).

Although it was a slight change, these results show the potential for future improvements in therapeutics targeting the VEGF-signaling pathways. Table 1.2 shows just a few examples of the continuing research into this area and the clinical trial stage at which they are currently.

Synthetic Protein Name and Type	Company	Target	Clinical Trial Phase	ClinicalTrials.gov Identifier
CT-322 - Adnectin	Adnexus	VEGFR2 – Inhibits binding of VEGF-C, D and potentially A	Phase I – Treating advanced solid tumours and non-Hodgkin's lymphoma Phase II – In combination with chemotherapy for treating metastatic colorectal cancer	NCT00374179 NCT00851045
PRS-050 – Anticalin	Angiocal	VEGF-A	Phase I – Treating patients with advanced solid tumours	NCT01141257
BIIBO21 – Small molecule inhibitor	Biogen	Hsp90	Phase I – In combination with exemestane in female patients with hormone receptor positive, advanced metastatic cancer	NCT01004081
MP0 112 - DARPin	Allergan	VEGF	Phase I/II - Safety study for patients with diabetic macular oedema Phase I/II – Safety study in patients with wet age-related macular degeneration	NCT01042678 NCT01086761
Abicipar Pegol - DARPin	Allergan	VEGF	Various phase I/II/III– Testing safety in patients with neovascular AMD and diabetic macular oedema	NCT02859766 NCT03539549 NCT03335852 NCT02462486 NCT02462928 NCT02181517 NCT02181504 NCT02186119

Table 1.2. Synthetic Antibody Mimetics in Clinical Trials. Clinical trial progress of several antibody mimetics with targets in the VEGF signalling pathways. Trial data is from www.clinicaltrials.gov

1.7.2 Synthetic proteins directed against VEGFRs

Lymphangiogenesis is a phenomenon where lymphatic vessels are generated from pre-existing vessels. This is mediated by VEGF-C and -D binding to VEGFR3. The lymphatic system regulates fluid and macromolecule movement from the tissues into the blood circulation as well as transporting lymphocytes as part of the immune response (Podgrabinska *et al.*, 2002). Angiogenesis is the process which is the most commonly targeted when it comes to cancer treatment. VEGFR3- associated lymphangiogenesis, however, is also an important precursor in tumour metastasis. Tumour cells may travel to the bloodstream either through a possible shunt between the lymphatic and vascular system or via the thoracic duct (Stacker *et al.*, 2002). This has been seen by the increased expression of VEGF-C and -D in tumour cells and tumour lymphangiogenesis and metastasis being suppressed by VEGFR3 inhibition, sometimes even more so than VEGFR2 inhibition (He *et al.*, 2002; Mattila *et al.*, 2002; Schoppmann *et al.*, 2002; Roberts *et al.*, 2006).

VEGF-A may also have a link to lymphangiogenesis as overexpression of VEGF-A has been found to generate “giant lymphatics,” in mouse ears which were functionally and structurally abnormal (Nagy *et al.*, 2002). This leads to the possibility that therapies which target VEGF-A signaling and therefore angiogenesis may also be able to target pathological lymphangiogenesis. As discussed previously, VEGF Trap is a synthetic antibody mimetic which selectively binds to VEGF-A and therefore not VEGF-C or -D.

A mouse model of inflammatory corneal neovascularization showed that VEGF Trap inhibited both hemangiogenesis and lymphangiogenesis. This was accompanied by a significant reduction in monocytes and macrophages which express VEGF-C and -D, backing up previous assumptions that their recruitment by VEGF-A through VEGFR1 is an essential step in lymphangiogenesis (Cursiefen *et al.*, 2004). It should also be noted that there are other theories about the exact role of VEGF-A in

lymphangiogenesis, such as increasing the expression of adhesion molecules involved in leukostasis or acting through VEGFR2 to promote lymphatic vessel formation and organization (Hong *et al.*, 2004; Liu *et al.*, 2017). Regardless of the reason, VEGF Trap could potentially prove as useful to cancer treatment as it does to ocular disorders.

Another synthetic protein has been produced which specifically targets VEGFR3, VEGFR31-Ig. VEGFR31-Ig is a combination of $VEGFR3_{12}$ (combining the first and second domains of VEGFR3) and VEGF Trap fused to the heavy chain constant region of human IgG1 and the light chain of the human κ constant region. This fusion protein bound to both VEGF-A and VEGF-C with similar affinities to that of VEGF Trap and a soluble VEGFR3-Ig fusion protein. It was capable of inhibiting both tumour growth and metastasis to both lungs and lymph nodes (Zhang *et al.*, 2010). Overall, reducing lymphangiogenesis through VEGFR inhibition may add another effective strategy to treating carcinomas, specifically tumour metastasis.

1.8.1 Synthetic proteins called Affimers

The established therapies previously described do have, overall, a good track record. Antibodies are well-established biological therapeutics with high affinities for their targets. They are, however, large bivalent structures with multiple chains and are dependent on disulphide bonds, thus making it harder for them to fold into the correct functional form within the cytoplasm. Antibodies also have low thermostability and their production in animals means they are difficult and expensive to manufacture. Oftentimes it is more economical for large production lines to favour *in vivo* methods, there are additional costs to be considered such as optimal subclone selection for antibody characteristics and their ability to grow in serum-deprived conditions. This is not even including worker associated costs such as for paying technicians and the maintenance of animal houses (National Research Council (US), 1999; Löfblom *et al.*, 2010; Wojcik *et al.*, 2010). There are other solutions which could retain the high specificity of antibodies while being more cost-effective and stable. Very promising therapeutics have been produced in the form of synthetic scaffold proteins called

antibody mimetics. Some of these engineered scaffolds are affibodies, monobodies, and designed ankyrin repeat proteins (DARPins) (Löfblom *et al.*, 2010; Wojcik *et al.*, 2010; Stahl *et al.*, 2013b) (Fig. 1.8). DARPins specific to VEGF-A have even been shown to have significantly reduced vascular leakage and angiogenesis in rabbit eyes when administered topically (Stahl *et al.*, 2013). These antibody mimetics are small with a high stability and can be easily expressed in bacterial strains (Löfblom *et al.*, 2010). They also have no cysteines, therefore showing low aggregation. Highly selective DARPins to their targets are also able to be acquired through the *in vitro* selection strategy known as ribosome display (Münch *et al.*, 2011). The advantage of this form of target acquisition is increased randomisation and thus diversification of the already large DARPin libraries (10^{12} clones) using PCR. In brief, a PCR fragment which encodes the DNA of a DARPin library is ligated into a vector with a ribosome binding site and a promoter. *In* vitro transcription of the DARPin DNA to mRNA is followed by ribosomal translation, which in turn creates complexes containing ribosomes, mRNA and its matching DARPin. The lack of a stop codon in the vector means that the DARPin remains attached to the tRNA of the ribosome, meaning that this complex can be screened against an immobilised target of interest. Specific DARPins to the target can then be eluted and reverse transcription can elucidate their genetic information for use in PCR. This creates a template for a new cycle starting with *in vitro* transcription in order to find highly selective DARPins for the protein of interest (Dreier B, 2012). Another method for scaffold production is phage display (Smith, 1985). A library of antibody mimetics can be created using the *E.coli* filamentous bacteriophage, M13, which has the unique ability of reproducing without killing its host cells (Rakonjac *et al.*, 2011). This allows introduction of a fusion protein consisting of the coding sequence for a protein of interest and either a major (pVIII) or minor (pIII) phage coat protein. In the case of pIII, which is the most commonly used in phage display, it is integrated into the membrane of the host cell and ultimately allows the now anchored M13 to release the desired single-stranded DNA (ssDNA) into the cytoplasm of said host (Bennett and Rakonjac, 2006). The

fusion gene is incorporated into a cloning vector called a phagemid for optimal infection. This phagemid is usually aided by a helper phage called M13K07, which has a defective origin of replication and allows the packing of the fusion protein into M13 (Chasteen *et al.*, 2006; Bazan *et al.,* 2012).

A novel scaffold protein which has shown to have some promise is the Affimer (Fig. 1.9A). These are highly thermostable synthetic protein scaffolds based on a consensus plant protease inhibitor called phyocystatin (Tiede *et al.*, 2014). The Adhiron coding region, a DsbA secretion signal peptide, an amber stop codon (TAG) and the C-terminal region of gene III of the M13 bacteriophage were cloned into the phagemid vector, pBSTG1. This results in a phagemid called pBSTG1-Adh, which can produce different results depending on the *E.coli* strain it is cloned into. In non-suppressor *E.coli* strains such as JM83, the amber stop codon effectively stops protein translation. However, if the pBSTG1 phagemid is cloned into a suppressor bacterial strain known as ER2738, translational read-through will be allowed past the in-frame amber stop codon, allowing the creation of an truncated Adhiron-(M13)pIII fusion protein (Tiede *et al.*, 2014).This is due to suppressor codons which can recognise and inhibit the amber stop codon, such as glnV (suppressor E). glnV in particular is a glutamine-specific tRNA mutation which can stop amber nonsense mutations and therefore translation termination, increasing the growth of M13 phagemid (Gold Bio, 2019). A phage display library has been constructed consisting of more than $3x10^{10}$ independent Affimer clones, and this phagemid library can be used to screen against biotinylated proteins to produce clonal proteins directed to an antigen of interest. This type of synthetic protein and screening technique offers many advantages. This has recently been demonstrated to be highly effective for the study of mammalian cell surface receptors and with efficacy on a mouse tumour model (Tiede *et al.*, 2017).

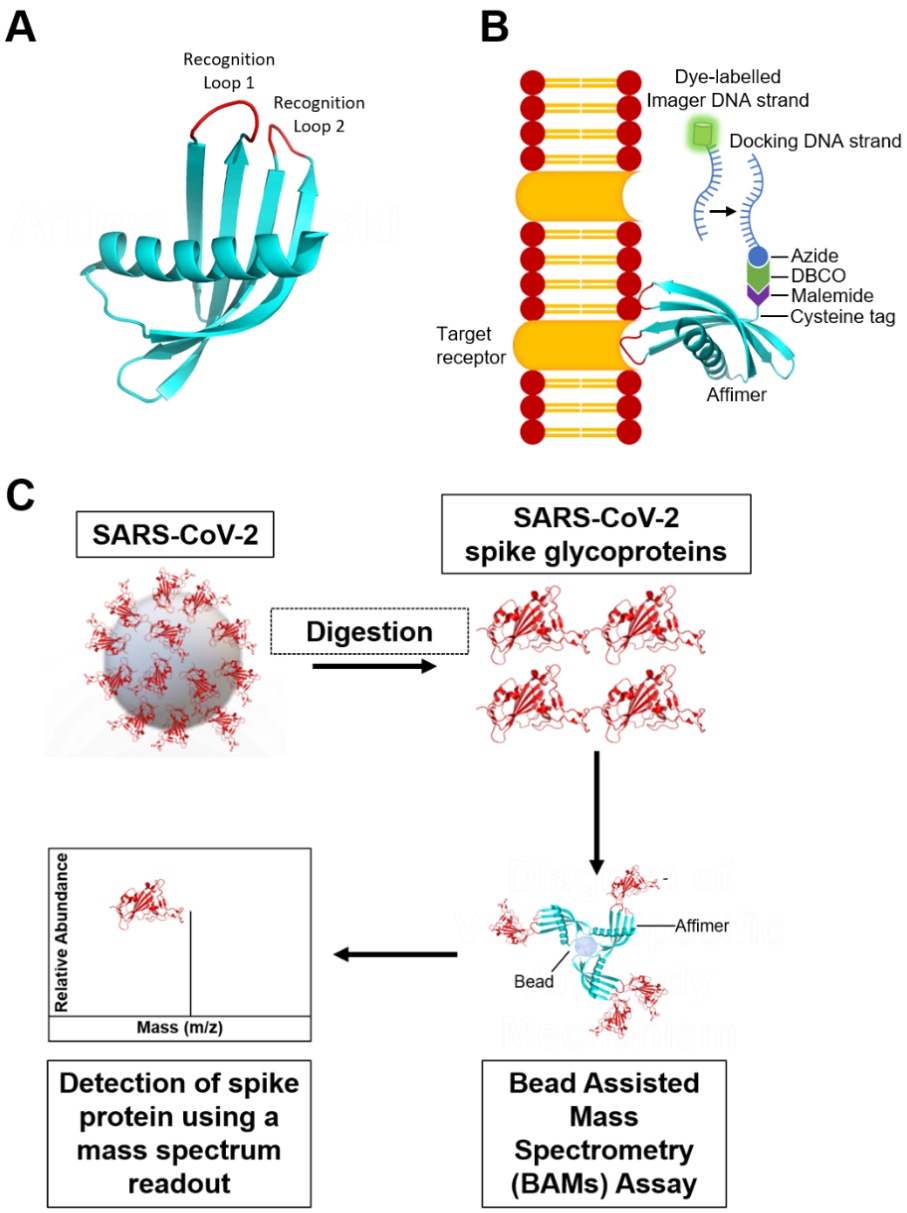

Figure 1.9. Affimer applications. **(A)** The Affimer scaffold contains two variable recognition loops which can recognize specific targets. **(B)** DNA-paint microscopy, where an Affimer can link a target protein to a conjugated DNA docking strand which is recognized by a fluorescently-tagged complementary DNA strand. **(C)** Ongoing research into new COVID-19 diagnosis methods using bead assisted mass spectrometry (BAMs). Samples are run over SARS-CoV-2-specific Affimers immobilized on beads. These beads are run through a mass spectrometer to identify the presence of SARS-CoV-2 glycoproteins for diagnosis. Image adapted from (Mahapatra and Chandra, 2020).

1.8.2 Affimers and COVID-19

COVID-19 is a Coronavirus infection in humans which has been difficult to both treat and diagnose. Rapid-testing is currently being implemented throughout the UK via Innova lateral flow devices despite concerns about their effectiveness. The Government also commissioned two laboratories, one at University of Oxford and the other at Public Health England's Porton Down to assess the specificity of these lateral flow devices towards SARS-CoV-2 via a 4-phase evaluation. These showed positive results overall with a specificity reported at 99.6% and a total false positive rate of 0.32% (95% CI:0.21-0.47%). It should be noted, however, that the accuracy of these tests would vary depending on the individuals using them. Laboratory scientists would report 79.2% positive tests (95% CI: 72.8-84.6%) vs trained healthcare-workers at 73% (95% CI: 64.3-80.5%). This number, however, would drop to 57.5% (95% CI: 52.3-62.6%) when tested by members of the public who were self-trained (Care *et al.*, 2020). The self-trained professionals were from Boots, the pharmacy company, and one could argue that they should be some of the most likely people to be used in testing the general public (Deeks and Raffle, 2020). Although everyone who took part in this study were highly trained professionals, this emphasises the point that rapid testing should be made simpler to use, especially since there are at-home COVID-19 tests for the general public. It is general knowledge that these particular tests require swabs from both the nose (nasopharynx) and back of the throat (pharynx), which once again could compromise test results due to causing discomfort to the person taking the test. There is anecdotal evidence that the general public do not often perform the tests correctly.

The potential for incorrectly carried out Covid -19 tests, strongly suggests it would be useful to consider new avenues for mass testing, such as the use of Affimers. The commercial company which has licensed the IP technology for Affimers, Avacta Group (www.avacta.com), announced its aim to produce its own lateral flow devices through a collaboration with Cytiva (previously known as GE Healthcare Sciences) and Adeptrix in May 2020 (Fig. 1.9C). The Avacta group reported Affimer reagents highly specific to

the SARS-COV2 viral antigen without cross-reactivity to SARS, MERS and other coronaviruses (Avacta, 2020). These Affimers can apparently work in pairs, allowing for binding to both intact virus particles and detached spike proteins (Fig. 1.9C). Spike proteins usually become detached in the pathology of COVID-19, meaning that Affimers could potentially allow disease progression monitoring as well as confirming an initial diagnosis. Cytiva would aid in producing antigen test strips based on saliva analysis, which could potentially eliminate the need for previous testing methods which were more painful (Avacta, 2020; *Business Wire*, 2020). Adeptrix's Bead-Assisted Mass Spectrometry (BAMS^{TM}) technology allows a higher sensitivity to samples taken as well as providing the opportunity for mass screenings in hospital laboratories which could potentially be greater than currently seen with PCR testing (Mahapatra and Chandra, 2020). A recent update from Avacta in November 2020 stated progress in producing the tests with help from the manufacturer, BBI Solutions. The Affimers have been reported to detect the coronavirus spike protein with a sensitivity exceeding 300 pg/ml in laboratory samples as compared to previous ELISA tests which detected these same proteins at 67.02 pg/ml (Avacta, 2020; Malik *et al.*, 2021). It was also stated that tests are still ongoing in both saliva and in anterior nasal swab samples, both of which are still more accessible and less painful than previous tests (Avacta,2020).

1.8.3 Recent research developments using Affimers

Affimers have enabled finding new forms of synthetic proteins e.g., foldamers. Foldamers work on the basic tendency of natural polymers to change the arrangements of their structures, such as α-helices and β-sheets, to compact conformations which are kinetically and thermodynamically stable. These arrangements also present active sites for a variety of chemical processes necessary for biological phenomena, such as catalysing reactions. In essence, foldamers are artificially-designed polymers which can form specific secondary, tertiary or quaternary structures in order to improve their biological function (Gellman, 1998; Arrata *et al.*, 2017). A *proteomimetic* aromatic oligoamide foldamer was previously designed to copy the structure of the α-helix in order to identify

inhibitors to protein-protein interactions (PPIs) controlled by the α-helix. The use of Affimers allowed the identification of peptide sequences which allowed specific binding to different foldamer sequences. The sequence of these Affimers also allowed for the potential identification of natural amino acids which would bind to these foldamers. Therefore, the use of Affimers could potentially enhance research into various disease targets for foldamers by identifying potential molecular recognition sequences (Arrata *et al.*, 2017).

Affimers also have potential non-medical uses, such as environmental protection. This can be seen in a study based upon methylene blue, which is a water-soluble dye often used to stain biological samples in research as well as materials like cotton and silk (Koutsoumpeli *et al.*, 2017). Methylene blue is therefore easily distributed in waste-water and can contaminate the environment as a result. A quartz crystal microbalance with dissipation monitoring (QCM-D) allowed the quantification of methylene blue-specific Affimer binding in a recreation of an aquatic environment. The Affimers were shown to have high specificity for their targets even within limnetic (lake water) samples which can contain many other contaminants to which to bind. This demonstrates the potential for future work on other small nonimmunogenic targets, as well as adding an environmental aspect to the many potential uses already found for Affimers (Koutsoumpeli *et al.*, 2017).

The structure and size of Affimers have also allowed them to be used in various imaging applications. Conventional antibodies can be directly labelled using one or more lysine residues for various applications, but this can be tricky due to unspecific ε-amino acid labelling which could accidentally prevent an antibody binding to its antigen. As stated previously, Affimers have two variable binding loops by which they bind to antigens. A cysteine amino acid residue can be added onto the C-terminus of the Affimer, after production via phage display, allowing site-specific labelling with dyes. The loops are far away from this added cysteine residue, reducing the chance of fluorescent-labelling of the Affimer to interfere with antigen binding. The small size of the Affimers also allows for the better

penetration of the cell, and therefore the ability to conduct intracellular imaging, something which is difficult for the larger antibodies to do. This means Affimers are useful for precise imaging techniques such as super-resolution microscopy (Carrington *et al.*, 2019).

Successful imaging of the cytoskeletal skeleton, tubulin and f-actin, have shown the potential of fluorescently-labelled Affimers in both fixed-cell and live microscopy (Lopata *et al.*, 2018; Tiede *et al.*, 2017). Further, the use of Affimers has recently been implemented in a relatively new imaging technique, DNA points accumulation for imaging in nanoscale topography (DNA-PAINT) microscopy DNA-PAINT involves the fluorescent labelling of short, 'imager' DNA strands to their complementary 'docking' strands, where the 'blinking' of the dye molecules allows visualisation through super-resolution microscopy (Schnitzbauer *et al.*, 2017) (Fig 1.9B). Using cysteine-malemide labelling, Affimers were conjugated to the docking strands in and allowed quantitative analysis in 3D of actin binding within the cell (Schlichthaerle *et al.*, 2018). These new techniques add an extra laboratory research aspect to the possible use of Affimers, as well as to their many uses for the possible influence on biological functions.

1.8.4 Affimer use in cancer and cardiovascular disease research

Carcinoembryonic antigen (CEA) is a blood-based biomarker for diagnosing colorectal cancer (CRC) as well as monitoring CRC disease progression. However, CEA is known to also be overexpressed in tumours in other epithelial-derived cancers such as lung, pancreatic and breast cancers. Its role in colorectal cancer has led to CEA becoming a target for phage display screening to produce specific Affimers. One study found that Affimer binders could not only bind to the soluble form of CEA, which is useful for monitoring the stages of colorectal cancer but could also detect both its glycosylated and deglycosylated forms, which did not affect binding to the protein epitopes. This allows a potential for Affimers to be used in a clinical setting for not only diagnosing colorectal cancer but also to be used in therapeutic applications (Shamsuddin *et al.*, 2021).

Affimers have also been found to bind to other proteins important in cancer, such as the BCL-2 family which regulates the apoptosis pathway. Interestingly, the selected Affimers could not only distinguish between different family members but could also select an ideal conformation of its target proteins to create certain outcomes. This could potentially allow future researchers to tailor conformations of their targets using Affimers in order to produce different functional effects (Miles *et al.*, 2021). Affimers have also been used in the first impedimetric biosensors to detect fibroblast growth factor receptor 3 (FGFR3). FGFR3 is frequently observed in bladder cancer, so this novel method could allow inexpensive (due to being label-free) and yet highly sensitive detection in the future (Thangsunan *et al.*, 2021).

The detection of soluble Receptor of Advanced Glycation End-products (sRAGE), a biomarker in chronic obstructive pulmonary disease (COPD) in human serum has also been possible by using Affimer reagents in liquid chromatography-mass spectrometry (LC-MS). The results were comparable to that of traditional antibody-based LC-MS assays as well as data showing the successful detection of sRAGE at clinical levels, 0.2-10 ng/ml (Klont *et al.*, 2018).

Although Affimers have been shown to be good binders for a wide variety of proteins, there are relatively few in literature which primarily focus on the cardiovascular system. The potential success for these can be seen in research focusing on blood loss and fibrogen-specific Affimers. The usage of these reagents enabled improvements in fibrin network stabilizing as well as prolonging clot lysis. One of the Affimers was also found to not influence clot permeability, thereby maintaining the physiology of the clots and further reducing the chances of lysis. This particular Affimer was brought forward to assess plasma which replicated common blood clotting disorders, such as haemophilia A, whereupon it also showed improved clot lysis times (Kearney *et al.*, 2019).

The data showing the prospective uses of Affimers in both cancer and cardiovascular disease shows that they could also have the capability to influence one of the major processes involved in all of these conditions, angiogenesis. This demonstrates a need for further experimental analyses of both VEGFR1-and VEGFR2-specific Affimers with respect to their effects on angiogenesis. The use of these reagents could possibly be used in the future as therapeutics for either promoting recovery in the cardiovascular system (via VEGFR1 inhibition) or impede the development of various carcinomas (via VEGFR2 inhibition).

1.9. Project aims and objectives

Although targeting VEGF-A and VEGFR2 are established therapeutic avenues, it is unclear as to the functional contribution by VEGFR1 to angiogenesis and how this could be harnessed for therapeutic advantage. One possibility is that blocking VEGFR1 function could stimulate angiogenesis, and this could be of benefit for heart attacks and strokes where we need to stimulate angiogenesis to repair damaged blood vessels. There is also a benefit to testing VEGFR2-specific Affimers in order to assess their potential effects for the treatment of cancer through their anti-angiogenic effects. The scientific hypothesis for this research is that targeting VEGFR1 and/or VEGFR2 using Affimers will affect endothelial and epithelial cancer cell function *in vitro* (Fig. 1.10). To answer these questions, the objectives were 4-fold:

- Identify Affimers that bind VEGFR1 or VEGFR2
- Characterise VEGFR1-specific Affimers for effects on VEGF-A-stimulated signalling and endothelial cell responses
- Characterise VEGFR1-specific Affimers for effects on VEGF-A-stimulated signalling and endothelial cell responses
- Characterise VEGFR1- and VEGFR2-specific Affimers for effects on cancer epithelial cell responses

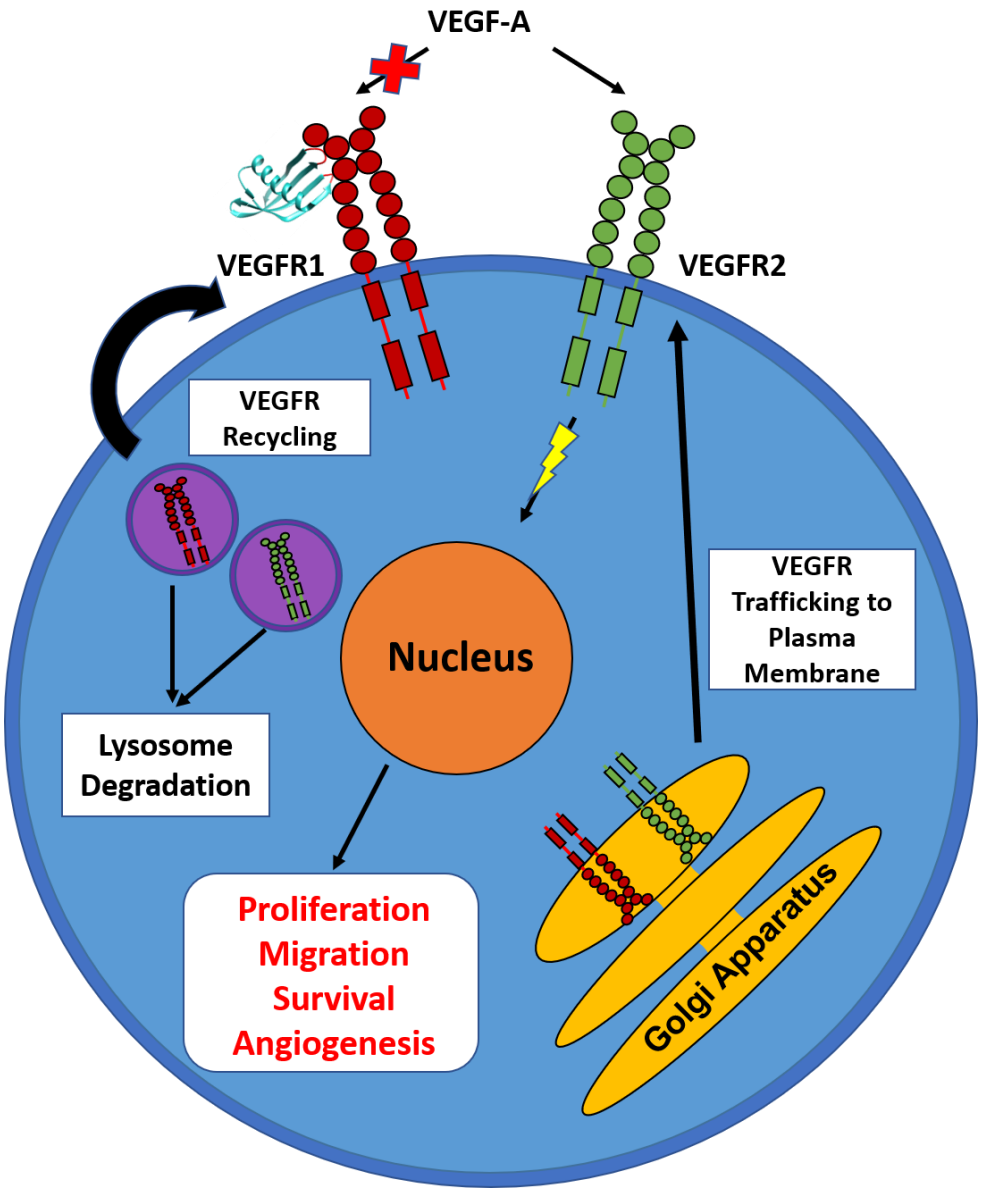

Figure 1.10. Schematic of VEGFR1-Affimer effects in endothelial cells. VEGFR1-specific Affimers could bind to the ligand binding domains (2 and 3) of the VEGFR1 receptor or preventing heterodimerization with VEGFR2. This would enable increased activation of VEGFR2 by VEGF-A binding and trigger multiple signalling pathways including p38 MAPK, eNOS, AKT and PLCγ1. This would increase gene transcription and the activation of endothelial cell proliferation, migration, survival and angiogenesis. Increased VEGF-A binding may also cause additional VEGFR2 trafficking from the Golgi membrane or recycling from endosomes to the plasma membrane.

Chapter 2

Materials and Methods

2.1 Materials

2.1.1 Chemicals

Chemicals were purchased from Melford Laboratories, Sigma-Aldrich, Thermofisher and VWR unless stated otherwise. Molecular biology chemicals and enzymes were purchased from Fermentas, New England Biolabs, Promega, and Stratagene. Tissue culture medium and supplements were purchased from Invitrogen Technologies /ThermoFisher and Promocell unless stated otherwise.

2.1.2 Buffers

All Buffers were made with distilled or double distilled/autoclaved water (ddH_2O) unless stated otherwise.

2.1.3 Primers

All primers were purchased from Integrated DNA Technologies and only underwent standard desalting measures.

2.2.1 Cell lines

Human umbilical vein endothelial cells (HUVECs) were isolated from human umbilical cords. These umbilical cords were obtained with the informed consent of patients undergoing Caesarean surgery at Leeds General Infirmary. Ethical approval (reference CA03/020) was obtained from the Leeds NHS Hospitals Local Ethics Committee (UK). Normal Human Dermal Fibroblasts (NHDF) were purchased from Promocell (Heidelberg, Germany). A human epithelial cancer cell line, A431, was stably transfected with the FUCCI system by Dr. Sreenivasan Ponnambalam.

2.2.2 Primary HUVEC isolation

The umbilical cord was cut at both ends with a sterile razor to fully expose the two arteries and single vein for effective HUVEC isolation. A blunt-ended needle attached to a 20ml syringe was inserted into the umbilical vein (the largest of the three openings) followed by repeated flushes with pre-warmed PBS containing penicillin (100 units/ml), streptomycin (100 units/ml) and amphotericin B (50 µg/ml) to remove any blood clots. To detach the HUVECs from the endothelium, the umbilical cord was clamped at one end and ~20 ml MCDB131 media (Life Technologies, Paisley, UK) containing 0.1% (w/v) type IIS collagenase was added. The clamped cord was incubated for 20 min at 37^{O}C, 5% CO_2, to allow HUVEC detachment. Cells were flushed out with PBS and centrifuged at 4000 rpm for 5 min to pellet the cells. HUVECs were seeded into T75 flasks (Nunc, Copenhagen, Denmark) containing 0.1% (w/v) pig skin gelatin (PSG) and endothelial cell growth medium (ECGM) (Promocell). These HUVECs would then be washed with PBS 4 times after 24 h so as to remove any residual red blood cells. HUVECs were cultured until passage 5 (Fig. 2.1).

2.2.3 Cell culture

All cell lines were usually cultured in T75 flasks and incubated at 37^{O}C, 5% CO_2.

HUVECs, as stated above were seeded into flasks pre-coated with 0.1% (w/v) PSG and grown in ECGM. NHDF (Fig 2.2) and A431-FUCCI (Fig 2.3) cells were both cultured in DMEM (Gibco Life Technologies) containing 10% (v/v) FBS, 1% (v/v) non-essential amino acids, 1% (v/v) sodium pyruvate. All of the cell lines used in the project were passaged using TrypLE^{TM} Express (Invitrogen, Amsterdam, Netherlands) and the same method. All of the reagents used were pre-warmed prior to trypsinization. The growth medium was aspirated from the flasks when the cells were at ~70-80% confluency, followed by three washes with PBS and incubation with 1 ml of TrypLE Express at 37C for 4 min. The trypsinization was then stopped by the addition of ~5 ml of the medium required depending on the cell lines. Centrifugation of the cells at 4000 rpm for 5 min created a cell pellet which could be resuspended in 3 ml of medium. This suspension would be split

1:3 in T75 flasks containing ~7-9 ml medium and this medium would be replaced every 2-3 days. The primary cell lines would be cultured up to passage 5 and 12 for HUVECs and NHDFs respectively.

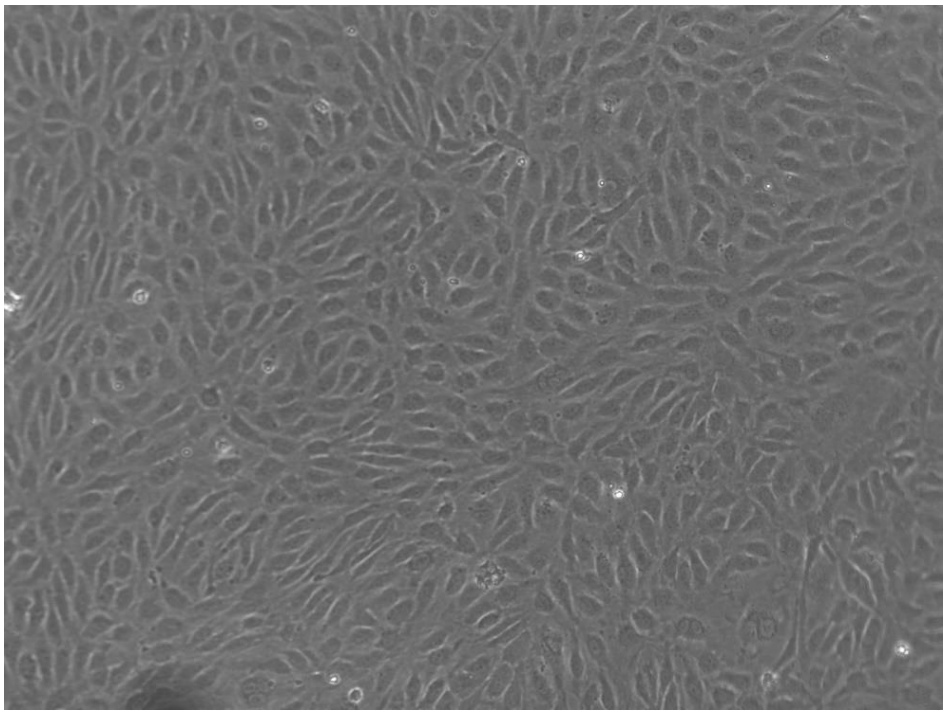

Figure 2.1. Human umbilical vein endothelial cells (HUVECs). HUVECs were grown to confluence (~70-80%) and display a characteristic 'cobblestone' morphology. Image of passage 0 (P0) HUVECs taken at 10x magnification after ~1 week of growth. Image was taken on an EVOS Auto fluorescence microscope.

2.3 Rapid transformation of bacteria

This technique was often used to transform Affimer plasmid DNA into XL10 *E.coli* for increasing stocks prior to protein expression. 10-1000 ng in 1-10 µl volume of plasmid DNA was added to 50 µl of XL10 competent cells and incubated on ice for 5 min. The cells were heat-shocked in a 42^0C water bath for 2 min followed by incubation at room temperature for 5 min. Cells were plated out onto LB Ampicillin plates and incubated at 37^OC, 5% CO_2.

2.4 High efficiency transformation of bacteria

Transformation of Affimer plasmid DNA into either ER2738 or BL21*DE3 *E.coli* was also carried out as previously described (Tiede *et al.,* 2017). 5-10 ng of plasmid DNA was pre-chilled before incubation on ice with 10 µl BL21*DE3 cells for 30 min. Cells were heat-shocked in a 42^OC water bath

for 45 sec before incubation on ice for 2 min. 450 µl SOC medium was added and incubated at 37^{O}C for 1 h in a shaker at 150-180 rpm. 100 µl of the transformation mixture was plated onto LB Ampicillin (100 µg/ml) plates and incubated overnight at 37^{O}C, 5% CO_2.

2.5 ELISAs to test cross-reactivity of Affimers

The BioScreening Technology Group (BSTG) at the University of Leeds, UK, used phage display to screen for human VEGFR1-specific Affimers (Fig. 2.2). Screening was against soluble VEGFR1 purchased from Sino Biological (Beijing, China). The potential use of Affimers in the future for *in vivo* applications led to a cross-reactivity study of these Affimers against the rat version of the VEGFR1 protein, once again purchased from SinoBiological. Phagemid vectors containing the Affimer clones were transformed into ER2738 cells and grown on LB Ampicillin plates as previously described in the high efficiency transformation protocol (incubated at 37^{O}C, 5% CO_2). Colonies were picked and grown in 100 µl of 2TY containing 100 µg/ml of Ampicillin in a 96-deep well plate overnight at 37^{O}C, 1050 rpm in an incubating microplate shaker. 25 µl of this culture was added to fresh 200 µl 2TY containing 100 µg/ml of Ampicillin and grown at 37^{O}C, 900 rpm for 1 h prior to the addition of M13KO7 helper phage (1/1000) and 25 mg/ml kanamycin stock (1/20) before incubation at 25^{O}C, 450 rpm overnight. 2x casein blocking buffer (Sigma) was also added to Streptavidin-coated plates and incubated overnight at 37^{O}C, 5% CO_2. Biotinylated human and rat VEGFR proteins were added to the blocked Streptavidin plates and incubated for 1 h prior to the addition of 40 µl Affimer phage-containing supernatant. Plates were washed prior to the addition of 1/1000 dilution of HP-conjugated anti-phage antibody for 1 h and visualisation with 3,3’5,5’-tetramethylbenzidine (TMB) (Seramun). Measurements of absorbance were taken at 620 nm on a 96-multiwell plate reader.

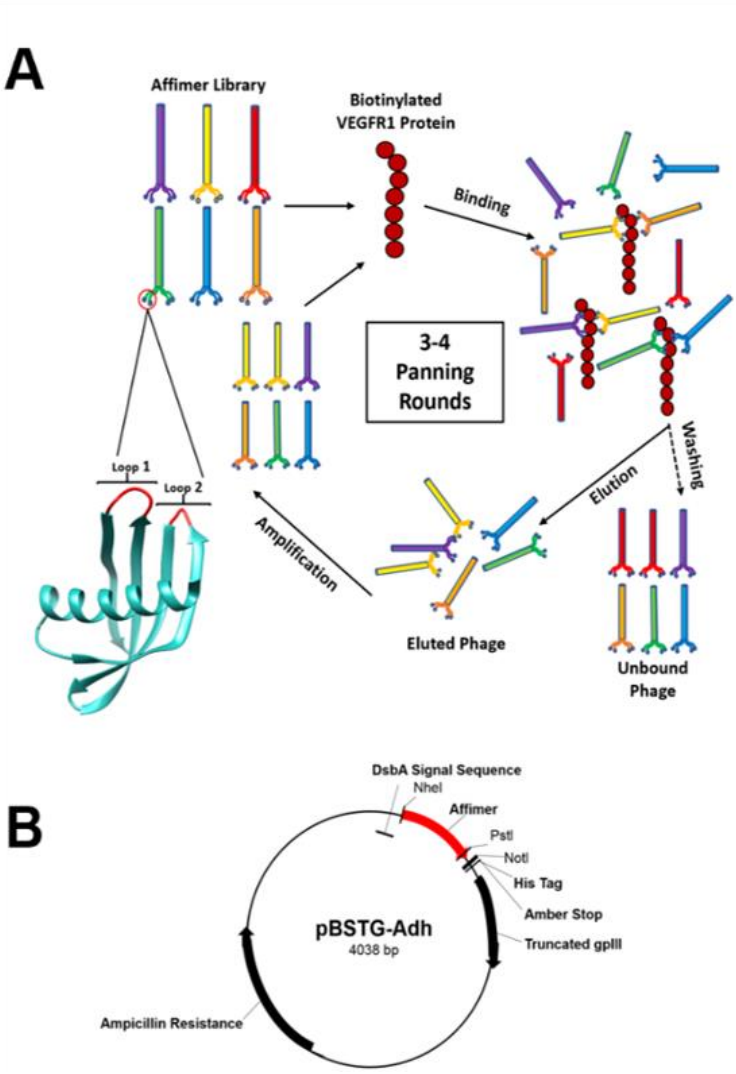

Figure 2.2. Phage display for isolating VEGFR1-specific Affimers. (A) shows a cartoon representation of how VEGFR1- and VEGFR2-specific Affimers were generated by the BSTG using phage display to find specific binders before elution and amplification. Each Affimer is a scaffold with two loops each containing nine randomized amino acids; these allow for specific binding to the target of choice. Biotinylated VEGFR proteins bound to streptavidin-coated wells were incubated with phage (pBSTG-Adh) containing the Affimer library (10^{10} clones). The wells were washed several times to remove any Affimers which did not bind to the VEGFR proteins. The phage containing the successfully bound Affimers was eluted using glycine and triethylamine. *E.*coli (ER2738) cells were infected with the eluted phage prior to the addition of M13K07 helper phage and kanamycin for amplification of successful binders. This process was repeated in 3-4 panning rounds to produce highly specific binders for these VEGFR proteins. **(B)** shows the pBSTG-Adh vector containing the Affimer coding region.

2.6 Subcloning Affimers

The VEGFR-specific Affimers were previously conjugated to a cysteine tag to allow ease of use in multiple experiments including the addition of biotin or a fluorescent tag. These are titled pET11c in subsequent methods and experimental results, whilst non-conjugated Affimers are named pET11a for ease of use. The non-conjugated forms of the Affimers, however, were also tested in order to identify whether beneficial effects found in experiments were due to the cysteine tag alone, rather than to the Affimer itself. To test this, a couple of the Affimers had their cysteine tag removed *via* the subcloning method as per the BSTG protocol.

2.6.1 Digestion of the Affimer pET11a vector

The following protocol for digestion of the pET11a plasmid vector was carried out using materials from NEB unless stated otherwise. 20 µg of Affimer in the pET11 vector was added to a mixture of 20 µl of both the NheI-HF and NotI-HF restriction enzymes (20,000 units/ml), Cutsmart Buffer, and sterile deionised water in a microcentrifuge tube. These were mixed and incubated overnight at 37^{O}C, 5% CO_2. This mixture was divided into several aliquots and incubated with 1 µl of Antartic Phosphatase (5000 units/ml) and Antartic Phosphatase Reaction Buffer for 15 min at 37^{O}C. The Antartic Phosphatase was heat inactivated at 65^{O}C for 5 min. 10x Orange G Loading Dye was added to each tube to allow easy visualisation of the digested vector after being run on a 0.7% agarose gel. The digested vector was extracted from the gel using a NucleoSpin Gel and PCR Clean-up kit (Macherey-Nagel, Düren, Germany) before the concentration was measured on a Nanodrop spectrophotometer (using the calculated extinction coefficient for an Affimer) and storage at -20^{O}C.

2.6.2 Amplification of the Affimer DNA sequence using PCR

PCR amplification of the required Affimer sequences without the cysteine tag on the C terminal was required. The following primers were used at 10 µM:

Forward Primer:

5' - ATG GCT AGC AAC TCC CTG GAA ATC GAA G - 3'

Reverse primer:

5' – TAC CCT AGT GGT GAT GAT GGT GAT GC – 3'

This reverse primer was used in order to amplify the core Affimer DNA sequence without the cysteine tag. A master mix was set up containing 0.8 µM of the forward and reverse primers, Phusion HF Buffer, 200 µM dNTP Mix, 3% DMSO, 0.02 units/µl Phusion DNA Polymerase and sterile water. 24 µl of the master mix was added to 1 µl of pET11c plasmids (template DNA) in 0.2 ml PCR strips and transferred to a PCR machine. Thermocycling conditions were as follows: 1 cycle for initial denaturation at 98^{O}C, 30 sec; 30 cycles of denaturation at 98^{O}C for 20 sec, annealing at 54^{O}C for 20 sec, and extension at 72^{O}C for 20 sec; 1 cycle for the final extension at 72^{O}C for 10 min and holding at 4^{O}C. DpnI (NEB) was added to each reaction and incubated at 37^{O}C for 1 h to remove *dam* methylated template DNA. The amplified DNA was purified using the NucleoSpin Gel and PCR Clean-up kit (Macherey-Nagel) and eluted in sterile water.

2.6.3 Digestion of the amplified Affimer sequences and ligation into the pET11a vector

Nhel-HF and Notl-HF enzymes were added to the PCR product along with Cutsmart buffer and sterile water in order to do a restriction digest of the sequence. These were mixed and incubated overnight at 37^{O}C, 5% CO_2 before the digested insert DNA were purified using the NucleoSpin Gel and PCR Clean-up kit (Macherey-Nagel) and the concentrations measured on a Nanodrop spectrophotometer. Ligation of the Affimer sequence into the previously digested pET11a vector DNA was carried out in the following manner: 25 ng of the Nhel-Notl digested insert DNA was added to 75 ng pET11a vector, T4 DNA Ligase, T4 DNA Ligase buffer and sterile water. These were mixed and incubated at room temperature overnight alongside a vector only ligation to act as a negative control.

2.6.4 Transformation of Ligated Affimer DNA into *E.coli* and Purification

1 µl of the ligated Affimer plasmid DNA mix was pre-chilled on ice before the addition of thawed XL10 *E.coli* cells and incubation on ice for 30 min. The cells were heat-shocked at 42^{O}C for 45 sec to allow insertion of the DNA into the cells followed by another ice incubation for 2 min. 190 µl SOC medium was then added and incubated at 37^{O}C for 1 h at ~150-180 rpm. This transformation mixture was plated onto LB Ampicillin plates and incubated overnight at 37^{O}C, 5% CO_2. This procedure was also carried out for the vector only ligation negative control. Single colonies were picked into LB Ampicillin for incubation overnight at 37^{O}C, 150 rpm. The Affimer plasmid DNA was extracted and purified using a QIAprep Spin Miniprep kit (Qiagen) before an aliquot was sent away for sequencing using a T7 primer: 5’ -TAA TAC GAC TCA CTA TAG GG- 3’.

2.7 DNA purification and agarose gel analysis

Affimer DNA was frequently extracted and purified throughout the studies in order to maintain a stock for future experimental procedures. Instructions were carried out as stated in mini, midi, and maxiprep kits from Qiagen depending on the amount of DNA needed to be prepared. The success of these purifications was determined both by the concentration of DNA measured on a Nanodrop spectrophotometer and *via* agarose gel electrophoresis. 2.4 g of agarose was added to 300 ml 0.5x TBE buffer and microwaved for 5 min. 10 µl ethidium bromide stock solution (10 mg/ml) per 100 ml of agarose gel solution was added once the solution was cooled to ~50^{O}C to allow visualisation of electrophoresed DNA. The solution was poured into a gel and a comb was placed at one end before being allowed to set. The comb was taken out once the gel had set, creating wells for the DNA to be loaded in. The set gel was placed in an electrophoresis tray containing ~700 mls of 0.5x TBE buffer. 1 kB DNA ladder was loaded at both ends of the gel at 4 µl and 2 µl respectively to allow easier identification of the lanes. 10 µl of DNA was added to 2 µl 6x DNA loading dye and loaded into each remaining well. The gel was allowed to run at 100 V for ~1.5 h or until the ladder had travelled ¾ the distance of the gel. Imaging was carried out on the Syngene G-Box (Frederick).

2.8 Affimer production

Phage display was used to screen for VEGFR1 and VEGFR2 Affimers with thanks to the BSTG. Screening was against soluble VEGFR1 and VEGFR2 proteins purchased from Sino Biological. Expression was carried out as previously described (Tiede et al., 2017). Affimer clones in pET11 vectors either missing or containing a cysteine tag were transformed into BL21*DE3 *E.coli* cells followed by inoculation of a single colony into ~5 ml of 2TY/100 µg ampicillin for an overnight culture. 1 ml of this overnight culture was added to 50 ml LB-ampicillin media and grown for ~2 h at 37^{O}C, 230 rpm to an OD_{600} of ~0.6. IPTG was added at a final concentration of 0.1 mM for a 6 h/overnight induction at 25^{o}C, 150 rpm. The cells were pelleted and lysed in 1 ml of lysis buffer (50 mM NaH_2PO_4, 300 mM NaCl, 20 mM Imidazole, 10% (v/v) glycerol, pH 7.4). Lysates were incubated with 300 µl Ni^{2+}-NTA

affinity resin (ThermoFisher) for ~2 h, followed by several washes (50 mM NaH_2PO_4, 500 mM NaCl, 20 mM Imidazole, pH 7.4) through centrifugation. The proteins were eluted (50 mM NaH_2PO_4, 500 mM NaCl, 300 mM Imidazole, 20% (v/v) glycerol, pH 7.4) and dialysed in PBS containing 10% glycerol. Purification was checked using a 15% SDS-PAGE gel stained with Coomassie blue dye.

2.9 BCA protein assay

BCA protein assays were frequently carried out during the project to analyse the concentration of protein in lysed cells, or of Affimers in comparison to BSA (Thermofisher) standards. The BSA standards were made at the following concentrations from a 1 mg/ml stock and sterile water: 0.2 mg/ml, 0.4 mg/ml, 0.6 mg/ml, 0.8 mg/ml and 0 mg/ml (sterile water only). These standards were kept at $4^{O}C$. 10 µl of each standard were loaded in duplicate along the top row of a 96 well plate. Standards were loaded starting from 0.2 mg/ml up to 1 mg/ml followed by the 0 mg/ml negative control. 5 µl of each protein to be tested were added to the remaining wells in duplicate. A BCA assay reagent was made using a 50:1 ratio of BCA reagent A:BCA reagent B so that 200 µl of reagent could be added to each well containing either protein standard (BSA) or test sample (in duplicate). The plate was incubated at $37^{O}C$ for 20 min before a reading was taken at 562 nm on a spectrophotometer (Varioskan).

2.10 Biotinylation and labelling Affimers with fluorescent tags

It was stated previously that the Affimers could have a cysteine tag conjugated to their C-terminal. This allows the addition of biotin and fluorescent tags for several experiments.150 µl TCEP resin was washed 3 times with PBS containing 1 mM EDTA and resuspended in PBS containing 4 µl 50 mM EDTA. The washed TCEP resin was incubated with 0.5 mg/ml Affimer in PBS for 1 h at room temperature. The mixture was centrifuged in a tabletop centrifuge at 1000 rpm for 1 min to pellet the TCEP resin. 130 µl of supernatant was mixed with 6 µl of 2 mM biotin-maleimide (Sigma) and incubated at $4^{O}C$ for 2 h on a rotator. Unbound biotin was removed by using Zeba Spin Desalting Columns (7K MWCO, Thermofisher) as per

manufacturer's instructions. The protocol for adding a fluorescent tag was the same apart from the use of AlexaFluor Maleimide 488 or 594 (green and red dye respectively) in place of the Biotin. The volume and concentrations were kept the same.

2.11 Endothelial cell proliferation assay

To measure the effects of Affimers on endothelial cell proliferation, a colourimetric ELISA assay was used. Here, the incorporation of BrdU in the DNA of actively proliferating cells can be quantified using a spectrophotometer after incubation with an anti-BrdU antibody. The following protocol used the cell proliferation assay kit (Roche Diagnostics, Burgess Hill, UK). HUVECS were seeded at 2 $x10^3$ cells per well in 0.1% (w/v) PSG coated 96-well plates in ECGM and incubated overnight at 37^OC, 5% CO_2. Cells were serum starved in MCDB131 containing 0.2% BSA (w/v) for 2 h at 37^OC, 5% CO_2 prior to the addition of various concentrations of Affimer reagents (0.1-100 µg/ml). After a 30 min incubation at 37^OC, 5% CO_2, the cells were stimulated with 25 ng/ml VEGF-A for 24 h. 10 µM BRDU reagent was added to each well at the 20 h mark followed by further incubation for 4 h at 37^OC, 5% CO_2. The medium was aspirated and fixed for 30 min followed by incubation with anti-BRDU-peroxidase antibody for 90 min. The wells were washed 3 times with washing buffer followed by incubation with TMB substrate solution for 30 min. The degree of a colour change to yellow was noted alongside readings taken at 5, 10, 20, and 30 min on a spectrophotometer 450 nm. 1M H_2SO_4 was added at 30 min for a final reading. Readings were recorded for every time-point but final assessments on proliferation were made based on the results after the addition of H_2SO_4.

2.12 Endothelial cell homeostasis assay

The concept of the cell homeostasis assay is similar to that of the previously used BrdU-mediated proliferation assay. However, the colourimetric ELISA technique is used to measure the degree of 3-(4,5-dimethylthiazol-2-yl)-2,5-diphenyltetrazolium bromide (MTT) reduction to insoluble formazan by the mitochondria of viable cells (since they lose this ability during cell death). Quantification can be carried out on a spectrophotometer as the amount of

formazan present is proportional to healthy cells (Clifford and Downes, 1996). A 5 mg/ml stock solution of MTT tetrazolium salt was made and wrapped in foil to protect it from the light. HUVECs were seeded at 2 $x10^3$ cells per well in 0.1% (w/v) PSG coated 96-well plates in ECGM and incubated overnight at 37^OC, 5% CO_2. Cells were serum starved in MCDB131 containing 0.2% BSA (w/v) for 2 h prior to the addition of various concentrations of Affimer reagents (0.1-100 µg/ml). The medium was aspirated and replaced with 50 µl 1 mg/ml MTT (diluted in ECGM) and incubated in the dark for 3 h. The MTT solution was aspirated and the purple formazan dye was dissolved in propan-1-ol. Formazan accumulates within cells since it is insoluble, so the addition of propan-1-ol solubilizes this reagent and thus allow it to pass through cell membranes to be measured (Clifford and Downes, 1996). The plates were read at 570 nm on a spectrophotometer.

2.13 Endothelial cell migration assay

A chemotactic gradient was created by adding 400 µl MCDB131 medium (Gibco Life Technologies) containing 25 ng/ml VEGF-A and/or various concentrations of Affimer reagents to 24 well plates (0.1-100 µg/ml). Transwell inserts (8 µm pore size, BD Biosciences, Oxford, UK) coated with 0.1% (w/v) PSG were placed into each of the wells, making sure that there was no air trapped between the insert and medium. HUVECs were seeded in MCDB131 containing 0.2% BSA (w/v) at 3 x 10^4 cells per well followed by the addition of Affimer reagents for 30 min. The cells were allowed to migrate towards the medium containing 25 ng/ml VEGF-A for 18-24 h at 37^OC, 5% CO_2. The medium was aspirated and each transwell insert was placed into fresh wells containing 400 µl 3-4% (w/v) paraformaldehyde (PFA) to allow fixation for 5 min at room temperature. The inserts were washed 3 times in PBS and transferred to wells containing 400 µl 0.2% (w/v) crystal violet in 20% (v/v) methanol at room temperature for 10 min. Transwell inserts were washed in PBS and cells were removed from the upper side of the filter using a cotton bud. Cells were imaged on the EVOS FL Auto microscope (ThermoFisher) at 10x magnification.

2.14 Endothelial cell tubulogenesis assay

NHDFs were obtained (Promocell) and cultured (Fig. 2.3) for use in the tubulogenesis assay to create a co-culture with HUVECs. HUVECs were suspended at $1x10^4$ cells in DMEM: ECGM (1:1) and added to confluent NHDF cells at a density of 5000 cells per well of a 48 well plate. HUVECs were cultured on top of the NHDF cells overnight at 37^OC, 5% CO_2. The medium was aspirated and Affimer reagents (0.1-10 µg/ml) were added 30 min at 37^OC, 5% CO_2 prior to 25 ng/ml VEGF-A stimulation in a total of 500 µl DMEM: ECGM. Cells were cultured at 37^OC, 5% CO_2 over the course of seven days with the medium being replaced with the experimental conditions every 48 h. After 7 days, the medium was aspirated and cells were fixed for 20 min at room temperature with 200 µl 3-4% PFA (w/v). This was followed by washes with PBS and the addition of 500 µl 1% (w/v) BSA in PBS, to block non-specific antibody binding, for 60 min at room temperature. The solution was aspirated and the cells were incubated with 100 µl of mouse anti-PECAM1 antibody (0.4 µg/ml) in 1% (w/v) BSA in PBS overnight at 4^0C. Following this, the cells were washed 3 times with PBS and incubated with 100 µl anti-mouse secondary antibody conjugated to AlexaFluor 488 (1 in 100) and DAPI (1 in 1000) for 2 h. This was followed by 2 washes with PBS and 1 wash with distilled H_2O. Images were taken on the EVOS FL Auto microscope at 20x magnification. The number of tubule branches and their lengths were quantified using AngioQuant. (www.cs.tut.fi/sgn/csb/angioquant).

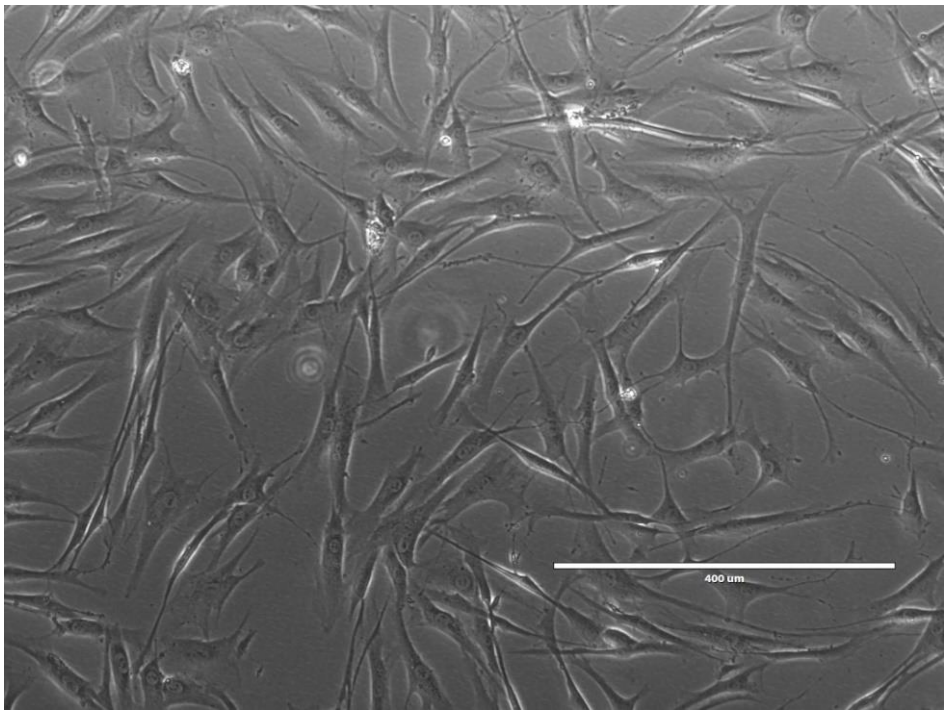

Figure 2.3. Normal human dermal fibroblasts (NHDFs). Cultured NHDFs shown using a transmitted light microscope. The image was taken at 10x magnification on an EVOS Auto fluorescence microscope after 3 days of growth. Bar, 400 mm.

2.15 Analysing HUVEC lysates

2.15.1 Cell lysis

Whole cell lysates of HUVECs were used for studies involving techniques like immunoblotting. To prepare these samples, the medium covering the HUVECs followed by two washes with ice-cold PBS. HUVECs were lysed in PBS containing 2% (w/v) SDS and 1 mM PMSF and isolated from the flask using a sterile cell scraper. The lysates were then homogenised using a sonicator 3-5 times for ~5 sec with 5 sec breaks on ice in between. These sonication times could be altered depending on the size of the sample. Lysate concentration was measured using a BCA assay (see above) and divided into 25 µg aliquots for storage at -20 or -80^{0}C.

2.15.2 SDS-PAGE

25 µg of each cell lysate was subjected to sodium dodecyl-sulfate polyacrylamide gel electrophoresis (SDS-PAGE) under reducing conditions. A 10-12% (w/v) SDS-resolving gel with a 5% (w/v) SDS-polyacrylamide stacking gel was prepared in advance. A sample was prepared with 2X SDS sample buffer (1 M Tris-HCl pH 6.8, 20% (v/v) glycerol, 4% (w/v) SDS, 0.1% (w/v) bromophenol blue and 4% (v/v) mercaptoethanol) at a 1:1 with the lysate. The lysate/buffer solutions were incubated at 95^0C for 5 min and kept on ice prior to loading onto the SDS-PAGE gel. These samples were run at 130 V for ~90 min in SDS-running buffer (192 mM glycine, 25 mM Tris, 0.1% (w/v) SDS).

2.15.3 Western blotting

SDS-PAGE gels containing the proteins were placed onto 0.2 µm nitrocellulose membranes (GE Healthcare Life Sciences). The membranes would then be placed into cassettes fitting into a tank containing transfer buffer (106 mM glycine, 25 mM Tris, 0.1% (w/v) SDS, 20% (v/v) methanol). A second electrophoresis procedure at either 300 mA for 3 h or 30 mA overnight (both at 4^0C) would then allow transfer of the separated proteins onto the membranes. The membranes were blocked with 5% (w/v) non-fat milk in 20 mM Tris-HCl pH 7.6, 137 mM NaCl, 0.1% (v/v) Tween-20) (TBS-T) for 1 h – overnight on a rocker at 4^0C. Rinses with TBS-T was followed by incubation of the membranes with goat anti-VEGFR1/VEGFR2 primary antibodies (R&D Systems) overnight at 4^0C for immunoblotting. This was followed by three washes with TBS-T for 10 min at a time prior to incubation with secondary anti-goat IgG HRP conjugates for 1 h at room temperature (Jackson Laboratories). A second round of 3x 10 min TBS-T washes was followed by the addition of EZ-ECL reagent (GE Healthcare Life Sciences). This would allow imaging using a G-Box digital imaging system for transmitted light and chemiluminsescence capture and quantification of images using densitometry (Syngene, Cambridge, UK).

2.15.4 Cell stimulation studies

Cell stimulation studies on endothelial and epithelial cell lines were carried out in order to study several signalling pathways. Cells were plated out in 6 or 12 well plates in ECGM until confluency of ~70% confluency was reached. The medium would be removed and the HUVECs would be starved in MCDB131 (+0.2% (w/v) BSA) for 2 h prior a 30 min, incubation with Affimers (0-100 µg/ml) at 37^{O}C, 5% CO_2. Stimulation with 10 or 25 ng/ml VEGF-A or PlGF-1 at various time points (0-60 min). This would be followed by cell lysis and immunoblotting as described above.

2.16 Immunofluorescence studies with antibodies and Affimers

2.16.1 General immunofluorescence analysis

Various immunofluorescence studies were carried out to either analyse the effects of Affimers on VEGFR1 and VEGFR2 expression on cells, or to test the efficacy of fluorescently-tagged Affimers. HUVECs were cultured as previously described on PSG-coated glass coverslips in 24 well plates. ECGM medium was aspirated followed by fixation with 3-4% (w/v) Paraformaldehyde (PFA) for 20 min at 37^{O}C, 5% CO_2. The cells were washed 3 times with PBS, this procedure being henceforth repeated between each step, unless otherwise stated. 50 mM ammonium chloride was added for 10 min at room temperature to quench the fixation solution. 0.2% (w/v) Triton-100 was added for 4 min at room temperature to permeate the cells. The cells were blocked (5 mg/ml BSA, 0.02% (w/v) sodium azide in PBS) for 1 h at room temperature, prior to incubation overnight at 4^{O}C with the primary antibody to the target receptor (in concentrations ranging from 1:100-1000) diluted in blocking buffer. 3 washes with washing buffer (1 mg/ml BSA, 0.02% (w/v) sodium azide in PBS) followed, this being repeated in between each step that follows. Corresponding secondary antibody (1:200-500) in buffer, was added for 1-2 h at room temperature and 4′,6-diamidino-2-phenylindole (DAPI; 1 mg/ml) diluted in blocking buffer. 3 washes with washing buffer and 2 washes with PBS preceded coverslip

mounting onto slides with Fluoromount-G. Imaging was carried out on either an EVOS FL Auto or a confocal microscope and fluorescence quantified using Fiji/ImageJ.

This protocol was repeated with the use of Affimers conjugated to either AlexaFluor 488 or 594 using maleimide linkage but with a few changes. Primary antibodies were excluded from the wells destined for Affimer incubation; these wells were instead covered with blocking buffer. The next day, AlexaFluor-conjugated Affimers were diluted in blocking buffer at concentrations ranging from 1:100-1000 and added to the wells for 1 h alongside DAPI (see above). The subsequent washes and mounting onto coverslips using Fluromount-G remained the same.

2.16.2 Fixation with glyoxal

Different fixation methods were also trialled to optimise immunofluorescence studies using AlexaFluor-tagged Affimers. This included fixation of the endothelial cells with 3% (v/v) deionised glyoxal. HUVECs were washed once with PBS (37^{O}C) before the addition of glyoxal (1:10 in glyoxal buffer, pH 5) for 10 min at room temperature. Cells were washed with PBS 3 times before the use of permeabilization buffer (0.2% Triton X-100 in PBS) for 15 min at room temperature on a shaker. Cells were blocked (10% normal donkey serum (NDS), 0.05% Triton X-100 in PBS) for 1 h at room temperature on a shaker. Cells were incubated overnight at 4^{O}C with primary antibodies diluted in antibody buffer (5% NDS, 0.05% Triton X-100 in PBS). 5 washes with washing buffer (1% NDS, 0.05% Triton X-100 in PBS) preceded the addition of secondary antibody or Affimer for 45 min at room temperature. Cells were washed 5 times with washing buffer followed by 1 wash with PBS before mounting on slides with Fluoromount-G. Images were taken on an EVOS FL Auto Microscope and fluorescence quantified using Fiji/ImageJ.

2.17 Isolation of VEGFR1 from endothelial cells using Affimers

A standard immunoprecipitation protocol was adapted in order to separate VEGFR1 from endothelial cells to further confirm the specificity of Affimers. HUVECs cultured in T75 flasks were washed 3 times with PBS before lysis (1% DDM, 1% Digitonin, 150 mM NaCl, 50 mM TrisHCl, 1 mM PMSF, pH 7.5) and scraping into microcentrifuge tubes. The samples were sonicated for 3-5 sec, 3 times, with ice incubation in between. 25 µg lysate was taken out as a loading control alongside 250 µg being taken out for each experimental sample. Lysates were centrifuged at 13000 rpm for 20 min at $4^{O}C$. Lysates were incubated with Affimers ranging 0.1-10 µg or with VEGFR-specific antibodies overnight at $4^{O}C$ on a rotator. Ni^{2+}-NTA affinity resin (for the Affimers) and protein G Sepharose beads (for the antibodies) were blocked for 1 h with 1% BSA in PBS before centrifugation for 10 min at 13000 rpm. These binding beads were washed and resuspended in lysis buffer (see above) before being incubated for 3 hours at $4^{O}C$ with the lysate/Affimer mix on a rotator. The samples were centrifuged at 13000 rpm for 10 min at $4^{O}C$, and the supernatant was removed. Samples were run on an SDS-PAGE gel before the standard western blotting protocol was carried out using primary VEGFR antibodies to detect potential binding.

2.18 Membrane receptor recycling assay using Affimers

Fluorescently-tagged Affimers were added to serum-starved HUVECs (in MCDB131 +0.2% BSA (w/v)) to analyse changes in membrane VEGFR1 recycling by using microscopy. 10 µg/ml of fluorescently-tagged VEGFR1-specific Affimers were added to HUVECs on gelatin-coated coverslips and incubated at $37^{O}C$, 5% CO_2 for 1 h. Primary antibodies to VEGFR1 and VEGFR2 were added as controls. The cells were chilled on ice and washed with acidic MCDB131 medium (pH 2.0) to remove the Affimers. Fluorescently-tagged secondary antibodies were added to the wells containing the primary antibody controls only, and incubated at $37^{O}C$, 5% CO_2 for 1 h followed by acid washing. The only primary antibodies available for secondary antibodies to bind are those which have attached to cell surface VEGFR1 which has gone on to be internalized and subsequently

recycled back to the membrane at least once (Smith *et al.*, 2017). Therefore, comparisons of the fluorescence to the wells containing antibodies permitted an estimation to be made of VEGFR1 recycling after incubation with the fluorescently-tagged Affimers. The cells were fixed using 3-4% PFA (w/v) and visualized using an EVOS Auto FL microscope. Fluorescence was quantified using Fiji/ImageJ.

2.19 Cell cycle monitoring using FUCCI-expressing A431 cell line

The effects of Affimers on epithelial adenocarcinoma cancer cell (A431) expressing the FUCCI fluorescent markers (from S. Ponnambalam, University of Leeds, UK) were monitored. A431-FUCCI cells, grown in DMEM/10% FBS with additives including puromycin (1 mg/ml), were split into 48 well plates and starved in Optimem for 2-3 h at 37^{O}C, 5% CO_2. The cells were incubated for 30 min at 37^{O}C, 5% CO_2, with Affimers ranging from 0.1-10 µg, prior to stimulation with 10 ng/ml VEGF-A or PlGF-1 (Promocell). Changes in cell cycle regulation was monitored at 24 h and 48 h intervals, using a digital fluorescence microscope, fitted with RFP and GFP filters, at 10x magnification. Overlay images of the RFP and GFP filters were created and the numbers of red, green and yellow cells (Fig. 2.4) were counted using Fiji/Image J.

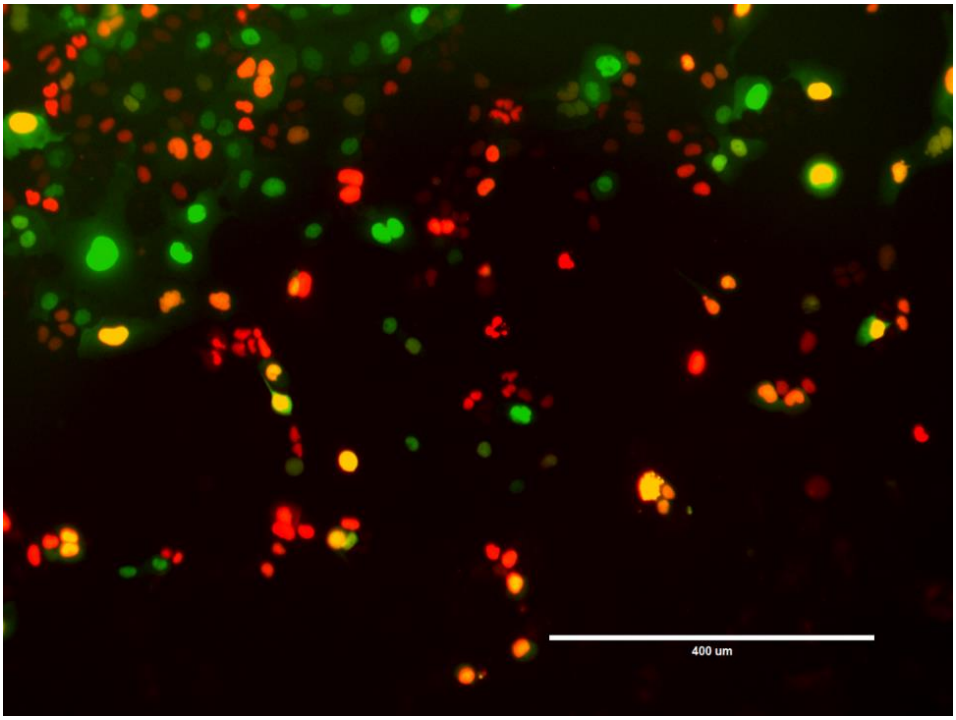

Figure 2.4. A431-FUCCI epithelial cancer cell line The FUCCI system allows visualization of cell cycle progression in A431 epithelial cancer cells. Cells are visible in G1 (red), S (yellow) and G2/M (green) phases of the cell cycle in the image shown above. Image taken at 10x magnification on an EVOS Auto fluorescence microscope. Bar, 400 mm.

2.20 Statistics

Statistical analysis for two groups was performed using unpaired two-tailed Student's t-tests. One-or two-way analysis of variance (ANOVA) followed by Tukey's or Dunnett's multiple comparison tests using GraphPad Prism VERSION 9.0.0 for Windows (San Diego, California, USA). Significance values between experimental and control groups were denoted on graphs with *p* values less than 0.05 (*), 0.01 (**), 0.001 (***) and 0.0001 (****). Error bars showed ± Standard Error of the Mean (SEM).

Chapter 3

Characterisation of VEGFR1-Specific Affimers

3.1 INTRODUCTION

Biochemistry is a wide and diverse involving the study of many proteins. There is usually a reliance upon methodologies relying on reducing specific proteins in order to identify their roles in signalling pathways (Tiede et al., 2017a). There are several loss-of-function techniques which can either knock-down DNA/RNA and therefore protein, or even ablate a gene which is an important process for protein expression. These technologies include RNA interference (RNAi), transcription activator-like effector nucleases (TALENs) and the latest arrival, the CRISPR-Cas9 system (Boettcher and McManus, 2015). Research in this field demonstrates, however, that these techniques must not be the only means used to assess the effects on functionality. For example, using the RNAi and CRISPR tools can often result in a multitude of off-target mutations (Kim *et al.*, 2015; Haussecker, 2016). These mutations can cause changes to the normal cellular phenotype, thereby potentially giving an inaccurate result. One theory goes further in this criticism, and postulates that these reverse genetic techniques may result in genetic compensation, leading to the possibility that the amount of RNA or protein may be altered to expiate the changes caused by loss-of-function (El-Brolosy and Stainier, 2017). For example, a study into zebrafish embryo morphology identified differences when comparing knockdowns and knock-outs for the *vegfaa* gene. Here, qPCR showed a compensatory increase in *vegfab* expression within the knock-out mutants as compared to the knockdowns; this upregulation was not seen *vegfaa* dominant-negative embryos. It was concluded from these results that this compensatory mechanism may be induced upstream of the function of the protein (Rossi *et al.*, 2015). These unintended effects suggest that there should be alternative techniques available for testing the genetic mutation of protein expression in order to assess its molecular physiology.

One of the main pharmacological agents used often to monitor or test protein distribution and/or function are antibodies. Antibodies are large glycoproteins and can be polyclonal, can bind to different epitopes within one antigen, or monoclonal (mAb), where the antibody binds to the same epitope of a specific antigen. The affinity of an antibody for an antigen is determined by factors such as hydrogen bonds, electrostatic forces, including van der Waals. These factors operating together, contribute to a to highly specific recognition and high-affinity binding (Yu *et al.*, 2017). This specificity allows for less harmful side-effects, meaning that antibodies have become some of the most profitable new drugs over the past five years. In fact, they contributed to 80% of the top 10 drugs available in 2018 (Lu *et al.*, 2020). The FDA approved its 100th mAb-based drug in April 2021, a programmed death receptor-1 (PD1) blocker named dostarlimab (GlaxoSmithKline). The 50th antibody was approved back in 2015, and it only took 6 years to double this figure (Mullard, 2021). It must be accepted, however, that the usage of antibodies does have some limits. The cost of their production means that they are sometimes reconstituted in unpurified sera, which further decreases their purity and thereby their specificity. Their large size can also be problematic as this factor heavily reduces the systems in which they can be used, including drug delivery and diagnostics. They also are not very thermostable and therefore are hard to both transport and store effectively for clinical use (Yu *et al.*, 2017).

Antibody-mimetics have become a rapid and ever-expanding area of research because of the aforementioned potential limitations on the usage of antibodies. There are often large libraries of these highly-specific synthetic molecular scaffolds, which, largely in part to their both time-saving and cost-effective for screening and production. Their small size, which is often due single domain proteins with no disulphide bonds and/or protein glycosylation, means that they can also penetrate into the cell interior. There are multiple antibody-mimetics currently being researched, such as Adnectins, designed ankyrin repeat proteins (DARPins) and Fynomers (Yu *et al.*, 2017). The function of this project is to add to the body of knowledge

encompassing synthetic proteins, by focussing upon the place of the Affimer within it.

One such synthetic protein scaffold is the Affimer which is utilised in this project. Affimers are highly specific reagents produced by the BioScreening Technology Group (BSTG) at the University of Leeds, but they are now commercially available through Avacta Life Sciences (Tiede et al., 2017a). Affimers are actually a group of two different scaffolds which includes the Adhiron, based on a plant-based phytocystatin (protease inhibitor), and a human cysteine protease inhibitor, Stefin A. A variant called Stefin A Quadruple Mutant-Tracy (SQT) has been engineered for such use. Both the Adhiron and SQT scaffolds have high thermostability, with the maximum melting temperatures (Tm) reaching 101^{O}C and 79.7^{O}C respectively. The Tm may not always be this high, but it is often still higher than that of the standard IgG antibodies (Kurt *et al.*, 2011; Tiede *et al.*, 2014). The stefin- and phyocystatin-based scaffolds have become the basis of two separate libraries, with them being named Affimer 1 and Affimer 2 respectively. There are suitable Affimers available which recognise a large number of target proteins, which can be used in a variety of applications, including the modulation of ion channel function, and both fixed-cell and *in vivo* imaging. They have previously been also found to inhibit VEGFR signalling, which is the focus of this PhD project (Tiede et al., 2017a).

In this chapter, the production of VEGFR1-inhibitory Affimers through phage display is explored. ELISA assays were also carried out in order to identify whether there was cross-reactivity between the human and murine versions of the previously attained VEGFR1-specific Affimers. This was to not only confirm whether or not they have their specificity to the protein, but also to enable an insight into their potential for use in future animal studies. The purification of the Affimer proteins and their subsequent biotinylation was also assessed. Finally, these Affimers were conjugated to Alexa Fluor 488 using maleimide-linkage to pinpoint their potential use in *in vitro* fluorescence imaging. This diverse set of experiments would not only confirm the efficacy and purity of the Affimers, but also evaluate whether they would be good diagnostic as well as functional agents.

3.2 RESULTS

3.2.1 VEGFR1 recombinant proteins as target antigens

Designing drugs for targeting a specific receptor requires a knowledge of both its structural conformation and how it influences other biochemical structures within a signalling cascade. In structural research, the focus is often on identifying the complex molecular assembly and interactions between a ligand and its receptor. This can be a good basis for identifying key traits of a target receptor so that novel pharmaceuticals can be produced and used in further functional assays. This approach is equally valid for research into VEGFRs, which are part of the type IV receptor tyrosine kinase (RTK) family. These RTKs share a common structure containing four domains with distinct purposes: these are the extracellular, transmembrane, cytoplasmic juxtamembrane and tyrosine kinase (TK) regions (Shaik *et al.*, 2020). Although the full structure of the VEGFRs have yet to be solved, tools such as X-ray crystallography and electron microscopy (EM) have accurately revealed the complexes formed between the extracellular (ECD) domain and VEGF ligands.

For example, these techniques have revealed that both VEGFR1 and VEGFR2 have seven immunoglobulin-like (Ig) domains (D1-D7) which trigger receptor activation in very specific ways. One model involves VEGF-A attaching to the D2-D3 ligand pocket, resulting in homodimerization of the VEGFR monomers. This dimer is stabilized by D4-7 which not only increases the binding affinity of VEGF-A but also potentially causes conformational changes around the transmembrane/cytoplasmic juxtamembrane regions of the VEGFR. This in turn would activate the signalling cascade through phosphorylation of the intracellular kinase domains (Ruch *et al.*, 2007; Markovic-Mueller *et al.*, 2017). This analysis of the VEGFR ECD opens a potential avenue for drug development. Leading on from this, Figure 3.1A depicts representations of the truncated forms of VEGFR1 and VEGFR2 in comparison to their full-length counterparts (Swiss UniProt ID P17948 and P35968 respectively). These truncated soluble forms comprised of the VEGFR ECDs are fused to a polyhistidine

(His) tag at the C-terminus and secreted from transfected human HEK293 cells (UniProt Consortium *et al.*, 2021). Using the purified VEGFR ECDs was the most sensible option to screen for specific Affimers since this was the region of interest. Another factor which had to be considered was that VEGFR proteins are relatively large, as demonstrated by the Western blots in Figure 3.1B. In these, the mature forms of VEGFR glycoproteins can be seen at ~180 kDa (soluble VEGFR1) and ~200-230 kDa (soluble VEGFR2) respectively. These high molecular weights did slightly complicate the calculations which were necessary for biotinylating the proteins for screening, since target proteins researched in the past have usually been very small (e.g., ~10 kDa). It would seem, therefore, that there could be great benefits to be accrued for the purposes of experimentation, by being able to use the truncated, smaller forms of the VEGFRs, which would not only serve to isolate the key binding site for the Affimers, but also potentially allow for better results overall to be achieved.

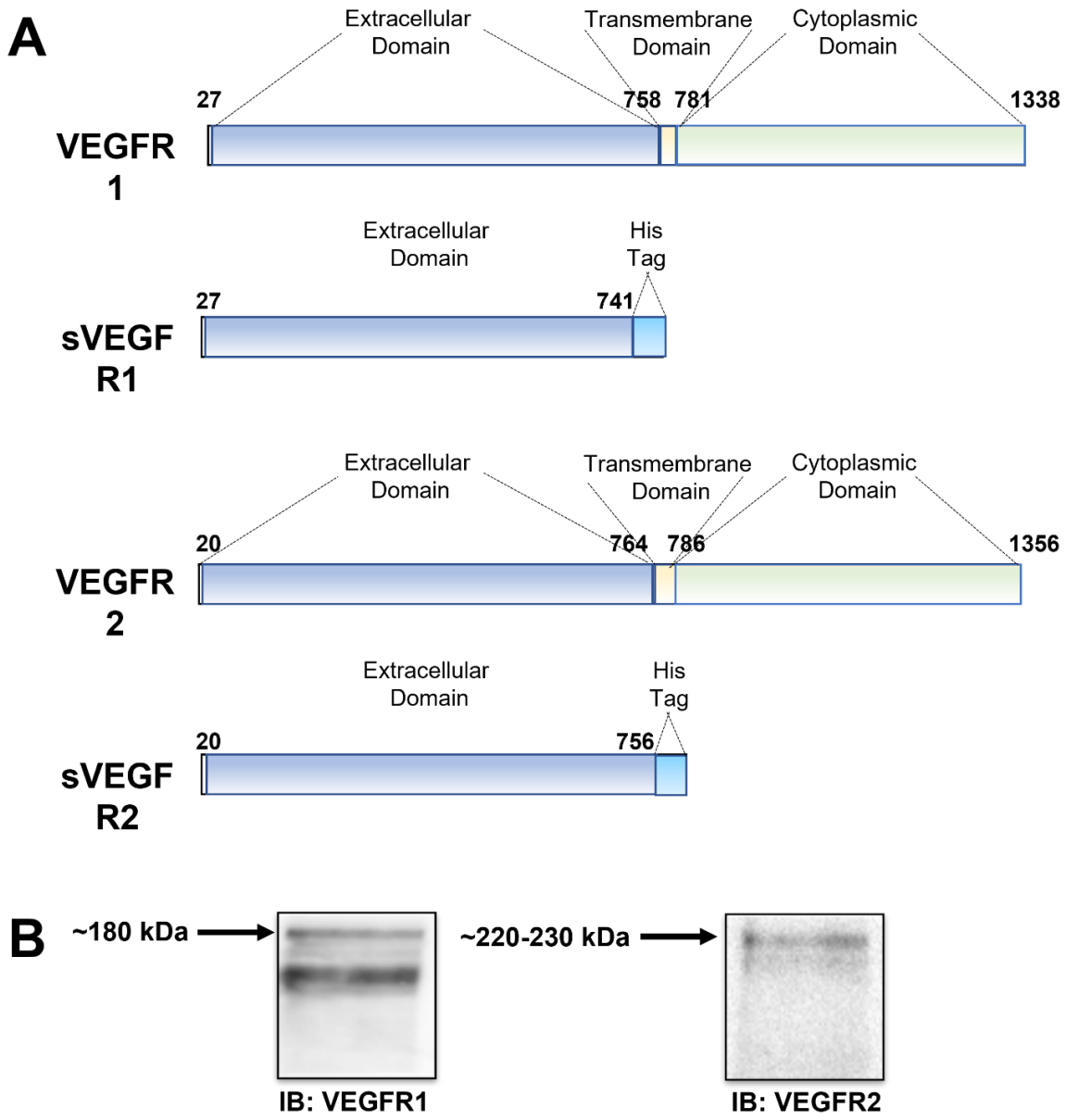

Figure 3.1. The VEGFR Proteins. (A) Schematic view of the full-length VEGFR1 and VEGFR2 proteins and domains with depiction of the truncated soluble proteins (sVEGFR1, sVEGFR2) used in phage screening. (B) Immunoblotting of native full-length VEGFR1 and VEGFR2 proteins in human endothelial cells (HUVECs). Estimated molecular mass of the mature, glycosylated proteins are indicated as ~180 kDa and ~220-230 kDa for VEGFR1 and VEGFR2 respectively.

3.2.2 Isolation of VEGFR1-specific Affimers using phage display

In this research, the main focus at the start was VEGFR1. Therefore, an initial screen was carried out by the BTSG isolated a panel of VEGFR1-specific Affimers. However, these Affimers had only been screened against the human soluble VEGFR1 protein, so we also wished to identify VEGFR1-specific human and murine cross-reactive Affimers. Figure 3.2 depicts results using the mouse (Fig. 3.2A) and rat (Fig. 3.2B) soluble VEGFR1 proteins respectively. In brief, the same phage display method was used as used in the standard BSTG protocol (Tiede et al., 2017). But, instead of using the same biotinylated human VEGFR1 protein throughout each of the three pans (rounds of enrichment screening), the proteins were instead switched to the mouse/rat form during the second round. This was done to see if this produced more effective yet cross-reactive Affimers for VEGFR1 from different species.

The final isolated Affimer clones were expressed and tested against the human and murine soluble VEGFR1 proteins using a phage ELISA alongside a negative control. These were also compared to a yeast SUMO-specific Affimer (Yeast SUMO 10), which acted as another negative control since it theoretically would not be able to bind to the VEGFR1 proteins. The data in Figure 3.2 shows two initial screens using in order to identify potential human/mouse and human/rat cross-reactive VEGFR1 specific Affimers. These graphs show that there was generally little enrichment in VEGFR1-specific Affimers. This is why the rest of the thesis mainly focuses on human-specific VEGFR1 inhibitory Affimers, seen in Figure 3.3, from a separate screen prior to this particular project. In terms of the data in Figure 3.2, the assays overall did not seem to demonstrate a great deal in terms of showing increased absorbance. One potential reason is that the mouse VEGFR1 was a in fact a soluble VEGFR1-Fc protein fusion attached, which could have reduced the efficiency of labelling, and screening efficiency. However, the soluble rat VEGFR1 protein also showed a low number of specific Affimers despite the lack of possible interfering tags or fusions. Despite these set-backs, there was one Affimer from this set of experiments

which showed some potential, named 53. The ELISA results showed that Affimer 53 bound to both the human and rat versions of VEGFR1, inferring some possible cross-reactivity (Fig. 3.2B). Further testing would reveal whether this particular Affimer could prove useful in functional assays that use both human and murine tissue.

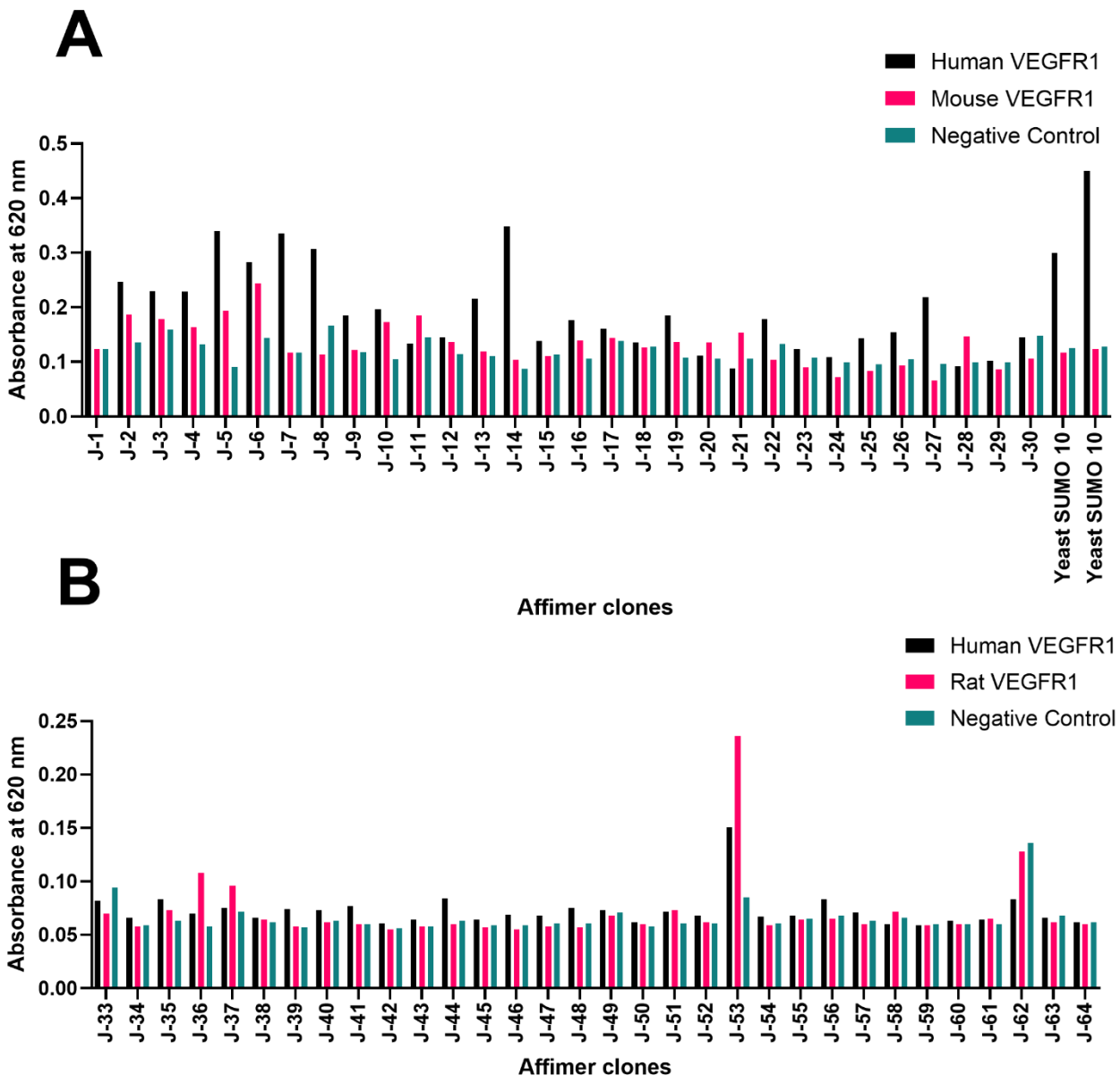

Figure 3.2. Phage displays screens to identify Affimers which recognise mouse and human VEGFR1. Phage display was carried to find VEGFR1-specific Affimers which could bind to both human and rodent VEGFR1 orthologs. Trials were carried out using (A) human and mouse, and (B) human and rat sVEGFR1 proteins. Clones were numbered based on the wells of the 96-well plate and are prefixed by the letter 'J' to distinguish these screens from the Affimers used later on in the project. Binding of the clones to sVEGFR1 was compared to two negative controls: a yeast SUMO-specific Affimer ('Yeast SUMO 10') and 2x Casein blocking buffer only ('Negative Control'). Absorbances were measured at 620 nm on a spectrophotometer to give an indication of Affimer recognition of sVEGFR1 (n=1).

3.2.3 VEGFR1-specific Affimer characterisation

Affimer 53 was carried forward alongside the previously isolated human VEGFR1-specific Affimers and analysed using ELISA (Fig. 3.3). Figure 3.3A depicts a comparison between binding of the Affimer clones to either the human or mouse versions of the VEGFR1 protein. The majority of VEGFR1-specific Affimers showed increased binding to human VEGFR1 protein when compared to the negative control, with the increases ranging from ~63-97% (Fig. 3.3A). This, however, raised some perplexing results, such as Affimer 53 showing very little specificity and the Yeast SUMO 10 binder also potentially binding to VEGFR1 as seen by the increased absorbances (Fig. 3.3A). Some VEGFR1-specific Affimers seem to show valid species cross-reactivity, such as Affimer 66 with an increase of 58% as compared to the control.

These factors led to a repetition of ELISA using soluble rat VEGFR1 protein (Fig. 3.3B). The Affimers were also tested against the biotinylated form of the yeast SUMO protein to further confirm or deny their specificity. This was in fact fruitful as the yeast SUMO 10 Affimer did not seem to bind to the VEGFR1 protein and vice versa, suggesting this assay was more reliable. Affimer 53 once again looked non-specific in binding specificity, but having this repeat with a different murine model at least helped save on time and resources in the long run. The majority of the other Affimers still displayed highly specific binding to soluble human VEGFR1 protein with an average signal increase of 93% compared to the negative control. Affimer 66 also once again seemed to show some cross-reactivity, this time showing an increase of 85% in signal intensity as compared to the blocking buffer. Therefore, not only do these previous VEGFR1-Affimers seem highly specific to human VEGFR1, but it was also discovered that one Affimer also shows cross-activity to murine VEGFR1. This work led to the basis for use of Affimer 66 in the later cell biology studies in this PhD thesis.

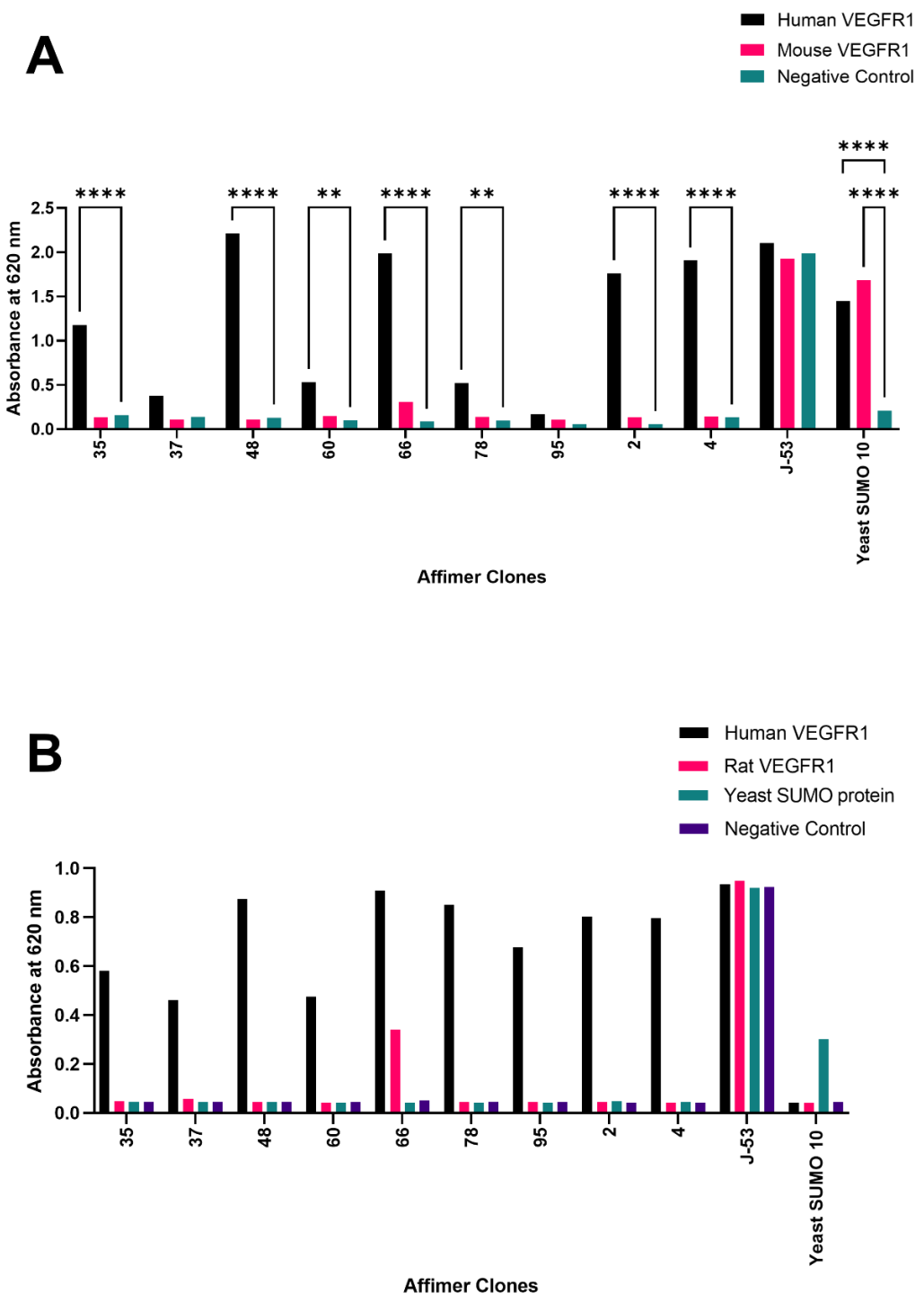

Figure 3.3. Cross-reactivity of isolated VEGFR1-specific Affimers. VEGFR1-specific Affimers which had been previously isolated from screens against the human sVEGFR1 protein (35, 37, 48, 60, 66, 78, 95, 2 and 4) were tested against (A) mouse and (B) rat sVEGFR1 proteins. One clone, J-53 from the cross-reactivity screen against rat VEGFR1 (Fig. 3.2B) was also tested against these previously established VEGFR1-inhibitory Affimers to further elucidate its specificity. These Affimers were also tested against yeast SUMO protein and 2x Casein blocking buffer ('Negative Control'), with these wells acting as negative controls. Absorbances were measured at 620 nm on a spectrophotometer to give an indication of Affimer recognition of sVEGFR1. Error bars denote ±SEM. Significance, ** p<0.005, **** p<0.0001 (n=3).

3.2.3 Affimer carboxy-terminal cysteine tagging

The potential practicality of Affimers in future research is extensive. These reagents not only have the capability to alter cellular function, but they are also able to have a more diagnostic function. This is due to the addition of a C-terminal cysteine through the sub-cloning methodology as per the BSTG lab (Tiede et al., 2017). Cysteine is useful because it is a strong nucleophile and can target molecules with sulphur atoms (thiols) in their side chains, such as maleimides (Kumar *et al.*, 2017). This allows site-specific modification and the added benefit of a naturally low abundance means that cysteine has good regio-and chemoselectivity (Gunnoo and Madder, 2016). The addition of a cysteine aids protein ligation, cyclization and labelling, such as with fluorescent tags or biotin (Kimple et al., 2013). This tagged version has proved useful in several research studies on Affimers. It may, however, be of use to also check whether the Affimers themselves are purely the reason for any physiological effects, or whether the cysteine tag may be having some contribution. For instance, the commonly used glutathione S-transferase (GST) tag has been found to dimerize in solution and thus thought to occasionally affect the biological protein that it is bound to (Kimple, et al., 2013). This, however, could have been due to the GST tag being attached to the N-terminus, whereas the cysteine tag is attached to the C-terminus of the Affimers, thereby potentially reducing this problem. This potential for a reduction in the problem does not mean, however, that there is no value in further experimentation to test whether or not unusual effects in cells are at least partly due to the addition of this tag.

The difference between cysteine-tagged and non-cysteine tagged purified Affimers is clear in SDS-PAGE gels which incorporate Coomassie blue staining. Figure 3.4 depicts each stage of the Ni^{2+}-NTA -mediated purification process for Affimer 66, which was previously found to be cross-reactive to human and rat VEGFR1. Here, the standard ~12.5 kDa Affimer protein scaffold is detected, but the cysteine-tagged Affimer 66 (Fig. 3.4A) shows either protein aggregates and/or dimers within as seen by multiple bands in early eluate fractions (#1-4; Figure 3.4). This would correlate with the general action of cysteine residues, where they create intermolecular

disulphide bridges within proteins to increase stability (Rotoli et al., 2018). The number of bands decreases in the later elution stages which could possibly be due to lower amounts of protein This possible conclusion is indicated by a single band getting fainter. The non-cysteine tagged version (Fig. 3.4B) shows very little dimerization in the first four elutions, which would be expected. However, elutions 5-8 did show some aggregation/dimerization, although it was less pronounced than with the cysteine tag. It should be noted that there was also a higher amount of protein within these elutions, which could potentially explain why there are multiple bands here.

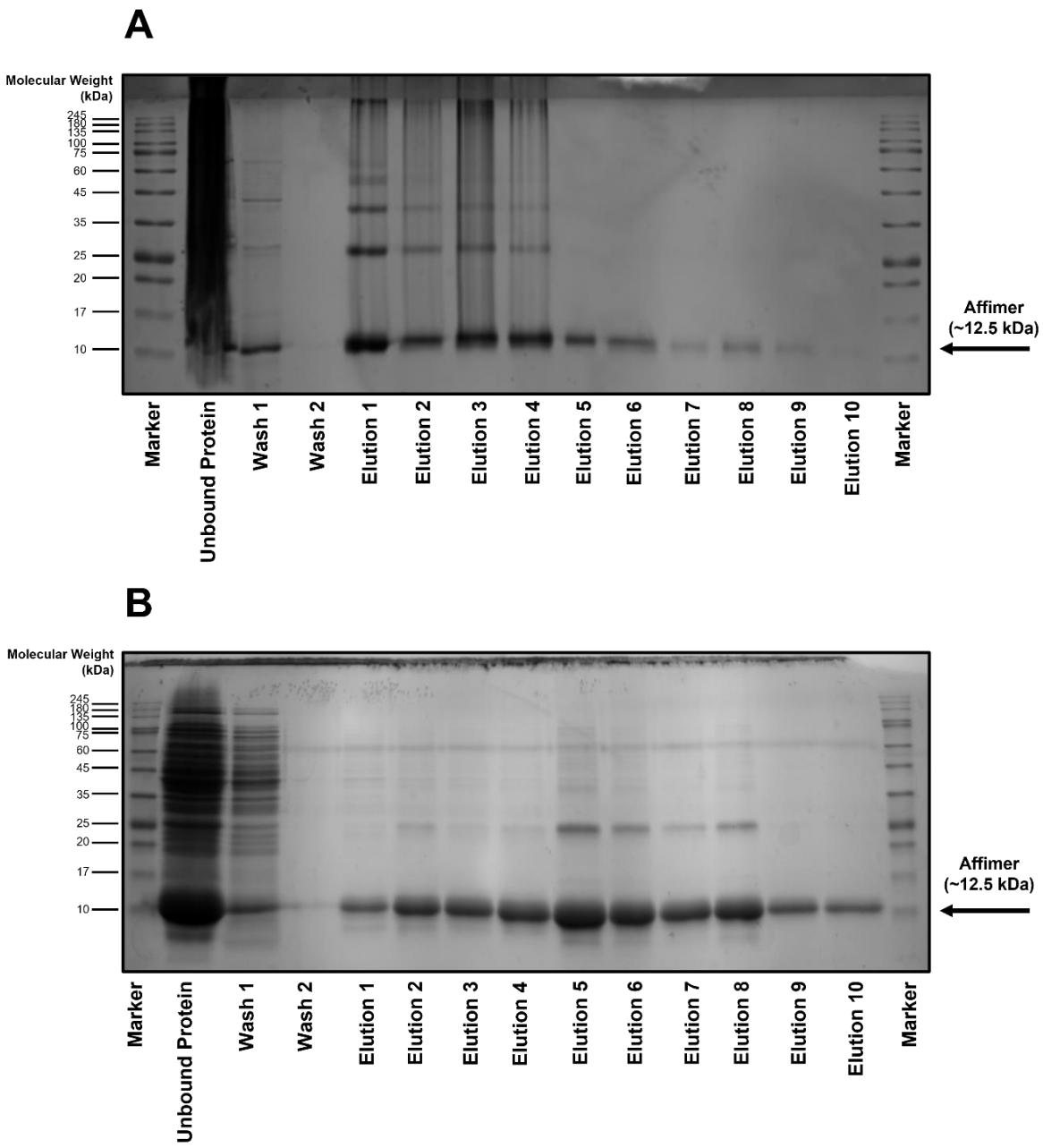

Figure 3.4. Bacterial expression and purification of recombinant Affimer. All Affimers were expressed in E. coli and purified prior to experiments. The Affimers had a His-tag which aided purification with a Ni^{2+}-NTA affinity resin. Fractions of protein were taken from each stage of the purification process, including the protein which did not bind to the resin ('Unbound protein'). 'Wash 1' and 'Wash 2' represents the first and final of ~10 washes of the resin which purified the protein. Elution fractions were also taken at each stage to confirm the presence of Affimer at ~12.5 kDa. Analysis of each purification stage was carried out using SDS-PAGE and Coomassie blue staining. Here, purification of the of the cross-reactive Affimer 66 is shown. Purification of either (A) cysteine-tagged Affimer 66, and (B) non-cysteine tagged Affimer 66 are shown.

Figures 3.4 and Figure 3.5 both depict differences between cysteine and non-cysteine-tagged Affimers. Cysteine and non-cysteine tagged Affimers will have the letters “c” and “p” after their names respectively in this and subsequent chapters. An immunoprecipitation (IP), or pulldown, method was adapted in order to isolate the VEGFR1 protein from HUVECs as compared to antibodies (Fig. 3.5A). For instance, Ni^{2+}-NTA affinity resin was tried instead of standard IgG specific beads used for pulldowns with antibodies, such as protein G sepharose, since it was thought that this may work better for the poly-Histidine (His)-containing Affimers. Each Affimer was incubated with the HUVEC lysate alongside the Ni^{2+}-NTA affinity resin and finally run on an SDS-PAGE gel. Western blotting was used to assess the success of this protocol with the aid of an anti-VEGFR1 antibody. Overall, the ~180 kDa VEGFR1 protein was detected in all of the lanes containing VEGFR1-specific Affimers bar 66c (which there was not a non-cysteine tagged version of at the time) (Fig. 3.5A). This could be an indication of stronger association with the receptor but could also mean that the beads containing the bound Affimers were not flushed off the HUVEC lysate as well as the other reagents. Analyses of the anti-VEGFR1 integrated density of the bands show that there did not appear to be a significant difference between the cysteine- and non-cysteine tagged versions of each VEGFR1-specific Affimer (Fig. 3.5B). For instance, the highest intensity seemed to be at the 35p (non-cysteine tagged) lane, which was about ~67% higher than that of its cysteine tagged counterpart. This was also matched by Affimer 48, where the non-cysteine tagged version was more than 67% greater than that of the cysteine-tagged. The reverse is seen with Affimer 37, where there was a ~<45% higher amount of protein seen with its cysteine- versus non-cysteine tagged versions.

There were, however, strong bands also detected in the lanes containing the VEGFR2-specific Affimer, B8c and the yeast SUMO specific Affimer, yeast SUMO-10. This would initially be cause for concern since these were technically the negative controls, but the lack of bands in the beads only lane means that these results are somewhat reliable. That aside, it is worth noting that there still appears to be a greater amount of bound VEGFR1

protein when comparing the anti-VEGFR1 and anti-VEGFR2 Affimers. For instance, if we compare the versions of the VEGFR1-specific Affimers which showed the greater intensities (35p, 37c and 48p), they are ~120% higher on average as compared to B8c. Affimers 35c and 37p also showed ~82% higher intensity on average as compared to B8c. The non-cysteine tagged B8p also appeared to show low binding to VEGFR1 as seen by the relatively reduced intensity, further indicating the higher specificity of the VEGFR1-specific Affimers for VEGFR1. Replicates of this experiment would have further elucidated whether these preliminary results could be officially confirmed.

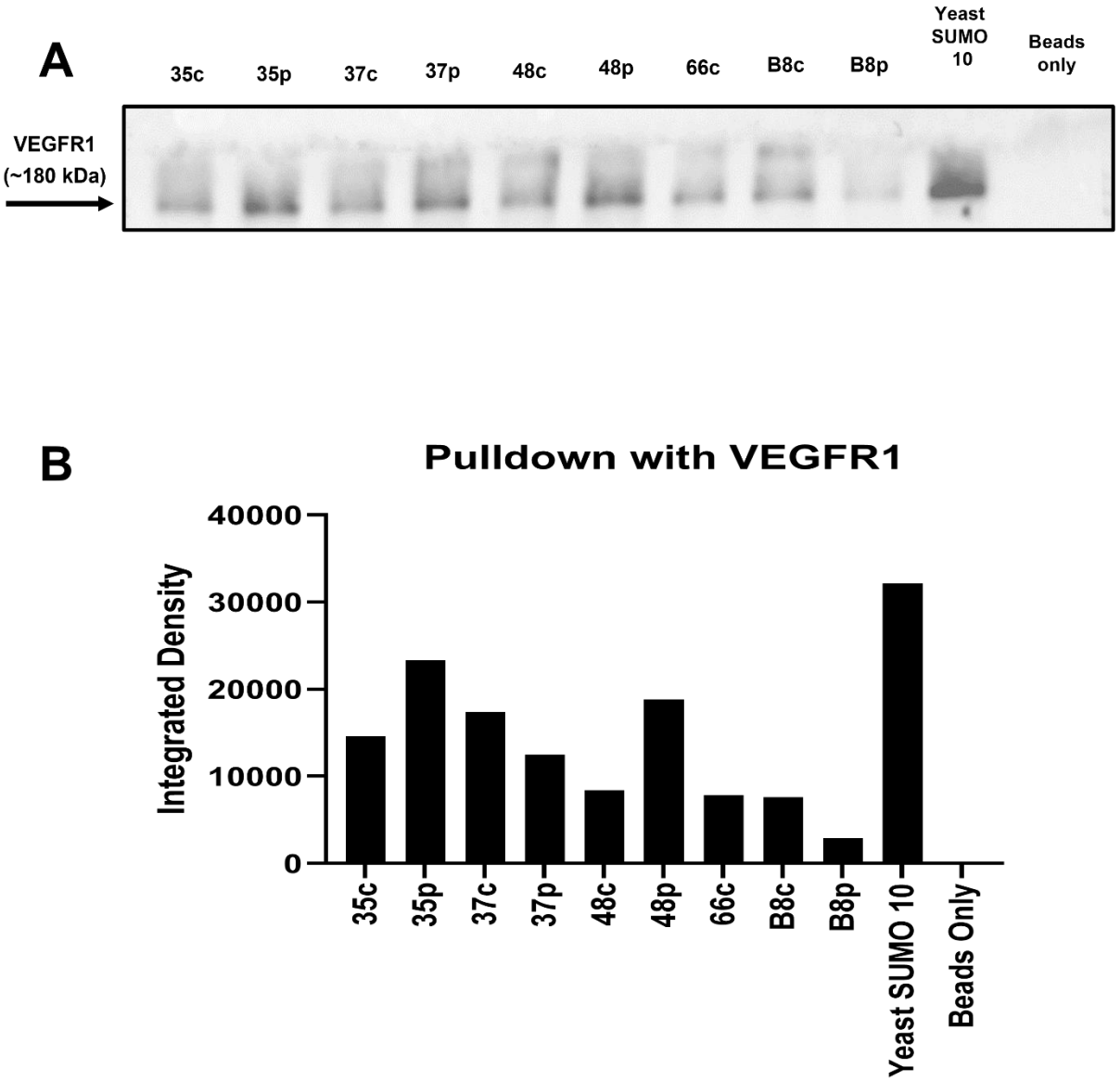

Figure 3.5. Affimer-specific isolation of VEGFR1. Isolation of human VEGFR1 protein from HUVECs using both cysteine- and non-cysteine tagged VEGFR1-specific Affimers. These were tested alongside VEGFR2 (B8) and yeast SUMO specific Affimers ('Yeast SUMO 10'). HUVECs were lysed and incubated with Affimers pre-incubated with a Ni^{2+}-NTA affinity resin. The resin ('Beads') was also used as a further control. These were analysed using SDS-PAGE and (A) immunoblotting using goat anti-VEGFR1 antibody. (B) Quantification of the binding of the Affimers to VEGFR1 was done using the integrated densities of each immunoblot band in Fiji/ImageJ and plotted (n=1).

The yeast SUMO 10 Affimer continued to dominate the results though. None of these, however, were significant differences, perhaps showing that the addition of this tag may be of no real detriment to their ability as binders. This could be because the binding of the cysteine tag to the c-terminus would not block the binding site of the Affimer, which would not be the case if it was labelled at the n-terminus site. There is also a possibility that the Affimers themselves have dimerized, resulting in the multiple bands seen on the blots. Further confirmation through techniques such as mass spectrometry would be useful to elucidate the identities of these proteins.

This led onto look an examination of the protein sequences of both the human and yeast forms of SUMO, using Clustal Omega 2.1 (Fig. 3.6A, 3.6B). Sequence alignments revealed the human and yeast SUMO share much similarity, particularly for SUMO1 (over 40% similarity). This is backed-up by percentage matrices and studying the phylogenetic tree, where SUMO1 and yeast SUMO originate from the same point and are therefore sister taxa. It is especially possible since previous studies involving Affimers have produced versions which were non-specific to each of the human isoforms of SUMO (Hughes et al., 2017). It would have been beneficial to try and test the yeast SUMO Affimer further in order to confirm these theories, but the unexpected binding to VEGFR1 in several experiments meant that a switch was made later on in the research to an alternative non-specific control Affimer.

A

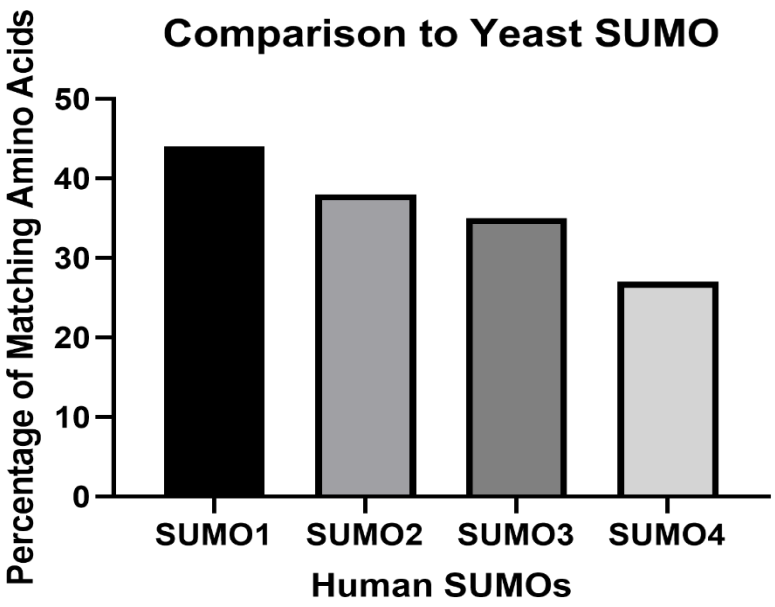

B

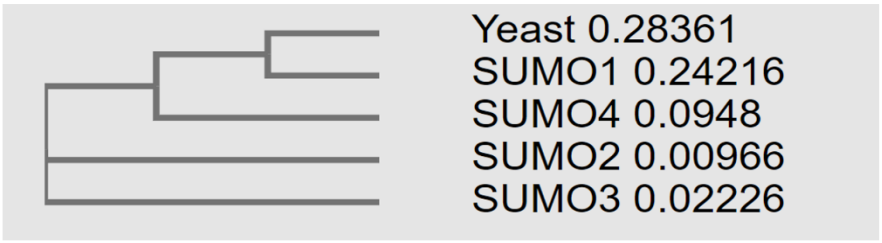

1: Yeast	100.00	47.42	39.13	42.39	42.39
2: SUMO1	47.42	100.00	42.11	47.37	46.88
3: SUMO4	39.13	42.11	100.00	86.32	84.04
4: SUMO2	42.39	47.37	86.32	100.00	96.81
5: SUMO3	42.39	46.88	84.04	96.81	100.00

Figure 3.6. Affimer-based isolation of VEGFR1 in comparison to yeast SUMO. (A) Sequence alignment and (B) percentage matrices were used to compare VEGFR1 and SUMO proteins to determine whether there was a link between the sequences of SUMO proteins and the non-specific results of Yeast SUMO 10 previously seen. Sequence analysis was carried out using Clustal Omega 2.1 (www.ebi.ac.uk).

3.2.4 Affimer biotinylation

Biotinylation is a very popular technique within the proteomics community. This is primarily due to the knowledge that biotin has a very strong association with avidin/streptavidin (Kd = 10^{-15}M); this is much higher than a lot of antibodies and also can have a lot less non-specific binding as a result. Therefore, a protein bound to biotin could be very easily detected within a system using its specificity for avidin/streptavidin (De Boer *et al.*, 2003). The biotinylation of target proteins has proved successful in isolating specific Affimers, showing that this process does not affect their efficacy. Therefore, it was decided to take advantage of this strong biotin/avidin detection system by biotinylating the Affimers themselves to see how well they may bind to either soluble VEGFR1 or to be able to detect this receptor in HUVEC lysate. The standard BSTG biotinylation protocol was carried out on the majority of the VEGFR-specific Affimers using malemide linkage (Tiede et al., 2017). Maleimide linkage involves the attachment of biotin (or dye)-conjugated maleimide to a free sulfhydryl bond on a protein via a stable thioether bond, such as to the cysteine tag on an Affimer (Nanda and Lorsch, 2014). Biotinylated Affimers were run on SDS-PAGE gels followed by Western blotting with a streptavidin HRP-conjugated antibody to specifically detect the biotin. Both the biotinylated and native cysteine-tagged forms of the Affimers were run on the gel to compare the success of the procedure (Fig. 3.7A). Bands corresponding to the Affimers were indeed seen at ~12.5 kDa for only the biotinylated forms. However, the dimers/aggregates representing the cysteine tagged forms were once again seen in all of the lanes including the native forms. This was particularly prevalent in the biotinylated Affimers 66c and B8c, where there were multiple, dense bands within the lanes. This could of course indicate the protein degradation over time, but it should be noted that there have been other studies where the biotinylation of proteins have also caused multiple bands to appear in the lanes of western blots. Theories include that biotinylation increases the aggregation of the proteins, which could even be due to changes in pH (Wadsley and Watt, 1987; Schamel, 2001).

As a test case, VEGFR1-specific Affimer 1 was biotinylated and used in an adapted version of the IP protocol (Fig. 3.7B). This method was trialled in order to identify potential binding regions on the VEGFR1 protein for this Affimer. The protocol was similar to the one above apart from the fact that the biotinylated Affimer was incubated with purified soluble VEGFR1 (sVEGFR1) proteins instead of cell lysate. Using an anti-biotin antibody allows a distinct band to be seen at ~180 kDa on a Western blot when incubated with the full-length human sVEGFR1, which consists of 6 domains. It is also possible to see a band within the lane containing human sVEGFR1 D1-4 at around 60 kDa, whilst nothing could really be seen in the lane containing human sVEGFR1 D1-5. There is also a faint band within the mouse sVEGFR1, suggesting weak cross-reactivity with murine VEGFR1. This set of experiments not only showed the efficacy of the biotin/avidin system in conjunction with Affimers, but also to provide further potential evidence for this synthetic scaffold's specificity to VEGFR1. Although this was a trial experiment, there was recognizable binding of the VEGFR1-specific Affimer to the full-length VEGFR1 as well as its ligand-binding domain using this technique. Further replicates and adding other VEGFR1-specific Affimers may therefore also prove useful in this context.

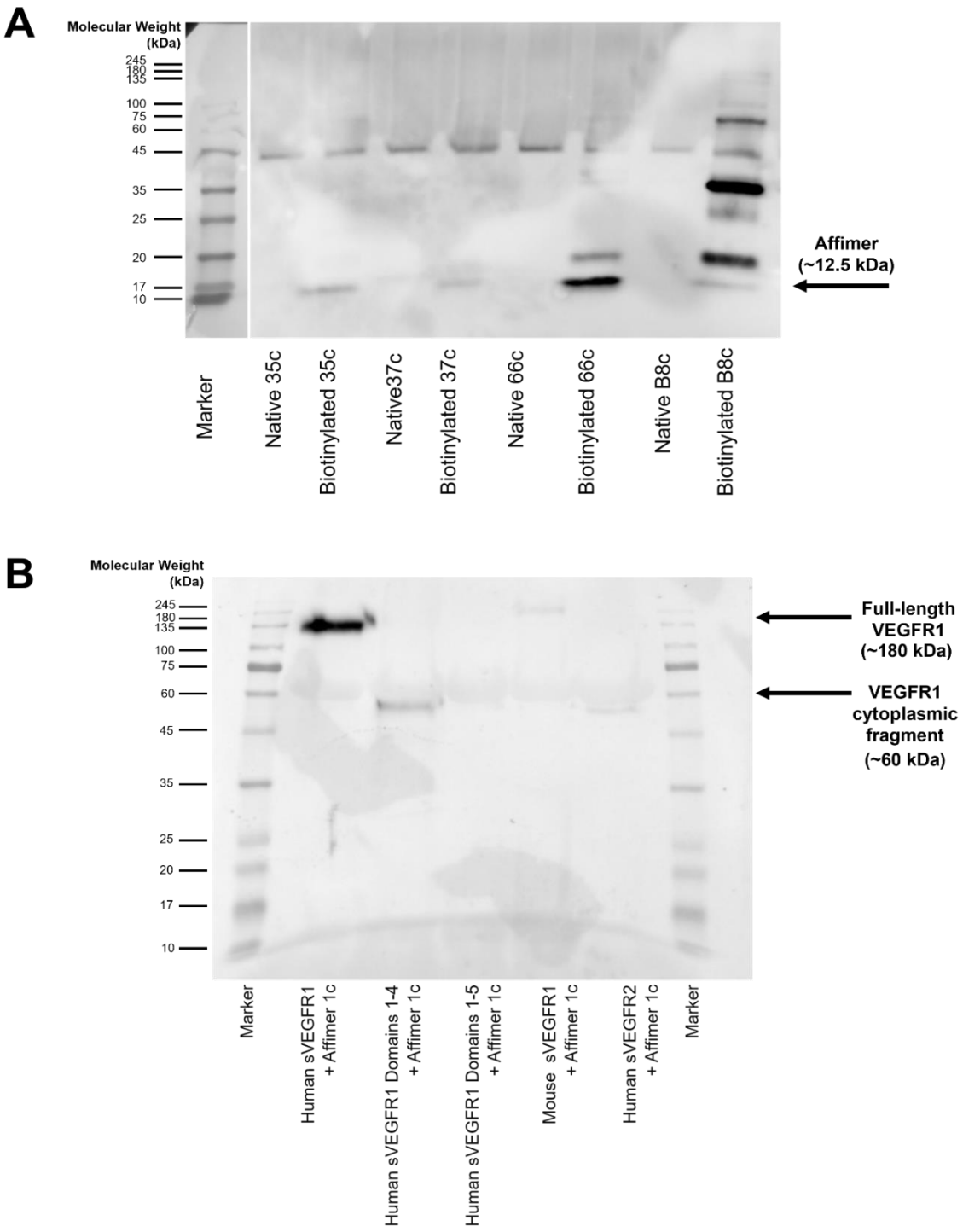

Figure 3.7. Biotinylation of VEGFR-specific Affimers. VEGFR-specific Affimers were biotinylated via their cysteine tags throughout the project. (A) Western blotting using both VEGFR1 and VEGFR2-specific Affimers in both their native and biotinylated forms. (B) VEGFR1-specific Affimer 1c was also biotinylated and incubated with different domains of human and mouse VEGFR1 proteins to identify potential binding sites. This was done using a similar protocol to the use of Affimers to isolate VEGFR1 from HUVECs (Fig. 3.5) (n=1).

3.2.5 Affimer labelling with fluorescent tags

The cysteine tag on Affimers not only allows one to biotinylate a protein, but also to add a fluorescent tag. Figure 3.8 shows an SDS-PAGE gel analysing Affimers conjugated to the green dye, AlexaFluor 488 *via* maleimide (cysteine-based) linkage. This direct conjugation allows one to not only use the Affimers like a fluorescently tagged antibody, but also provides the added potential benefit accrued from their small size, meaning that they may need less time to bind to the cells. The Affimers were compared to their fluorescently tagged form and also to their native form, using a fluorescent gel imager, to enable an assessment as to whether this conjugation had been successful. Here, the gel shows bright bands at ~10-12 kDa in the lanes containing the two AlexaFluor tagged VEGFR1 Affimers, 35c and 66c (Fig. 3.8). There was also a bright band in the lane Alexa-Fluor tagged VEGFR2 Affimer, B8c, but, unexpectedly, it was also found to be present in its native form. It is at present unknown as to why this should be the case, but it could potentially be due to a contamination issue.

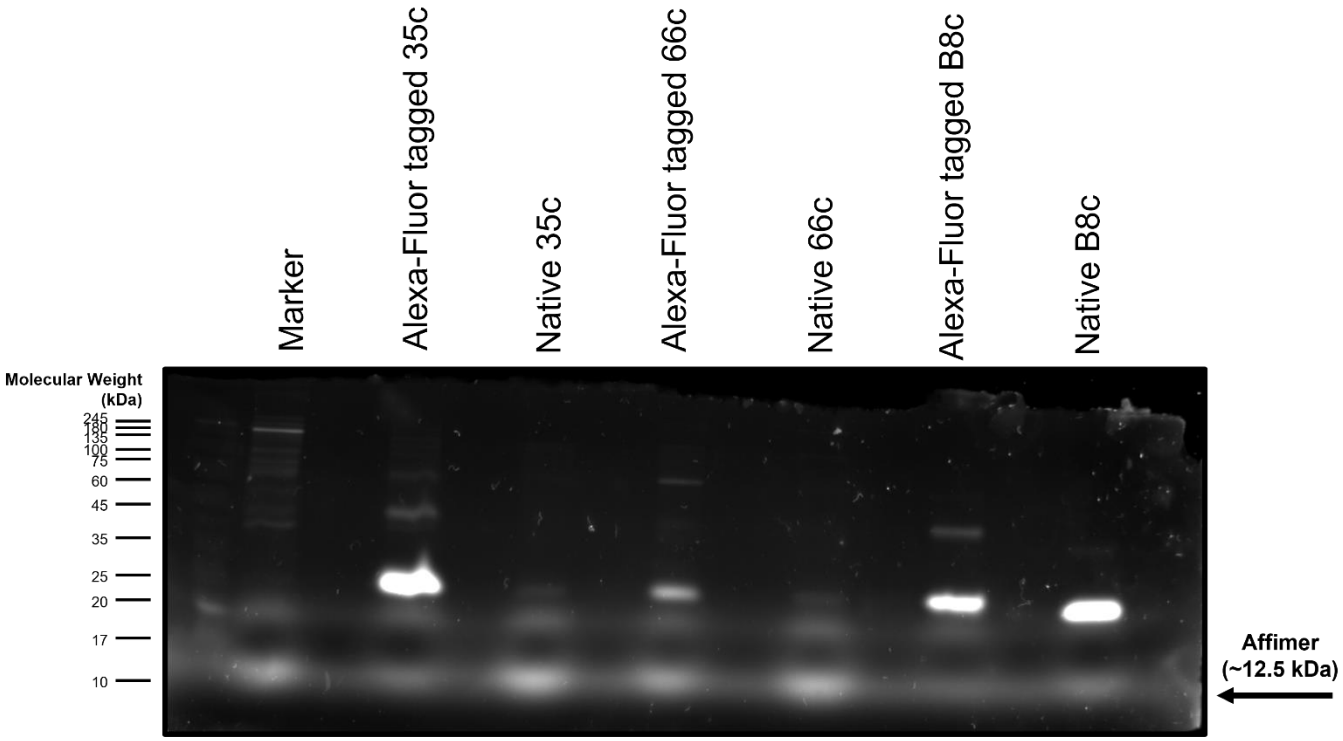

Figure 3.8. Affimer tagging using a fluorescent AlexaFluor 488. VEGFR-specific Affimers were fluorescently tagged with maleimide-activated AlexaFluor 488 dye by conjugation to the cysteine tags engineered into the Affimers. SDS-PAGE and fluorescence imaging using a 488 nm (excitation) and 510 nm (emission) filter-set using a digital imaging workstation (see Materials and Methods) to compare both fluorescent and non-fluorescent Affimers (n=1).

These VEGFR-specific Affimers were considered sufficiently promising to be taken forward for immunofluorescence studies. The majority of the available Affimers were fluorescently tagged and used in fluorescence imaging to ascertain which ones best labelled VEGFR1. From these studies, it was concluded that VEGFR1-specific Affimer 37 was one of the better Affimers in terms of VEGFR1 detection. It is common practice for conventional antibodies to be used at different concentrations depending upon the application chosen is functional or for imaging. Therefore, it was decided to test various concentrations of Affimer 37 on HUVECs, as well as test different fixation methods (Figs. 3.9-3.11). This protocol was chosen because previous trials with the lab standard, 3-4% paraformaldehyde (PFA) (w/v) had variable results in terms of producing clear staining patterns. This could have been due to its tendency to either damage the plasma membrane or change the morphology of cells (Richter et al., 2018; Cheng et al., 2019). It was decided to test other fixation protocols which may not only show specific binding sites clearly, but also keep the overall integrity of the experiment. The most novel method of the three involved using fixation using 5% (v/v) glyoxal, which is a small dialdehyde. The small size of glyoxal would hypothetically reduce cell damage to and penetrate the membrane quicker alongside preserving cellular proteins (Richter et al., 2018). Ice-cold 100% methanol can also show intracellular structures quite well, which would be useful for observing staining of internal VEGFR1 using the Affimers. Methanol and glyoxal based fixation techniques have been compared previously (Channathodiyil and Houseley, 2021). Overall, there was a general dose-dependent increase in fluorescence staining with all three methods of fixation which can also be seen numerically in the graph in Figure 3.12. It appears that the brightest images occurred when using 10 µg/ml of VEGFR-specific Affimer for all of the fixation methods, which would be expected with increased amounts of protein. This concentration also shows a lot of background fluorescence intracellularly, meaning it is trickier to see where exactly the VEGFR1s may be. There is also some staining in the wells incubated with 2 µg/ml of Affimer although the cell walls were more prominent with glyoxal and PFA.

In conclusion, it seems that 5 µg/ml of Affimer would be the ideal concentration to use, as it provides a good balance between the competing requirements to achieve both a bright image and also better intracellular/membrane staining.

There is some (non-specific) nuclear staining within the images. For instance, leaving the Affimer on for a shorter period of time may be found to be beneficial. The total corrected cell fluorescence (TCCF) was calculated using Fiji/ImageJ and the data acquired from the GFP channel of the EVOS fluorescence microscope. The following calculation was used to plot the graph in Figure 3.12: TCCF = Integrated density – (area of the selected cell x mean background fluorescence readings) (Cheng et al., 2018). The TCCF was calculated for both the cytoplasmic and nuclear sections of the cell to identify where there was the most staining. Overall, there seems to be highly significant differences in the amount of fluorescence between the cytoplasm and nucleus for the majority of Affimer concentrations and fixation methods. It seems that both glyoxal and methanol benefit the most from having concentrations ranging from 5-10 µg/ml. The best concentrations for PFA, however, seemed to be 2-5 µg/ml, indicating some increased sensitivity overall, even though the fluorescence was lower when compared to the other fixation methods.

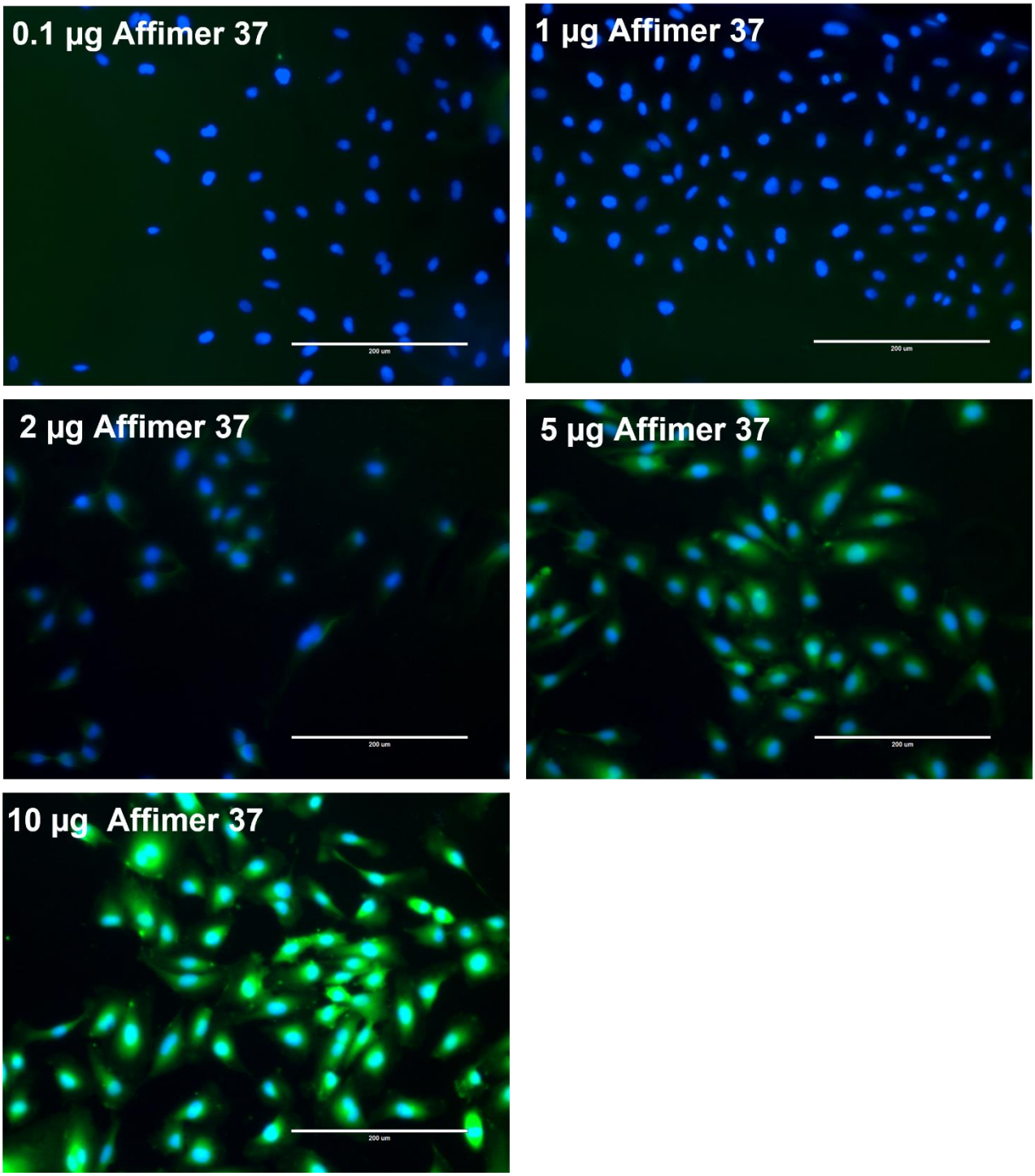

Figure 3.9. Analysis of Affimer 37 binding using glyoxal fixation. HUVECs were fixed with 5% (v/v) glyoxal (see Materials and Methods) and incubated with various concentrations of AlexaFluor488-labelled Affimer 37 (green). Digital fluorescence microscopy was used to visualize bound Affimer 37 (green) and cell nuclei were stained with DAPI (blue). Images were taken on an EVOS FL Auto microscope. Bar, 200 µm

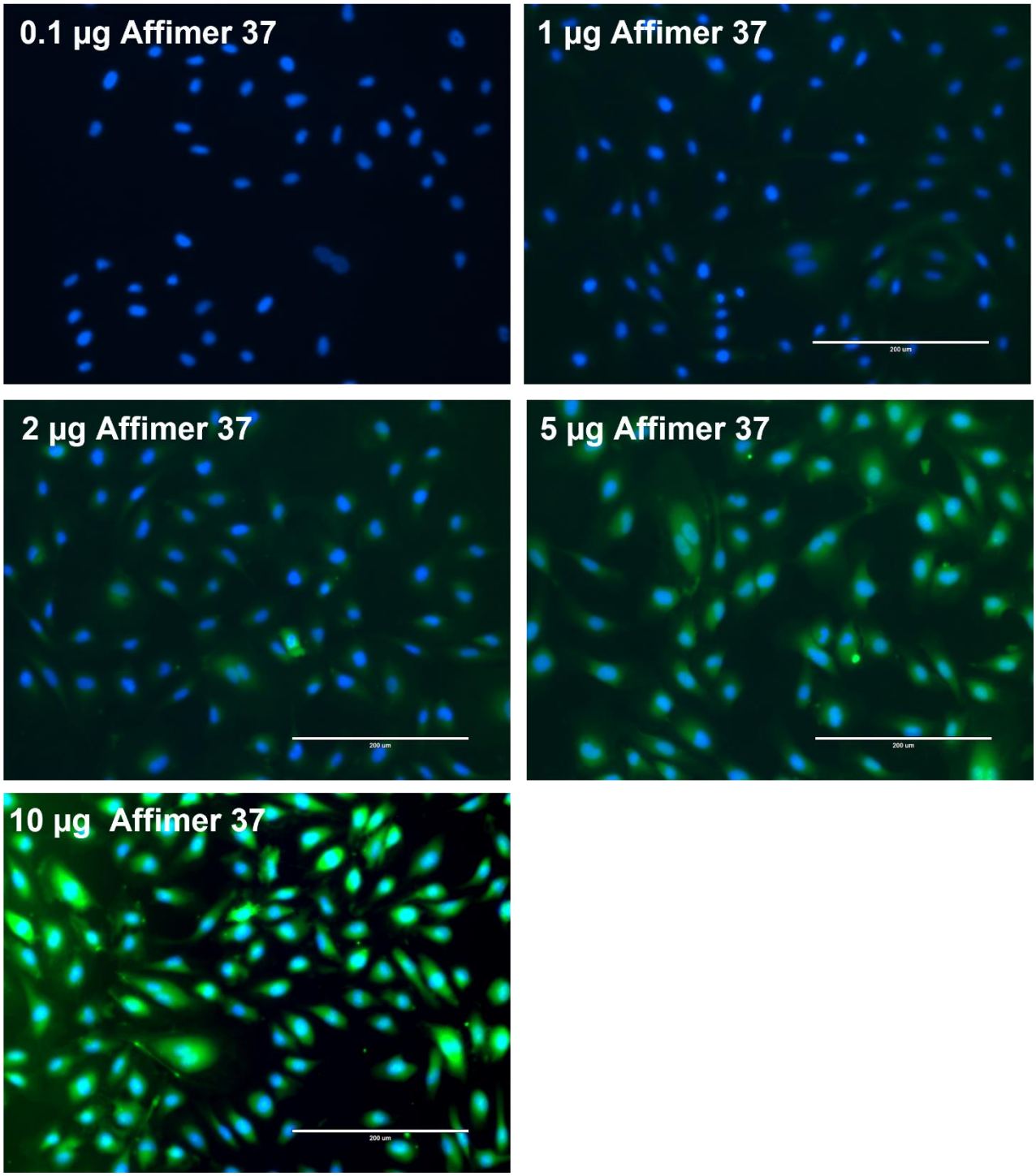

Figure 3.10. Analysis of Affimer 37 binding using methanol fixation. HUVECs were fixed with ice-cold methanol (see Materials and Methods) and incubated with various concentrations of AlexaFluor488-labelled Affimer 37 (green). Digital fluorescence microscopy was used to visualize bound Affimer 37 (green) and cell nuclei were stained with DAPI (blue). Images were taken on an EVOS FL Auto microscope. Bar, 200 μm

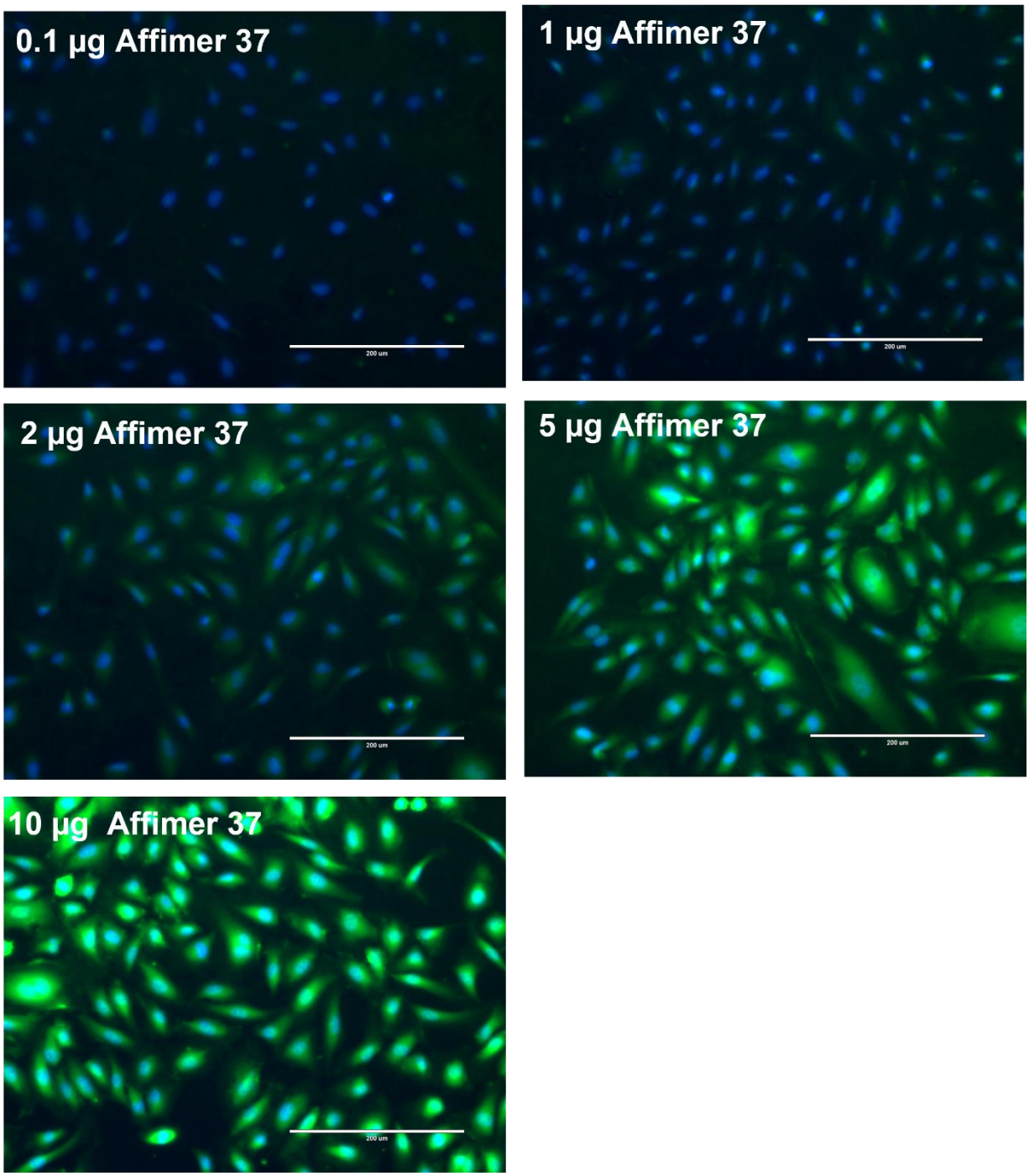

Figure 3.11. Analysis of Affimer 37 binding using paraformaldehyde fixation. HUVECs were fixed with 3-4% (w/v) PFA (see Materials and Methods) and incubated with various concentrations of AlexaFluor488-labelled Affimer 37 (green). Digital fluorescence microscopy was used to visualize bound Affimer 37 (green) and cell nuclei were stained with DAPI (blue). Images were taken on an EVOS FL Auto microscope. Bar, 200 μm.

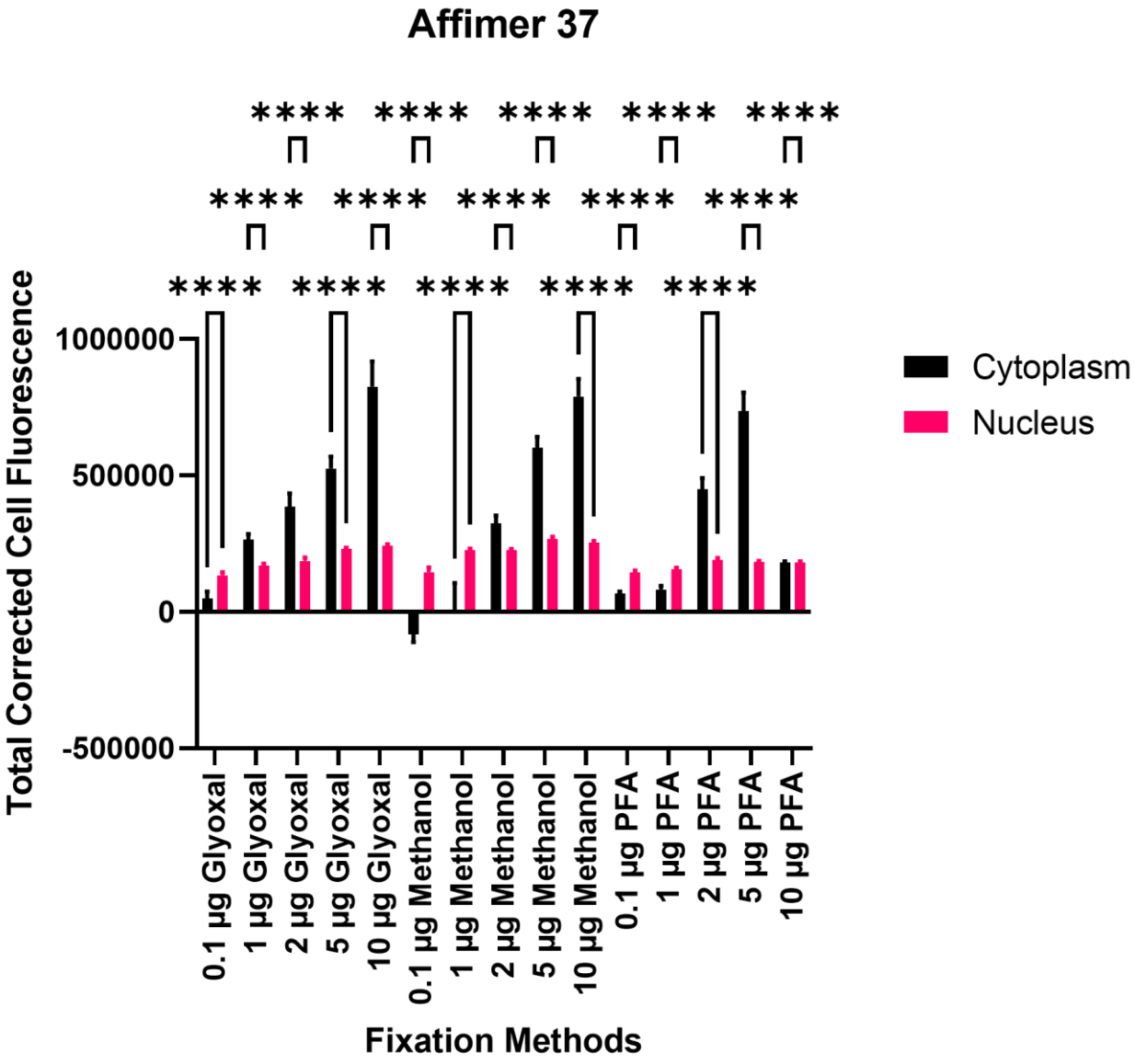

Figure 3.12. Comparison of different chemical fixation methods to visualise Affimer 37 binding to endothelial cells. Quantification of Affimer 37 binding to endothelial cells using 3 different chemical fixation methods. Three fields of view were taken from each corresponding well. Images were analysed Fiji/Image J in order to calculate the total corrected cell fluorescence seen in the green channel. Staining was mainly seen in the cytoplasm of the HUVECs but there was also some staining in the nuclei. Error bars denote ±SEM. Significance: ****, p<0.0001 (n=3).

Finally, confocal microscopy was used in to discover whether more information about VEGFR-Affimers binding to HUVECs could be discovered by using a higher resolution microscope (Figs. 3.14-3.15). In Figure 3.14, Affimer 37 was once again titrated to see if the confocal images would correlate with standard recordings using a digital fluorescence microscope with glyoxal fixation. An interesting finding is that using 10 µg/ml of the Affimer showed brighter fluorescence as compared to the higher 25 µg/ml. In addition, there was also still some nuclear staining at all the concentrations as well, although more defined peri-nuclear regions of AlexaFluor 488 staining can be observed, after using 5 µg/ml of the Affimer. The fact that this concentration seemed to perform better specificity-wise overall, correlates well with the data elicited from previous images. Confocal images with 10 and 25 µg/ml of the cross-reactive VEGFR1-66 and the VEGFR2-specific A9 are seen in Figure 3.15, using in conjunction with glyoxal fixation. These were also compared to a standard goat anti-VEGFR1 antibody which acted as a positive control. Here, despite the intracellular background staining, there do appear to be pockets of specific binding of the Affimers for 10 µg/ml of both Affimer 66 and Affimer A9. It is interesting, however, that 25 µg/ml of Affimer 66 seemed to be even more specific, as the nuclei did not appear to be stained in the majority of the cells. This was an interesting result, as it contrasts with the observations made from previous microscopy images, where a higher concentration of Affimers showed brighter fluorescence, yet less specific binding. It would be of value in future experimentation, to make more replicates of these experiments to enable a calculation to be made as well, for the TCCF for confocal images. These results, overall, indicate that Affimers have the potential to be good binders, if the protocols were either optimised or they were titrated further.

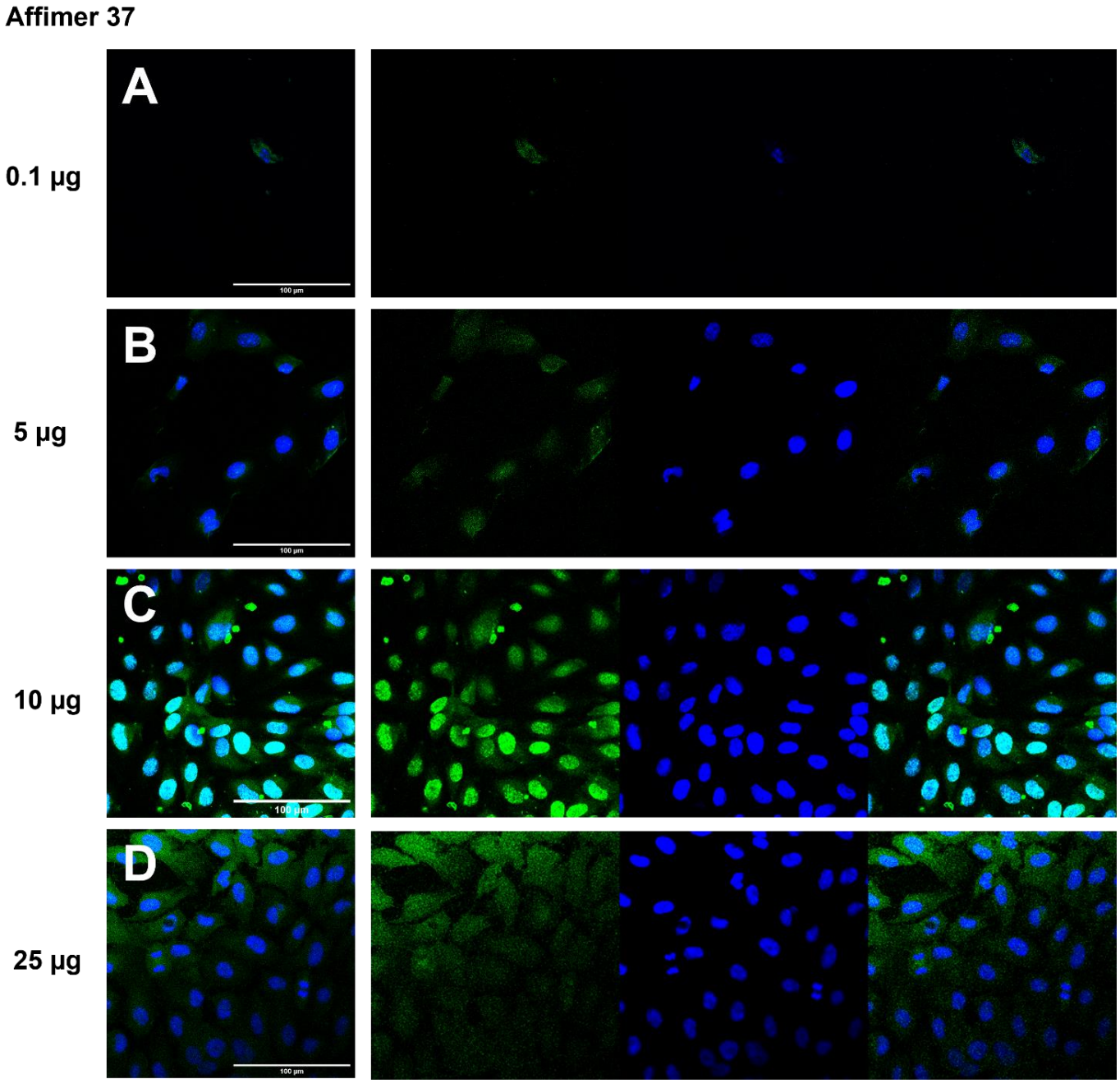

Figure 3.14. Confocal microscopy using Affimer 37. AlexaFluor488-labelled Affimer 37 was diluted to different concentrations and incubated with HUVECs, before fixation with 5% glyoxal. Nuclei were stained with DAPI (blue). Images were taken on a Zeiss LSM510 confocal laser microscope 63x magnification. Montages were also created on Fiji/ImageJ to show both cytoplasmic and nuclear staining. Bar, 100 µm.

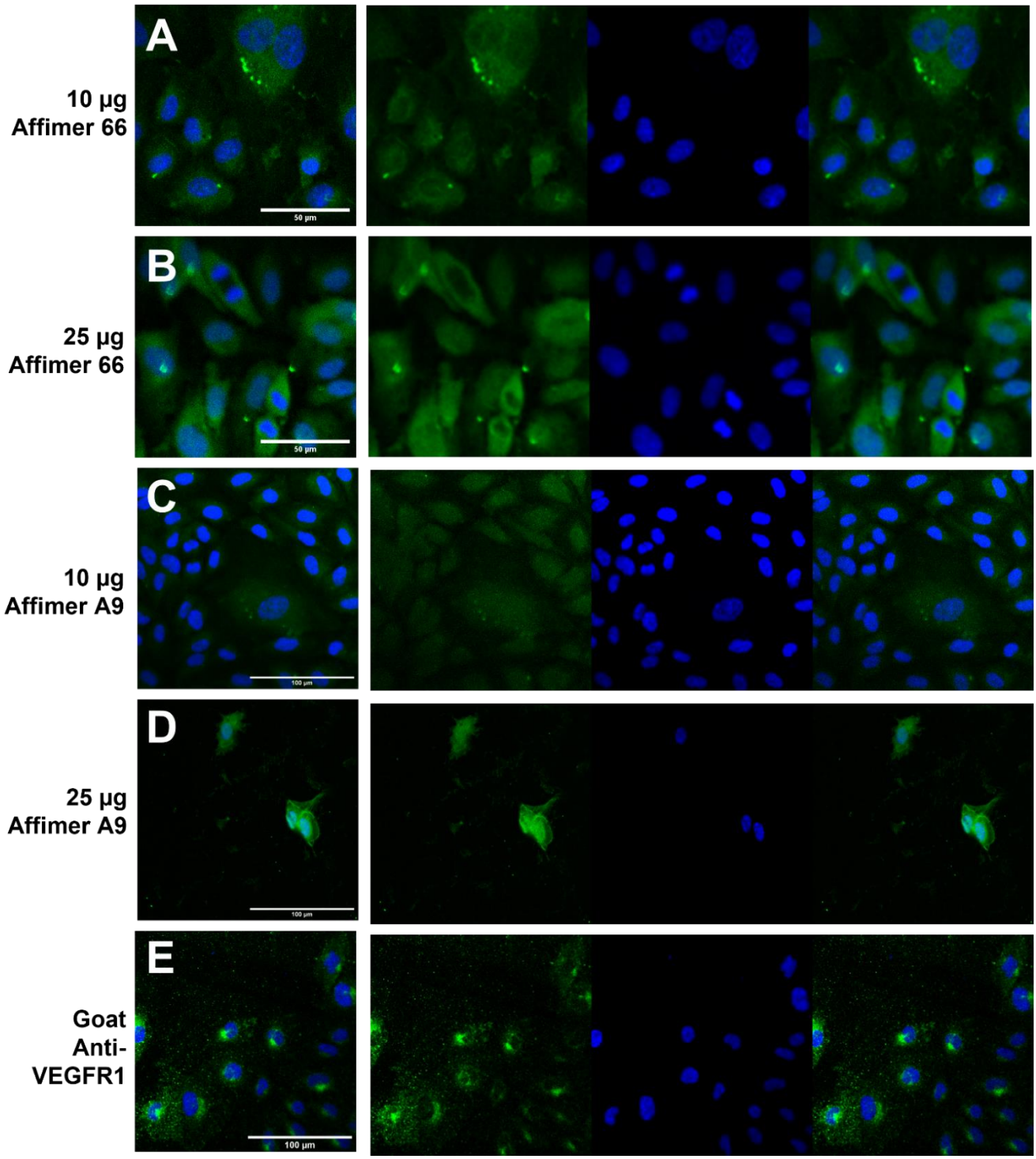

Figure 3.15. Confocal microscopy to compare different VEGFR1 and VEGFR2-specific Affimers. AlexaFluor488-labelled Affimers (green) were used to detect (A, B) VEGFR1 using Affimer 66, and (C, D) VEGFR2 using Affimer A9. (A, C) 10 μg/ml or (B, D) 25 μg/ml labelled Affimer was used in the experiments. HUVECs were then fixed with 5% glyoxal and processed for fluorescence microscopy. (E) Goat anti-VEGFR1 antibody staining of HUVECs was used as a control. Nuclei were stained with DAPI (blue). Images were taken on a Zeiss LSM510 confocal laser microscope at 50x and 63x magnification. Montages were also created on Fiji/ImageJ to show both cytoplasmic and nuclear staining. Bar, 100 μm.

3.3 DISCUSSION

The experimentation detailed in this chapter has produced some interesting and unexpected results. At the start of the study, it was hoped to create more Affimers specific to VEGFR1. This aim, of course, would require the creation of cross-reactive Affimers specific to the human and murine versions of the VEGFR1 protein. It was discovered over time that one of the main reasons why this aim did not work out as hoped, was due to the premature degradation of the VEGFR proteins used in the phage display process. Since VEGFRs are receptor tyrosine kinases, being taken out of the fridge at 4^{O}C and being put back in multiple times throughout each screening stage may have potentially affected their stability. VEGFRs in serum can keep 90% of their initial concentration at -20^{0}C over 3 months and decades at -75^{0}C and withstand up to five cycles of freeze-thawing, but they can still become unstable (Kisand *et al.*, 2011; Lee *et al.*, 2015). The lyopholization (freeze-drying) process can also potentially affect the activity of proteins. The VEGFR proteins used were prepared using mannitol and trehalose as lyoprotectants, but these could have potentially, not been fully protective, as demonstrated by a previous study where the use of trehalose did not fully prevent structural changes of lysozyme (Roy and Gupta, 2004).

Another important factor to consider was that though the yeast SUMO 10 Affimer, specific to *SMT3,* was used throughout the experimentation as a negative control, it often displayed the opposite effects to those expected. For instance, multiple phage display screens were disregarded due to the fact that the yeast SUMO 10 Affimer also appeared to bind to the VEGFR proteins in the screening stages. This was also seen in the IP studies, where the Affimer appeared to strongly bind to VEGFR1.

These results, however, do not mean that the Affimer may not have been able to bind to the human form to some degree, as *SMT3* shares ~50% sequence homology with that of the human SUMOs (1, 2 and 3) (Newman *et al.*, 2017). There is currently a working model of SUMOylation which in turn affects SENP1-mediated VEGFR2 trafficking. Similar to ubiquitination, the theory is that there is a small pool of SUMOylated VEGFR2 within the Golgi. During ischaemic conditions, SENP1 is upregulated and therefore

causes VEGFR2 to be de-SUMOylated and trafficked to the plasma membrane to induce angiogenesis. Hyper-SUMOylation can occur during diseases such as diabetes, which decreases SENP1 (Zhou *et al.*, 2018). SUMO1 has also been found to increase endothelial tubule formation, highlighting its role in angiogenesis; SUMO2 and 3 may also be able to compensate for these functions if necessary (Rabellino et al., 2020). In fact, the HexaHis blot reveals a band at ~60 kDa, which could be a cytoplasmic fragment produced from proteolytic cleavage, which is possibly due to matrix metalloproteinase 14 (MMP14) (Han *et al.*, 2016). In previous studies with IPs on HUVECs, a 60 kDa cytoplasmic fragment was also seen alongside cleaved VEGFR1 protein (Rahimi et al., 2009). In this PhD project, this band was not detected with the anti-VEGFR1 antibody, which only binds to the extracellular domain of the receptor. Although precautions were taken to prevent proteolysis during HUVEC cell lysis, there may have still been some that occurred. However, as the anti-HexaHis antibody purely recognises the Affimers, it is possible that it represents the binding of yeast SUMO 10 to this VEGFR1 fragment since it is meant to the intracellular SUMO. It is also possible that it is the His tag itself, which could be generating a non-specific response, as there can be a lot of background in mammalian cell lines due to the presence of native histidine residues (Young *et al.*, 2012). Previous studies have also shown high variability between blotting results depending on the brand of HexaHis antibody used (Debeljak *et al.*, 2006).

The studies implementing a protocol similar to an IP also show a potential binding site for one VEGFR1-specific Affimer,1. Interestingly, this binding site appears to be between domains 1-4 rather than 1-5, which is puzzling since domains 4-5 are closely associated with one another. In a structural study by Mueller *et al.,* (2017) a complex is said to be formed between VEGF-A and D2-3 of the VEGFR1. There are in fact three sockets within this complex: the top D3-D4 bound by VEGF-A; the centre consisting of D4-D5 and finally the bottom D5-D7 which aids stability. VEGF-A binding causes a conformational change within the receptor, including the interlinking between the chains for D4-5, to bring closer the gap between

protomers, which ultimately aids homodimerization (Markovic-Mueller *et al.*, 2017). Although it is too early to tell, there may be a possible mechanism of action which could be deduced from these findings. It is accepted fact that heparan sulfate proteoglycans (HSPGs) and neuropilin receptor-1 (NRP-1) are key co-receptors which enhance VEGFR activity. Heparin is a form of HSPG for use in research and has been found to strongly bind to D1-4 of the mouse form of VEGFR1 (sFLT) at physiological concentrations in baculovirus and insect cells. It was found, however, that it is not able to bind to D1-2 or D1-3 of the sFLT, indicating that the fourth domain of FLT-1 was the main heparin binding site (Park and Lee, 1999). In another study, the affinity of immobilized heparin for VEGFR1 was 5x higher than it was to that of NRP-1 (11 nM and 50 nM respectively), whilst there was no binding to VEGFR2 at all (Teran and Nugent, 2015). This is an unexpected result, as heparin is known to increase HUVEC proliferation, which is typically a VEGFR2-mediated function (Park and Lee, 1999). It is of interest, however, that when VEGF-A_{165} was added, which has a binding site for heparin, there was a significant increase in the binding of heparin to VEGFR2, which could explain this beneficial contribution towards cell growth (Teran and Nugent, 2015). It could be possible to inhibit the strong interaction of VEGFR1 with the HSPGs, thereby allowing VEGF-A_{165} to bind to this endogenous heparin and therefore stimulating angiogenesis. It is possible, therefore, that Affimer 1 is in fact inhibiting this heparin binding region on the fourth Ig-like loop of VEGFR1. This would provide a description of one possible mechanism by which VEGFR1-specific Affimers may ultimately be able to enhance VEGFR2 signalling. However, as previously mentioned there would need to be further repetition of this experiment in order to confirm this suggestion, in combination with testing more Affimers at various concentrations.

Finally, the immunofluorescence studies showed that AlexaFluor-tagged Affimer binding varied depending on their concentration and the fixation type used. Although PFA is the standard fixation type in most labs, it has previously been found that Affimers may react better to other fixation types. Methanol has previously been found to be a good alternative choice, but it can also cause a loss of proteins in the membrane and cytosol similar to

that of PFA (Richter et al., 2018). It would be of great value in the future to carry out a full study on all of the available Affimers, with each of these fixation methods and concentrations, so as to ascertain more concrete information. The results may also appear less conclusive due to the fact that there is also some nuclear staining. This would usually be attributed to non-specific staining by the antibody/antibody-mimetic in question, either to do with technique or too high a concentration has been used. However, the small size of the Affimers could mean that they penetrated the cell membrane more easily and traversed further than intended, perhaps into the nucleus. One way to potentially decrease the chance of this happening would be to reduce the amount of time that the Affimers are incubated with the fixed cells. ~1-2 h was used during this study, but incubation for even less time could be more optimal. There may also be another potential explanation where there may indeed be some VEGFR proteins present within the nucleus. For instance, Domingues *et al.* (2011) found that VEGFR2 may translocate to the nucleus after VEGF stimulation, with their results even showing a potential role in the regulation of its own transcription (Domingues *et al.*, 2011). A similar study has also identified the potential presence of VEGFR1 within the nucleus after γ-secretase cleavage (Carpenter and Liao, 2009). The results from these studies, however, only supply tentative additional indications, when taken along with the evidence from these studies, further experimentation is required to determine whether or not there is specificity of binding to cells. If the immunofluorescence studies seen in Figures 3.9-3.11 were to be repeated in the HUVECs, to do knockdown or knockout studies on VEGFR1 using siRNA and CRISPR Cas9 transfection respectively. There is also a possibility that attempting a transient transfection of human embryonic kidney 293 (HEK293) cells with a soluble splice variant of VEGFR1 would be possible; this would create a cell line overexpressing VEGFR1 which could be compared to non-transfected HEK293 cells using this same IF protocol.

In general, the evidence from this chapter demonstrates that VEGFR-specific Affimers are strong binders on a molecular level, regardless of whether they are cysteine or non-cysteine tagged. They may also have a

particular use *in vivo* studies in the future due to their cross-reactivity with animal VEGFR1, as well as finding a purposeful function in the diagnosis of underlying illness. The following chapters will focus more on the effects of these Affimers on cellular function.

Chapter 4

Modulation of signal transduction, trafficking and tubulogenesis by VEGFR1-specific Affimers in endothelial cells

4.1 Introduction

The function of VEGFR1 within endothelial cells is currently not very well understood. This VEGF receptor tyrosine kinase can exist as either soluble or membrane-bound isoforms generated by alternative RNA splicing. Both of these protein isoforms of VEGFR1 have an affinity for VEGF-A that is 10-100-fold greater than that exhibited by VEGFR2, indicating VEGFR competition for VEGF-A ligand could regulate endothelial responses. VEGFR1 can also form a heterodimer with VEGFR2, but ~50-90% of these are non-productive or non-signalling complexes (Chappell et al., 2016; Shaik et al., 2020). VEGFR1 is, therefore, often attributed as to being an indirect inhibitor of VEGFR2 signalling and function. VEGFR1, however, can also play a key role in cell survival and proliferation via binding to other ligands such as VEGF-B and PlGF. This aspect will be explored in more detail in Chapter 6 studies into a human epithelial cancer cell line.

There are a multitude of studies focusing on inhibiting pathological angiogenesis in order to treat diseases such as wet AMD and cancer. A particular problem with cancer therapy is caused by the large number of different tumour mutations (in different cancer patients) which modulate multiple signal transduction pathways. The increased use of anti-angiogenic therapies in cancer is becoming more established as a route to reducing tumour angiogenesis. Previous studies *in vivo* have already shown that there is an up-regulation of pro-angiogenic factors including VEGF-A during myocardial ischaemia in mice. In combination with *in vitro* angiogenesis and cell migration, experimentation has suggested that VEGF-A administration can have an overall cardioprotective effect (Zou et al., 2019).

In this chapter, we explore the use of primary human endothelial cells (HUVECs) to evaluate how targeting VEGFR1 using Affimers modulates cellular responses. A working hypothesis was that inhibiting VEGFR1 using Affimers could be beneficial for VEGFR2-specific responses. The use of different concentrations of different VEGFR1-specific Affimers to modulate endothelial function was also explored. These studies provide a foundation for future work in establishing how targeting VEGFR1 could be useful in a disease context.

4.2 RESULTS

4.2.1 VEGFR1-specific Affimer titration and cell viability

One of the main concerns about drug development is whether such agents are safe for clinical use. To address this issue, dose-dependent titration of potential drug molecules to assess cell viability is important. Such assays often rely on monitoring mitochondrial activity e.g. MTT or MTS assays. These assays rely on the conversion of MTT/MTS to purple formazan crystals by healthy mitochondria. The larger the number of healthy cells, the greater the purple colour increase, which can be easily monitored at 570 nm using a spectrophotometer (Moradi, 2018). Three different concentrations of Affimer were tested, at 0.1, 10 and 100 µg/ml, on endothelial cells (HUVECs). These were tested as well at different cell numbers; this process being followed by stimulation with 25 ng/ml of VEGF-A_{165} (named VEGF-A throughout). Analysing the Affimers against different HUVEC seeding densities would potentially not only help optimise future cellular experiments, but also to observe any patterns which might be seen with different VEGFR1 inhibitor concentrations. These concentrations of Affimers were used in order to identify whether a change in dosage would potentially affect cell survival, especially the highest concentration. These concentrations would not necessarily be used in the future experiments due to wanting to keep to relative safe physiological levels but using a high dosage now could at least help in developing future safety protocols. It would of course be *in vitro* cells being used for comparison with animal experiments, but nevertheless, they could at least provide a good reference for future use. An assessment of the cross-reactive VEGFR1-specific

Affimer 66, was also necessary due to the potential for it to be used in animal-based experiments. The absorbances were measured at three time points i.e. 0, 24 and 48 h.

Figure 4.1 shows cell viability assays at not only different initial HUVEC seeding densities, but also different concentrations of the two key Affimers, 35 and 66. These were compared to cell treatment with a VEGFR tyrosine kinase inhibitor, Sutent (sunitinib malate, SU11248; SUTENT^{TM}) and cells cultured in either serum-free (MCDB131 + 0.2% BSA) or complete medium (ECGM+VEGF-A) (le Tourneau *et al.,* 2007). Results are also seen for cells which were incubated with only VEGF-A. Initially, it was decided to measure the effects of the Affimer VEGFR1-specific Affimer 35 (non-cysteine tagged) due to it being effective in previous experiments (Dr. G. Smith, unpublished data). In the previous experiments, cell viability was high even at Affimer concentration of 100 µg/ml. An additional two lower concentrations were added for the experimentation carried out in this thesis in order to aid in the assessment of HUVEC viability at more clinically relevant concentrations.

Looking at the graphs in both of the figures shows a general trend: that seeding 1000 cells showed enhanced viability for the majority of the conditions after 48 h (Fig. 4.1). This was an expected result as there is often more successful growth with lower cell seeding densities due to the lack of competition for potential growth factors within the serum. However, the seeding density of 3000 cells overall seemed to show the most change in terms of cell proliferation, especially with Affimer 35. Here, 100 µg/ml of Affimer 35 showed the greatest increase in absorbance and therefore viability over the course of 24-48 h of ~900% (0.06 to 0.6). The inhibition of VEGFR1 using Affimer causes an almost 3-fold increase in cell viability (Fig. 4.1). This was similar to that observed with Affimer 66 at 100 µg/ml, although it was not as great an increase in cell viability at ~30% (0.07-0.1). One thing to note would be that the use of the VEGFR1-specific Affimers often showed larger increases in cell survival as compared to the controls, including with ECGM.

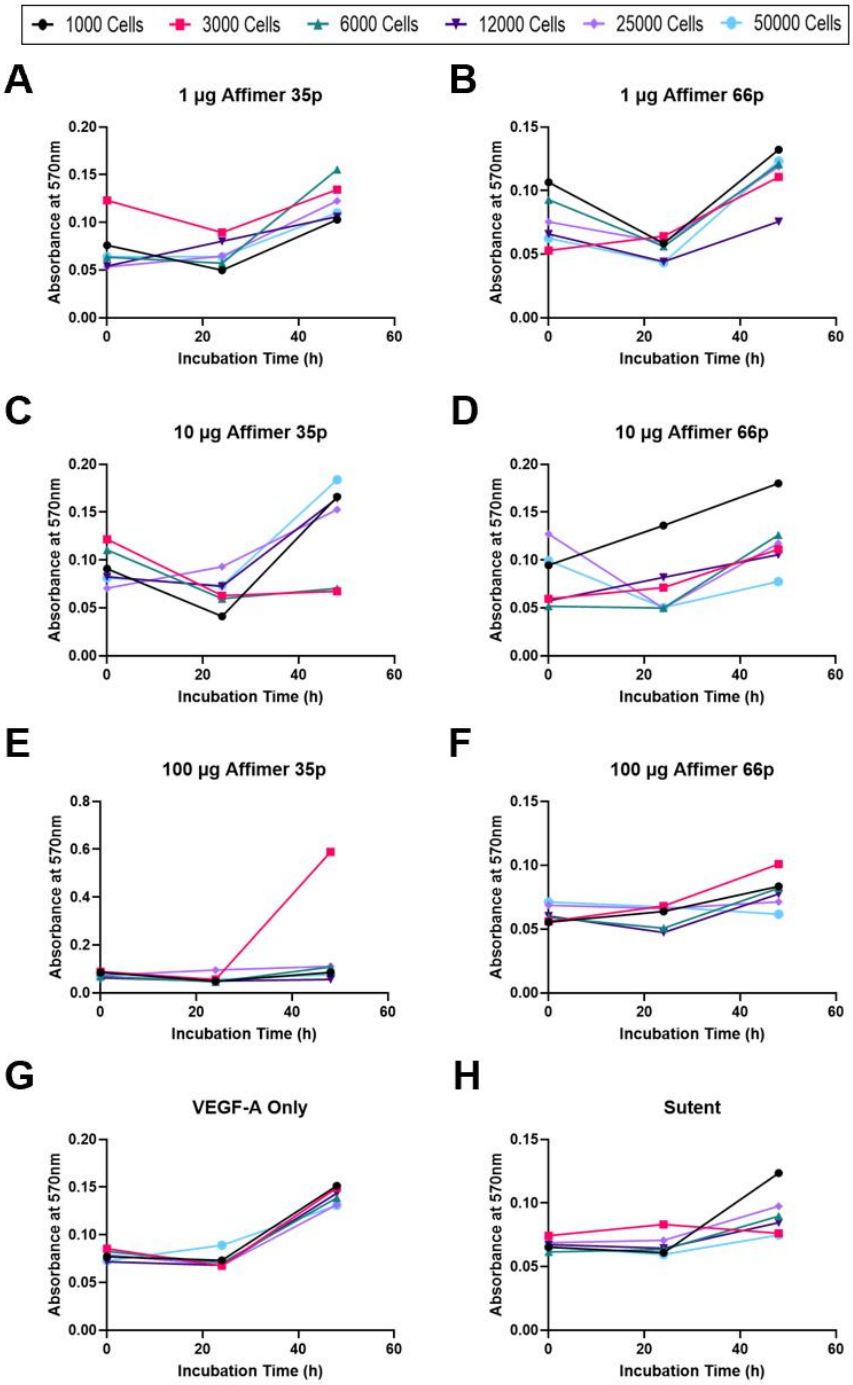

Figure 4.1 Comparing the effects of VEGFR1-Affimer concentration and HUVEC cell number on viability. HUVEC cell viability was determined by an MTT assay at 24 and 48h. HUVECs were starved in MCDB131 medium prior to incubation with the Affimers for 30 min followed by stimulation with 25 ng/ml VEGF-A. MTT was added at 24h prior to measurement on a spectrophotometer at 570 nm. This measurement was repeated at 48h. Graphs represent the effect of the initial number of cells plated against (A-F) two different VEGFR1-specific Affimers at different concentrations (1-100 µg/ml) and (G) VEGF-A stimulation only as a positive control with (H) 1 µM Sutent as a negative control (n=1).

In Figure 4.2 analysis of the final recording of cell viability at 48 h was totalled, and an average made for each treatment. This graph depicts a comparison being made to ECGM+VEGF-A, to compare how Affimer inhibition influences HUVEC viability in contrast to their ideal growth conditions. All of the treatments seemed to generally show increased cell survival as compared to ECGM, including the serum-free medium containing VEGF-A alone. The average cell viability for all of the concentrations of Affimer reagents combined were 69% and 23% higher than that of ECGM for 35 and 66 respectively. In particular, the average of Affimer 35 was higher than the 66% increase seen with VEGF-A alone. Also, the highest individual increase was seen with 100 µg/ml of Affimer 35 by over 106% as compared to ECGM. These experiments potentially highlight the important fact that even the highest concentrations of these new inhibitors would be safe for the human body.

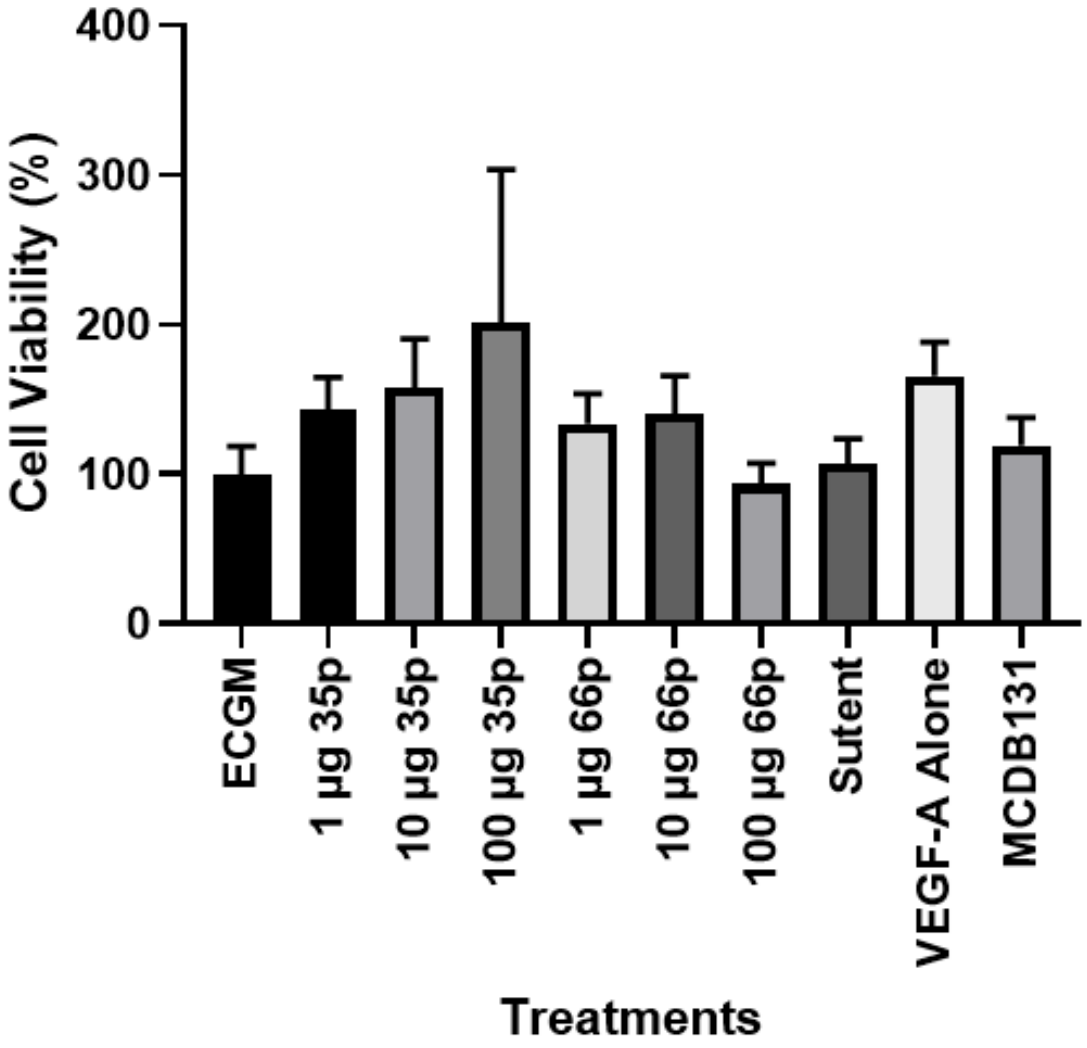

Figure 4.2 VEGFR1-specific Affimers are not toxic to endothelial cells. The cell viability of HUVECs were assessed using MTT assays and calculated against a positive control (ECGM medium+VEGF-A). The two VEGFR1-specific Affimers tested, 35p and 66p, were trialed at three different concentrations (1-100 µg/ml) (n=6).

4.2.2 VEGFR1-specific Affimers promote VEGF-A-stimulated endothelial cell proliferation

MTT assays measure cell viability but are not an effective assay for measuring cell proliferation. Instead, measuring the Bromodeoxyuridine (BrDU) incorporation into new DNA using ELISA is a more accurate measure of cell proliferation (Bergler *et al.*, 1993; Clifford and Downes, 1996). The BrDU assay, as used over the course of 24 and 48 h of Affimer treatment, is well illustrated here (Fig. 4.3). A comparison of 9 VEGFR1 Affimers, some cysteine and non-cysteine tagged, at 100 µg/ml along with the Yeast SUMO 10 Affimer were evaluated. This evaluation demonstrates that the majority of VEGFR1-specific Affimers stimulated VEGF-A-regulated endothelial cell proliferation (Fig. 4.3), as compared to the control. This was particularly notable with Affimers 37c, 48c and 2p, where HUVEC proliferation was 50% greater than treatment with VEGF-A alone. There was also an increase in endothelial proliferation using Yeast SUMO 10-specific Affimer (Fig.4.3). Although there were slightly higher values seen with the cysteine tagged versions of VEGFR1-specific Affimers, these were not significant in comparison to their counterparts. Interestingly, Affimer 35c treatment caused ~50% decrease in cell proliferation compared to the control (Fig. 4.3).

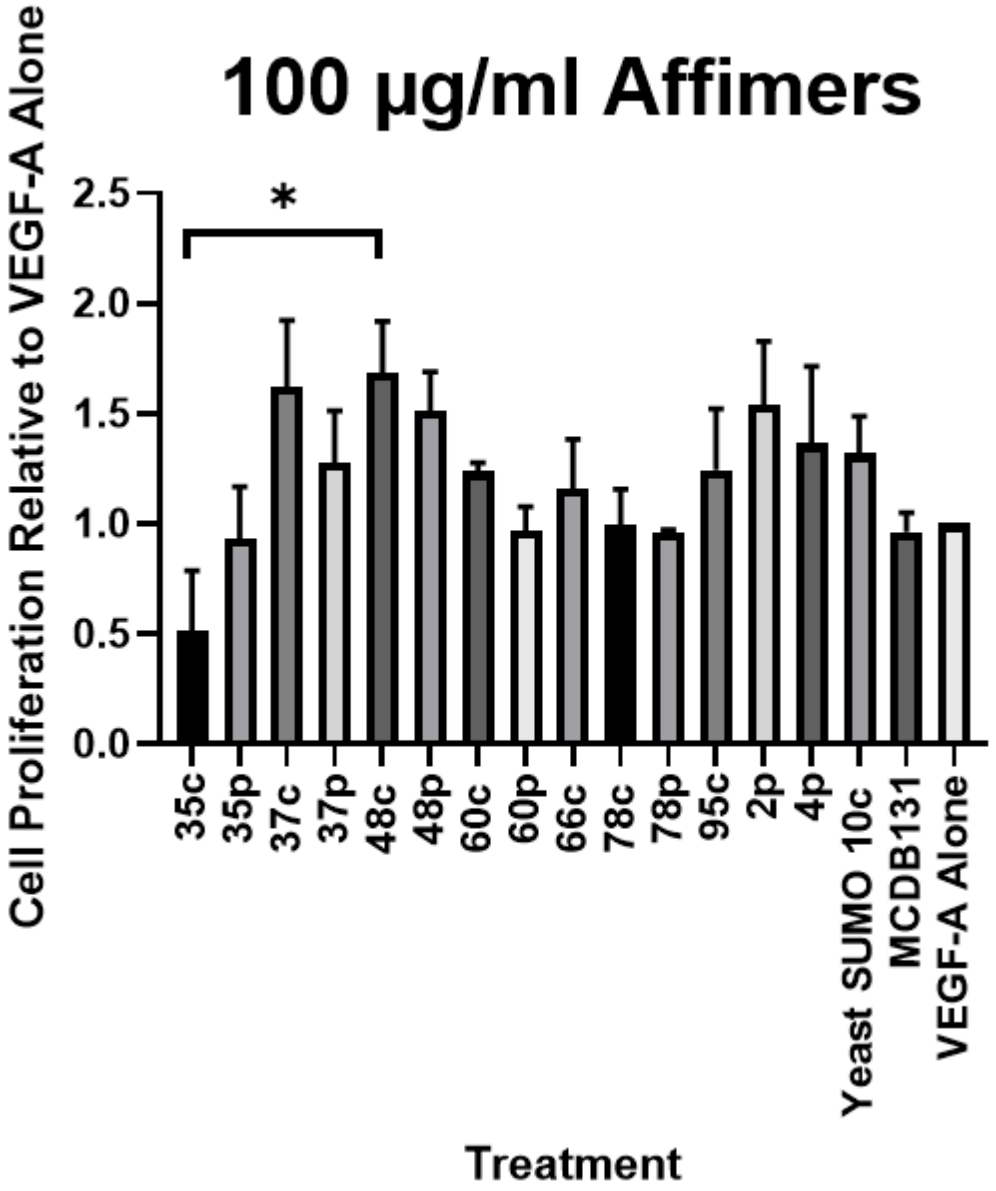

Figure 4.3 Both forms of VEGFR1-specific Affimers mediate endothelial cell proliferation. The effects of both cysteine and non-cysteine tagged (labelled "c" and p") Affimers on HUVEC BrDU incorporation which was quantified using a colorimetric proliferation ELISA. HUVECs were treated with 100 µg/ml of the VEGFR1-specific or Yeast SUMO10c (control) Affimer prior to stimulation with 25 ng/ml VEGF-A. BrDU reagent was added to the cells for four hours prior to fixation and incubation with a BrDU-specific antibody. Serum-free medium+VEGF-A (MCDB131) was used as an additional control. The final absorbances were calculated against cells which had only been stimulated with VEGF-A. Error bars denote ±SEM. Significance: *, $p<0.05$. (n=3).

One possibility is that Affimer concentration could be influencing VEGFR1-specific Affimer effects. HUVEC proliferation assays were carried out using 0.1, 1, and 10 µg/ml of the non-cysteine tagged VEGFR1-specific Affimers, in conjunction with VEGF-A (Fig. 4.4) or VEGF-B (Fig. 4.5) stimulation respectively. Comparisons were made relative to endothelial growth in ECGM+VEGF-A, labelled as the control, due to endothelial cells typically being cultured in this medium. Both of these figures show that the ECGM control generally had the highest amount of proliferation out of all the conditions. This was, however, to be expected as this medium allows optimal conditions for the growth of the endothelial cells. In Figure 4.4**,** we can see a range of effects on endothelial cell proliferation based on the concentrations of the Affimers used. These numbers were often higher than that of controls such as VEGF-A alone, but this ultimately depended on the Affimer concentration present. For example, Affimer 11 showed the lowest amount of cell proliferation when compared to the other VEGFR1 inhibitors at 1 µg/ml, with it in fact being ~ 25% lower than that of VEGF-A alone. However, it exceeded isolated VEGF-A stimulation by ~3% when used at 10 µg/ml. The majority of these Affimers showed a general trend of increased proliferation with increased concentration. However, some of the Affimers remained consistent at every concentration such as cross-reactive VEGFR1-specific Affimer 66. This, however, was the opposite for VEGFR1-specific Affimer 60, which provided more effects at lower concentrations (Fig. 4.4). This Affimer was in fact the best in terms of enhancing stimulation out of all the Affimers at both 0.1 and 1 µg/ml. However, Affimer 60 had the least effects at 10 µg/ml. This was the opposite of Affimer 2, which was worst at 0.1 µg/ml (30% decrease from VEGF-A), but best at 10 µg/ml (5% increase from VEGF-A). Figure 4.5 shows the cell proliferation results using VEGFR1-specific Affimers alongside VEGF-B stimulation. It can also be seen from this figure, that when using Affimer 35, increasing dosage decreases endothelial cell proliferation. This is in contrast to Affimer 1, where cell proliferation is consistently high at all Affimer concentrations, indicating that it may not bind specifically to VEGFR1. These results were

largely in opposition to those effects observed using Affimers alongside VEGF-A.

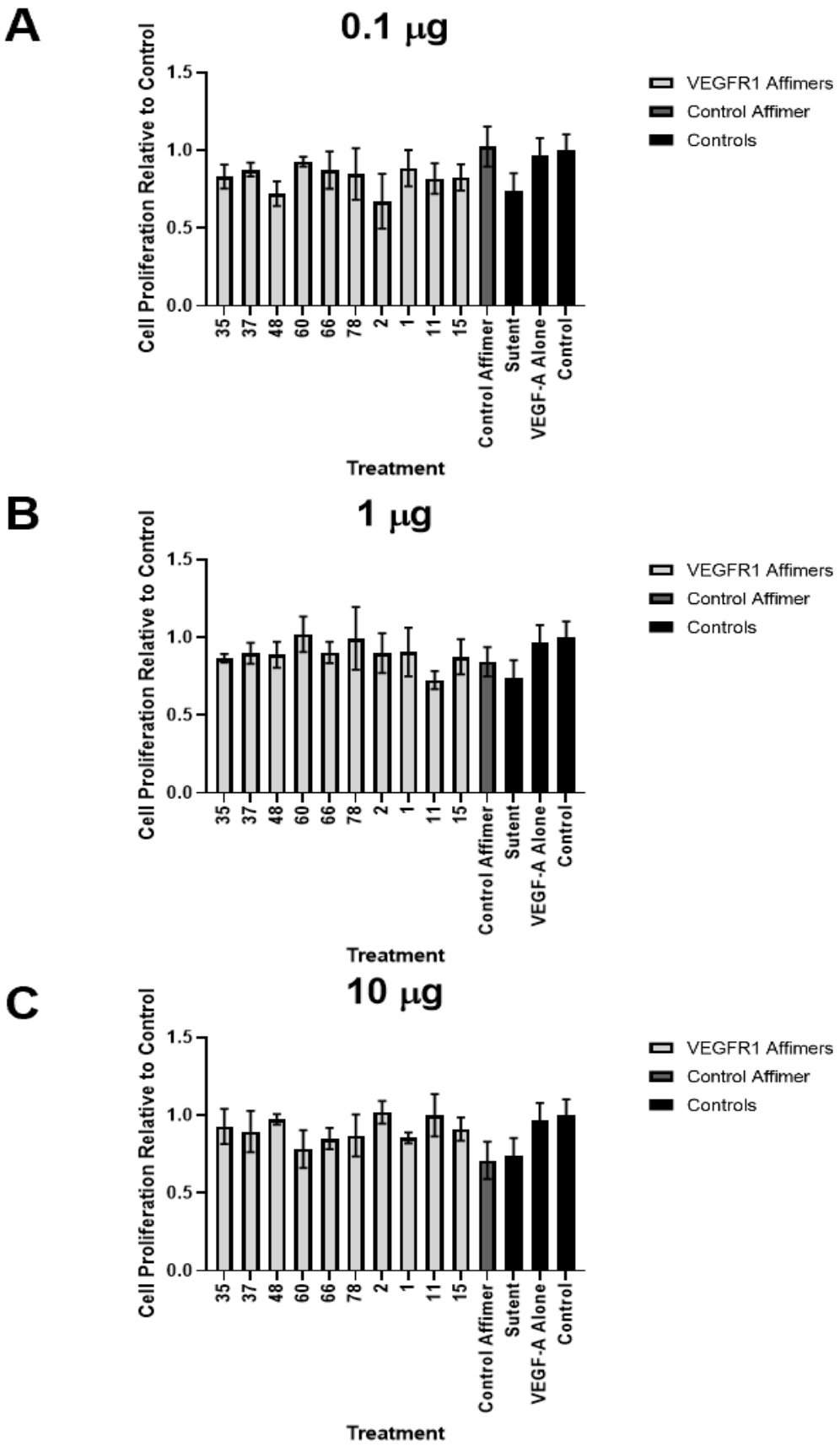
A
0.1 μg
Cell Proliferation Relative to Control
1.5
1.0
0.5
0.0
35
37
48
60
66
78
2
1
11
15
Control Affimer
Sutent
VEGF-A Alone
Control
Treatment
VEGFR1 Affimers
Control Affimer
Controls
B
1 μg
Cell Proliferation Relative to Control
Treatment
VEGFR1 Affimers
Control Affimer
Controls
C
10 μg
Cell Proliferation Relative to Control
Treatment
VEGFR1 Affimers
Control Affimer
Controls

Figure 4.4 VEGFR1-specific Affimers can positively influence VEGF-A mediated endothelial cell proliferation at a range of concentrations. Affimers at three different concentrations were incubated with HUVECs, followed by the measurement of BrDU incorporation using a colorimetric proliferation ELISA. HUVECs were treated with (A) 0.1, (B) 1 and (C) 10 µg/ml of VEGFR1-specific Affimer for 30 min prior to stimulation with 25 ng/ml VEGF-A. These were also compared to a non-specific control Affimer (control) along with 1 µM Sutent, VEGF-A alone and ECGM medium+VEGF-A (control). BrDU reagent was added to the cells for four hours prior to fixation and incubation with a BrDU-specific antibody. The final absorbances were calculated against cells which had been incubated with ECGM+VEGF-A. Error bars denote ±SEM (n=3).

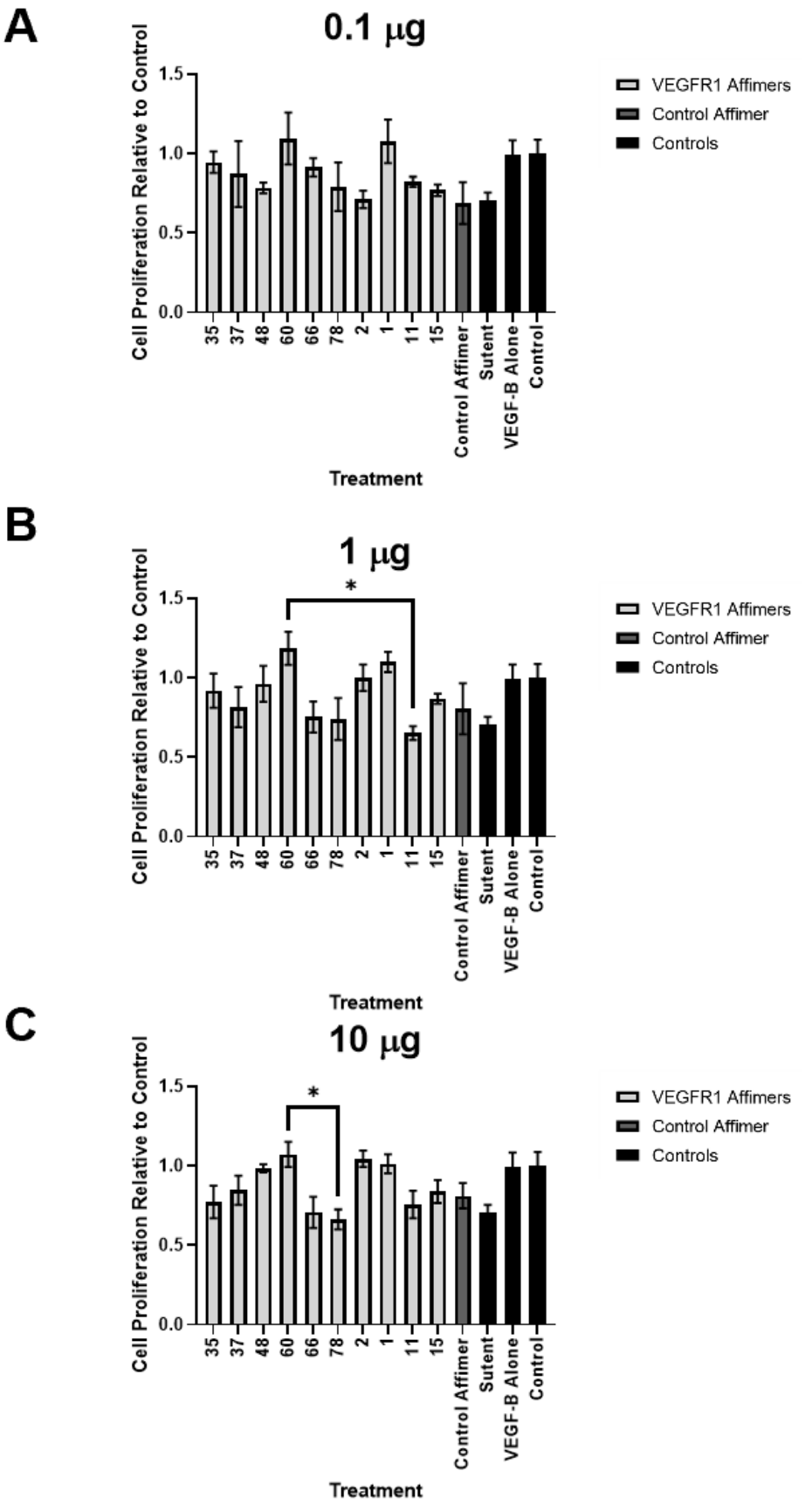
A
0.1 μg
Cell Proliferation Relative to Control
1.5
1.0
0.5
0.0
35
37
48
60
66
78
2
1
11
15
Control Affimer
Sutent
VEGF-B Alone
Control
Treatment
VEGFR1 Affimers
Control Affimer
Controls
B
1 μg
*
Cell Proliferation Relative to Control
Treatment
VEGFR1 Affimers
Control Affimer
Controls
C
10 μg
*
Cell Proliferation Relative to Control
Treatment
VEGFR1 Affimers
Control Affimer
Controls

Figure 4.5 VEGFR1-specific Affimers can have differing effects on VEGF-B mediated endothelial cell survival depending on concentration. Affimers at three different concentrations were incubated with HUVECs, followed by the measurement of BrDU incorporation using a colorimetric proliferation ELISA. HUVECs were treated with (A) 0.1, (B) 1 and (C) 10 µg/ml of VEGFR1-specific Affimer for 30 min prior to stimulation with 25 ng/ml VEGF-B. These were also compared to a non-specific control Affimer (control) along with 1 µM Sutent, VEGF-B alone and ECGM medium+VEGF-B (control). BrDU reagent was added to the cells for four hours prior to fixation and incubation with a BrDU-specific antibody. The final absorbances were calculated against cells which had been incubated with ECGM+VEGF-B. Error bars denote ±SEM. Significance: *, $p<0.05$ (n=3).

A

VEGFR1 Affimer	Potential concentration for promoting VEGF-A stimulated proliferation
35	10 µg
37	1 µg
48	10 µg
60	1 µg
66	1 µg
78	1 µg
2	10 µg
1	1 µg
11	10 µg
15	10 µg

B

VEGFR1 Affimer	Potential concentration for allowing VEGF-B stimulated survival
35	0.1 µg
37	0.1 µg
48	10 µg
60	1 µg
66	0.1 µg
78	0.1 µg
2	10 µg
1	1 µg
11	0.1 µg
15	1 µg

Table 4.1 Concentrations of each VEGFR1 Affimer for differing effects on endothelial cell proliferation. The concentration of each VEGFR1-specific Affimer tested at which they may have favourable outcomes on (A) VEGF-A mediated proliferation or (B) VEGF-B mediated survival.

4.2.3 VEGFR1-specific Affimers promote VEGF-A-stimulated endothelial cell migration

Another important *in* vitro assessment of VEGF-A-regulated endothelial function is cell migration. One of the best-known methods to use in this area of work, is the transwell cell migration assay, which measures single-cell migration in response to soluble diffusible agents such as growth factors and small molecules. This type of assay allows the researcher the ability to assess the effects of extraneous chemo-attractants on single-cell migration without interference from cell-cell interactions. The experiment usually consists of two chambers separated by a porous membrane across which cells can migrate across a chemo-tactic gradient (Boyden, 1962; Chen, 2005). During this project, HUVECs were pre-treated with various VEGFR1 Affimers for 30 min prior to their addition to the inner chamber. Over the next 24 h, HUVECs were allowed to migrate across the 8 µm porous membrane towards the medium containing 25 ng/ml VEGF-A in the lower chamber. Any successfully migrated cells were chemically fixed and stained prior to counting.

Figure 4.6B shows the effects of two of the Affimers, 35 and 37 at 100 µg/ml both for cysteine and non-cysteine tagged Affimers. Once again, this was to compare whether there was any great difference between the two versions on cellular function and calculate the change against VEGF-A stimulation alone. Here, there is generally an increase in HUVEC migration as compared to VEGF-A treatment alone. There is a slight decrease of about 20% after using the non-cysteine tagged version of 37, which was the opposite of its cysteine-tagged counterpart. Although there was not a significant difference between the two, this could either indicate that this Affimer is less effective in general or should be used at a different concentration. In contrast, both the cysteine and non-cysteine tagged versions of Affimer 35 both showed an average increase of 26% with only a 3% difference. This negligible difference between the two led to a trial of differing concentrations of the non-cysteine tagged versions in further experiments, seen in Figures 4.6A and Figure 4.6C. These Affimers were

also compared to the cross-reactive Affimer 66 and the non-specific control Affimer.

There was an unexpected decrease in HUVEC migration with all three concentrations of Affimers 37 and 66. This finding, however, does not mean that there cannot be some other pieces of information found here. For instance, using Affimer 66 at 0.1 µg/ml increased migration ~6-fold more than its higher concentration. This could indicate a dose-dependent response, whereupon a lower concentration than 0.1 µg/ml may have potentially shown more successful migration. There is also some information to be gathered from both Figures 4.6A and Figure 4.6C with regards to Affimer 37. Although the mean migration was low at all three concentrations, there is a slight increase in migration at 10 µg/ml (Fig. 4.6C), which is backed-up by the microscopy image (Fig. 4.6A). There was at this concentration, however, a great deal of variability, which might have been explained by further replications of the experiment. It could also indicate that the optimal concentration for Affimer 37 is higher than 10 µg/ml and lower than 100 µg/ml, as seen in the previous results. A more positive effect on migration is seen with Affimer 35, where all two out of three concentrations were shown to increase HUVEC migration. This once again seemed to be dose dependent as concentration was inversely correlated with motility; this is particularly noticeable at 0.1 µg/ml, where cell migration was almost double that of the control. These migration results may therefore once again emphasise that the success of these experiments may depend a great deal upon Affimer concentration, as observed in Table 4.2.

A

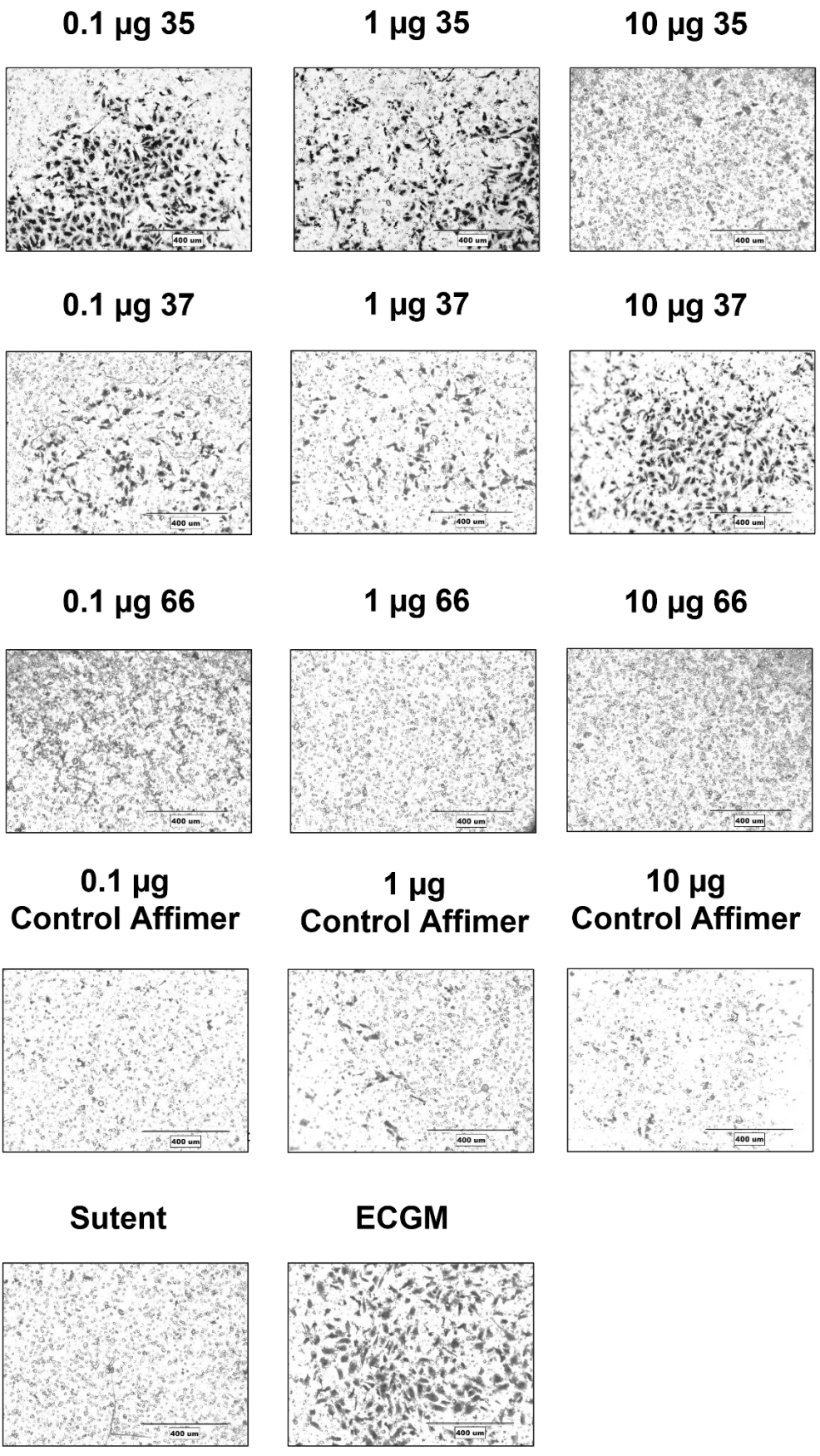
0.1 µg 35
1 µg 35
10 µg 35
0.1 µg 37
1 µg 37
10 µg 37
0.1 µg 66
1 µg 66
10 µg 66
0.1 µg
Control Affimer
1 µg
Control Affimer
10 µg
Control Affimer
Sutent
ECGM
400 um

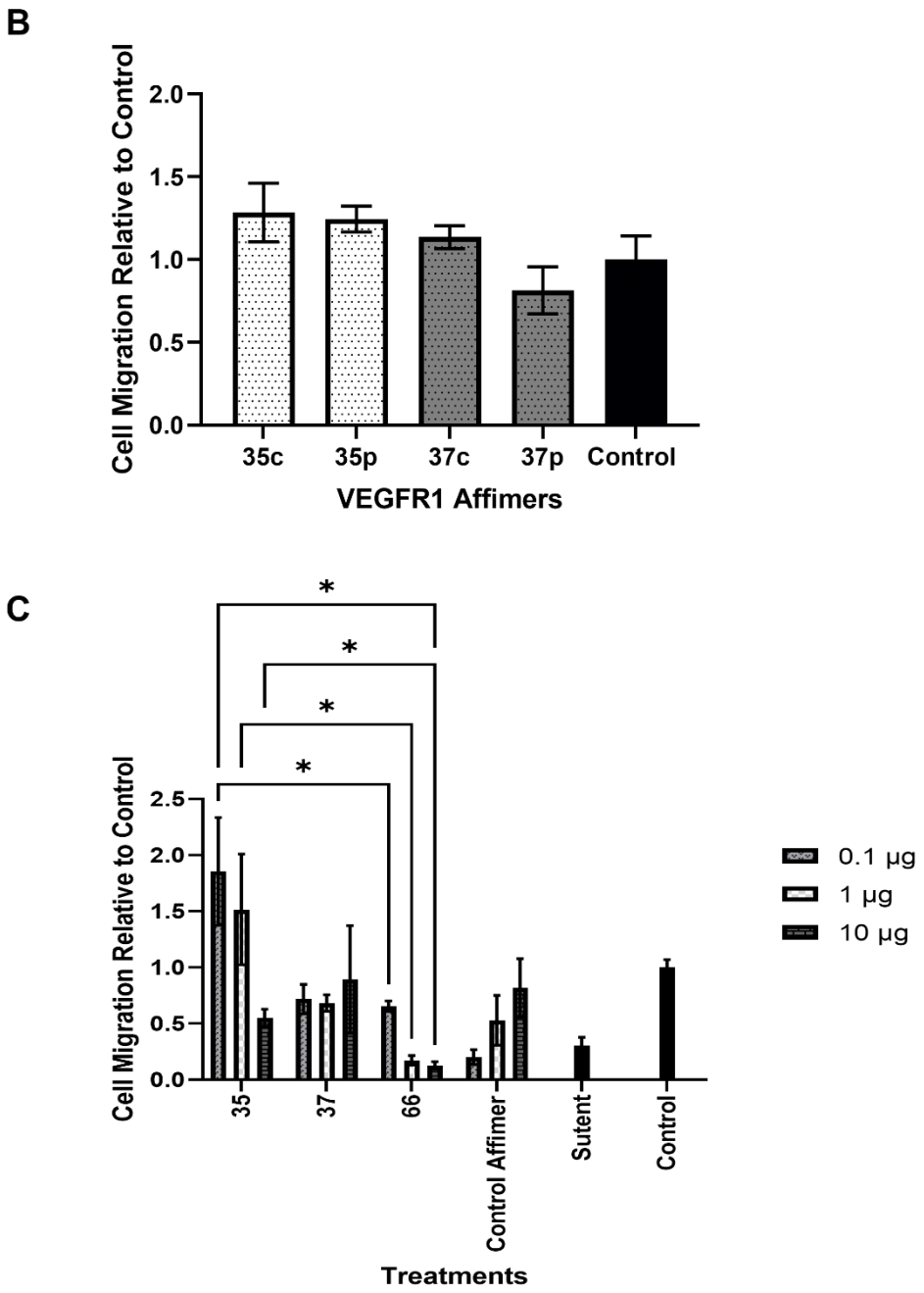

Figure 4.6 VEGFR1-specific Affimers can positively influence VEGF-A mediated endothelial cell migration depending on concentration. Analysis of the effect of Affimer concentration on transwell cellular migration. HUVECs were incubated with VEGFR1-specific Affimers at a range of concentrations (0.1-10 µg/ml) for 30 min followed by stimulation with 25 ng/ml VEGF-A. Controls including 1 µM Sutent, ECGM medium+VEGF-A and the non-specific control Affimer were also used. (A) Cells were stained using 0.2% crystal violet at 24h and pictures were taken on a digital fluorescence microscope (EVOS FL Auto) at 10x magnification. Bar, 400 µm. Migrated cells were counted using Fiji/Image J analysis and calculated against ECGM medium+VEGF-A. Quantified migrated cells were compared between (B) cysteine and non-cysteine tagged versions of VEGFR1 Affimers at 10 µg/ml as well as (C) at different concentrations. Error bars denote ±SEM. Significance: *, ;<0.05 (n=3).

VEGFR1 Affimer	Potential concentration for promoting VEGF-A stimulated migration
35	0.1 µg
37	10 µg
66	0.1 µg

Table 4.2 Concentrations of each VEGFR1 Affimer tested for differing effects on endothelial cell migration. The concentration of each VEGFR1-specific Affimer tested at which they may have favourable outcomes on VEGF-A mediated transwell migration.

4.2.4 VEGFR1-specific Affimers promote VEGF-A-stimulated endothelial tubulogenesis

Angiogenesis is one of the most important physiological phenomena in the body, yet it is hard to reproduce it in an experimental setting. To model this process, we can measure the *in vitro* tubule formation of endothelial cells: this is known as tubulogenesis (Jopling et al., 2014). Assays for tubulogenesis can evaluate the effects of drugs on the growth and branching of vascular tubes formed by endothelial cells in culture *in vitro.* Here, growth of tubules of primary human umbilical endothelial cells (HUVECs) on top of primary human dermal fibroblasts (NHDFs) is termed an endothelial fibroblast organotypic assay. The fibroblasts act as a structural framework with the aid of secreted collagen and other ECM proteins, to aid the development of 3-D vascular tubes by primary endothelial cells (Newman et al., 2011).

Nine VEGFR1-specific Affimers were administered to the HUVECs on “day 0,” which was one day after these cells were initially distributed on top of the fibroblast cells. These Affimers were added 30 min prior to the addition of 25 ng/ml VEGF-A in order to allow proper binding of these binders to the VEGFR1 receptors. These cells were cultured for seven days allowing for the replenishment of Affimers and VEGF-A every two days. In brief, cells

were fixed and stained with PECAM-1 on the final day to allow the visualisation of the resultant tubules. It has been previously stated that VEGFR1 is potentially an inhibitor of the processes usually controlled by VEGFR2, particularly angiogenesis. Therefore, the hypothesis of this experiment was that the addition of non-cysteine tagged Affimers which inhibited the VEGFR1 receptor would in fact enhance tubulogenesis, which would be demonstrated by an increase in the number of tubules and branches. To ascertain evidence that the Affimers worked at the same concentrations as conventional antibodies, each of the Affimers were tested at three different dosages: 0.1 µg, 1 µg, and 10 µg/ml. These Affimers were also compared to an established 1 µM of Sutent, a potent VEGFR inhibitor, as a negative control and the addition of VEGF-A^{165} alone. The usage of three different concentrations of Affimers was not only to check how applicable they were at standard concentrations used in established therapeutics, but also to identify which dosage worked best for each of the Affimers.

Figures 4.7-4.9 shows the influence of 0.1, 1 and 10 µg/ml of each VEGFR1 respectively after 7 days. It was decided to try and measure tubule and branch growth to see if Affimers made a difference not only on VEGF-A stimulated cells but also on those with this growth factor absent. These were plated alongside and compared to cells which were only stimulated with VEGF-A. An α-PECAM-1 primary antibody was used prior to a fluorescently tagged secondary antibody in order to take images on the microscope. The Angioquant program was used to automatically count the numbers of tubules and branch points in each image. The microscopy images showed a general increase in tubule formation after the addition of VEGF-A, but this was sometimes more pronounced in the Affimer-containing wells. For instance, in Figure 4.7B the most significant change in tubule length was seen between the control and 0.1 µg/ml Affimer 60 after VEGF-A stimulation, which was four times greater than the former. There was also a significant change between the non-stimulated and stimulated wells containing 60, with a 300% increase, which was also seen with 48, almost a 900% increase. These results were also mirrored in Figure 4.7C showing

the number of branch points, where the most significant changes between stimulation were with Affimers 48, an increase of 900%, and 60, an increase of 360%. The number of branch points generally increased with all of the treatments in comparison to the negative control, Sutent, which was to be expected. Overall, the 0.1 µg/ml Affimer showed average increases of 601% and 657% in tubule length and branch number respectively. Based on these two graphs, we can also deduce the most effective reagents at this concentration based on comparisons to the control Affimer. At this concentration, we can conclude that the most effective were Affimers 37, 48 and 60.

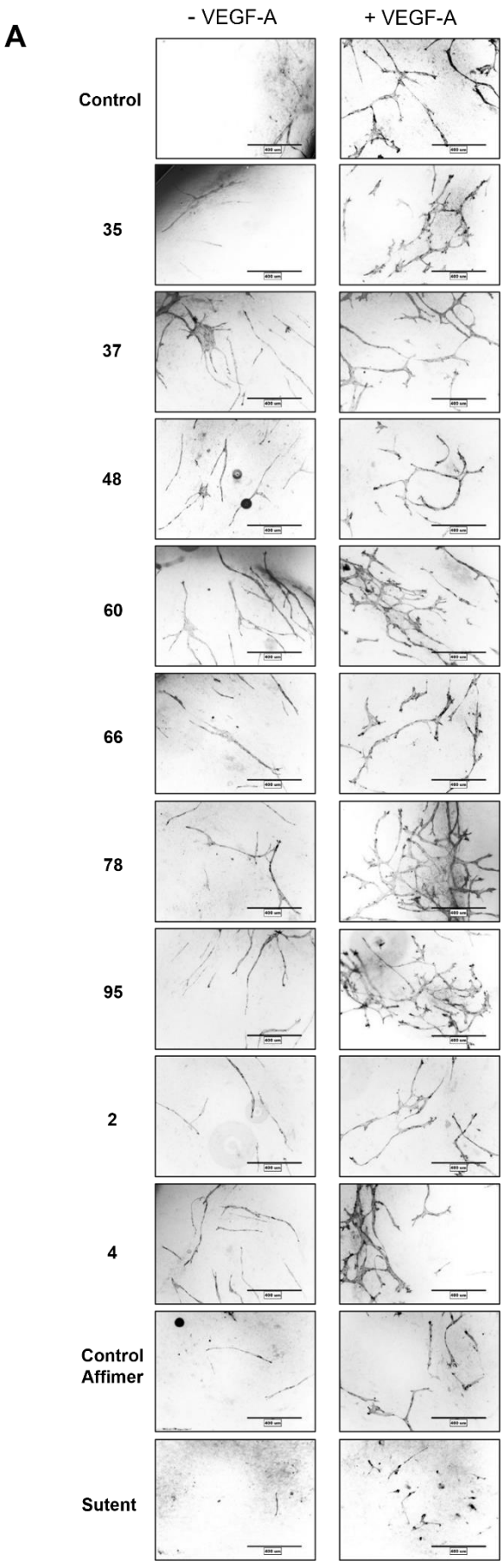
A
- VEGF-A
+ VEGF-A
Control
35
37
48
60
66
78
95
2
4
Control Affimer
Sutent

B

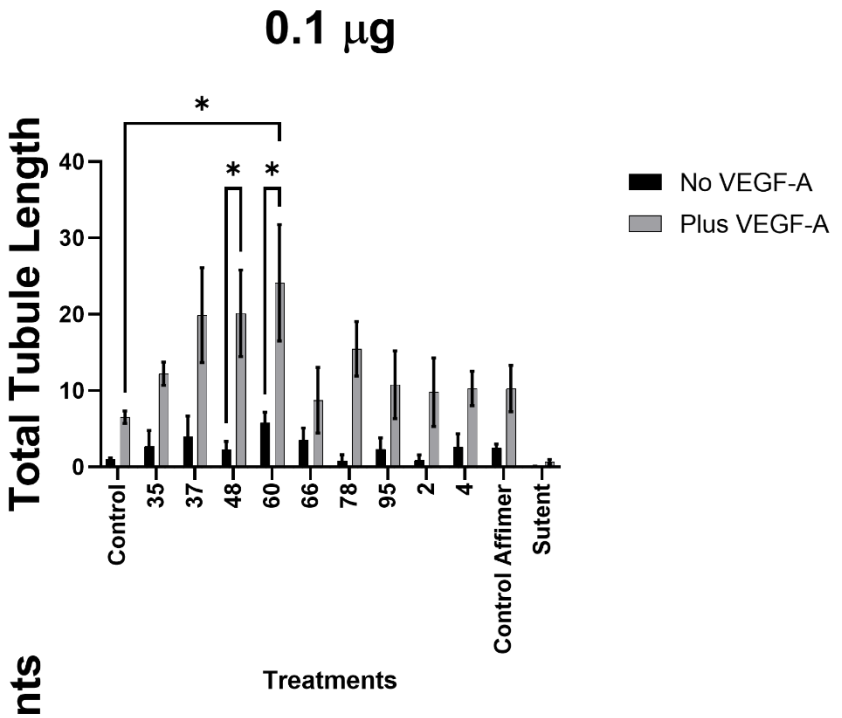

C

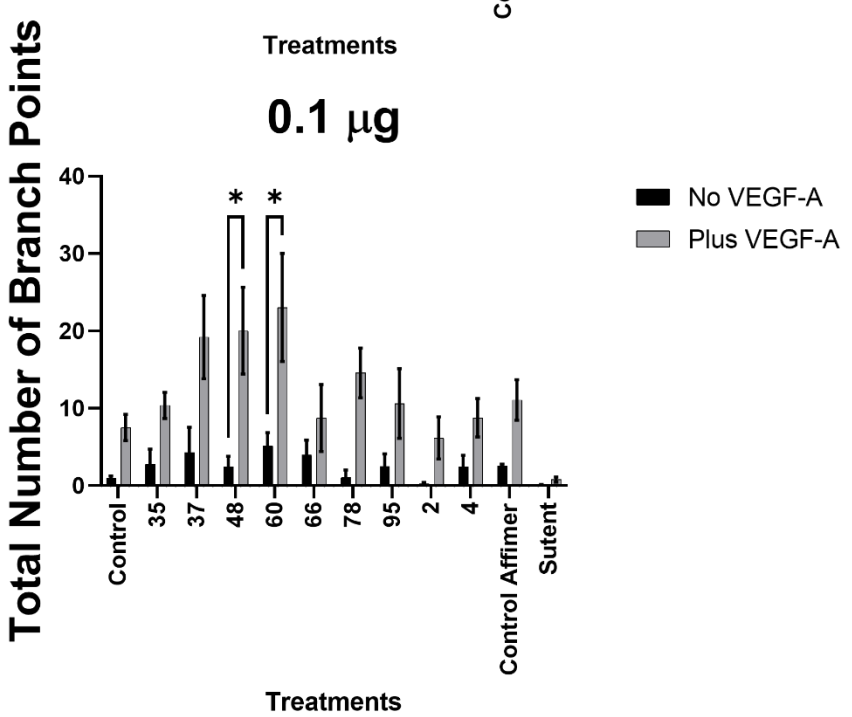

Figure 4.7: 0.1 µg/ml VEGFR1-Specific Affimers increase VEGF-A-stimulated tubulogenesis. *In* vitro HUVEC tubulogenesis on co-cultured fibroblasts. (A) HUVECs were incubated with 0.1 µg/ml of a control or VEGFR1-specific Affimers for 30 min prior to stimulation with 25 ng/ml VEGF-A. 1 µM Sutent was added as an additional control. Cells were fixed and stained with a PECAM-1 specific antibody with images being taken on a digital fluorescence microscope (EVOS FL Auto) after 7 days. Bar, 400 µm. Quantification was carried out using the Angioquant program to analyse (B) total tubule length and (C) the number of branch points of the tubules formed. relative to no stimulation respectively. Error bars denote ±SEM. Significance: *, $p<0.05$ (n=3).

Figure 4.8 shows a repeat of this experiment but with the Affimers at 1 µg/ml. Here, we can see more growth in tubule and branch numbers with the majority of the VEGFR1-specific Affimers, especially when compared to the control Affimer, with an average increase of 585% and 612% in tubule length and branch number respectively between the non- and VEGF-A stimulated cells. The most effective of these Affimers at this concentration appeared to be Affimer 78, where there was a significant ~20x increase in both tubule and branch number after VEGF-A stimulation. Finally, Figure 4.9 shows tubulogenesis at 10 µg/ml Affimer. There were once again increases in both tubule length and branch number seen at this Affimer concentration, although less overall, at an average of 275% and 285% respectively, as compared to the 1 µg/ml Affimer. However, the most significant change in both tubule length and branch number was seen at this concentration, that of Affimer 37. Tubule length and branch number was not only 4x and 3x higher than the control respectively, but also showed highly significant increases before and after VEGF-A stimulation. Tubule length was increased by 550% whilst branch number was increased by 525%. In fact, this final tubule length and branch number was the highest out of all the treatments and concentrations. There were varying degrees of success with each of the Affimers at 10 µg/ml, but there was relative success with them all, except for 95, as compared to the control Affimer. Overall, these results highlight the necessity to carry out dose-dependency experiments to analyse the effects on tubulogenesis. It could be assumed that the higher the concentration of a reagent, the greater the effect which can be seen. This, however, was not the case for these VEGFR1-specific Affimers, whereupon the majority of them worked best at the lower concentrations, namely 1 µg/ml. It is for further experimentation to determine whether the use of lower concentrations of the VEGFR1-specific Affimers would result in greater stimulatory effects on tubulogenesis, or whether the doses in these experiments are at the limits of their efficacy.

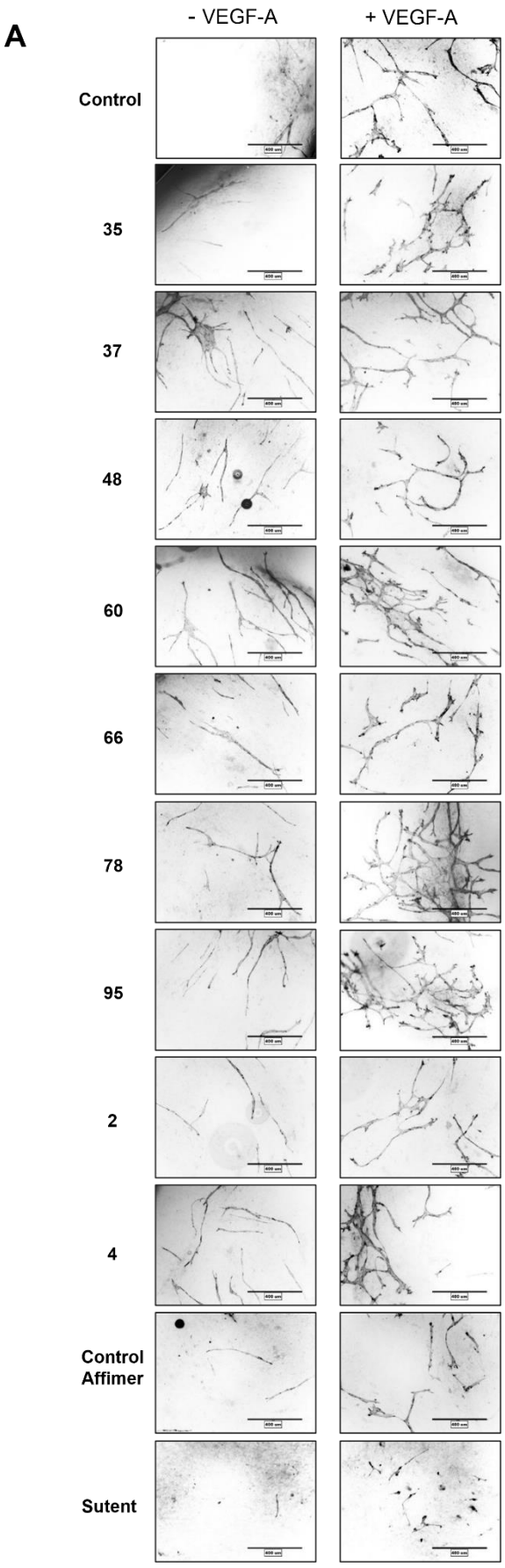
A
- VEGF-A
+ VEGF-A
Control
35
37
48
60
66
78
95
2
4
Control Affimer
Sutent

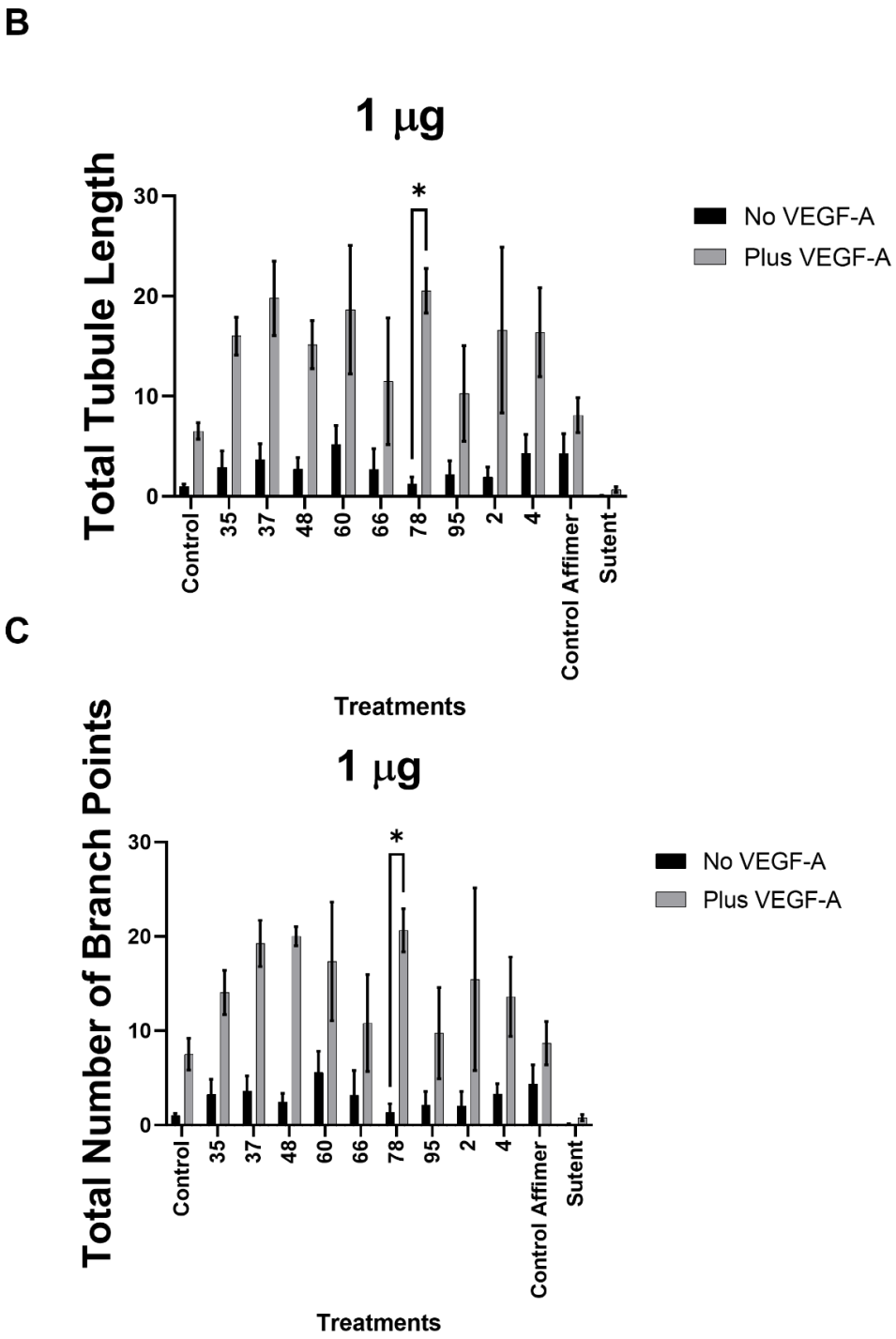

Figure 4.8: 1 µg/ml VEGFR1-Specific Affimers increase VEGF-A-stimulated tubulogenesis. *In vitro* HUVEC tubulogenesis assay on co-cultured fibroblasts. (A) HUVECs were incubated with 1 µg/ml of a control or VEGFR1-specific Affimers for 30 min prior to stimulation with 25 ng/ml VEGF-A. I µM Sutent was added as an additional control. Cells were fixed and stained with a PECAM-1 specific antibody with images being taken on a digital fluorescence microscope (EVOS FL Auto) after 7 days. Bar, 400 µm. Quantification was carried out using the Angioquant program to analyse (B) total tubule length and (C) the number of branch points of the tubules formed. relative to no stimulation respectively. Error bars denote ±SEM. Significance: *, $p<0.05$ (n=3).

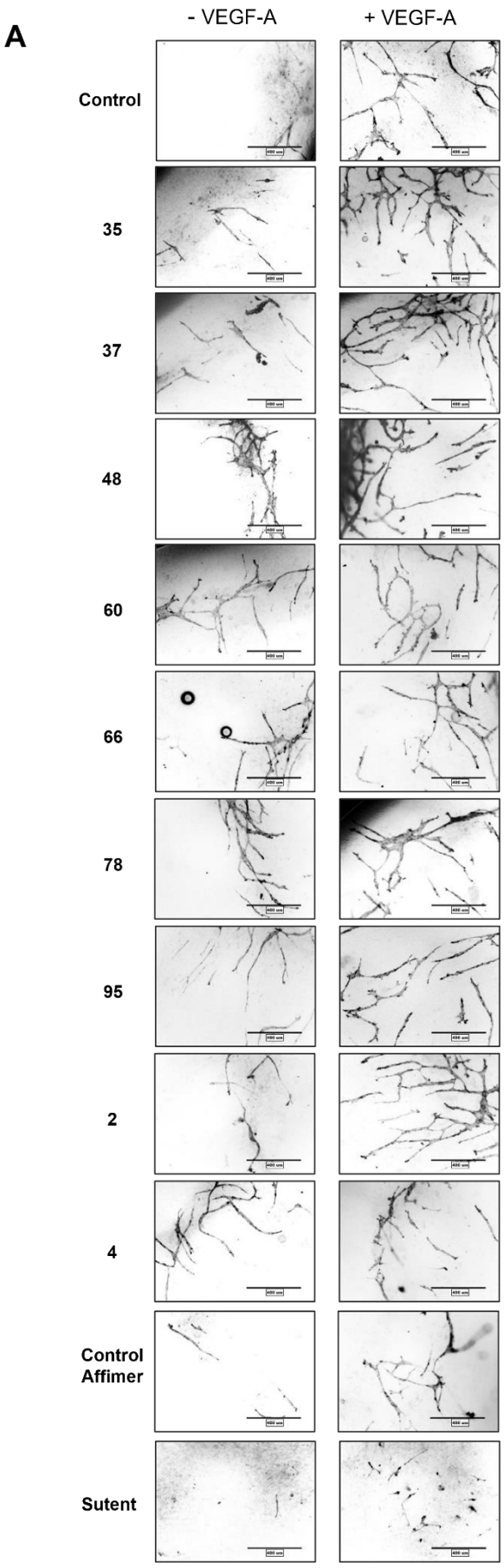
A
- VEGF-A
+ VEGF-A
Control
35
37
48
60
66
78
95
2
4
Control Affimer
Sutent

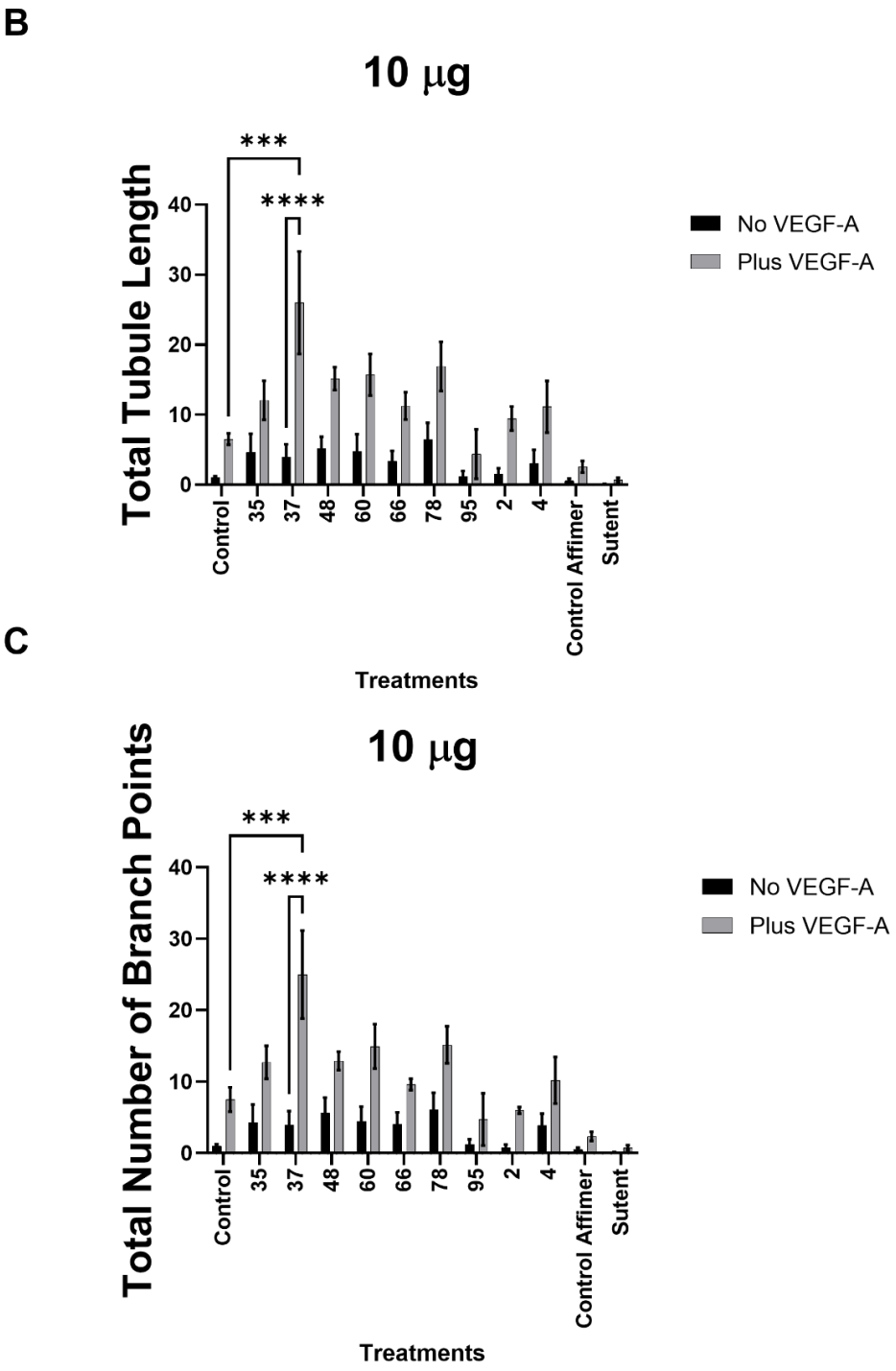

Figure 4.9: 10 µg/ml VEGFR1-Specific Affimers increase VEGF-A-stimulated tubulogenesis. *In vitro* HUVEC tubulogenesis assay on co-cultured fibroblasts. (A) HUVECs were incubated with 10 µg/ml of a control or VEGFR1-specific Affimers for 30 min prior to stimulation with 25 ng/ml VEGF-A. 1 µM Sutent was added as an additional control. Cells were fixed and stained with a PECAM-1 specific antibody with images being taken on a digital fluorescence microscope (EVOS FL Auto) after 7 days. Bar, 400 µm. Quantification was carried out using the Angioquant program to analyse (B) total tubule length and (C) the number of branch points of the tubules formed. relative to no stimulation respectively. Error bars denote ±SEM. Significance: *, $p<0.05$; ***, $p<0.001$; ****, $p<0.0001$ (n=3).

Table 4.3 shows the optimal concentrations for each of the VEGFR1-specific Affimers for enhancing tubulogenesis based on these results. It can be seen that the majority of these Affimers work well at a concentration of 1 µg/ml with the exceptions of 37, 48, and 60. 37 was the only Affimer which worked best at the highest concentration used of 10 µg/ml whilst the optimum for 48 and 60 was at the lowest concentration of 0.1 µg/ml. These results highlight the fact that finding the optimum dosage for each Affimer would be preferred to accurately find an effective yet safe dosage, but there is the potential for using all of them at a concentration at 1 µg/ml.

VEGFR1 Affimer	Potential concentration for promoting VEGF-A stimulated tubulogenesis
35	1 µg
37	10 µg
48	0.1 µg
60	0.1 µg
66	1 µg
78	1 µg
95	0.1 µg
2	1 µg
4	10 µg

Table 4.3 Concentrations of each VEGFR1 Affimer tested for stimulatory effects on endothelial cell tubulogenesis. The concentration of each VEGFR1-specific Affimer tested at which they may have favourable outcomes on VEGF-A mediated tubulogenesis.

4.2.5 Fluorescent-tagged VEGFR1-specific Affimers effects in endothelial cells

The ability of the Affimers to be conjugated to other reagents allows an opportunity to not only affect cell signalling on a molecular level, but also could allow them to be used as detection tools. The previous experiments within this thesis primarily focused on the effects of the Affimers on endothelial cell function. Conventional antibodies, however, often have an additional use for detecting specific proteins using immunofluorescent staining, so this was naturally the next step for the Affimers. This is why the VEGFR1-specific Affimers were conjugated to Alexa-fluor dyes using maleimide linkage. Recycling of VEGFR1 is potentially important to maintain steady-state VEGF1 levels and functionality. Conventional cell recycling assays includes the use of a 1 h incubation with a primary antibody which can bind to the receptor of choice, followed by an acid wash of the cells and the addition of a fluorescent secondary antibody. Only receptors which have recycled at least once are able to be visualised using a fluorescent microscope. It was desired, however, to try by-passing the need for a primary antibody. The use of fluorescently conjugated Affimers would allow a combination of functionality and visualisation. This method could not only determine whether cell cycling would be affected by the Affimers in comparison to the antibody, but also reveal whether this one-step method could make this experiment more efficient.

The effects of VEGFR1 Affimers on cellular function were not only dependent on the isoform of Affimer, but the concentration. This methodology involved incubation with the fluorescently conjugated Affimers for 1 h followed by the usual acid wash, but visualisation would be confirmed almost immediately without the need for a secondary antibody. Figure 4.10B shows a comparison of VEGFR1 Affimers which include 37 (one which seemed to conjugate well to the Alexafluor previously) and the cross-reactive 66 along with comparisons to VEGFR1 and VEGFR2 antibodies using the conventional method. The total corrected cell fluorescence of Affimer 37 was highly significant in comparison to all of the conditions

tested. Fluorescence was detected at triple the concentration of that of the VEGFR1 antibody using the previous method. This not only shows that this particular Affimer modulates VEGFR1 trafficking, but this is also a useful probe for detecting VEGFR1 (Fig. 4.10A, 4.10B). It may be worth noting that this increase in fluorescence could also have been due to the relative success of Alexafluor conjugation in comparison to the other VEGFR1 Affimers which were sometimes poorly tagged. However, comparing it to VEGFR1 antibody can show at least some credence to the fact that trafficking of the receptor may also be increased during the same time period.

A

Affimer 35

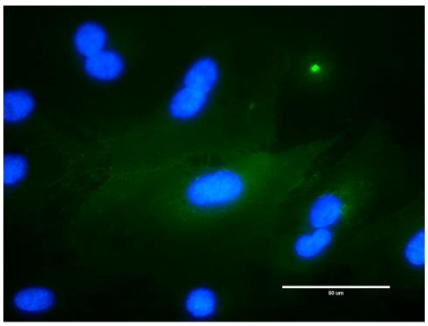

Affimer 66

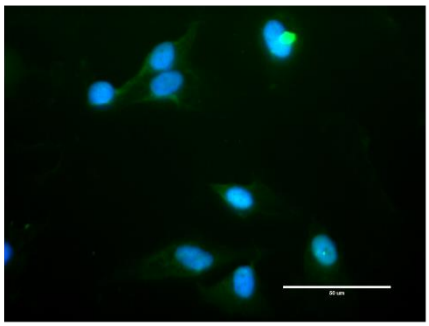

Affimer A9

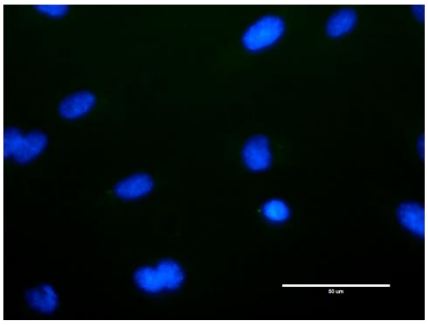

Affimer B8

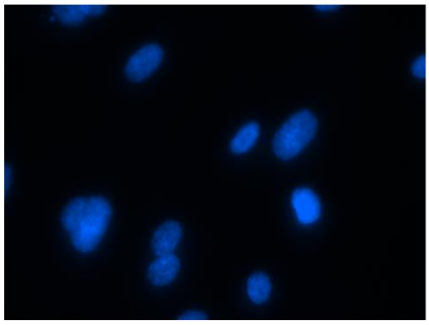

VEGFR1 Antibody

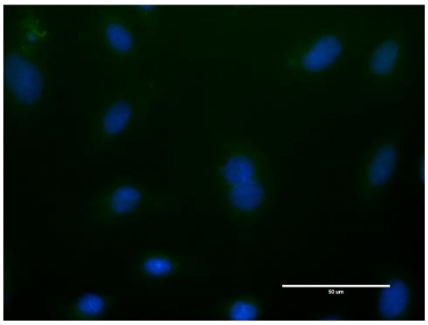

VEGFR2 Antibody

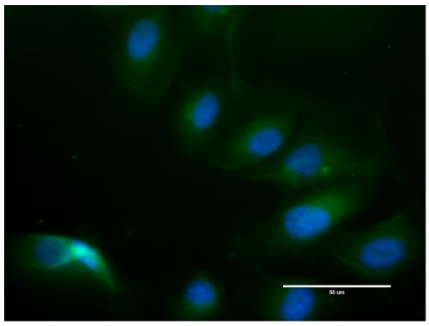

Negative Control Affimer

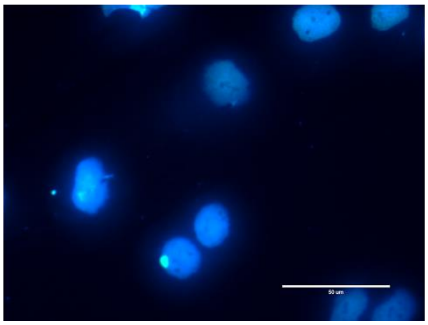

B

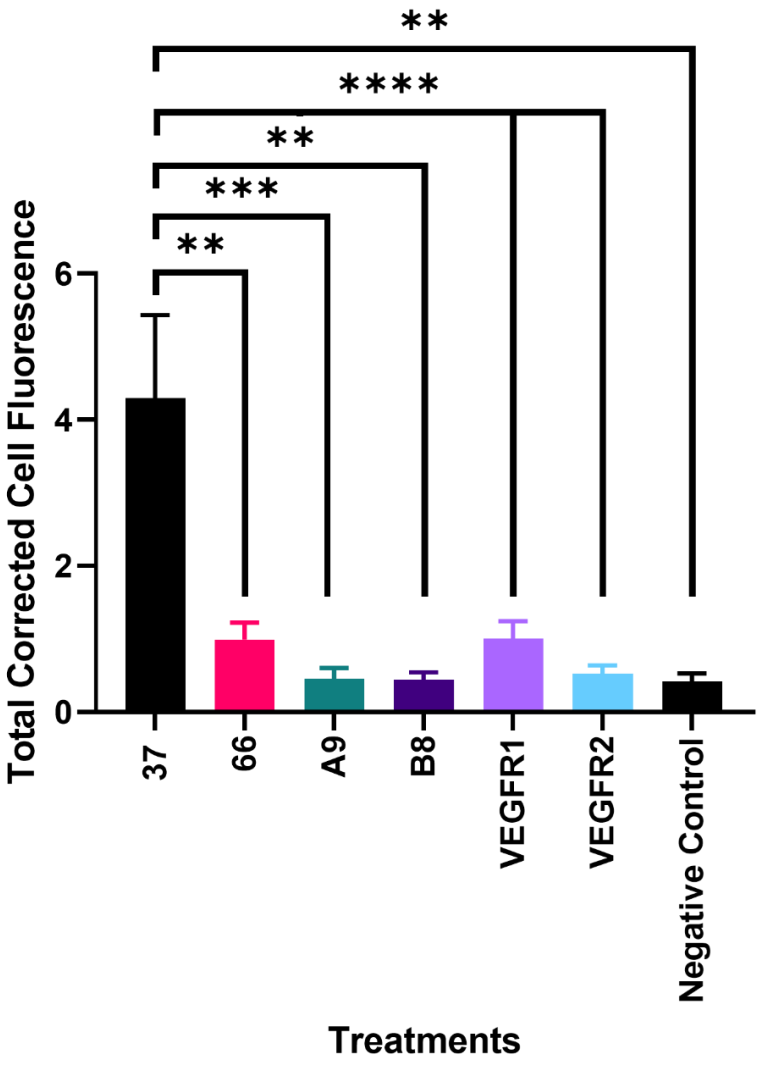

Figure 4.10. VEGFR recycling assay using Affimers. A VEGFR recycling assay in endothelial cells (HUVECs) was carried out using incubation of cells with 10 µg/ml AlexaFluor 488-tagged VEGFR1-specific Affimers (green) for 1 h. Cells were acid washed to remove bound Affimers on the surface of the cells prior to fixation and processing. (A) Imaging was carried out using a digital fluorescence microscope (EVOS FL Auto). Nuclei were stained with DAPI (blue), and pictures from three fields of view per well were taken at 40x magnification. Bar, 50 µm. (B) Quantification of relative recycling of VEGFR1 and VEGFR2. Total corrected cell fluorescence was calculated using Fiji/Image J analysis to compare VEGFR1, VEGFR2 and non-specific Affimers efficacy alongside goat anti- VEGFR1 or goat anti-VEGFR2 antibodies Error bars denote ±SEM. Significance, ** p<0.005, *** p<0.001, **** p<0.0001 (n=3).

4.3 DISCUSSION

VEGFR2 is a major therapeutic target in blocking angiogenesis in various diseases such as cancer and diabetic retinopathy. For instance, there is an array of synthetic proteins currently being produced specifically to block VEGFR2 and therefore reduce its role in promoting adverse effects in such diseases (Löfblom et al., 2010; Wojcik et al., 2010). However, an inhibitory role for VEGFR1 in angiogenesis could act to slow recovery damaged cardiac and vascular tissues after heart attacks. Ectodomain shedding of VEGFR1 also produces soluble VEGFR1 (sVEGFR1) which may either form a non-functional heterogenous dimer with VEGFR2 or sequester VEGF-A (Rahimi *et al.,* 2009). This is why the use of VEGFR1-inhibitory Affimers is a novel concept which was addressed using cell-based assays in this chapter.

Throughout this chapter, a range of Affimer concentrations were used to identify both safe and effective dosages (Table 4.4). This was started with the cell viability assays where even 100 µg/ml of Affimers did not adversely affect endothelial cell viability. MTT assays carried out by Spitzer *et al.,* (2006) also demonstrated the benefits of the titration of the VEGF-inhibitor, bevacizumab on several cell lines including on human retinal pigment epithelium (ARPE19) cells. Viability was steady between 0.008 up to 2.5 mg/ml, where after 48 h the number of cells decreased by 30% as compared to the control (Spitzer et al., 2006). During the course of the experimentation involved in this study, there was little cytotoxicity with the Affimers identified, but nevertheless, to ensure their safety in dosages for human consumption it would be of great value to use lower concentrations of each reagent in future experiments in order to definitively identify safe, yet effective working dosages similar to antibodies.

The positive effect on cell viability was confirmed by BrDU based proliferation experiments, where a lower concentration of 10 µg/ml Affimer seemed to be an optimal concentration for the majority of these reagents for enhancing VEGF-A mediated proliferation. This was comparable to research involving a slightly different proliferation assay undertaken by

Bussolati *et al.,* (2001), which involves [^{3}H]-thymidine incorporation instead of BrDU. Here, 30 ng/ml of an anti-VEGFR1 antibody was added to HUVECs, whereupon it increased proliferation by ~51% as compared to the basal control. This effect was later reduced after the addition of an anti-VEGF antibody, confirming that it was related to VEGF-A signalling (Bussolati et al., 2001). In the work detailed in this chapter, the effects of VEGFR1-specific Affimers on BrDU proliferation was also assessed after the addition of the survival factor, VEGF-B. Despite the absence of VEGF-A, cell proliferation was still increased after incubation with the majority of the Affimers and VEGF-B. This correlates well with known facts about VEGF-B and VEGFR1 signalling in general, where it has been shown to have a definite link to cell survival. Taking this into consideration, it is theorised that the most suitable Affimers would enhance both VEGF-A mediated proliferation and VEGF-B mediated survival when used at the same concentration, for example VEGFR1-60 (Table 4.1A and B).

Cell Assay Type	Most Effective VEGFR1 Affimer	Affimer Concentration
Viability	35	100 µg/ml
Proliferation	60	1 µg/ml
Migration	35	0.1 µg/ml
Tubulogenesis	37	10 µg/ml
Recycling Assay	37	10 µg/ml

Table 4.4 Most Effective VEGFR1 Specific Affimers. A summary of the previous VEGF-A mediated cellular assays. Based on the Affimers which were able to be tested, estimates were made about which Affimer was the best VEGFR1 inhibitor in each experiment along with its most effective concentration.

The difference in cell proliferation induction between VEGFR1 and VEGFR2-specific Affimers may be explained by differential activation of the MAP kinase (MAPK) pathway. This can be revealed from previous studies where migration may be induced through PI3-K signalling as seen with VEGFR1s on human monocytes, where inhibition of PI3-K resulted in a 55% decrease in migration. Akt inhibition has also led to a 30% decrease in monocyte chemotaxis (Tchaikovski *et al.,* 2008).

Examining the overall trend of cell migration data, there was a general effect of Affimer dose-dependence. One unusual finding is that Affimer 35 increased endothelial cell migration the most at 0.1 µg/ml in response to VEGF-A as compared to the other conditions. This result further highlights the importance of titrations and shows that it is possible to still induce beneficial effects even at the lower concentrations. The difference in cell proliferation induction between VEGFR1-specific and VEGFR2-specific Affimers may be explained by differential activation of the MAP kinase (MAPK) pathway. This can be revealed from previous studies where migration may be induced through PI3-K signalling as seen with VEGFR1s on human monocytes, where inhibition of PI3-K resulted in a 55% decrease in migration. Akt inhibition has also led to a 30% decrease in monocyte chemotaxis (Tchaikovski *et al.,* 2008).

There is experimental evidence that has also shown that the binding of another VEGFR1-specific ligand, placental growth factor (PlGF), may enhance VEGF-A mediated angiogenesis. Previous studies which may show this potentiation of VEGF signalling, include the observation of functional heterodimerization between VEGFR1 and the VEGFR2 receptor, and PlGF overexpression, causing increased numbers and branching of blood vessels in mice (Odorisio et al., 2002; Autiero et al., 2003).

What can also be noted is the difference membrane-bound (mVEGFR1) and soluble (sVEGFR1) isoforms of VEGFR1. To recap, mVEGFR1 is a ~180 kDa protein which contains 7 IgG-like domains within its extracellular region; it also remains attached to the membrane and can only be released by γ-secretase/presenilin (Rahimi *et al.,* 2009).

sVEGFR1 is a smaller ~110 kDa protein which consists of the IgG-like domains 1-6 and a cytoplasmic factor; it may be formed through either alternative splicing or proteolytic cleavage of the larger mVEGFR1 (Wu *et al.*, 2010). The mVEGFR1 and sVEGFR1 have opposing roles on angiogenesis; mVEGFR1 has been found to increase angiogenesis while sVEGFR1 is the opposite as an inhibitor of this process due to its ability to bind VEGF-A. This can be seen from the proangiogenic nucleoside, Adenosine, which has been known to upregulate the membrane form whilst downregulating the soluble form in the presence of HIF-1α (Leonard et al., 2011; Wang et al., 2019).

The use of Affimers at different concentrations could allow fine-tuning the regulatory effects mediated by VEGFR1, determining on cell growth inhibition or stimulation. PIGF and VEGF-A-mediated VEGFR1 tyrosine phosphorylation has previously been found to cause ectodomain shedding in leukemic cancer cells. This generates the soluble form of VEGFR1 (sVEGFR1), which consists of the IgG-like domains 1-6, and a cytoplasmic factor. The remaining VEGFR1 receptor is still attached to the membrane and requires γ-secretase/presenilin to release it. (Rahimi *et al.*, 2009)

Overall, there is a great potential for the use of VEGFR1 Affimers in pharmacological studies. There are not many inhibitors of VEGFR1 or its ligands currently on the market, often leading researchers to resort to alter gene expression instead (Carmeliet *et al.,*2001). The ability to give further control and choice for studying VEGFR1 signalling would allow greater insight into its function in healthy and diseased states.

The cell-based experiments of this research show the potential of the VEGFR1-specific Affimers. Although the murine cross-reactive Affimer, 66, was not as effective as the other reagents tested, it still showed some beneficial effects. This could mean that these experiments could still be trialled in animals as well as potentially being beneficial in human clinical studies. The *in vitro* tests used in this project still provide a very useful and safe insight as to how these reagents may react in a human body. *In vivo* studies could also prove useful for further elucidation of the specific Affimer

functions. For instance, FLT-1 tyrosine kinase-deficient homozygous mice (flt-1(TK-/-) have also been shown to have normal blood vessel development due to angiogenesis when the tyrosine kinase domain was deleted whilst the ligand domain was still present. There was, however, a marked decrease in VEGF-mediated macrophage migration as VEGFR1 is extremely specific to these cells, which is not ideal as macrophages are a key part of cardiac recovery (Hiratsuka et al., 1998; Lavine et al., 2018). This could potentially cause problems depending on how Affimer binding affects tyrosine kinase phosphorylation, but this could emphasise the necessity for drug dosage optimisation. Therefore, using the VEGFR1-specific Affimers could not only promote VEGFR2-mediated signalling but also not have deleterious effects on VEGFR1 as a whole.

Chapter 5

Modulation of signal transduction, trafficking and tubulogenesis by VEGFR2-specific Affimers in endothelial cells

5.1 INTRODUCTION

The role of VEGFR2 is well-studied unlike its counterpart, VEGFR1. Its ability to bind various ligands within the VEGF family promotes different signalling pathways important for many endothelial responses. This makes it an apt means for targeting not only cardiovascular responses, but also in the targeting of diseases such as cancer (Koch *et al.*, 2011). These pathologies not only influence normal cell proliferation and migration but notably angiogenesis.

The fact that cancer has a multitude of potential targets makes anti-cancer therapies more difficult to develop. Targeting tumour angiogenesis is important as immunohistochemical studies show the increased expression of VEGF-A and VEGFRS in almost 50% of all cancers (Salven *et al,* 1998). Tumour cells can influence sprouting angiogenesis in several ways, including secreting VEGF-A, which binds to healthy endothelial cells, potentially down-regulating angiogenic inhibitors such as angiostatin (Nishida *et al.*, 2006). These tumour cells can also form new vessels through a process called intussusceptive (or non-sprouting) angiogenesis, whereupon connections are formed through intravascular pillars located in the lumen of blood vessels (Mentzer and Konerding, 2014; Lugano *et al.,* 2020). For example, intussusceptive angiogenesis has been seen in melanoma along with higher levels of growth factors such as VEGF (Ribatti *et al.*, 2005).

Although we were not looking at non-sprouting angiogenesis, it is important to emphasise the role of angiogenesis in cancer pathology overall, specifically with regards to VEGFs and its membrane receptors. This is of particular importance due to the random genetic variants of cancer cells, meaning treatment can be nigh-on impossible. In contrast, endothelial cells

have genetically stable genomes which allows for reduced resistance to drugs (Kerbel, 1991; Aragon-Ching and Dahut, 2010). Not only that, but angiogenesis can also provide a useful target in androgen-responsive disease such as prostate cancer. This cancer can often be diagnosed in later stages due to its initially slow progression. Treatment can often involve a radical prostatectomy, but alternative therapeutics may be needed if there is still a relatively high level of prostate-specific antigen (PSA) post-operation. This can include hormone suppression therapeutics, chemotherapy or radiotherapy (which have been shown to decrease PSA levels by 50% in 82% of men studied) (Lange *et al.*, 1990; Aragon-Ching and Dahut, 2010). However, prostate cancer has been known to reoccur due to resistance to androgen depletion therapies. In fact, the androgen receptor could potentially adapt to lower levels of its hormonal ligands by several methods including overexpression and including more types of growth factors for activation (Gregory *et al.*, 2001). This could be a problem in other malignancies which are also influenced by the androgen receptor, such as breast cancer (Michmerhuizen *et al.*, 2020). The targeting of endothelial cell-mediated angiogenesis through VEGFR2 could, therefore, in fact bypass the difficulties seen with these other tumour-targeting therapeutics.

The aim in this chapter was to identify whether Affimers specific for VEGFR2 could inhibit endothelial cell proliferation, migration and angiogenesis (tubulogenesis). Providing a comparative and detailed analysis of dose-dependent effects of VEGFR2-specific Affimers on endothelial cells could indicate whether these reagents could compete with established treatments of abnormal angiogenesis.

5.2 RESULTS

5.2.1 VEGFR2-specific Affimers effects on endothelial cell viability

In Chapter 4, we analysed endothelial cell viability after incubation with VEGFR1-specific Affimers. We repeated such experiments to evaluate three different concentrations of the non-cysteine tagged version of the VEGFR2-inhibitory Affimer, A9 (named A9p throughout) (Fig. 5.1). A9 is the second of the two previously found Affimers obtained through phage display. Several experiments prior to this project found that B8 had more inhibitory effects than A9, so it was often focused on more later on. For this study, it was decided that it would be beneficial to test both of these VEGFR2-inhibitory Affimers to further clarify their effects. A9 was the focus of these studies on viability since it had not been used in these particular experiments previously.

This set of experiments was also pertinent due to the inclusion of 1 µM Sutent, allowing for a comparison to be made to the established tyrosine kinase inhibitor of VEGFR2, and an important anti-angiogenic cancer therapeutic. A reliance on lower cell number seems to be the norm for the majority of these conditions, due to the increased cell absorbance at cells seeded at 1000 cells, bar that seen with the complete medium. In fact, the cell absorbance was relatively low for all of the cell seeding conditions in complete medium apart from at 50,000 cells per well at the 48-hour mark, where absorbance reached 0.14. This absorbance, however, was pretty well-matched with regards to cells incubated with both 1 µg/ml A9p and VEGF-A, whereupon the average absorbance across all of the cell seeding counts was 0.12. This was in addition to higher overall absorbance seen around 0.1 at 0 h, which was higher than all of the other conditions tested. This, however, changed when compared to the two other concentrations of Affimer after 48 h, whereupon both 10 and 100 µg/ml showed absorbances of ~0.14 at the 1000 cell density. 10 µg/ml Affimer, though, showed slightly lower, and sometimes decreasing, absorbance with increasing cell density. This was not the case for the 100 µg/ml, where absorbance was consistently across at all the cell seeding densities after 48 h (average of ~0.11). This

was reflected in the values ascertained for cells only stimulated with VEGF-A, where absorbance was consistently high for all cell seeding densities (average of ~0.14). This could potentially be promising with regards to safety, where even the highest concentration of this Affimer did not significantly decrease cell viability as compared to cells incubated in their ideal environment, i.e., either complete medium or only with their preferred ligand, VEGF-A.

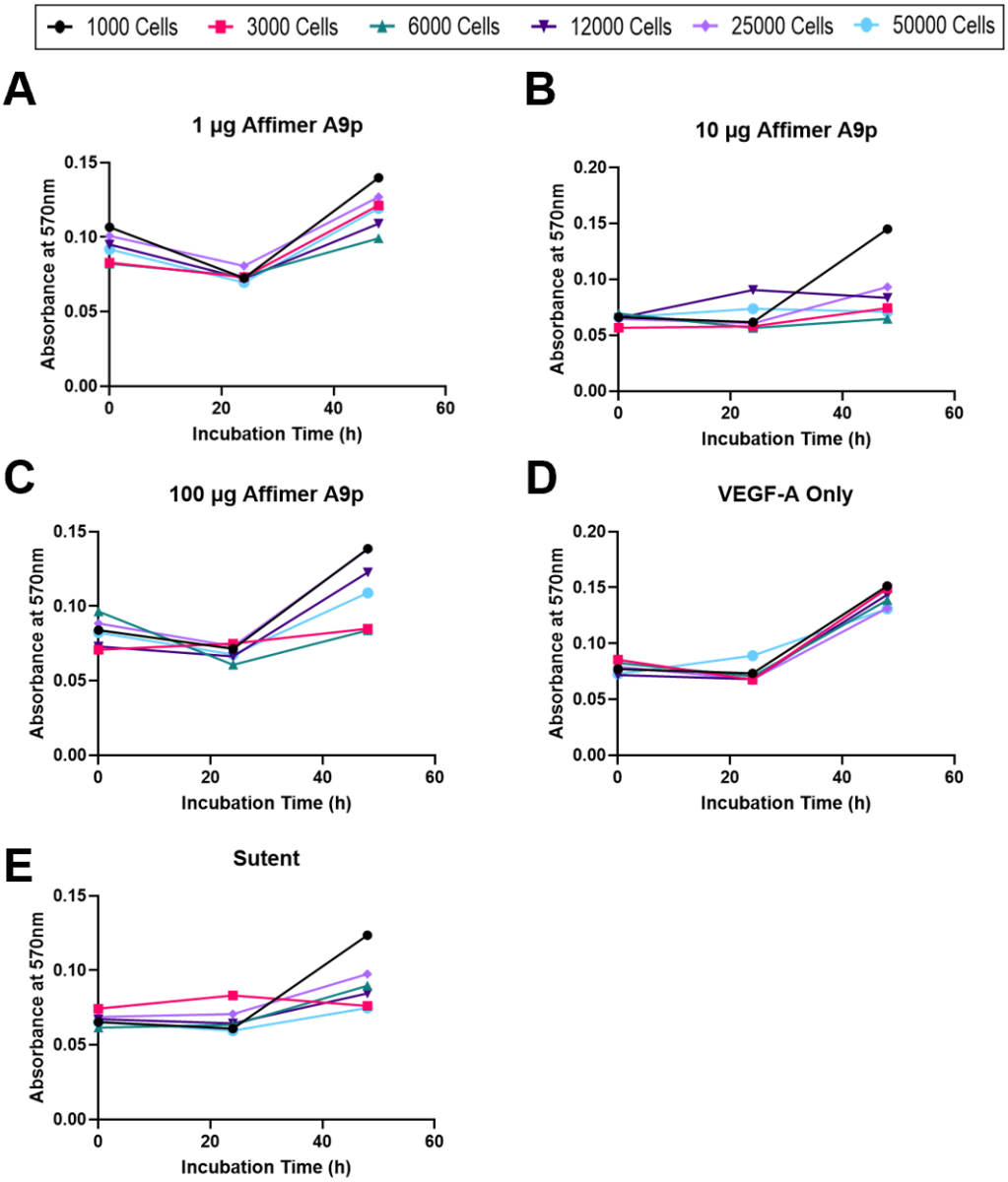

Figure 5.1 Comparing the effects of VEGFR2-Affimer concentration and HUVEC cell number on viability. HUVEC cell viability was determined by an MTT assay at 24 and 48h. HUVECs were starved in MCDB131 medium prior to incubation with the Affimers for 30 min followed by stimulation with 25 ng/ml VEGF-A. MTT was added at 24h prior to measurement on a spectrophotometer at 570 nm. This measurement was repeated at 48h. Graphs represent the effect of the initial number of cells plated against (A-C) one VEGFR2-specific Affimer at different concentrations (1-100 µg/ml) and (D) VEGF-A stimulation only as a positive control with (E) 1 µM Sutent as a negative control (n=1).

Finally, an average of total cell viability was calculated across all the cell seeding counts for each condition (Fig. 5.2). Cell viability was calculated from the conversion of cell absorbance to a percentage of ECGM+VEGF-A, this choice being made due to this being the standard medium in which HUVECs are culture. The wells containing VEGF-A alone showed significantly higher cell viability compared to the majority of the conditions, where it was higher even than that of ECGM, by 66%. There is, however, still slightly increased viability with all of the concentrations of Affimer compared to ECGM, these being 140, 104 and 133% for 1, 10 and 100 µg/ml respectively. Not only this, but we can also see a similarity in cell viability when comparing the standard VEGFR inhibitor, Sutent and 10 µg/ml of A9p (107 and 104% respectively). From these results three things might be concluded: that inhibition of VEGF-A signalling is effective *via* these inhibitory Affimers, that they could be comparable to current inhibitors, and that they are not so potent that they could damage any surrounding healthy tissue with increased cell division rates, such as in the bone marrow (which would alleviate safety concerns).

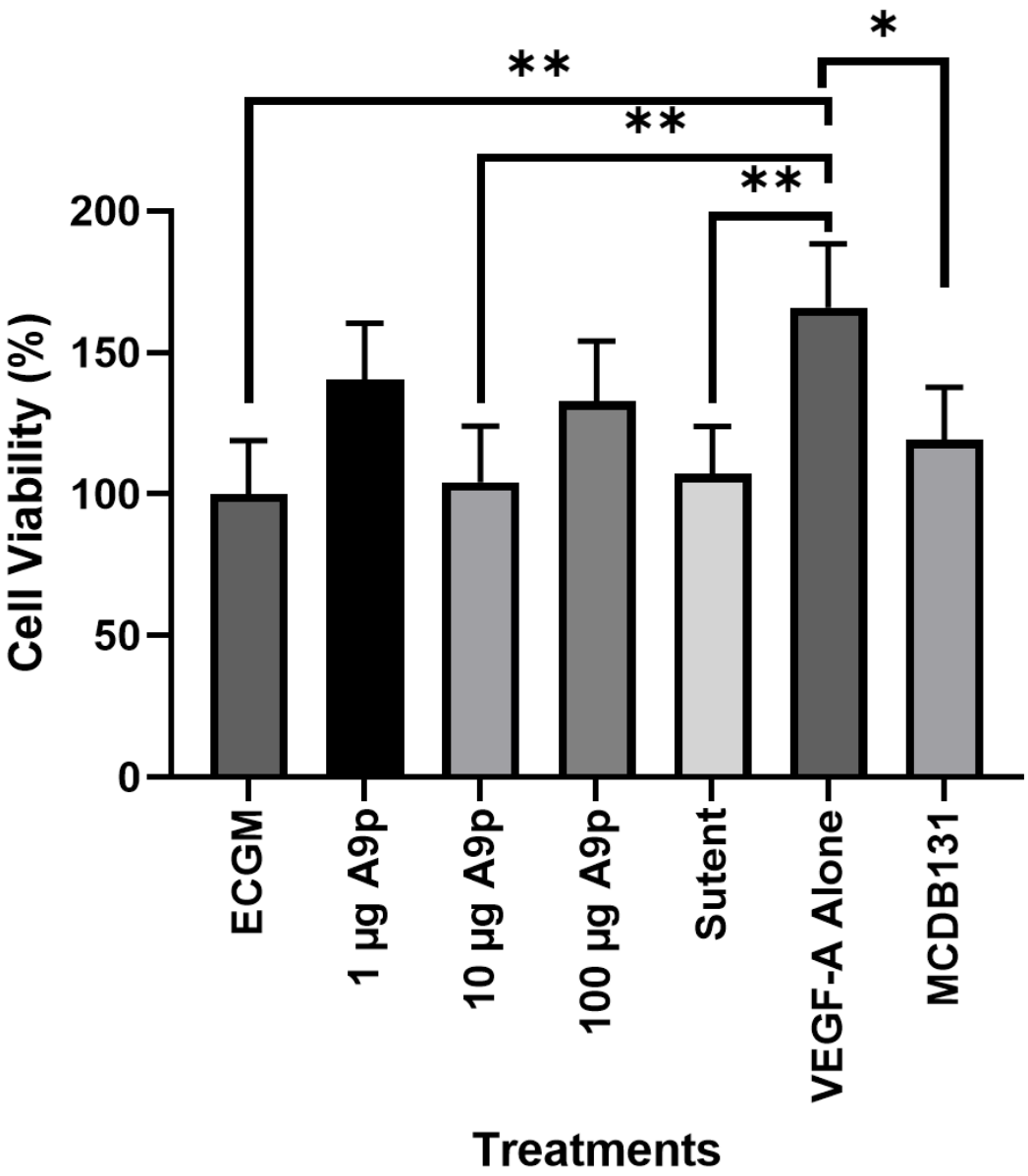

Figure 5.2 VEGFR2-specific Affimers are not toxic to endothelial cells. The cell viability of HUVECs were assessed using MTT assays and calculated against a positive control (ECGM medium+VEGF-A). The VEGFR2-specific Affimer tested, A9p, was trialed at three different concentrations (1-100 µg/ml) (n=6).

5.2.2 Assessing whether VEGFR2-specific Affimers can inhibit VEGF-A-stimulated endothelial cell proliferation

Once again, we evaluated endothelial cell proliferation by measuring BrDU incorporation using ELISA. For this assay, it was thought to be relevant to use the B8 VEGFR2-specific Affimer due to previously successful studies (Tiede et al., 2017). Figure 5.3 shows a comparison between the cysteine and non-cysteine tagged version of the B8 Affimer (B8c and B8p respectively) after stimulation with 25 ng/ml VEGF-A. These were also compared to a cysteine-tagged yeast SUMO-specific Affimer (Yeast SUMO 10c), serum-free medium (MCDB131) and medium with VEGF-A stimulation alone. The absorbances recorded were converted in order to compare the treatments to VEGF-A alone; this is due to the expectation that adding a VEGFR2 inhibitor may potentially inhibit this ligands' signalling. There were no statistically significant differences in proliferation between the Affimers at this concentration and when VEGF-A was used alone. In fact, there is a very slight increase in proliferation with B8p, but not as much as that seen with the Yeast SUMO 10 Affimer. One of the key results of this experiment to note though is that there was a negligible difference between the cysteine and non-cysteine tagged versions of B8. This could indicate that this tag did not influence the proliferations of these cells, showing that these Affimers could potentially be used interchangeably without worrying about the consequence.

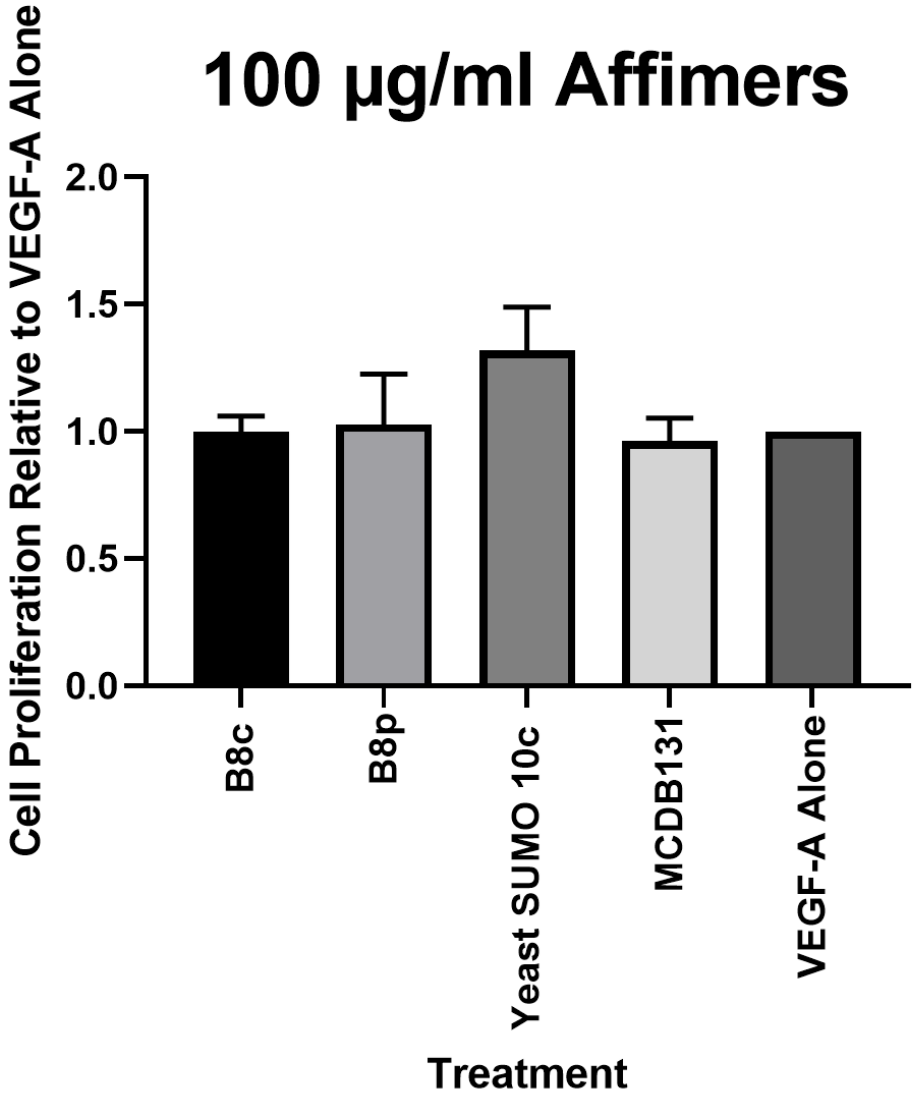

Figure 5.3 Assessing the effects of VEGFR2-specific Affimers on endothelial cell proliferation. The effects of both cysteine and non-cysteine tagged (labelled "c" and p") Affimers on HUVEC BrDU incorporation which was quantified using a colorimetric proliferation ELISA. HUVECs were treated with 100 µg/ml of the VEGFR2-specific or Yeast SUMO10c (control) Affimer prior to stimulation with 25 ng/ml VEGF-A. BrDU reagent was added to the cells for four hours prior to fixation and incubation with a BrDU-specific antibody. Serum-free medium+VEGF-A (MCDB131) was used as an additional control. The final absorbances were calculated against cells which had only been stimulated with VEGF-A. Error bars denote ±SEM (n=3).

Due to these results, it was decided to repeat these experiments with lower concentrations of Affimer. We analysed VEGF-A-stimulated HUVEC proliferation at three concentrations of three different non-cysteine tagged Affimers: B8, A9 and the aforementioned negative control Affimer with non-specific binding loops (Fig. 5.4). Each of these Affimers were also compared to 1 μM Sutent, ECGM+VEGF-A, and VEGF-A stimulation only. Comparisons were made to the ECGM wells, which were labelled as the control. Despite the use of Tukey tests within a 2-way ANOVA showing significance between several of the results, there does not appear to be a great difference in cell proliferation with any of the concentrations of the VEGFR2-specific Affimers and the positive controls. There was even a slight increase in proliferation with all three concentrations of the A9 Affimer, mirroring previous studies where this inhibitor was not as effective on a cellular level as compared to B8. B8 did show slight decreases in proliferation at all three concentrations (~0.06 difference on average), but this was still not as much as the more established Sutent. In fact, there was approximately a 16% decrease in proliferation with Sutent as compared to using all three concentrations of the B8 Affimer. If anything, it seems that the control Affimer decreased proliferation more than the VEGFR2-specific Affimers, especially at the highest dose of 10 μg/ml. This could indicate a need for further replicates or trials with more doses of the VEGFR2-specific Affimers along with clarifying their effects on proliferation signalling pathways using immunoblotting.

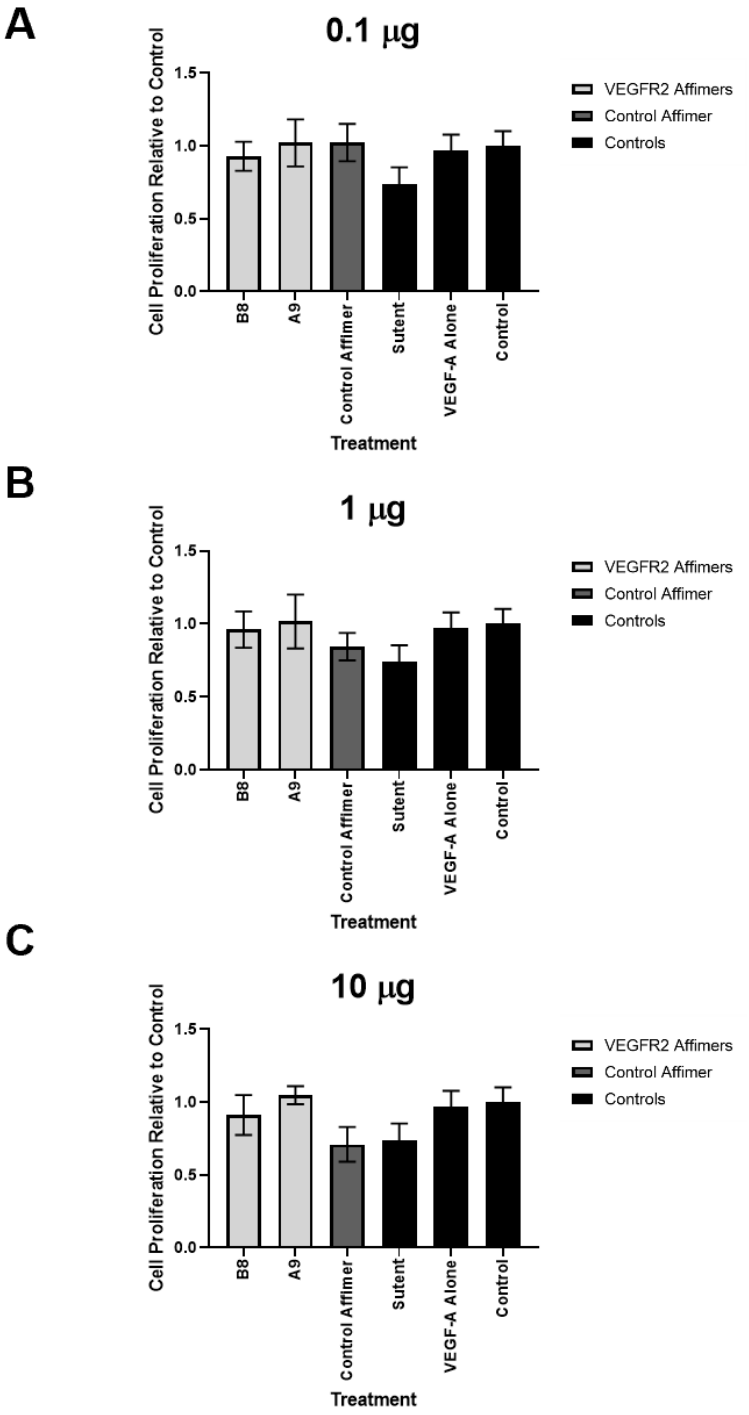

Figure 5.4 VEGFR2-specific Affimers can have differing effects on VEGF-A mediated endothelial cell proliferation depending on concentration. Affimers at three different concentrations were incubated with HUVECs, followed by the measurement of BrDU incorporation using a colorimetric proliferation ELISA. HUVECs were treated with (A) 0.1, (B) 1 and (C) 10 µg/ml of VEGFR2-specific Affimers for 30 min prior to stimulation with 25 ng/ml VEGF-A. These were also compared to a non-specific control Affimer (control) along with 1 µM Sutent, VEGF-A alone and ECGM medium+VEGF-A (control). BrDU reagent was added to the cells for four hours prior to fixation and incubation with a BrDU-specific antibody. The final absorbances were calculated against cells which had been incubated with ECGM+VEGF-A. Error bars denote ±SEM (n=3).

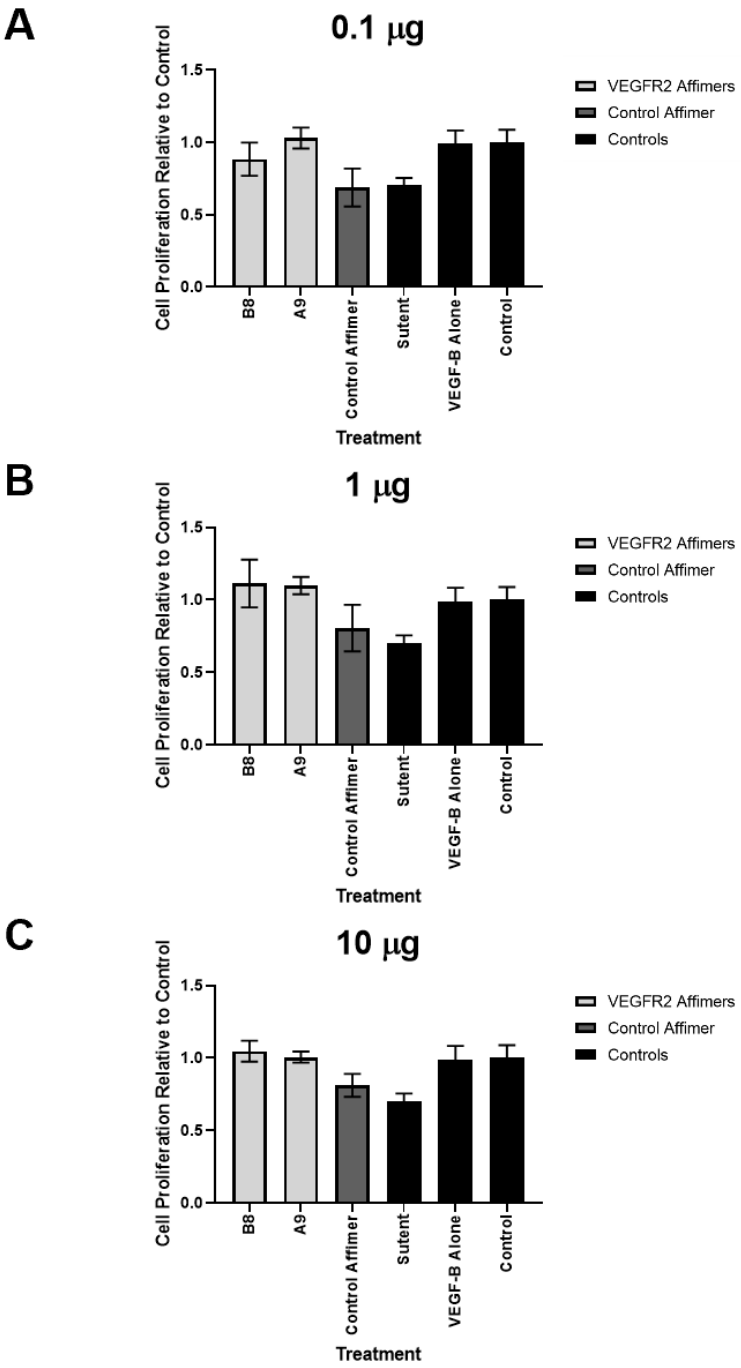

Figure 5.5 VEGFR2-specific Affimers can positively influence VEGF-B mediated endothelial cell survival at a range of concentrations. Affimers at three different concentrations were incubated with HUVECs, followed by the measurement of BrDU incorporation using a colorimetric proliferation ELISA. HUVECs were treated with (A) 0.1, (B) 1 and (C) 10 µg/ml of VEGFR2-specific Affimers for 30 min prior to stimulation with 25 ng/ml VEGF-B. These were also compared to a non-specific control Affimer (control) along with 1 µM Sutent, VEGF-B alone and ECGM medium+VEGF-B (control). BrDU reagent was added to the cells for four hours prior to fixation and incubation with a BrDU-specific antibody. The final absorbances were calculated against cells which had been incubated with ECGM+VEGF-B. Error bars denote ±SEM (n=3).

It was decided to repeat the VEGF-B mediated proliferation experiments which were carried out in the previous chapter. VEGF-B is specific to VEGFR1, so the expectation was that there would be little change in proliferation after inhibition with anti-VEGFR2 Affimers. Cell proliferation was once again compared to Sutent and ECGM+VEGF-B (control), but VEGF-B stimulation was used instead (Fig. 5.5). Tukey statistical tests show significant decreases in endothelial cell proliferation at all three concentrations of the Affimer as compared to VEGF-B alone and the control, where decreases of 20, 30 and 30% were seen for 0.1, 1 and 10 µg/ml respectively. This was comparable to the effects of Sutent, where there was also a 30% decrease in cell proliferation. However, there was almost an opposite trend with regards to the VEGFR2-specific Affimers. Once again, all three concentrations of the A9 Affimer showed slight increases in proliferation. These were similar to when VEGF-A was used as the stimulant, once again indicating that this may be the lesser of the two Affimers tested. There are, however, differences seen between the concentrations of the B8 Affimer. There was indeed a decrease in proliferation of about 10% by using 0.1 µg/ml of this reagent, but the opposite was seen for the remaining two where there were increases. This was most noticeable for 10 µg/ml of B8, where there was an 11% increase in proliferation. Although marginal, this was in fact the highest change in proliferation as compared to not only the other concentrations of B8, but all of the other treatments.

5.2.3 VEGFR2-specific Affimers inhibit VEGF-A-stimulated endothelial cell migration

The transwell cell migration assay was used once again in order to determine the effects of the VEGFR2-inhibitory Affimers. Addition of 100 µg/ml of the cysteine or non-cysteine tagged versions of Affimer B8 were once again tested (Fig.5.6A). One of the main aims of this experiment was to further clarify whether the addition of a cysteine tag could change the functionality of the Affimers. The Affimers were compared to cells which were stimulated with VEGF-A without inhibition (Fig 5.6B). Here, there was very little difference in the number of observed migrated cells between the cysteine and non-cysteine tagged B8, approximately 5%. Combined with an ~40% decrease in migration for both versions compared to the control, this highlighted that Affimer B8 effectively inhibits VEGF-A-stimulated endothelial cell migration.

An analysis of the effects of different concentrations of Affimers B8 and A9 was undertaken alongside comparisons to the negative control Affimer and 1 µm Sutent treatment. Successful HUVEC migration was calculated as a percentage of ECGM+VEGF-A (control), in order to assess the effects against un-inhibited HUVEC migration. We find that endothelial cell migration is dependent on both the concentration and strain of Affimer (Fig. 5.6C; Table 5.1). For instance, 0.1 µg/ml of Affimers B8 or A9 show ~50% and 40% decreases in endothelial cell migration respectively. However, the control Affimer also appeared to decrease migration at this concentration, indicating there was potentially some unreliability in this set of experiments looking at this specific concentration. A further examination of the effects of Affimer A9 shows that cell migration was actually slightly increased by ~4% at 1 µg/ml Affimer, but a reduction was noted once again at 10 µg/ml. Migration at 1 µg/ml Affimer B8 was also increased compared to its 0.1 µg/ml counterpart but was still approximately 30% lower than the control. The final set of experiments using the 10 µg/ml concentration could potentially have been the most reliable, due to the fact that there was little difference in the number of migrated cells between the control Affimer at this concentration and the ECGM control. This would have been expected given

the theoretical non-specificity of the control Affimer to VEGFR2. Incubation with 10 µg/ml A9 seemed to show a decrease of ~10%; this was not far off from the control Affimer results. On the other hand, B8 at 10 µg/ml showed a decrease in migrated HUVECs by ~84%, which was the lowest out of all the concentrations of Affimer tested. This was even a third lower than that of the established Sutent, which decreased migration by ~70%.

A

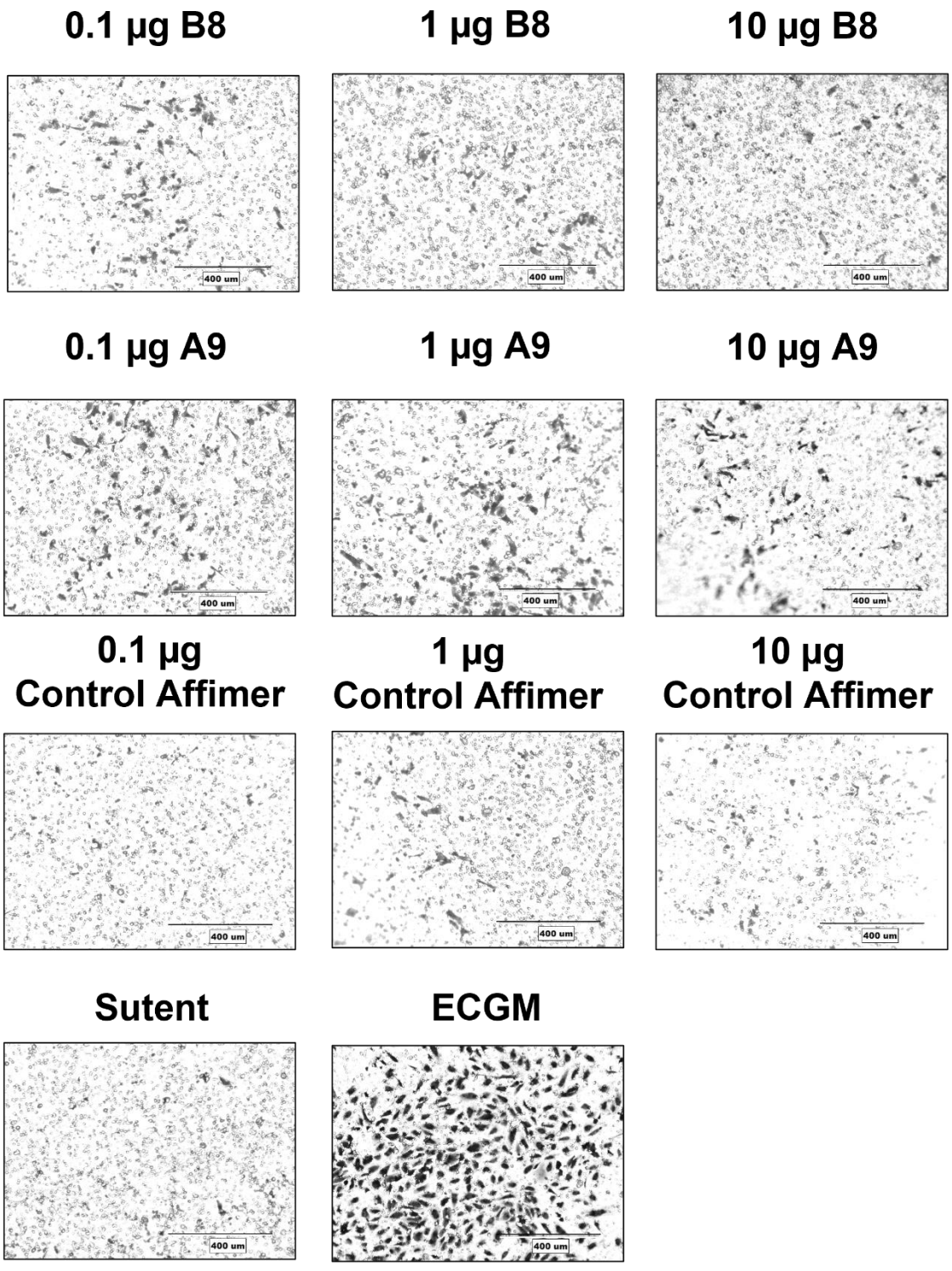
0.1 µg B8
1 µg B8
10 µg B8
0.1 µg A9
1 µg A9
10 µg A9
0.1 µg
Control Affimer
1 µg
Control Affimer
10 µg
Control Affimer
Sutent
ECGM
400 um

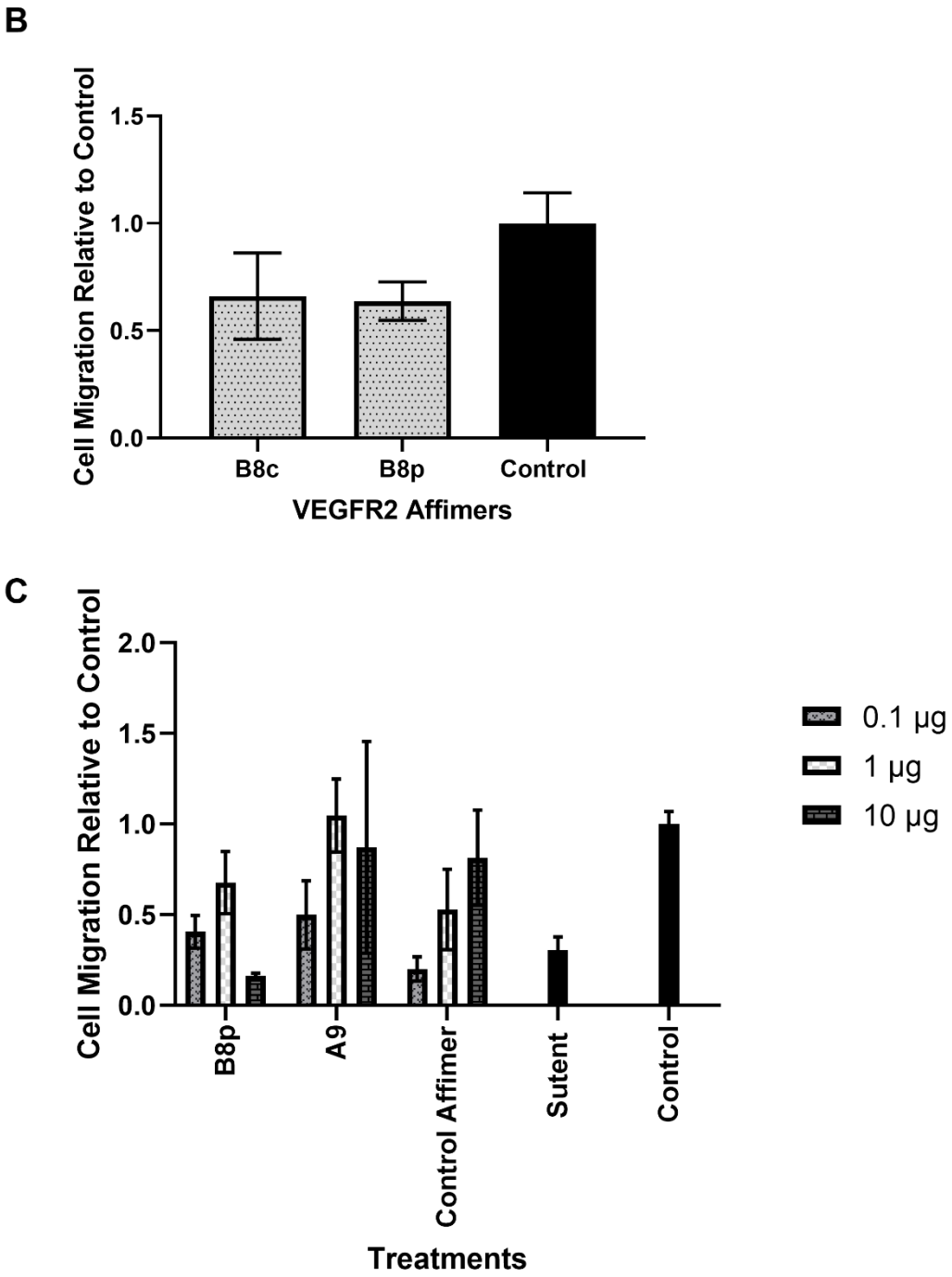

Figure 5.6 VEGFR2-specific Affimers can reduce VEGF-A mediated endothelial cell migration depending on concentration. Analysis of the effect of Affimer concentration on transwell cellular migration. HUVECs were incubated with VEGFR2-specific Affimers at a range of concentrations (0.1-10 µg/ml) for 30 min followed by stimulation with 25 ng/ml VEGF-A. Controls including 1 µM Sutent, ECGM medium+VEGF-A and the non-specific control Affimer were also used. (A) Cells were stained using 0.2% crystal violet and pictures were taken on a digital fluorescence microscope (EVOS FL Auto) at 10x magnification. Bar, 400 µm. Migrated cells were counted using Fiji/Image J analysis and calculated against ECGM medium+VEGF-A. Quantified migrated cells were compared between (B) cysteine and non-cysteine tagged versions of VEGFR2 Affimers at 10 µg/ml as well as (C) at different concentrations. Error bars denote ±SEM. Significance: *, $p<0.05$ (n=3).

VEGFR2 Affimer	Potential concentration for blocking VEGF-A-stimulated migration
B8	10 µg
A9	0.1 µg

Table 5.1 Concentrations of each VEGFR2 Affimer tested for differing effects on endothelial cell migration. The concentration of each VEGFR2-specific Affimer tested at which they could have favourable outcomes on VEGF-A mediated transwell migration.

5.2.4 Assessing whether VEGFR2-specific Affimers can inhibit VEGF-A-stimulated endothelial tubulogenesis

One of the key methods in which VEGFR2 signalling is analysed prior to clinical trials is the use of the *in vitro* endothelial fibroblast organotypic assay which allows evaluation of tubulogenesis. In Chapter 4, it was detailed that this assay was used to determine the effects of VEGFR1-specific Affimers on HUVEC tubulogenesis. In this current chapter it will be detailed that these experiments were repeated, but that this time their focus was on looking at the effects of VEGFR2-specific Affimers instead. This was hoped to provide the basis for a better understanding of the effects of VEGFR1-specific Affimers in this assay.

Figures 5.7-5.9 show the results of three concentrations of the two VEGFR2-specific Affimers, B8 and A9 alongside the control Affimer. Figure 5.7 shows the results from 0.1 µg/ml Affimer treatment on tubule length and branch points. Contrary to what was expected, the use of these Affimers at this concentration increased both the length and the number of branch points as compared to the control, both prior to and after VEGF-A stimulation. There was an average increase of 221% and 242% in tubule length and branch numbers respectively, with the most significant being upon treatment with Affimer B8. In fact, incubation with the Affimer B8 caused >2-fold increase in tubule length and branch number as compared to control. This was much the same result where the Affimers were used at

1 µg/ml (Fig. 5.8A-C). There was still a relatively high average increase in branch numbers of 275%, with them being double or slightly less than double of the control after incubation, with reference to B8 and A9 respectively. The increase was, however, less pronounced with regard to the tubule length, where there was an average of 190%. These changes were also not significant especially with A9, where there was only a slight increase of ~29% when compared to the control. Finally, the use of 10 µg/ml of the Affimers still caused increased tubule length and branch number (Fig. 5.9A-C), the averages were reduced compared to the previous concentrations at 117% and 138% respectively. This finding is emphasised, for example, in the results post VEGF-A stimulation; there was only a 5% difference in tubule length between the control and B8. In fact, tubule length was halved after A9 incubation when compared to the control. The branch number also showed some promising results, where the post-stimulation results showed reductions after the use of both B8 and A9 when compared to the control. The decreases were 13% and 63% for B8 and A9 respectively.

It is interesting, and in need of further study, that the results for all three concentrations were still higher than that of the control Affimer and Sutent. A possible explanation for this fact may be found in the finding that dosages of VEGFR2-specific Affimers higher than 10 µg/ml could show a greater inhibition of endothelial tubulogenesis. Further experimentation, along with the introduction of additional protocols, such as siRNA-mediated VEGFR-2 knockdown, may further clarify what these findings could mean.

A

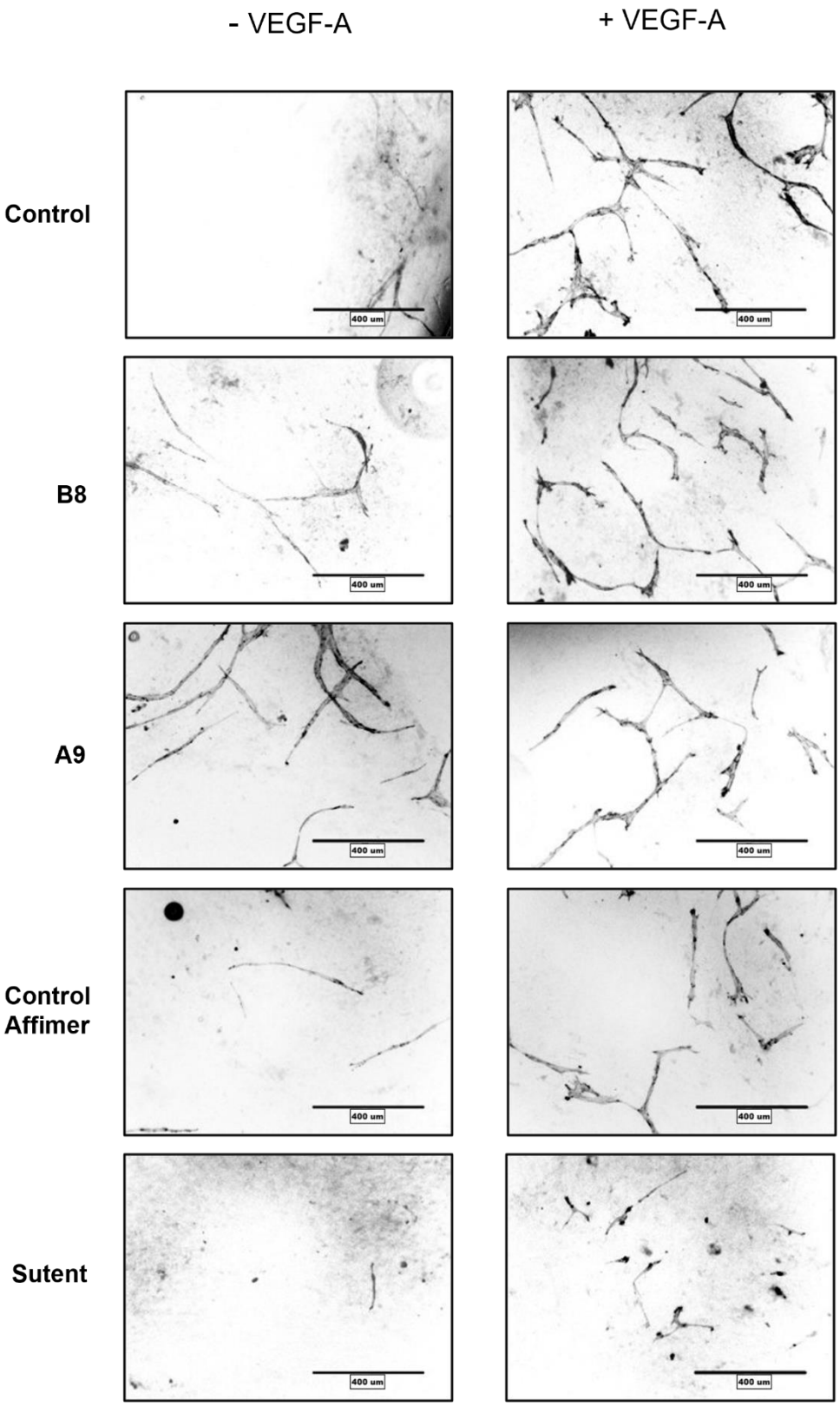

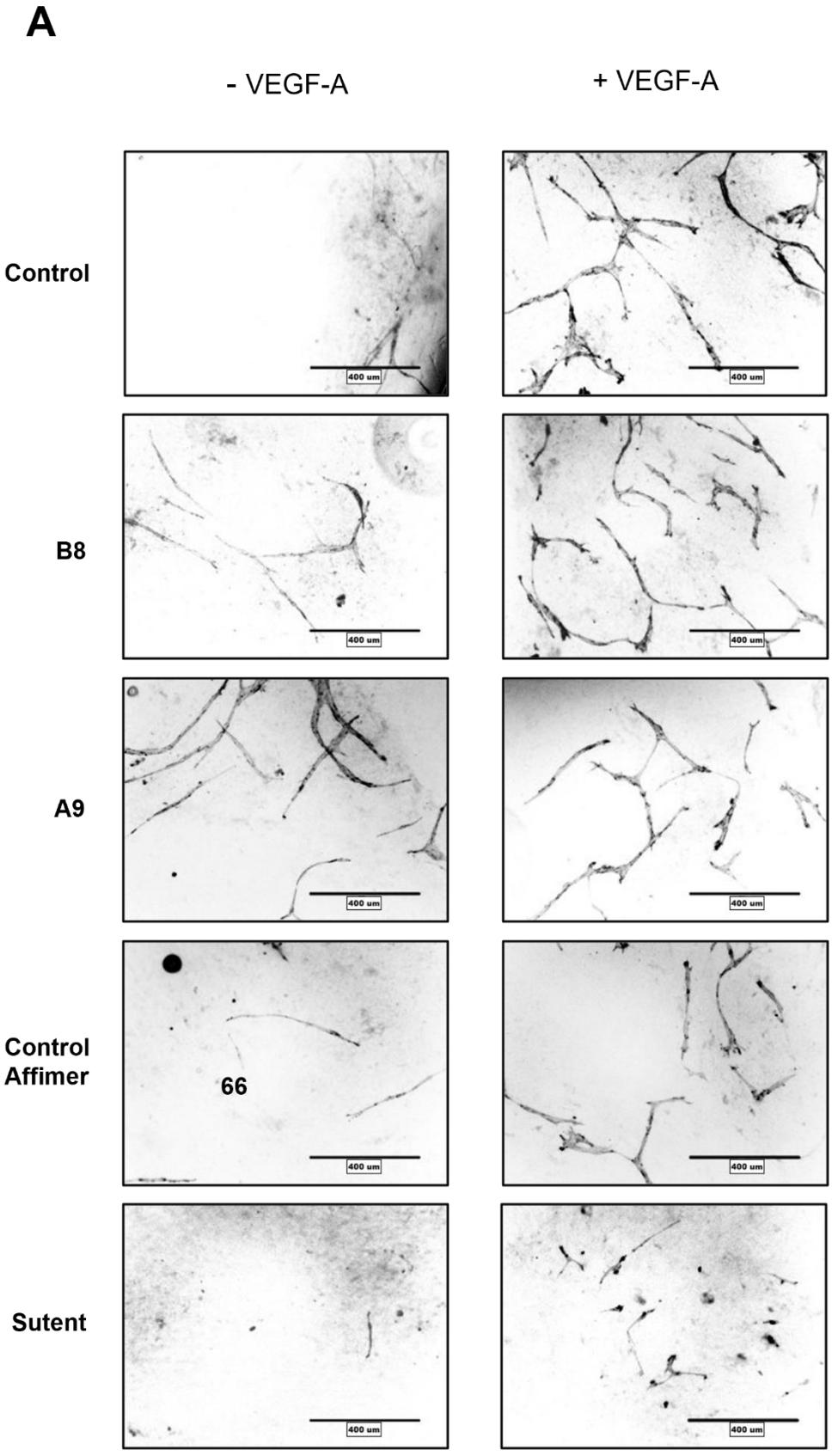
A
- VEGF-A
+ VEGF-A
Control
B8
A9
Control Affimer
Sutent
66
400 um

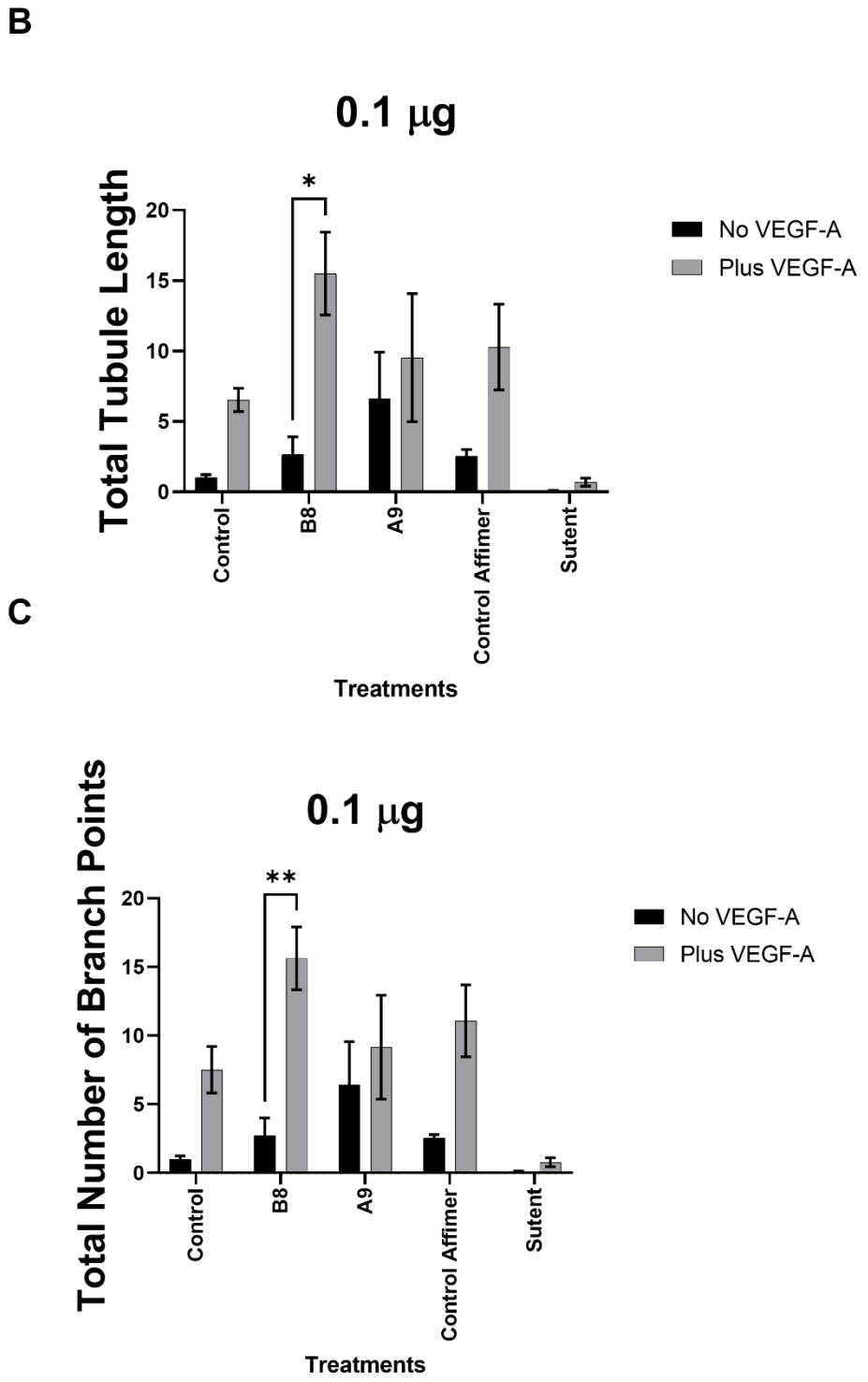

Figure 5.7: 0.1 µg/ml VEGFR2-Specific Affimers do not affect VEGF-A-stimulated tubulogenesis. *In vitro* HUVEC tubulogenesis assay on co-cultured fibroblasts. (A) HUVECs were incubated with 0.1 µg/ml of a control or VEGFR2-specific Affimers for 30 min prior to stimulation with 25 ng/ml VEGF-A. 1 µM Sutent was added as an additional control. Cells were fixed and stained with a PECAM-1 specific antibody with images being taken on a digital fluorescence microscope (EVOS FL Auto). Bar, 400 µm. Quantification was carried out using the Angioquant program to analyse (B) total tubule length and (C) the number of branch points of the tubules formed. relative to no stimulation respectively. Error bars denote ±SEM. Significance: *, $p<0.05$; **, $p<0.01$ (n=3).

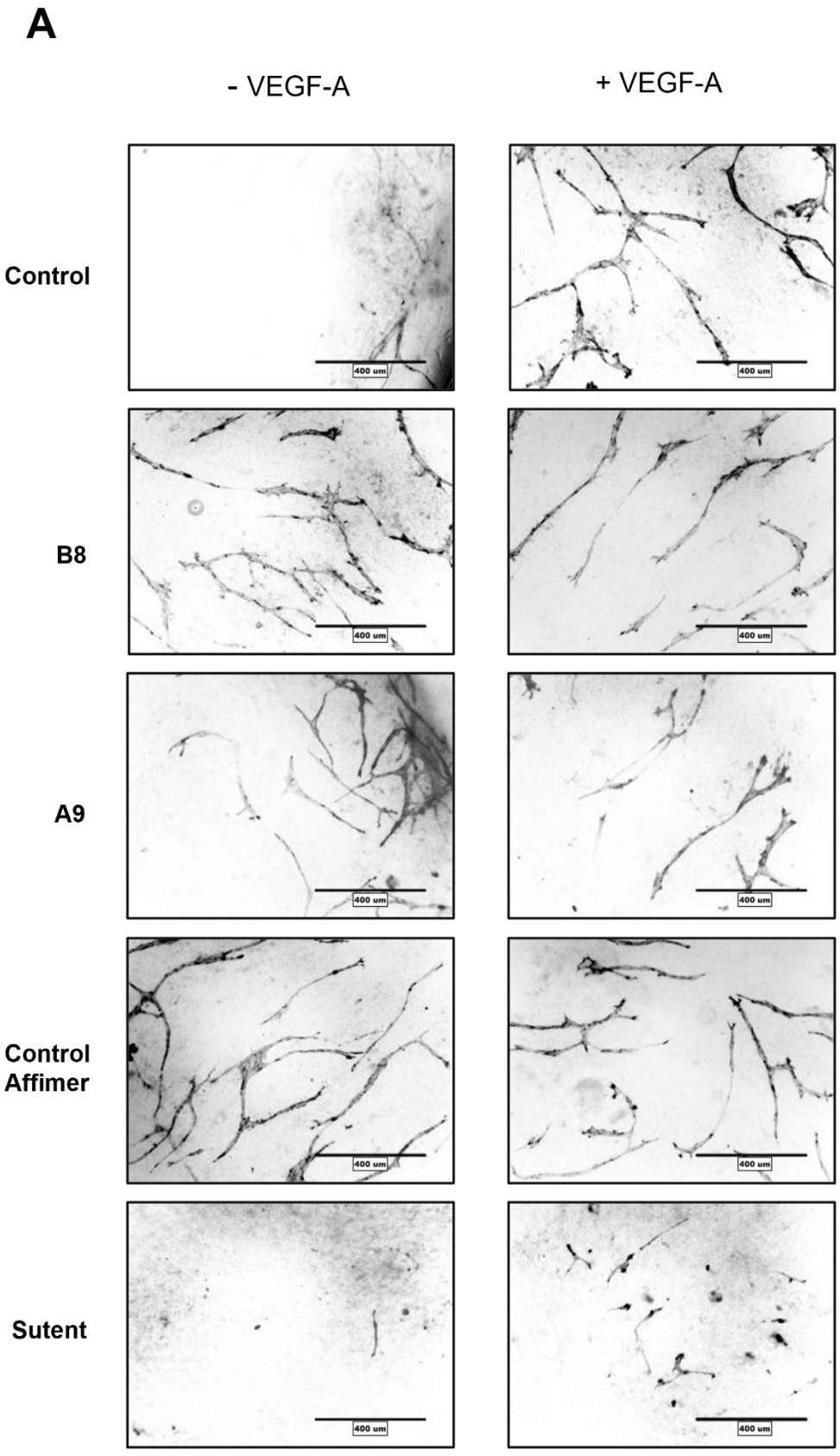
A
- VEGF-A
+ VEGF-A
Control
B8
A9
Control Affimer
Sutent
400 um

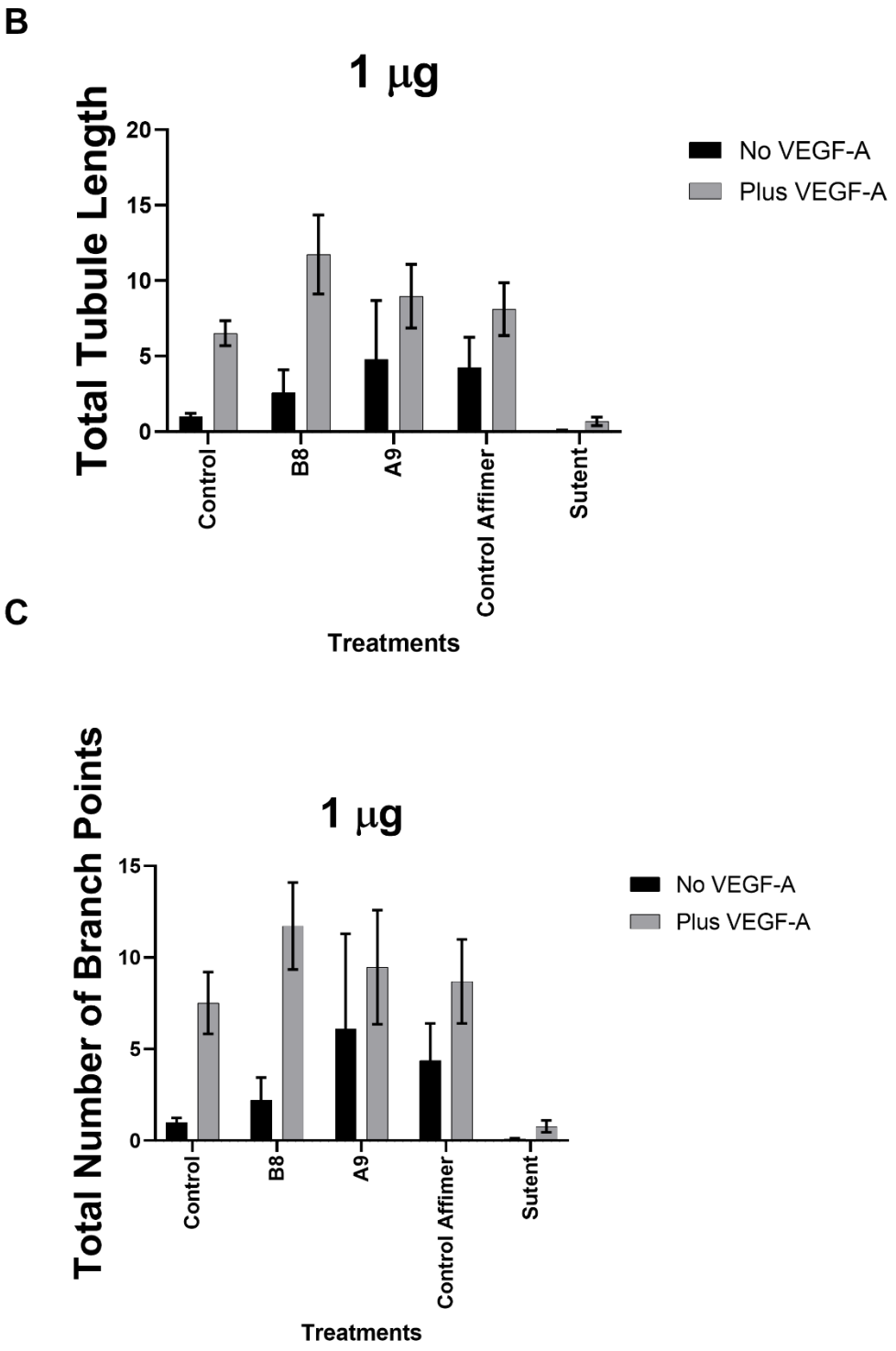

Figure 5.8: 1 µg/ml VEGFR2-Specific Affimers do not affect VEGF-A-stimulated tubulogenesis. *In vitro* HUVEC tubulogenesis assay on co-cultured fibroblasts. (A) HUVECs were incubated with 1 µg/ml of a control or VEGFR2-specific Affimers prior to stimulation for 30 min with 25 ng/ml VEGF-A. 1 µM Sutent was added as an additional control. Cells were fixed and stained with a PECAM-1 specific antibody with images being taken on a digital fluorescence microscope (EVOS FL Auto). Bar, 400 µm. Quantification was carried out using the Angioquant program to analyse (B) total tubule length and (C) the number of branch points of the tubules formed. relative to no stimulation respectively. Error bars denote ±SEM (n=3).

A

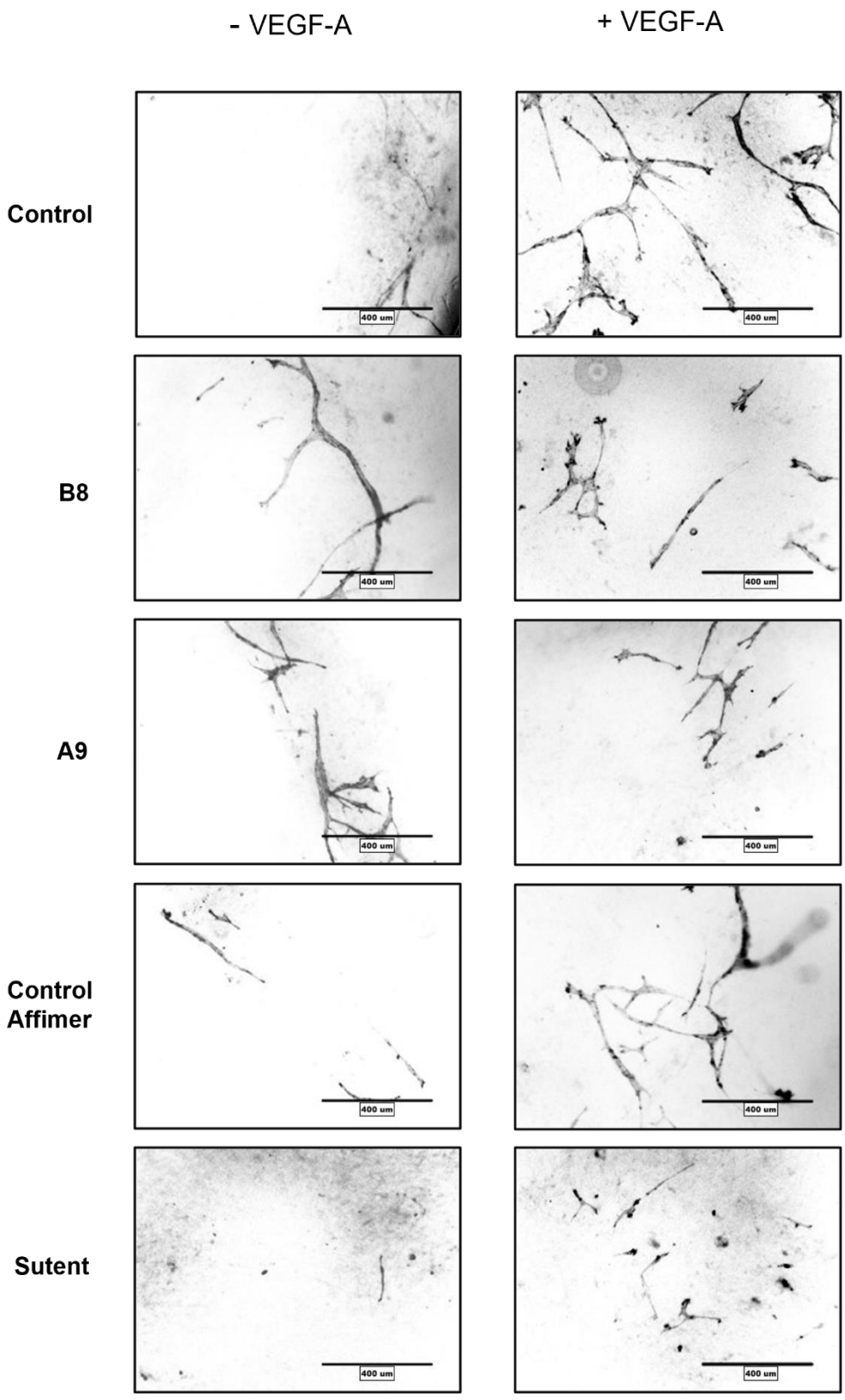

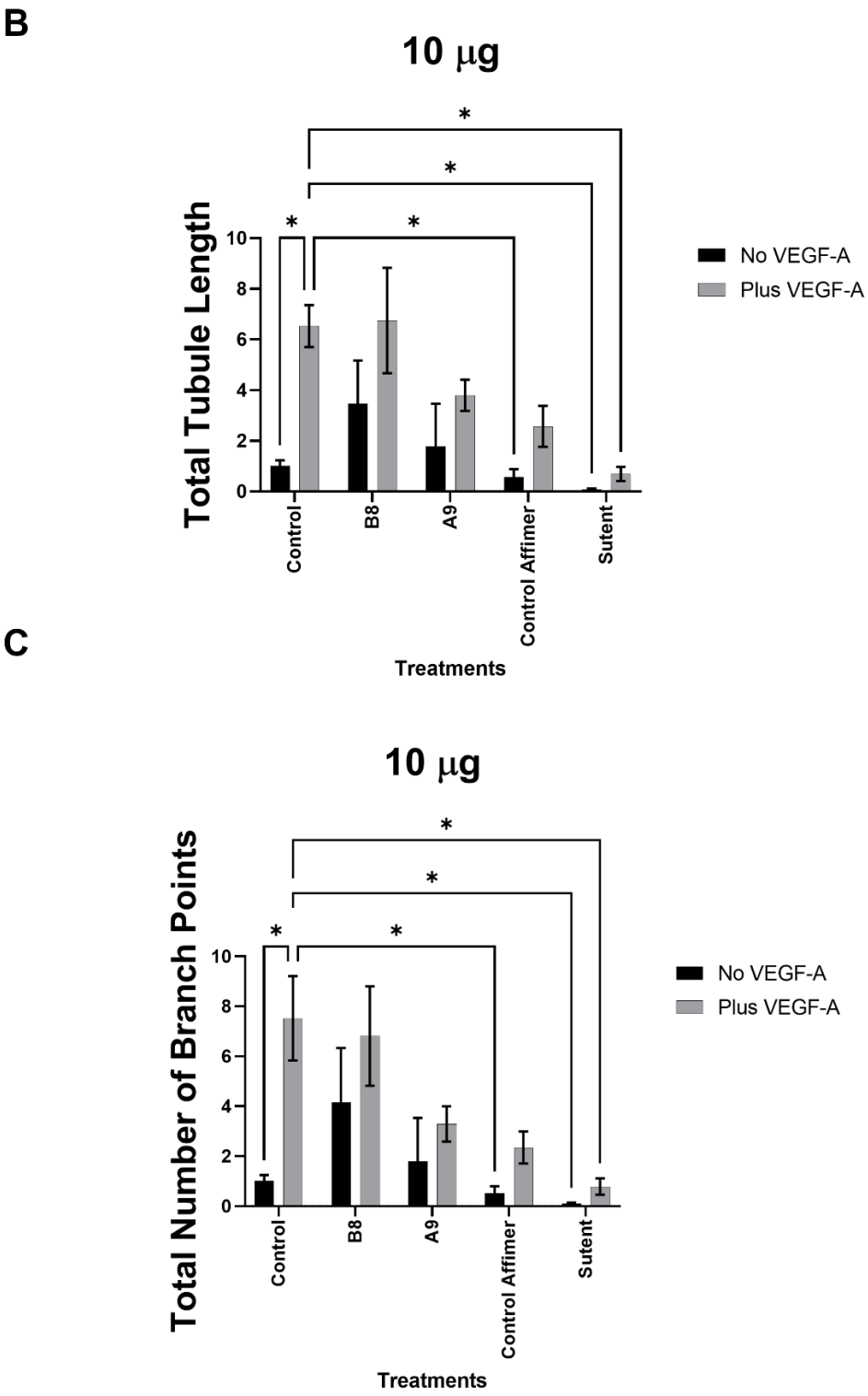

Figure 5.9: 10 µg/ml VEGFR2-Specific Affimers have low inhibitory effects on VEGF-A-stimulated tubulogenesis. *In vitro* HUVEC tubulogenesis assay on co-cultured fibroblasts. (A) HUVECs were incubated with 10 µg/ml of a control or VEGFR2-specific Affimers for 30 min prior to stimulation with 25 ng/ml VEGF-A. 1 µM Sutent was added as an additional control. Cells were fixed and stained with a PECAM-1 specific antibody with images being taken on a digital fluorescence microscope (EVOS FL Auto). Bar, 400 µm. Quantification was carried out using the Angioquant program to analyse (B) total tubule length and (C) the number of branch points of the tubules formed. relative to no stimulation respectively. Error bars denote ±SEM. Significance: *, $p<0.05$ (n=3).

5.3 DISCUSSION

The development of antibodies has played a huge part in treating VEGF-related diseases. VEGF/VEGFR was actually one of the top targets within the first 100 mABs to be approved by the FDA, with four antibodies being approved. The use of antibodies against VEGF and its receptors is not only special on a clinical level, but it is also a profitable one. For instance, the VEGF-targeting bevacizumab (Genentech) was one of the top selling mABs in 2019. This was followed by ranibizumab (VEGF-targeting Fab, Genentech) which was approved for age-related macular degeneration in 2006, and, thus far, is the only non-canonical antibody to break into the top-20 sales list for antibodies. It, and its cancer-treating counterpart, bevacizumab, are only commercially viable due to the facts that they are from the same mouse antibody and have, supposedly, an equivalent activity. Ranibizumab is also one-third of the price of bevacizumab, due to it being a Fab fragment which enables better retinal penetration. Overall, the association of the VEGF pathway to both cardiovascular and cancer has led to non-stop research on the topic, leading to probably more FDA approvals in the future (Mullard, 2021).

Although the VEGFR2 signalling pathways are well-studied, there are still some unanswered questions about how it may be activated or inhibited, especially with regards to VEGFR1. These receptors act in very similar yet drastically different ways depending upon the ligand which stimulates them. This is why it was a felt to be a key aim, in this project, to ascertain more information about how, in particular, these novel inhibitors would work on the VEGFR2 receptor. This project has demonstrated that the impact on cellular function was not only different between the Affimer scaffolds used, but their method of action was even varied by their concentration (Table 5.2).

Cell Assay Type	Most Effective VEGFR2 Affimer	Affimer Concentration
Viability	A9	1 µg/ml
Migration	B8	10 µg/ml

Table 5.2 Most Effective VEGFR2 Specific Affimers. A summary of the previous VEGF-A mediated cellular assays. Based on the Affimers which were able to be tested, estimates were made about which Affimer was the best VEGFR2 inhibitor in each experiment along with its most effective concentration.

The VEGF-A mediated proliferation and migration of endothelial cells were found to reduce depending upon the concentration of VEGFR2-Affimer, which was only to be expected. However, there were also increases in proliferation seen after VEGF-B stimulation, specific to VEGFR1, indicating that it may still promote cell survival even in the absence of proper VEGFR2 signalling. This could be related to the other VEGFR1-specific ligand, placental growth factor (PlGF). This growth factor is often overexpressed in tumour cells, although it can inhibit growth *via* VEGF/PlGF heterodimers in some models. In one study, using anti-PlGF mAbs inhibits the activation of the MAPK cascade pathway in VEGFR1-specific tumours (Yao et al., 2011). This emphasises the need to not only test the effects of VEGF-A stimulation on cancer progression, but also the specific ligands to VEGFR1, namely PlGF and VEGF-B. Ideally, the dose titrations used in this project serve to help to pin-point ideal inhibitory concentrations of VEGFR2-specific Affimers, such as 1 µg/ml, which would maintain endothelial cell survival through VEGF-B, yet effectively inhibit pathogenic migration towards tumour cells.

Tubule formation was slightly inhibited after VEGFR2 inhibition at higher concentrations of the Affimers, as compared to the cells incubated only with VEGF-A. Tubule branch number and length was also substantially lower after VEGFR2 inhibition compared to when VEGFR1-inhibitory Affimers

were used in chapter 4. This could potentially be explained by differences in phosphorylation and thus activation of the receptors. In previous immunoprecipitation studies on endothelial and fibroblast cell lines, it was revealed that overexpression of KDR (VEGFR2) showed significant increases in phospholipase C-γ (PLC-γ) phosphorylation. This was weaker in cells overexpressing Flt-1 (VEGFR1), indicating that it is in factor VEGFR2 which is the main receptor responsible for PLC-γ activation despite it also binding well to VEGFR1 (Sawano et al., 1997). One of the main tyrosine residues on VEGFR2 is 1175-Y, which is a major auto-phosphorylation site which binds PLCγ. The equivalent of this site in VEGFR1 is the tyrosine residue 1169-PY, although it is not a highly phosphorylated region. The PLCγ pathway contains protein kinase C (PKC), which is a major effector of tubulogenesis. Therefore, the higher kinase activity of VEGFR2 in response to VEGF-A could explain why it plays a major role in angiogenesis as compared to VEGFR1 (Shibuya, 2011).

Overall, the potential benefits of these VEGFR2-specific Affimers show potential, but still require a lot more optimisation. For instance, there were certain cellular experiment results which seem to imply that concentrations higher than 10 µg/ml would further potentiate inhibition *via* VEGFR2-Afifmers. Further experimentation would be useful for identifying what these concentrations may be, and if they would still be relevant physiologically and safe in future research.

Chapter 6

Affimer-Based Targeting of VEGFR Function in Cancer Epithelial Cells

6.1. INTRODUCTION

Cancer therapy is complicated by the multitude of biochemical pathways through which this disease develops and progresses leading to mortality. My initial project aims were to use Affimers to target VEGFR1 function in endothelial cells and assess whether this could be of potential therapeutic benefit. The previous development of VEGFR2-specific Affimers suggested that the endothelial response to VEGF-A could be dramatically modulated by such agents (Tiede et al., 2017). An alternative route to assessing Affimer efficacy to VEGF-regulated cellular responses is to evaluate VEGF-dependent responses in epithelial cancer cells, such as A431. Numerous studies on A431 cells have largely focused on the cellular response to epidermal growth factor (EGF) caused by elevated expression of EGF receptor or ErbB1 (EGFR/ErbB1) (Masui *et al.,* 1993). However, the VEGF-stimulated response of A431 cells means that these cells could also provide another test of our VEGFR-specific Affimers (Di Benedetto et al., 2003) .

Eukaryote cell cycle can be broadly split into four phases. The two main cell division periods are the DNA synthesis (S) phase, where chromosomes are doubled and the mitosis (M) phase, where the newly divided chromosomes are partitioned between the 2 daughter cells. There are also two growth (or gap) phases termed G1 and G2, which also act as checkpoints for the S and M phases respectively. G1 and G2 delay the cell division periods, not only to prohibit potential mutations in the DNA occurring, but also to allow more time for cells to grow in size and duplicate other cellular contents (Alberts et al., 2002). A major advance in the study of the cell cycle linked to cancer cell proliferation is the use of fluorescent reporter systems which are used to monitor living cells. One such is the Fluorescent Ubiquitination-based Cell Cycle Indicator (FUCCI) system (Zielke and Edgar, 2015; Sakaue-Sawano et al., 2008)

The FUCCI system relies on the concept of ubiquitin-regulated proteolysis of specific cell cycle proteins e.g. through the activity of ubiquitin E3 ligase complexes APC^{Cdh1} and SCF^{SKP2}, which are active during the M/G1 phase and S/G2 phase respectively. APC^{Cdh1} and SCF^{SKP2} reciprocally inhibit each other throughout the cell cycle due to their binding to specific substrates which are marked for degradation in different phases of the cell cycle. However, SCF^{SKP2} can also act as a APC^{Cdh1} inhibitor. APC^{Cdh1} binds to Geminin, which usually peaks during the S/G2 phases, whereas SCF^{SKP2} binds to Cdt1, which peaks during G1. The accumulation and degradation of both Geminin and Cdt1 at specific points ensures that each cell replication stage only occurs once throughout single cycle. The FUCCI system uses fluorescent probes in order to visualize the peaks and troughs of Geminin and Cdt1 throughout the cell cycle over time. These fluorescent reporters are monomeric Kusabira Orange (mKO2), fused to Cdt1, and monomeric Azami Green (mAG), fused to Geminin (Sakaue-Sawano et al., 2008). Figure 6.1 depicts the expression of FUCCI biomarkers during the cell cycle which could be detected by fluorescence microscopy. Visualization of red fluorescence (mKO) is emitted by cells at the G1 phase, whereas green fluorescence (mAG) by cells shows G2/M phases. An overlay of such staining patterns in a field of cells indicates which cells are in stationary or actively proliferating phases.

The FUCCI system has provided new ways to not only analyse cell kinetics in real-time but also to carry out *in vivo* studies (Zielke and Edgar, 2015). For example, zebrafish have often been used as animal models in cardiovascular research due to their increased ability to regenerate the damaged heart, such as after cardiomyocyte ablation or cryoinjury. A FUCCI-transgenic zebrafish line was created where Cdt1 and Geminin reporters of the FUCCI system were fused to the cardiac myosin light chain *2* promoter sequence *(CMLC2)* in cardiomyocytes. Drug screens on live FUCCI-zebrafish embryos showed roles for several signal transduction pathways, including Transforming growth factor β (Tgfβ) and Hedgehog (Hh) in cardiomyocyte proliferation (Choi et al., 2013).

The aims of the experiments in this chapter were to assess the effects of Affimers in combination with either VEGF-A or placental growth factor-1 (PlGF-1): these are known ligands for VEGFR1 and VEGFR2 or VEGFR1 alone. These effects were assessed using a stably transfected human A431-FUCCI cell line. Using VEGFR1- or VEGFR2-specific Affimers could thus evaluate VEGFR contribution to epithelial cancer cell responses to either VEGF-A or PlGF-1.

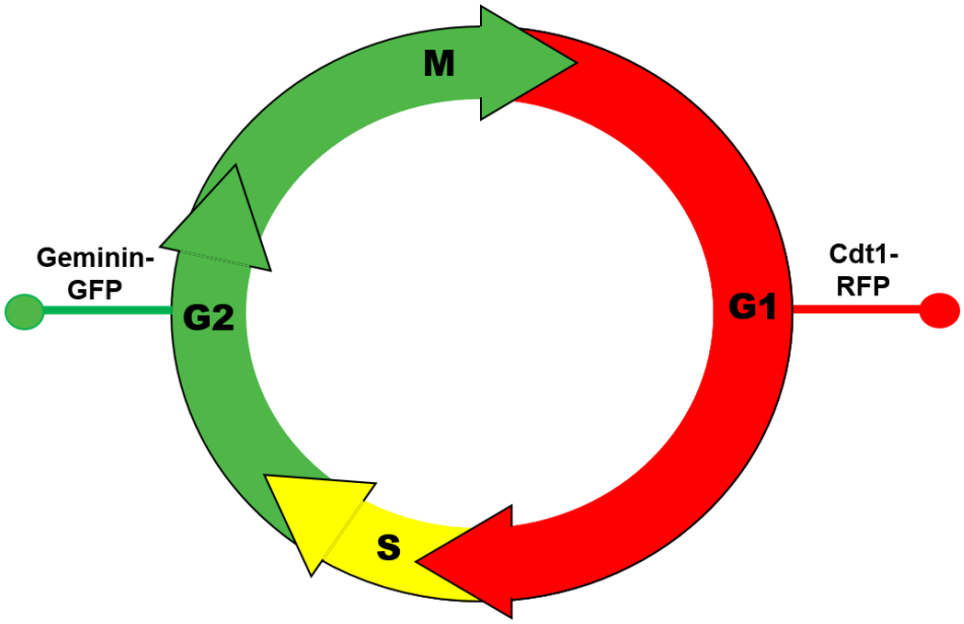

Figure 6.1. The FUCCI reporter system. The eukaryote cell cycle regulators Cdt1 and Geminin show cyclical changes in protein levels. Expression of chimeric or hybrid proteins comprising Cdt1-mKO (red) and Geminin-mAG (green) enables visualization of these cell cycle phases in living cells. G1 (red) represents the first stage of the growth cycle, DNA synthesis in the S phase (yellow), G2 (green) is the second growth phase of the cycle which includes mitosis (M). Abbreviations: monomeric Kusabira Orange, mKO; monomeric Azami Green, mAG.

6.2. RESULTS

6.2.1. VEGFR1-specific Affimers effects on VEGF-regulated A431 cell proliferation

Throughout this research, Affimers have been used in a dose-dependent manner to assess effects on cellular responses. This was to identify the optimal concentration of each Affimer in each assay in order to assess their effects on specific cellular processes. In these set of experiments, Affimer concentrations of 0, 0.1, 1 and 10 µg/ml of either VEGFR1- or VEGFR2-specific Affimers were tested for effects on A431-FUCCI cell growth and cell cycle kinetics. Based on previous studies on primary endothelial cells, 10 ng/ml of the chosen growth factors, VEGF-A and PlGF-1, were used as a maximal stimulatory condition in these studies. Previous experiments had mainly focused on using VEGF-A due to its ability to bind to both VEGFR1 and VEGFR2, but the effects of PlGF-1 were assessed, since PlGF-1 only binds to VEGFR1. A control Affimer (scrambled loop sequences) was used in comparison to VEGFR-specific Affimers. The VEGFR2 tyrosine kinase inhibitor, Sutent, was also used in conjunction with either VEGF-A or PlGF-1 to block VEGFR activation and signalling. The use of serum-free media such as OptiMEM was used to starve cells before VEGF stimulation in the presence or absence of Affimer.

A titration of VEGFR1-specific Affimer 35 and Affimer 37 after VEGF-A stimulation was evaluated on A431-FUCCI cells (Figs. 6.2, 6.3). There were an increased number of visible green cells (G2/M) observed upon combining VEGFR1-specific Affimer and VEGF-A, as compared to the application of the control Affimer and VEGF-A treatment, after an incubation period of 24 h (Fig.6.2A, 6.3A). After a 48-h incubation period, there was an overall increase in red cells (G1/S) with every treatment; there also, appeared to be an increase in the number of yellow cells in the VEGFR1-specific Affimer treatments. Quantification of these cell numbers for Affimers 35 (Fig.6.2B) and Affimer 37 (Fig. 6.3B) respectively confirm these trends.

Incubation with 0.1 µg/ml of either Affimer 35 or Affimer 37 showed the highest number of total cells after 24 and 48 h (Figs. 6.2B, 6.3B). For instance, Affimer 35 treatment showed a 64% increase in cell count over the course of 24 h, whilst Affimer 37 showed a 17% increase in total cell

numbers as compared to cell numbers with VEGF-A treatment alone Fig.6.3B). Interestingly, the total number of cells decreased with increasing concentrations of both Affimers, but still remained higher than treatment with VEGF-A alone. If we compare Affimer 37 and VEGF-A treatment vs. control (VEGF-A alone), we can see that all three concentrations exhibit greater cell numbers of 174% (0.1 µg/ml), 159% (1 µg/ml), and 138% (10 µg/ml) respectively. The number of cycling green and yellow cells is dose-dependent, as they are inversely correlated to increasing concentration of Affimer 37. Lower concentrations of Affimer 37 therefore may be allowing cells to progress through G2/M. This is in contrast to 10 µg/ml of Affimer 37, as there was a significant increase in the number of red cells (G1/S) over the 24 h time course (p=0.0001) of 131% (Fig. 6.3B). This could indicate that more cells are stuck within the G1 phase at this concentration.

This cell cycle pattern is also matched by the results showing Affimer 35, although there are some differences. (Fig.6.2B). Looking at only the 48h treatment, the total cell count is decreased by 44% upon addition of 0.1 or 1 µg/ml of Affimer 35, this is accompanied by a significant decrease in the number of red cells (0.0005) (Fig. 6.2B). 10 µg/ml of Affimer 35 also attenuated cell growth, with there being a 28% decrease over the course of 24 h. This final concentration is also 57% and 72% lower than VEGF-A alone and Sutent respectively. This could be explained by an almost negligible number of green cells, indicating that there are less cells progressing thorough S2/G2/M.= This is unexpected, as using a VEGFR1 inhibitor should allow for increased stimulation of VEGFR2 with VEGF-A, thereby increasing cell growth and viability.

There were both similarities and differences found in the effects of both VEGFR1-specific Affimers. Both Affimers caused increased cell proliferation over the course of 24 h and exhibited dose-dependent effects to a similar degree. Differences were evident when comparing Affimer dosage effects at the same time period vs. positive and negative controls. This is seen upon Affimer 35 treatment, where the highest concentration of 10 µg/ml showed lower numbers of A431-FUCCI cells as compared to either the VEGF-A

alone or upon Sutent addition (Fig. 6.2). Cell cycle progression can also be seen through increases in yellow and green cells, which show the S and G2 phases respectively. The quantity of cells in S and/or G2 seems to increase upon treatment with either VEGFR1-specific Affimer, but this and overall cell growth is decreased with increasing concentration.

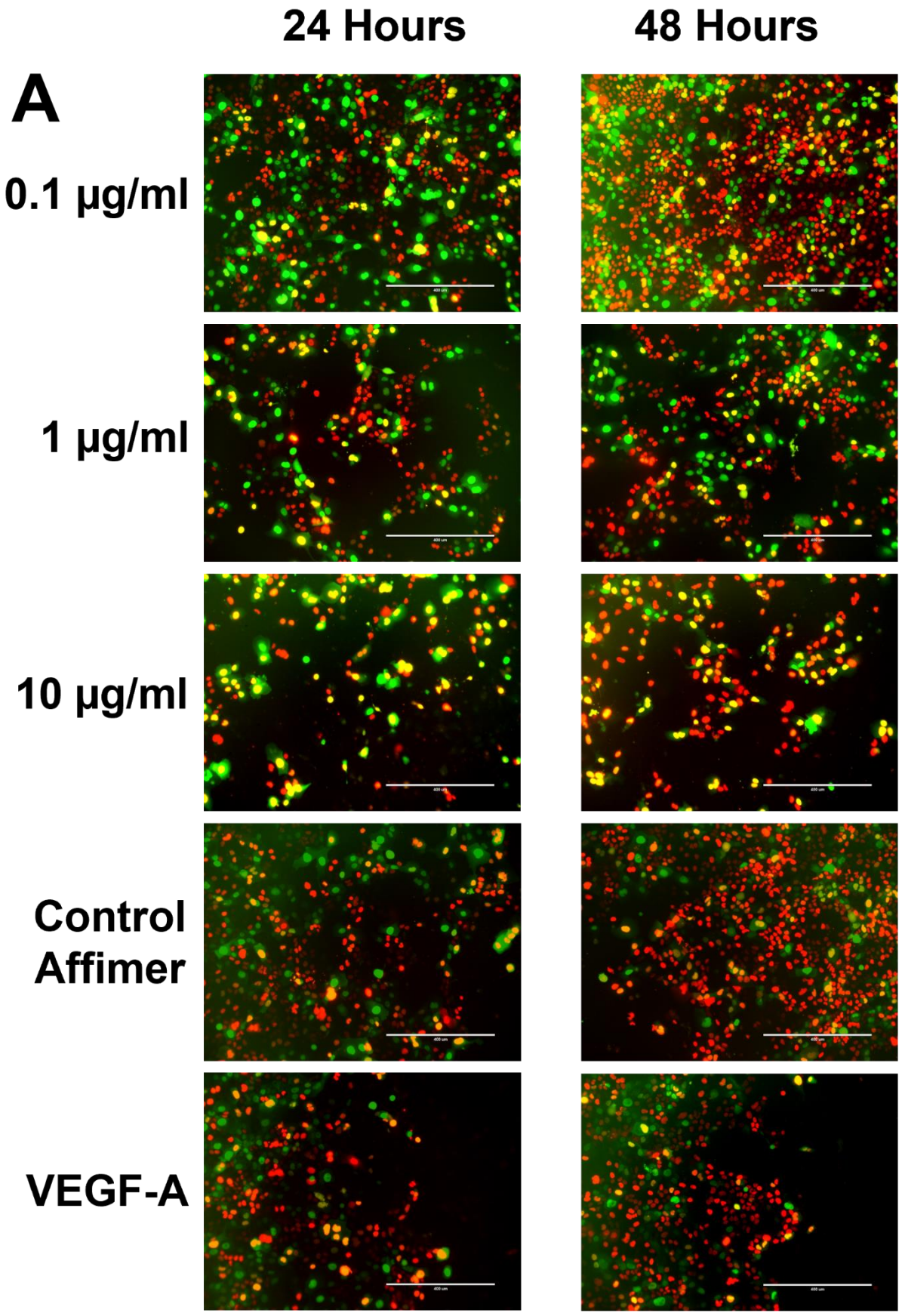
24 Hours
48 Hours
A
0.1 µg/ml
1 µg/ml
10 µg/ml
Control Affimer
VEGF-A

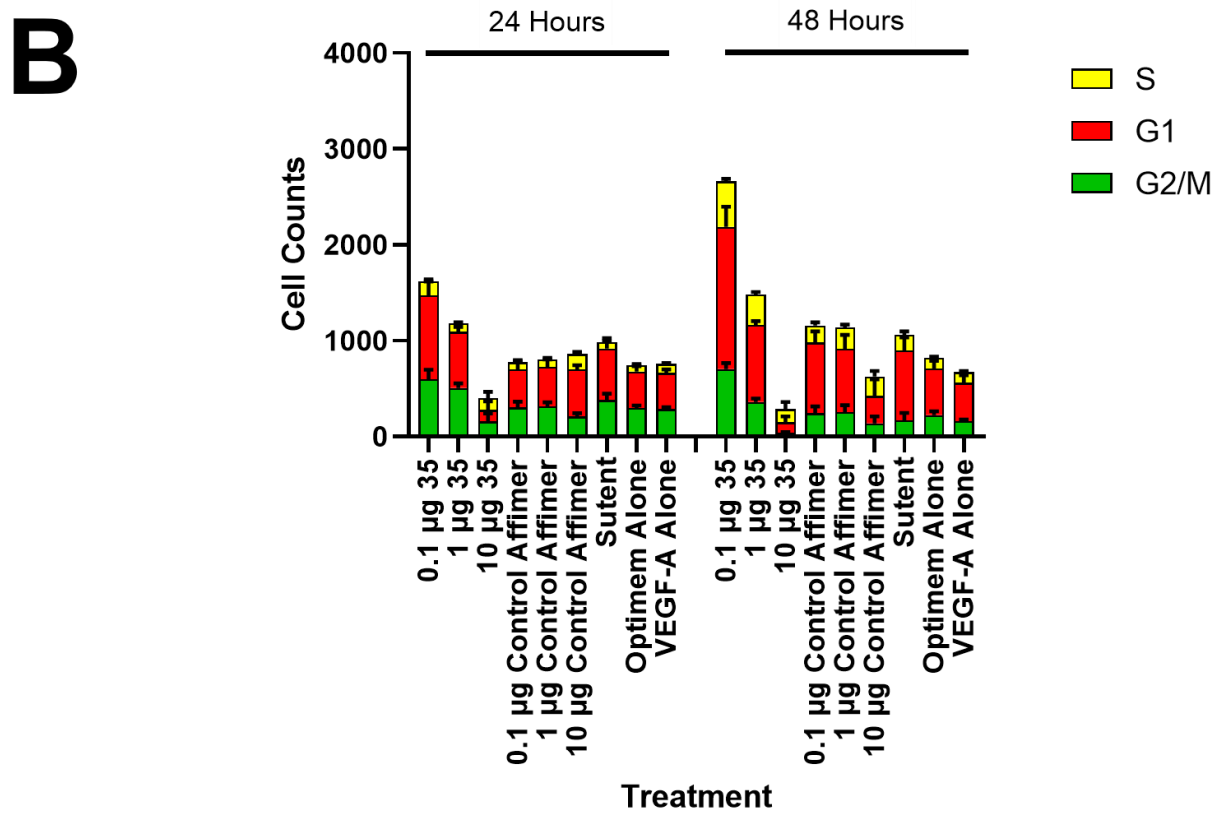

Figure 6.2. VEGFR1-specific Affimer 35 modulates VEGF-A-regulated epithelial cell proliferation. (A) A431-FUCCI cells were starved in Optimem medium for 2 h and incubated with the VEGFR1-specific Affimer 35 or control Affimer (0.1, 1 or 10 µg/ml) for 30 min prior to stimulation with VEGF-A (10 ng/ml). Wells containing 1 µM Sutent or Optimem+VEGF-A were used as additional controls. Representative images of three fields of view were taken on a digital fluorescence microscope (EVOS FL Auto) at 24 and 48 h. Images were taken with the GFP and RFP filters and cells counted using the overlays. Scale bar = 400 µm. (B) Quantification of the number of coloured cells depict the effects of 0.1, 1 or 10 µg/ml VEGFR1-specific Affimer blockage upon Affimer 35 treatment. Error bars denote ±SEM (n=3).

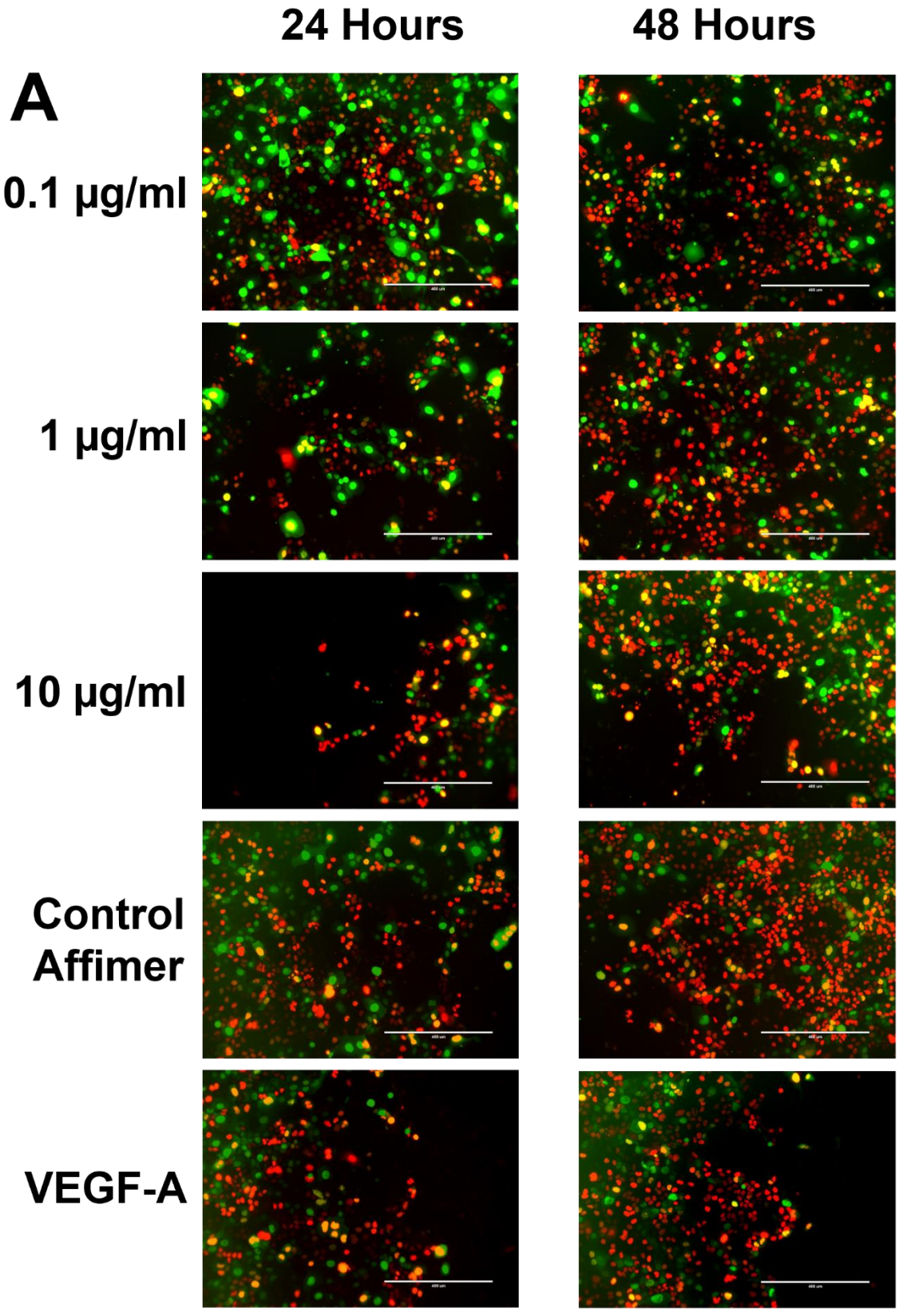
24 Hours
48 Hours
A
0.1 µg/ml
1 µg/ml
10 µg/ml
Control Affimer
VEGF-A

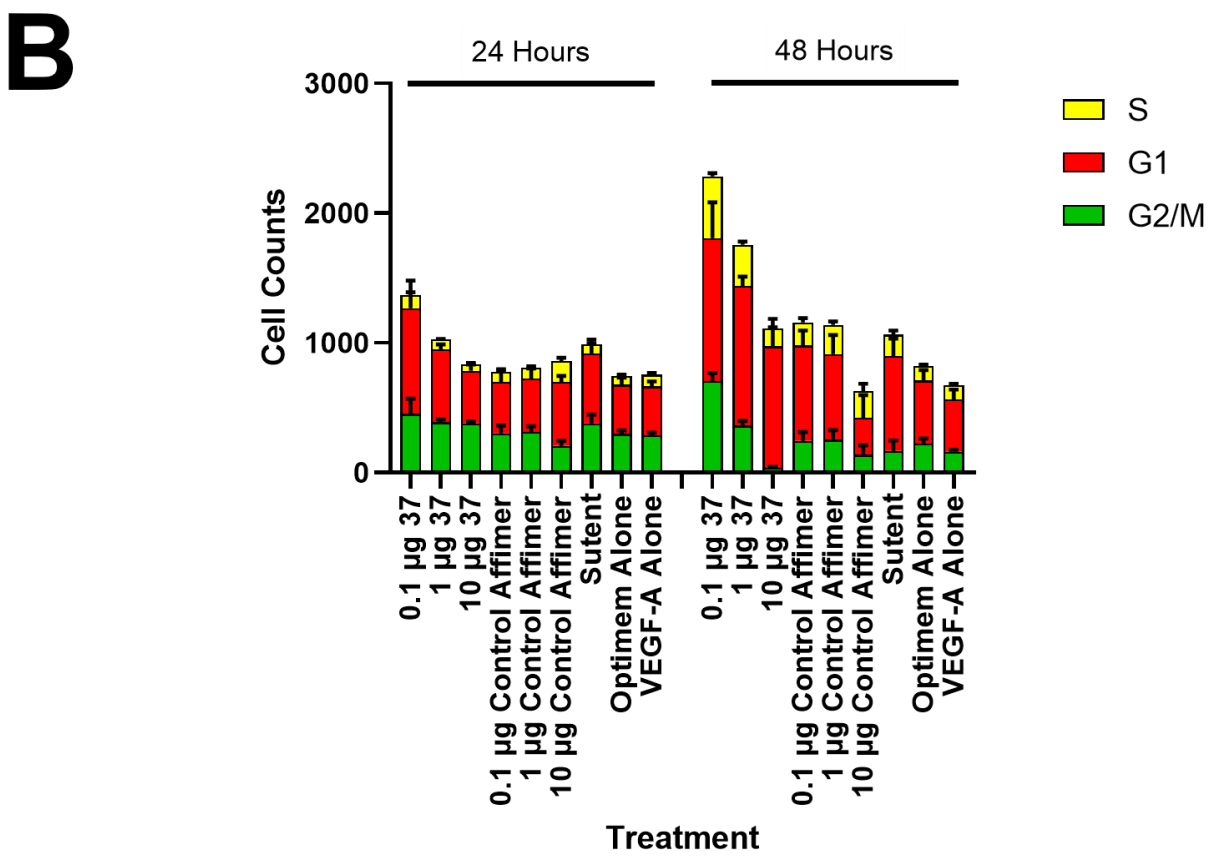

Figure 6.3. VEGFR1-specific Affimer 37 modulates VEGF-A-regulated epithelial cell proliferation. (A) A431-FUCCI cells were starved in Optimem medium for 2 h and incubated with the VEGFR1-specific Affimer 37 or control Affimer (0.1, 1 or 10 µg/ml) for 30 min prior to stimulation with VEGF-A (10 ng/ml). Wells containing 1 µM Sutent or Optimem+VEGF-A were used as additional controls. Representative images of three fields of view were taken on a digital fluorescence microscope (EVOS FL Auto) at 24 and 48 h. Images were taken with the GFP and RFP filters and cells counted using the overlays. Scale bar = 400 µm. (B) Quantification of the number of different coloured cells depict the effects of 0.1, 1 or 10 µg/ml VEGFR1-specific Affimer blockage upon Affimer 37 treatment. Error bars denote ±SEM (n=3).

6.2.2. VEGFR2-specific Affimer effects on VEGF-A-regulated A431 cell proliferation

Previous work has established that VEGFR2-specific Affimer B8 and Affimer A9 modulate VEGF-A-stimulated responses in endothelial cells (Tiede et al., 2017; work in this PhD thesis). Affimer B8 and A9 were subsequently used on A431-FUCCI cells, and the effects analysed (Figs .6.4,6.5). There were generally fewer A431-FUCCI cells remaining after treatment with either 0.1 µg/ml Affimer B8 (Fig. 6.4B) or Affimer A9 Fig.6.5B) at both 24 h and 48 h. Quantification of the total number of A431-FUCCI cells were lowest at 24 h for all three concentrations used of Affimer B8 or Affimer A9 (Figs. 6.4, 6.5). Interestingly, the cell counts after incubation with both of these Affimers were approximately the same at each corresponding concentration. For example, the overall number of cells decreased with concentration at 48 h, where there was a ~24% and ~32% difference between 0.1 vs. 1 µg/ml of Affimer B8 and Affimer A9 respectively. This was also mirrored in the difference between 1 and 10 µg/ml treatments for both of these Affimers, where there were changes of 77% and 66% in red cell numbers for Affimer B8 and Affimer A9 treatments respectively. There was an increase in cell count and therefore proliferation between 24 and 48h for both Affimers at 0.1 and 1 µg/ml, but these were still lower than their equivalent concentrations of control Affimer and alongside Sutent. The observation of a steady decrease in the numbers of both green and yellow cells as the concentrations of Affimers increases, in spite of the fact that the overall cell count is high, is an interesting finding. These factors could lead to the conclusion that the majority of the cells are remaining in the G1 phase after an initial burst of cell growth over 24 h. However, the expected VEGFR2-induced decrease in cell count from 24 h to 48 h was only seen with Affimer B8 at 10 µg/ml, which was 57%. There was also an almost equal number of green to red cells, with a ~10% difference (green>red cells) ‘as well as the lowest number of yellow cells (S phase). This indicates increased accumulation of A431-FUCCI cells in S phase upon such Affimer treatment.

The overall effects of both Affimer B8 and Affimer A9 were similar on A431-FUCCI cells. Both Affimers promoted cell proliferation at 0.1 and 1 µg/ml but B8 inhibited cell proliferation at 10 µg/ml, over a 24 hr period (Fig. 6.4B, 6.5B). This VEGFR2-specific Affimer dosage appeared more effective that using the VEGFR2 tyrosine kinase inhibitor, Sutent (Figs. 6.4, 6.5).

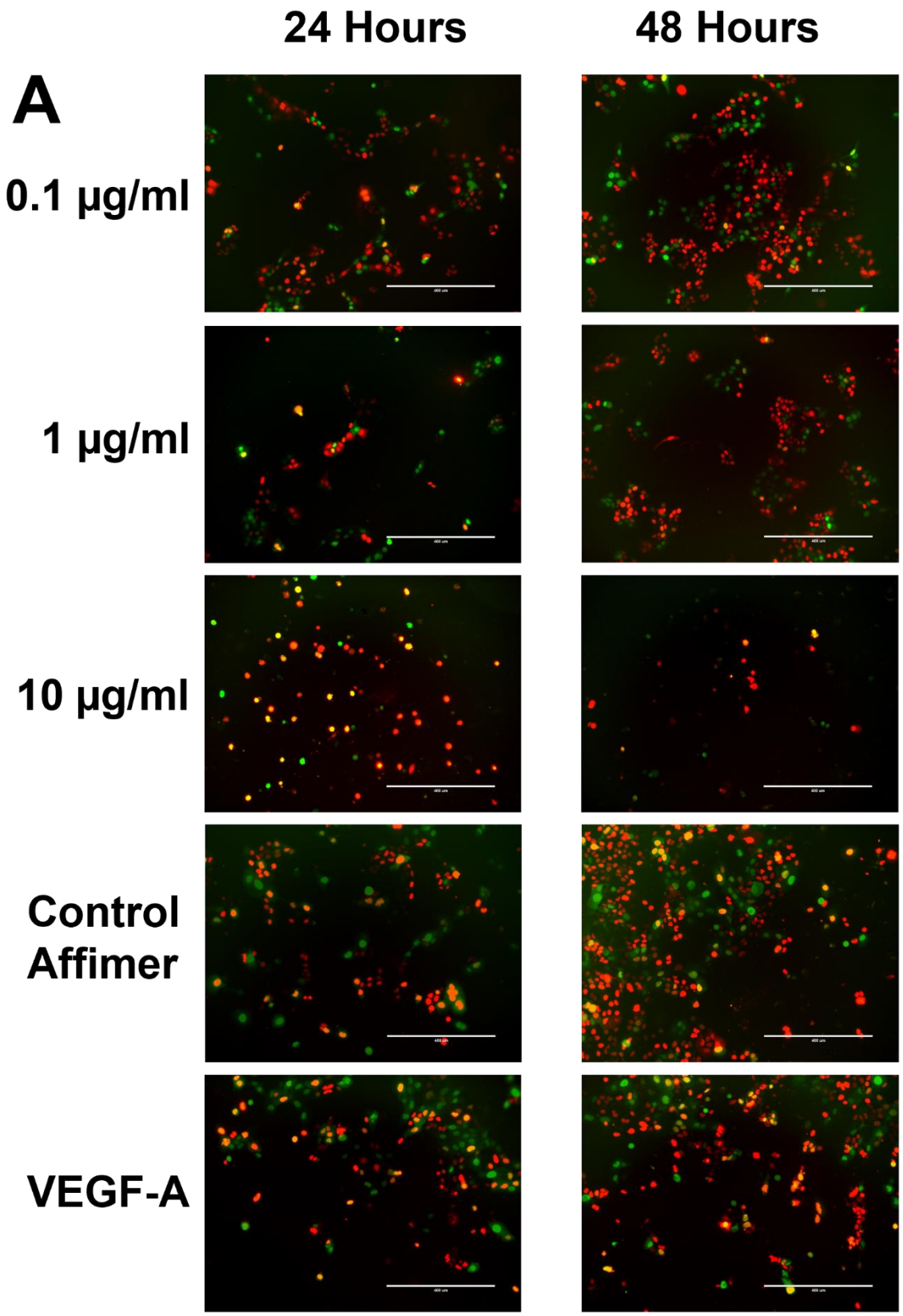
24 Hours
48 Hours
A
0.1 µg/ml
1 µg/ml
10 µg/ml
Control Affimer
VEGF-A

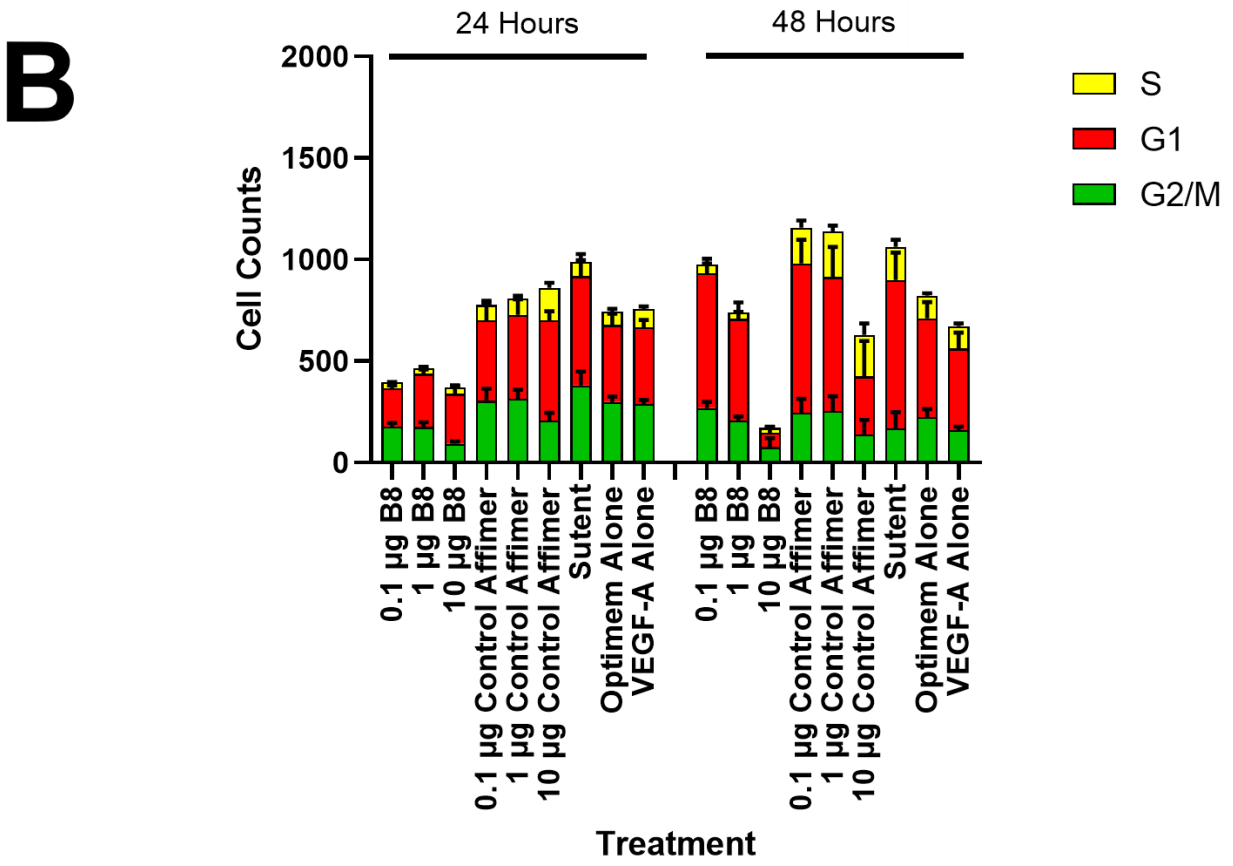

Figure 6.4. VEGFR2-specific Affimer B8 modulates VEGF-A-regulated epithelial cell proliferation. (A) A431-FUCCI cells were starved in Optimem medium for 2 h and incubated with the VEGFR1-specific Affimer B8 or control Affimer (0.1, 1 or 10 µg/ml) for 30 min prior to stimulation with VEGF-A (10 ng/ml). Wells containing 1 µM Sutent or Optimem+VEGF-A were used as additional controls. Representative images of three fields of view were taken on a digital fluorescence microscope (EVOS FL Auto) at 24 and 48 h. Images were taken with the GFP and RFP filters and cells counted using the overlays. Scale bar = 400 µm. (B) Quantification of the number of different coloured of cells depict the effects of 0.1, 1 or 10 µg/ml VEGFR2-specific Affimer blockage upon Affimer B8 treatment. Error bars denote ±SEM (n=3).

.

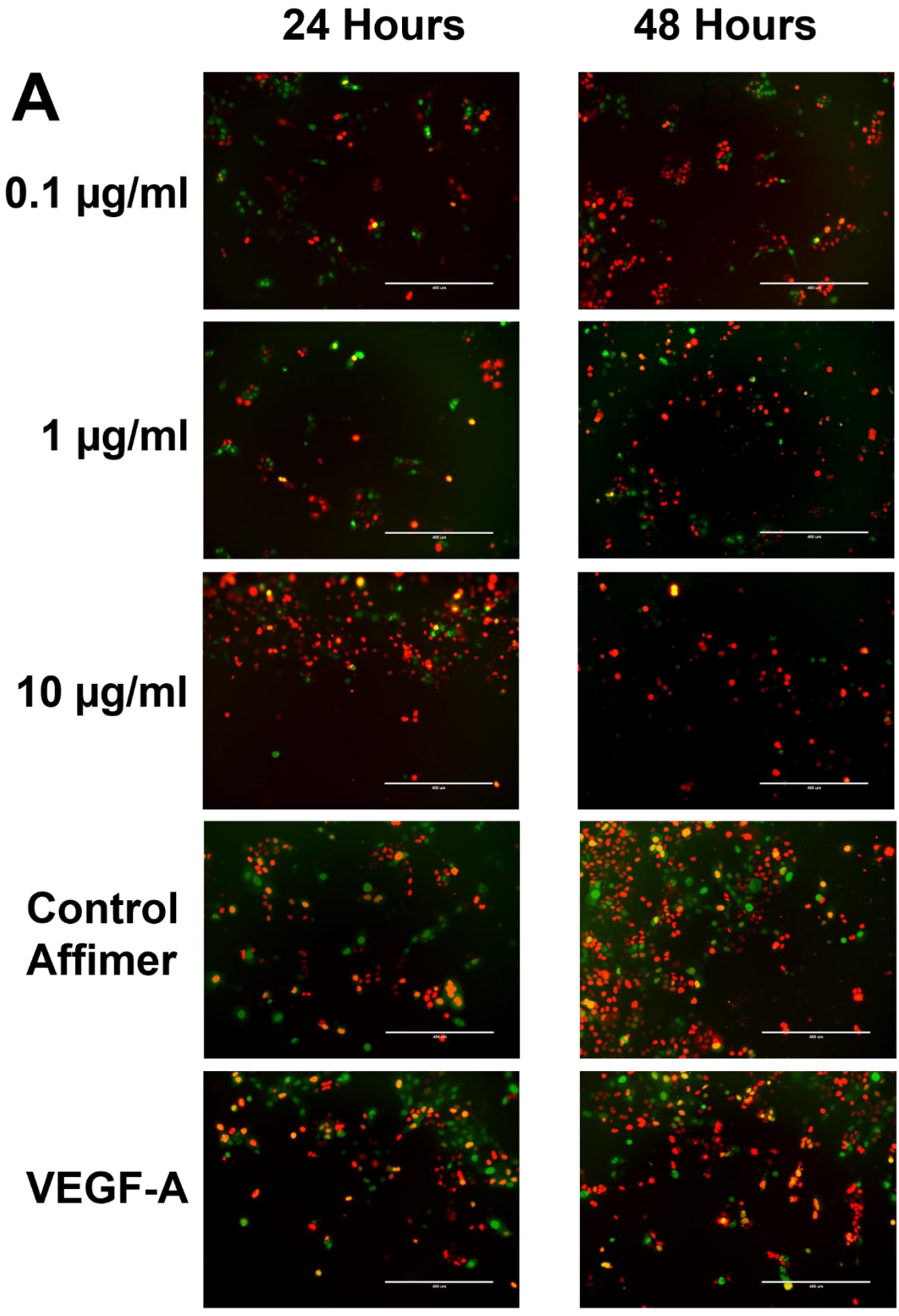
24 Hours
48 Hours
A
0.1 µg/ml
1 µg/ml
10 µg/ml
Control Affimer
VEGF-A

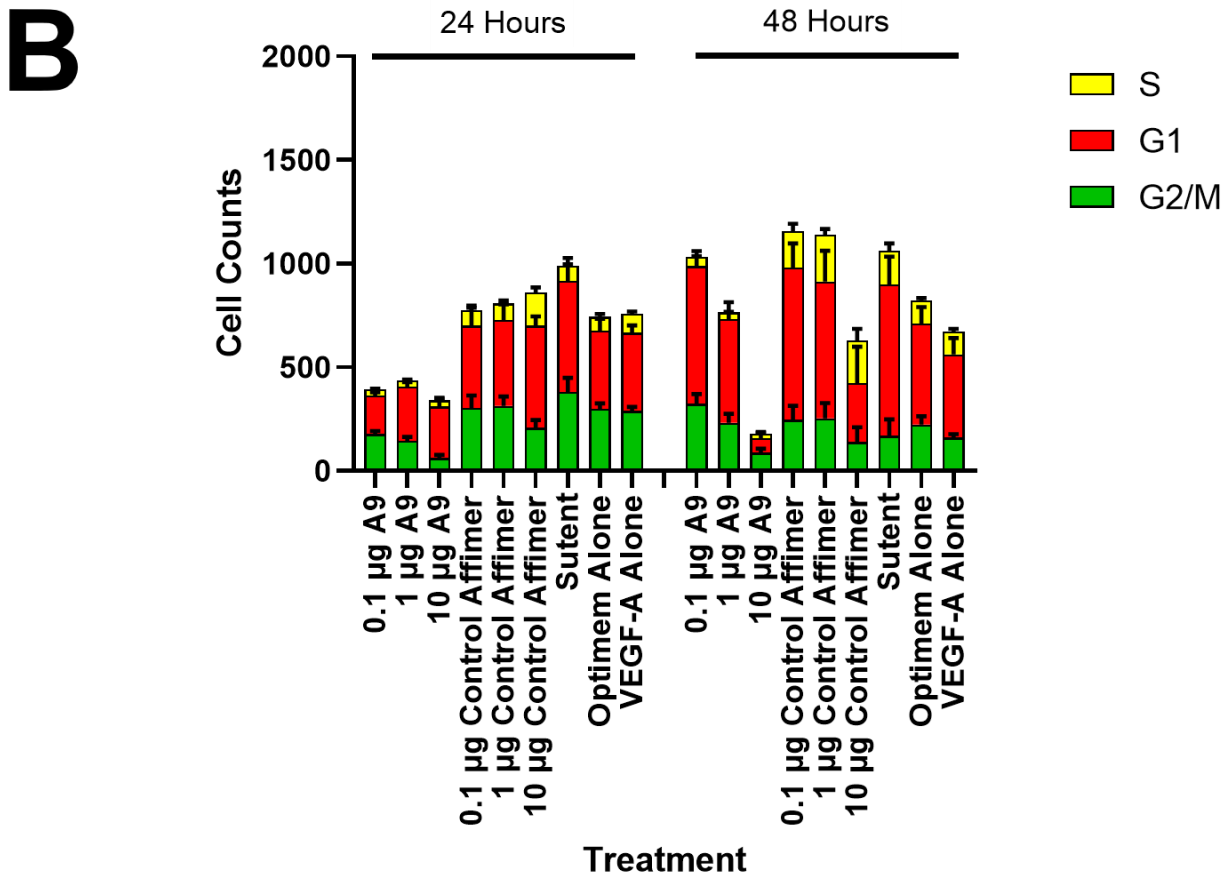

Figure 6.5. VEGFR2-specific Affimer A9 modulates VEGF-A-regulated epithelial cell proliferation. (A) A431-FUCCI cells were starved in Optimem medium for 2 h and incubated with the VEGFR1-specific Affimer A9 or control Affimer (0.1, 1 or 10 µg/ml) for 30 min prior to stimulation with VEGF-A (10 ng/ml). Wells containing 1 µM Sutent or Optimem+VEGF-A were used as additional controls. Representative images of three fields of view were taken on a digital fluorescence microscope (EVOS FL Auto) at 24 and 48 h. Images were taken with the GFP and RFP filters and cells counted using the overlays. Scale bar = 400 µm. (B) Quantification of the number of different coloured cells depict the effects of 0.1, 1 or 10 µg/ml VEGFR2-specific Affimer blockage upon Affimer A9 treatment. Error bars denote ±SEM (n=3).

.

6.2.3. VEGFR1- and VEGFR2-specific Affimer effects on PlGF-1-stimulated A431 cell proliferation

PlGF-1 binds specifically to VEGFR1 and promotes signalling and cellular responses in that context. Stimulation of A431-FUCCI cells in the presence of Affimer 35 or Affimer 37 combined with PlGF-1 revealed new effects (Figs. 6.6, 6.7). There was an increase in the proportion of cells in G1 (red) upon PlGF-1 treatment after 24 h (Figs. 6.6B, 6.7B). Increasing concentrations of Affimer 35 decreased the proportion of dividing green cells; however, similar effects were also observed with control Affimer treatment (Fig. 6.6B). Notably, the proportion of yellow cells (S phase) increased substantially upon Affimer 35 treatment (Fig. 6.6B), but increase was not as great with 37 (Fig.6.7B). In contrast, Affimer 37 increased the proportion of red cells (G1) but did not affect the proportion of actively dividing green cells substantially (Fig. 6.7B).

A similar analysis of VEGFR2-specific Affimer B8 and Affimer A9 on PlGF-1-stimulated A431-FUCCI cells were carried out (Figs.6.8, 6.9). There was again a notable and marked inhibition of A431 cell growth and viability upon VEGFR2 inhibition with either Affimer B8 (Fig.6.8B) or Affimer A9 (Fig. 6.9B). Affimer B8 showed substantial inhibition on A431 cell proliferation at all concentration ranges and at both 24 and 48 h after treatment (Fig. 6.8B). A similar inhibitory effect on A431 cell proliferation was observed upon treatment with Affimer A9 (Fig. 6.9B). Notably, there was almost a complete disappearance of yellow (S phase) cells upon treatment with either Affimer B8 or Affimer A9 (Figs. 6.8B, 6.9B) Finally an evaluation of the effects of the different VEGFR1- and VEGFR2-specific Affimers at the highest concentration (10 µg/ml) was carried out followed by stimulation with either VEGF-A or PlGF-1 (Fig. 6.10A, B). There were notable differences in overall cell growth between cells incubated with VEGFR1 and VEGFR2 Affimers after both VEGF-A and PlGF-1 stimulation (Fig. 6.10A, B). There was also, however, great differences in cell count depending on the type of VEGFR1 Affimer used, highlighting the fact that each of these synthetic structures may be different in their own way (Fig.6.10A). The increases in the number

of cells and those within the S phase (yellow) was also more prominent after PlGF-1 stimulation, especially with Affimers 35 and 37 (Fig. 6.10B). These results could therefore show that the majority of cells remain in the S phase for a longer period of time when stimulated with PlGF-1 after VEGFR1 inhibition.

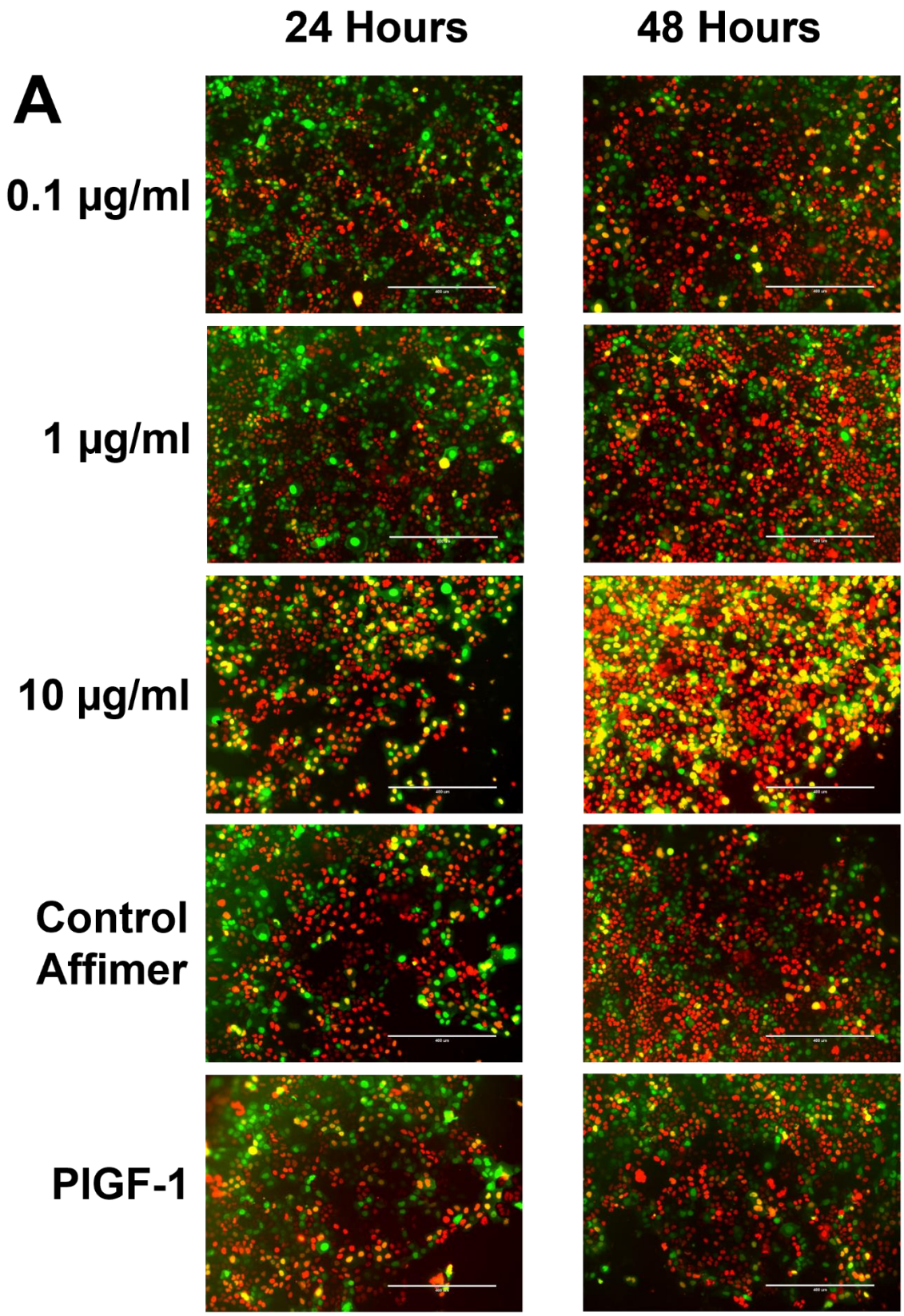
24 Hours
48 Hours
A
0.1 µg/ml
1 µg/ml
10 µg/ml
Control Affimer
PlGF-1

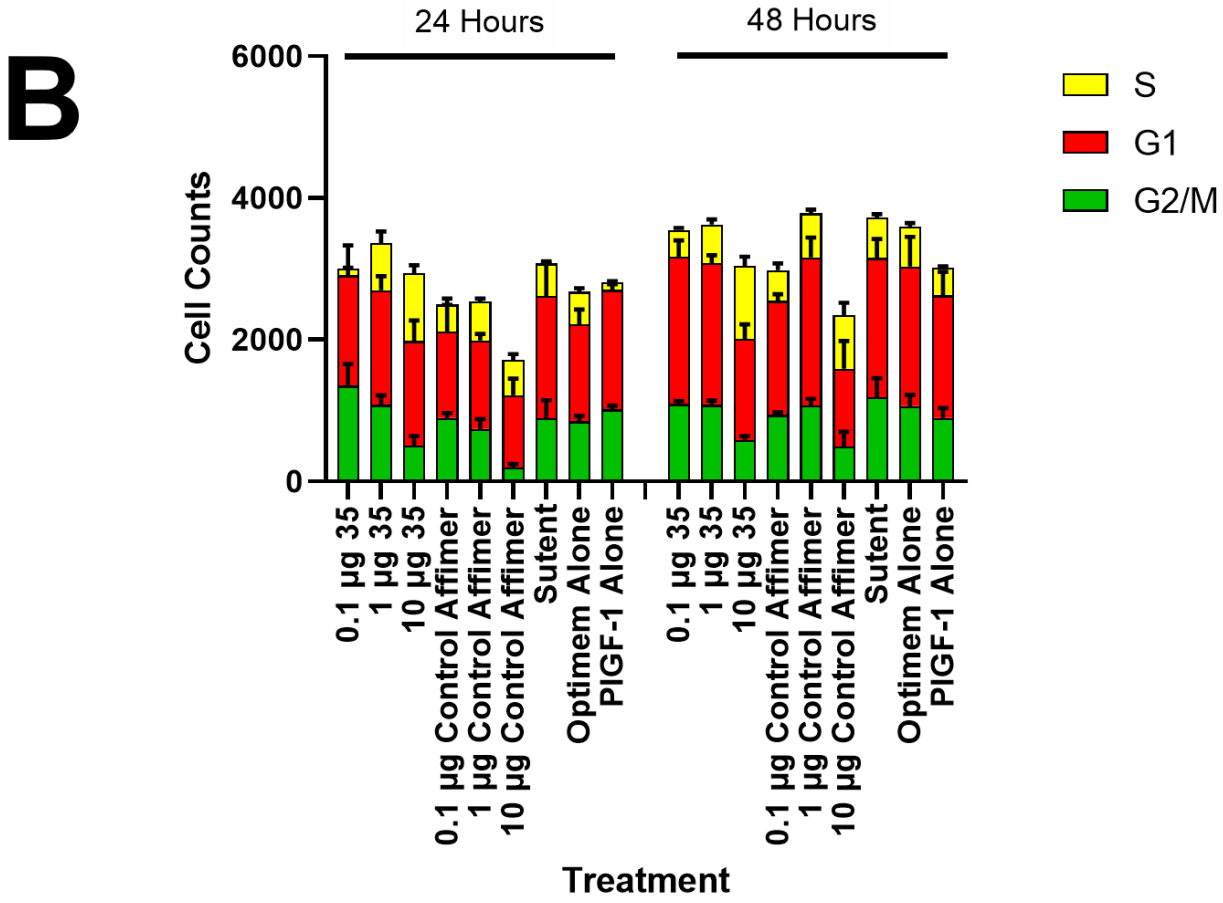

Figure 6.6. VEGFR1-specific Affimer 35 modulates PlGF-1-regulated epithelial cell proliferation. (A) A431-FUCCI cells were starved in Optimem medium for 2 h and incubated with the VEGFR1-specific Affimer 35 or control Affimer (0.1, 1 or 10 µg/ml) for 30 min prior to stimulation with PlGF-1 (10 ng/ml). Wells containing 1 µM Sutent or Optimem+PlGF-1 were used as additional controls. Representative images of three fields of view were taken on a digital fluorescence microscope (EVOS FL Auto) at 24 and 48 h. Images were taken with the GFP and RFP filters and cells counted using the overlays. Scale bar = 400 µm. (B) Quantification of the numbers of different coloured cells depict the effects of 0.1, 1 or 10 µg/ml VEGFR1-specific Affimer blockage upon Affimer 35 treatment. Error bars denote ±SEM (n=3).

.

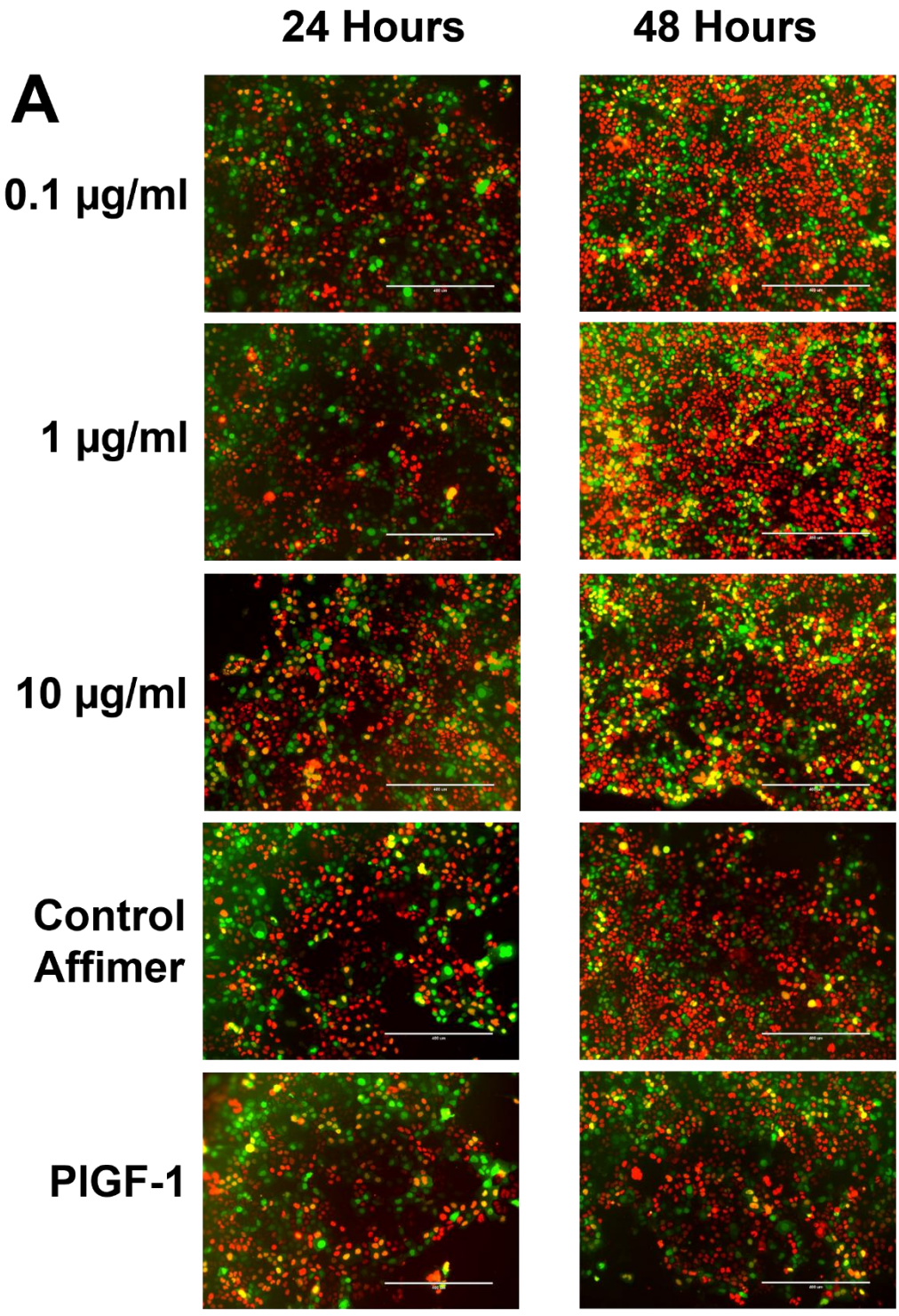
24 Hours
48 Hours
A
0.1 µg/ml
1 µg/ml
10 µg/ml
Control Affimer
PlGF-1

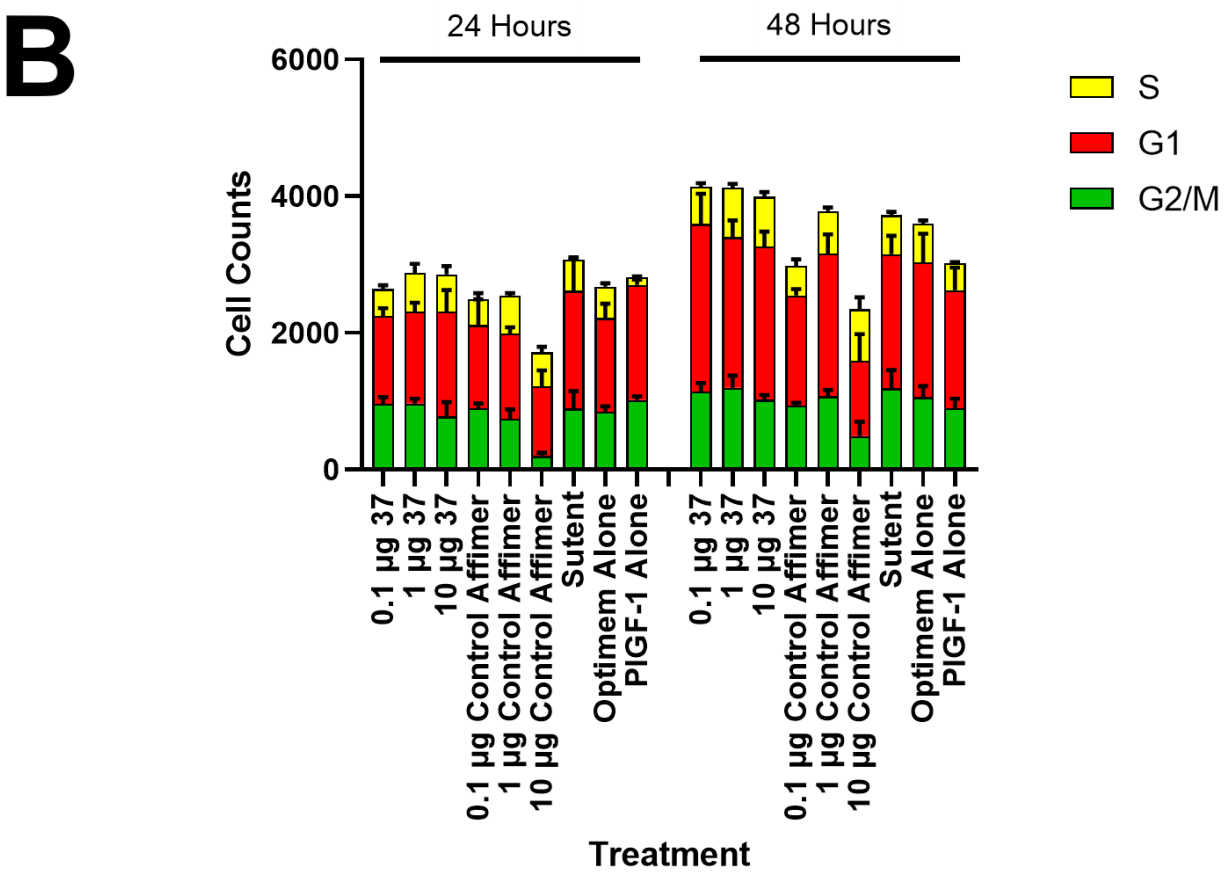

Figure 6.7. VEGFR1-specific Affimer 37 modulates PlGF-1-regulated epithelial cell proliferation. (A) A431-FUCCI cells were starved in Optimem medium for 2 h and incubated with the VEGFR1-specific Affimer 37 or control Affimer (0.1, 1 or 10 µg/ml) for 30 min prior to stimulation with PlGF-1 (10 ng/ml). Wells containing 1 µM Sutent or Optimem+PlGF-1 were used as additional controls. Representative images of three fields of view were taken on a digital fluorescence microscope (EVOS FL Auto) at 24 and 48 h. Images were taken with the GFP and RFP filters and cells counted using the overlays. Scale bar = 400 µm. (B) Quantification of the numbers of different coloured cells depict the effects of 0.1, 1 or 10 µg/ml VEGFR1-specific Affimer blockage upon Affimer 37 treatment. Error bars denote ±SEM (n=3).

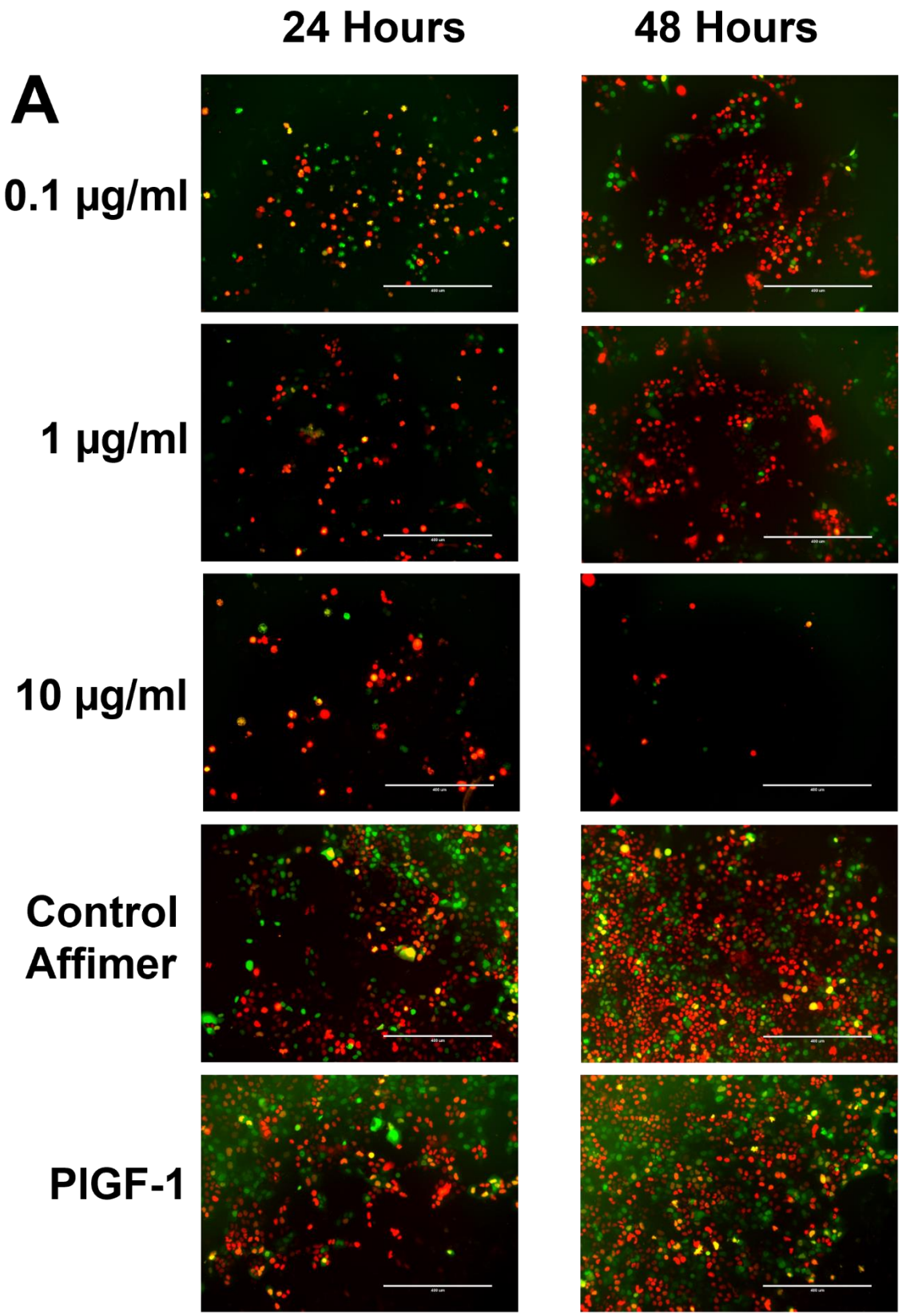
24 Hours
48 Hours
A
0.1 µg/ml
1 µg/ml
10 µg/ml
Control Affimer
PlGF-1

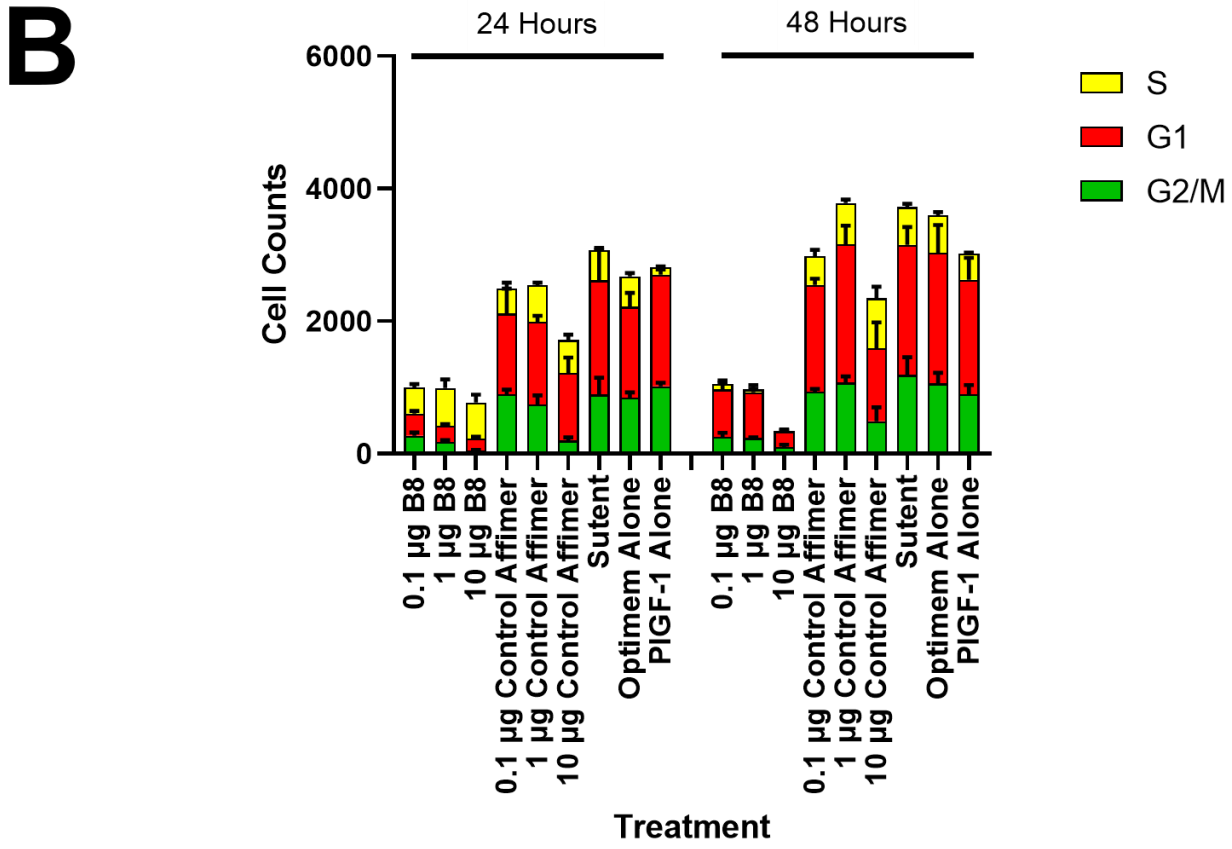

Figure 6.8. VEGFR2-specific Affimer B8 modulates PlGF-1-regulated epithelial cell proliferation. (A) A431-FUCCI cells were starved in Optimem medium for 2 h and incubated with the VEGFR1-specific Affimer B8 or control Affimer (0.1, 1 or 10 µg/ml) for 30 min prior to stimulation with PlGF-1 (10 ng/ml). Wells containing 1 µM Sutent or Optimem+PlGF-1 were used as additional controls. Representative images of three fields of view were taken on a digital fluorescence microscope (EVOS FL Auto) at 24 and 48 h. Images were taken with the GFP and RFP filters and cells counted using the overlays. Scale bar = 400 µm. (B) Quantification of the numbers of different coloured cells depict the effects of 0.1, 1 or 10 µg/ml VEGFR2-specific Affimer blockage upon Affimer B8 treatment. Error bars denote ±SEM (n=3).

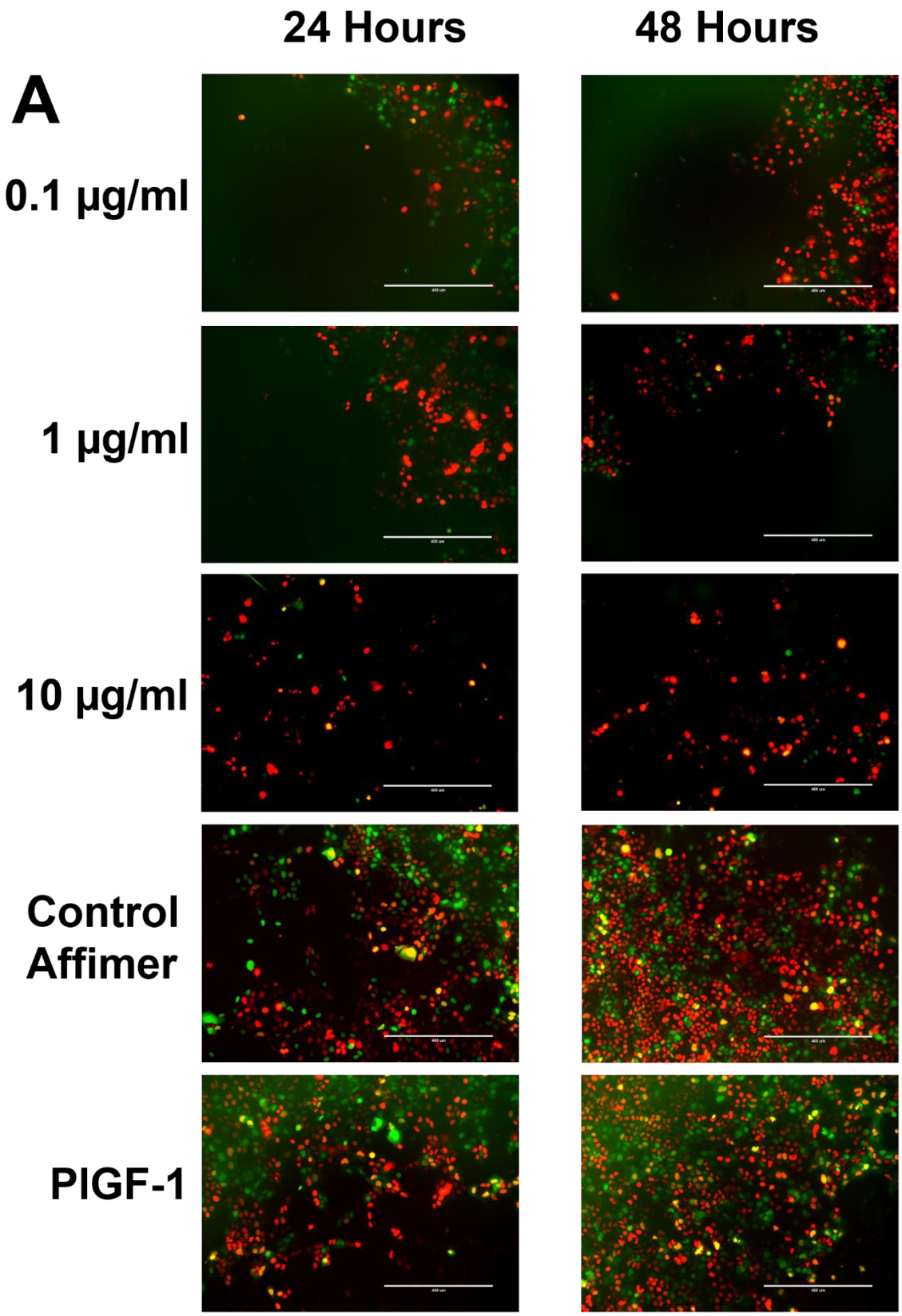
24 Hours
48 Hours
A
0.1 µg/ml
1 µg/ml
10 µg/ml
Control Affimer
PlGF-1

B

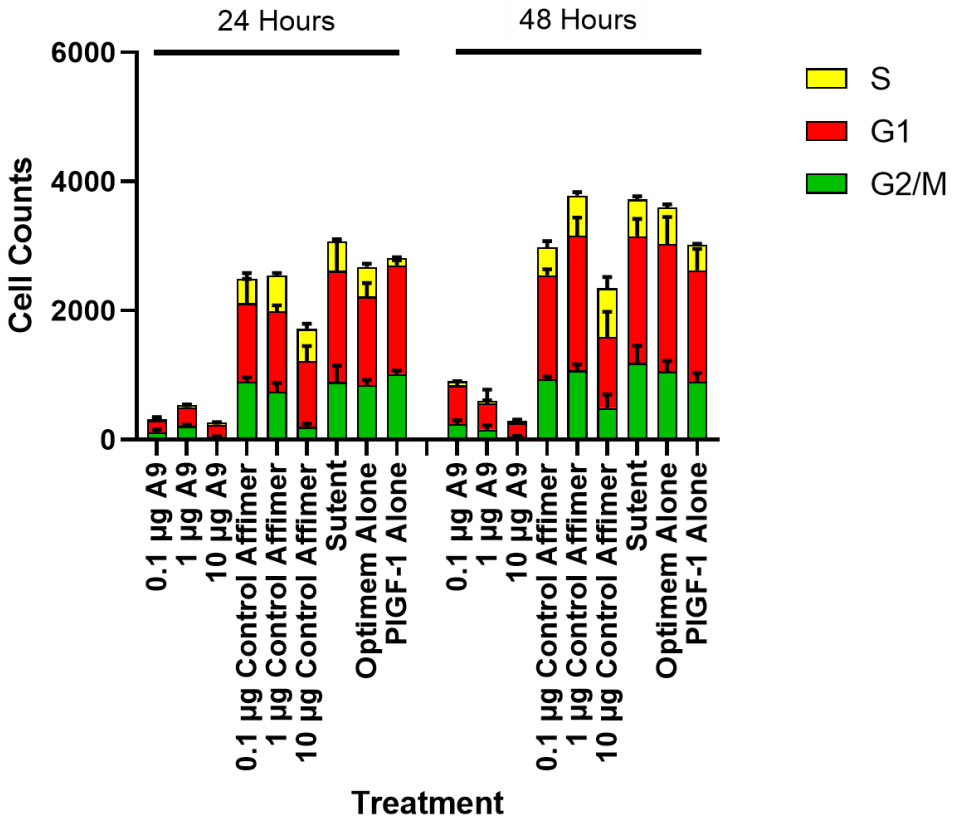

Figure 6.9. VEGFR2-specific Affimer A9 modulates PlGF-1-regulated epithelial cell proliferation. (A) A431-FUCCI cells were starved in Optimem medium for 2 h and incubated with the VEGFR1-specific Affimer A9 or control Affimer (0.1, 1 or 10 µg/ml) for 30 min prior to stimulation with PlGF-1 (10 ng/ml). Wells containing 1 µM Sutent or Optimem+PlGF-1 were used as additional controls. Representative images of three fields of view were taken on a digital fluorescence microscope (EVOS FL Auto) at 24 and 48 h. Images were taken with the GFP and RFP filters and cells counted using the overlays. Scale bar = 400 µm. (B) Quantification of the numbers of different coloured cells depict the effects of 0.1, 1 or 10 µg/ml VEGFR2-specific Affimer blockage upon Affimer A9 treatment. Error bars denote ±SEM (n=3).

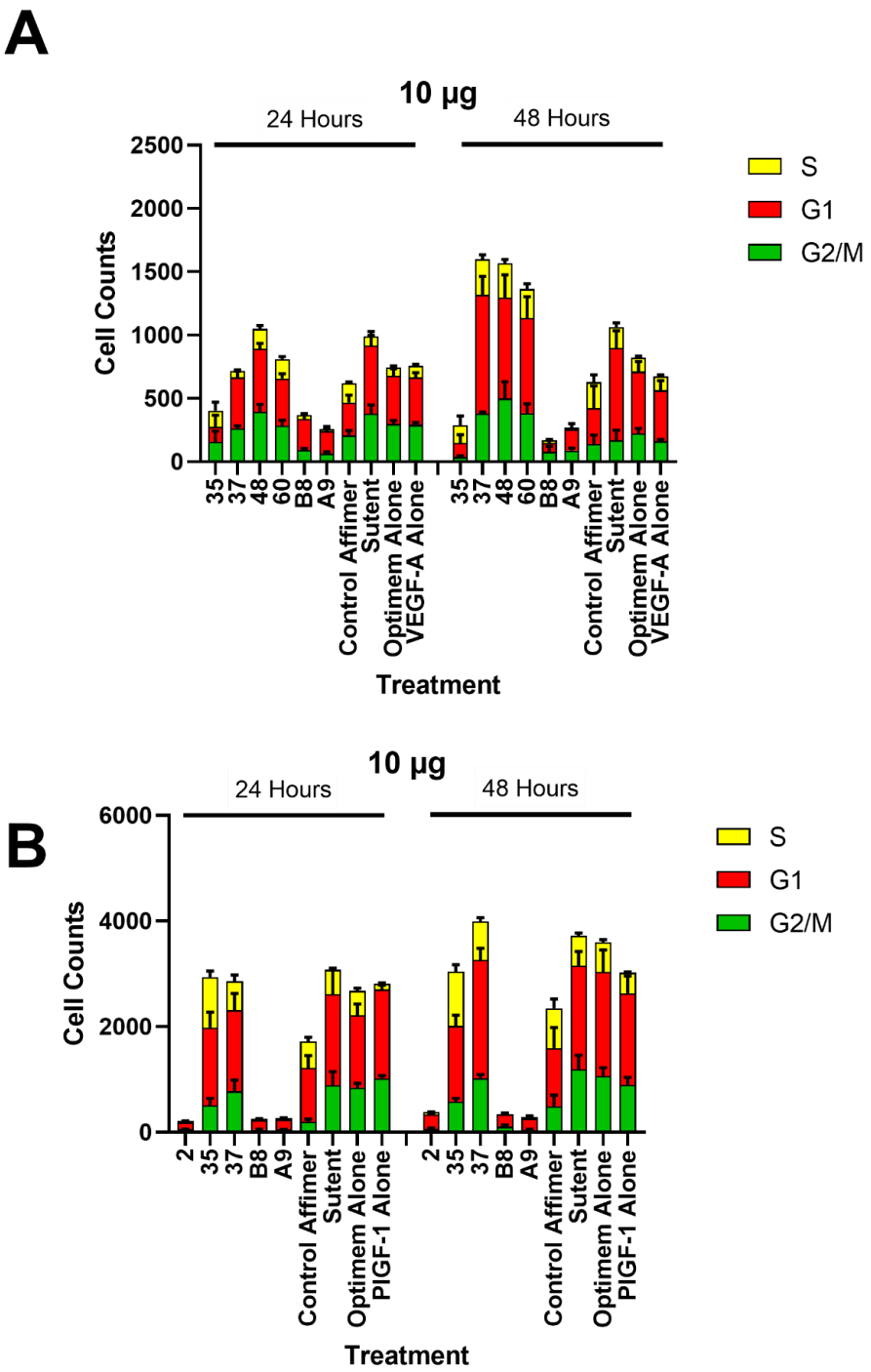

Figure 6.10. Comparison of maximal dosage of VEGFR1 and VEGFR2-specific Affimers on epithelial cell proliferation. A431-FUCCI cells were starved in Optimem medium for 2 h and incubated with maximal amounts of VEGFR-1 or -2 specific Affimer (10 µg/ml) for 30 min prior to stimulation with 10 ng/ml (A) VEGF-A, or (B) PlGF-1. Wells containing 1 µM Sutent or Optimem+VEGF-A/Optimem+PlGF-1 were used as additional controls. Representative images of three fields of view were taken on a digital fluorescence microscope (EVOS FL Auto) at 24 and 48 h. Images were taken with the GFP and RFP filters and cells counted using the overlays. Quantification of the numbers of different coloured cells depict the effects of 10 µg/ml VEGFR1 or -2 specific Affimer blockage. Error bars denote ±SEM (n=6).

6.3. DISCUSSION

The study of cell cycle progression is an important but complicated matter. Methodologies such as immunoblotting and quantitative-PCR (q-PCR) allow a more in-depth look into the cell signalling pathways. These tools, however, are limited by the notion that all of the cells within a sample would function in the same manner. This may not necessarily be the case, as there can be great differences in the distribution of RNA, proteins and cell organelles between individual cells (Matson and Cook, 2017). Cells, therefore, stably transfected with the FUCCI system, provide a great opportunity for assessing the intracellular dynamics without these potential variations or cell-cell interactions. Cancer is also an extremely complicated target for research, as there are a multitude of pathways which could be studied. For instance, the cyclic adenosine 3',5'-monophospohate (cAMP) can activate two different effectors, protein kinase A (PKA) and exchange protein activated by cAMP (Epac), which may either antagonize or work together to influence cancer cell signalling. Targeting Epac may be a larger problem since it can either promote or reduce cancer cell proliferation depending upon the cell line used (Wehbe et al., 2020). It would, therefore, be optimal to target a physiological process which is common to all cancer progression, namely VEGF-mediated angiogenesis. The results detailed in this chapter highlight the opposing effects of VEGR1- and VEGFR2-inhibitory Affimers on A431-FUCCI cell cycle progression.

Overall cell growth appeared to be upregulated with both of the VEGFR1 Affimers used after VEGF-A stimulation, and fluorescence microscopy revealed that this may have been due to increased numbers being within the G2/S part of the cell cycle (Figs. 6.2, 6.3). This was in contrast to incubation with the VEGFR2 Affimers, where an overall decrease in cell numbers was matched with potential stagnation within G1 (Figs. 6.4, 6.5). In repeats of these experiments, stimulation of the cells with the VEGFR1-specific ligand, PlGF-1 also revealed an overall increase in the number of cells as compared to after VEGF-A. This was particularly noticeable with the two VEGFR1-specific Affimers, where increased growth appeared to be

accompanied by a large number of cells remaining within the S phase of the cycle greater than that seen after VEGF-A stimulation (Figs. 6.6, 6.7). Incubation with VEGFR2-specific Affimers showed similar decreases in cell growth between PlGF-1 and VEGF-A stimulated cells. This, however, was initially accompanied by an initially large number of cells being within the S phase of the cycle after 24 h, but this was overtaken by a larger number being within the G1 phase after 48 h (Figs. 6.8, 6.9).

Both of the VEGFR1-Affimers, 35 and 37 showed inverse dose-dependent effects on A431 cell growth after VEGF-A stimulation. This correlates well with the fact that VEGF-A binding to VEGFR2 induces cell proliferation. It should also be noted that the highest concentration used, 10 µg/ml was not as effective especially with regards to Affimer 35, where cell growth was actually decreased as compared to the controls. In contrast, the lowest concentration of 0.1 µg/ml showed a great increase in cell growth for both of the Affimers used, which is not only a good working concentration as compared to traditional antibodies, but also means there would be less chance of cell toxicity. This cell growth was accompanied by an increased number of cells within the G2/M phase of the cell cycle after inhibition with both of the VEGFR1 Affimers. This relates well to *ex vivo* studies of cardiomyocytes from FUCCI-expressing transgenic mice, where the G2/M phases was also extended; it is possible that developmental differentiation is also mediated by VEGF-A (Hashimoto et al., 2014; Braile et al., 2020). Now we can turn our focus to the use of PlGF-1 as a growth factor. PlGF-1 primarily binds to VEGFR1 and is also known to have a role in tumour proliferation and metastasis (Weddell et al., 2018). The initial decrease in the number cells could be explained by a potential decrease in the autocrine VEGF-A produced by the cells. The increase over time could therefore be explained by another phenomenon seen in endothelial cells, where PlGF-1 can enhance VEGFR2-mediated angiogenesis via its binding to VEGFR1. PlGF-1 also has no real role in physiological conditions and instead influences pathological angiogenesis *via* a synergistic relationship with VEGF. Although they are upregulated during physiological angiogenesis, the roles of PlGF and VEGFR1 are limited to sensitizing endothelial cells to

VEGF. However, the ability of PlGF to enhance VEGF-mediated angiogenesis is potentially further confirmed in pathological conditions, as evidenced by a greater presence of PlGF and VEGF/PlGF heterodimers within tumours in hypoxic conditions. Further, there is a possibility that PlGF could induce angiogenic signals through VEGFR1 itself, as seen in an *in vitro* study where inhibition of this receptor decreases PlGF's enhancement of angiogenesis. (Carmeliet *et al.*, 2001). More evidence would be needed to confirm this in the case of this study, however, but there is a possibility that the addition of PlGF-1 has some sort of enhancement effect on VEGFR2-mediated cell growth even with VEGFR1 blockade.

VEGFR2 inhibition with Affimers B8 and A9 both showed similar decreases in cell growth after VEGF-A stimulation, depending upon their concentration. The overall cell count was decreased after incubation with both of these Affimers as compared to the control; however, both 0.1 and 1 µg/ml of each Affimer still showed increased cell growth from 24 to 48 h. This was not the case for 10 µg/ml of both B8 and A9, where there was in fact a decrease in cell growth over this same time period. This corroborates well with the fact that VEGF-A mediated cell proliferation is primarily through VEGFR2. This has been well researched in endothelial studies, but selective inhibitors of VEGFR2 have been found to decrease VEGF-A mediated MAPK phosphorylation and tumour angiogenesis (Nakamura *et al.*, 2004). The VEGFR2 Affimers also appeared to keep these cells within the G1 phase of the cycle at all concentrations, as demonstrated by the low number of red cells This observation is further backed-up by evidence that longer G1 phases are associated with a focus on cell differentiation rather than proliferation (Zielke and Edgar, 2015). With regards to the PlGF-1 studies, there remained a low number of cells as compared to the controls at all concentrations of both B8 and A9. There was a brief upregulation of cells in the S phase for both of these Affimers at the 24 h mark, but this soon decreased. This could be attributed to the ability of PlGF-1 to bind to VEGF in normal physiology, thus reducing the latter's concentration and therefore having the ability to reduce tumour angiogenesis (Eriksson *et al.*, 2002; Tarallo *et al.*, 2010). There, therefore, could also be some benefit to adding

both VEGF-A and PlGF-1 together, in future studies using A431-FUCCI cells.

In summary, the FUCCI system allowed a detailed visualization of the effects of the VEGFR-specific Affimers to be made on individual cell cycles. Data from additional future Western blot experimentation could be obtained in future studies in order to enable a precise idea of the signalling pathways affected, and as to how they may be related to these microscopy results.

Chapter 7

Final Discussion

7.1 OVERVIEW

The work from this PhD thesis has given an overview of the development and properties of VEGFR1-specific Affimers. By comparing these VEGFR1-specific Affimer properties to more well-established VEGFR2-specific Affimers, this work now establishes a framework for the further development of such agents towards their use in diseases ranging from cancer to cardiovascular disease.

7.2 VEGFR1-specific Affimers could be used as high affinity detection tools

The initial aim of this project was to identify and characterise Affimer reagents specific to VEGFR1 in the context of cardiovascular disease. These Affimers were previously screened for and assessed, finding binding affinities to VEGFR1 e.g. 18.37 nM and 10.97 nM for Affimer 35c and Affimer 37c respectively (O. Karpov, Ponnambalam laboratory, unpublished findings). These relatively high affinities for VEGFR1 also helped explain the enhancement of several pro-angiogenic cellular assays (G. Smith, Ponnambalam laboratory, unpublished findings). Affimer 35 seemed to perform better than Affimer 37 at promoting cell proliferation, but this was often dependent on Affimer concentration. Affimer 37 however, seemed to be a better probe for detecting VEGFR1, as seen by its effects in immunofluorescence and recycling assays. Its efficacy was further optimised by using different cell fixation methods such as using 5% glyoxal other than the traditional 3-4% PFA. Affimers conjugated to AlexaFluor dyes, were found to have an important potential to be a more rapid and direct method to detect VEGFR1 within cells. Using Affimer-based detection could well create a more efficient and easier method i.e., shorter incubation times, and not having to use secondary labelled antibodies (Richter et al., 2018; Im et al., 2019).

7.3 VEGFR1-specific Affimers promote pro-angiogenic outcomes

Conclusions drawn from the functional arm of this project, enable several points to be made about the manner in which Affimers work as inhibitors both in cardiovascular disease and cancer. Focusing firstly, on the cardiovascular aspect of the project, it was found that inhibiting VEGFR1 with these reagents generally increased endothelial cell proliferation, migration and tubulogenesis. This would most likely be due to modulation of VEGF-A mediated events occurring via VEGFR2, as VEGFR1 is postulated to act as an endogenous inhibitor of VEGFR2 signalling. *In vivo* studies also show that VEGFR1 deletion can induce physiological cardiac hypertrophy where normal function was still preserved without adverse side-effects (Kivelä et al., 2019). VEGFR1 has also been shown to be upregulated in hypoxic conditions, resulting in VEGF-B facilitating anti-apoptosis in cardiomyocytes myocardial infarction *in vivo* (Zentilin et al., 2010). These findings attest to the possible use of VEGFR1 to stimulate angiogenesis through inhibition and thereby improve cardiac recovery times.

The conclusion above does not seek to ignore the fact that VEGFR1 may also have pro-angiogenic effects, potentially delaying post-myocardial infarction recovery. For instance, heterodimerization between the transmembrane isoforms of VEGFR1 and VEGFR2 can itself promote angiogenesis and this is further highlighted by the overexpression of its specific ligand, PlGF-1. The expression of VEGFR1 has also been reported to have increased in a mouse cardiomyocyte cell line (H9c2) during recovery after a heart attack and this increase was maintained for 30 days after this event (Wang *et al.*, 2019). Studies of the myocardium in mice have also shown that co-administration of PlGF-1 and VEGF-A, enhanced post-ischaemia angiogenesis in endothelial cells. This effect was produced through the formation of VEGF-PlGF complexes, which in turn may have activated functional heterodimerization of mouse VEGFR1 and VEGFR2

(Autiero et al., 2003). The initial inhibition of VEGFR1 using an Affimer may not only promote angiogenesis through VEGFR2, but the rapid clearance rate of the Affimer from the body would potentially not permanently block the more beneficial effects of VEGFR1 in the long run (Tiede et al., 2017) (Tchaikovski *et al.*, 2008).

Immunoprecipitation studies have allowed insight into where one of the VEGFR1-specific agents, Affimer 1, could bind on the VEGFR1 extracellular region, namely domains D1-D4. This correlates well with the currently understood ligand binding domains of VEGFR1, but it should be noted that there did not seem to be much binding to D5. D5 is necessary for VEGFR activation via dimerization of the receptor through the formation of hydrogen bonds, as well as enhancing ligand binding (Markovic-Mueller et al., 2017) This explains the fact that this VEGFR1 Affimer was not as potent in its effect when compared to its counterparts, given that D5 would still be present and enhance the effects of VEGF-A binding.

7.4 VEGFR1-specific Affimers promotes epithelial cancer cell progression involving VEGF-A or PlGF-1

A cancer-related study in this project was related to VEGFR1 function in A431 cancer epithelial cells. The original hypothesis was that VEGFR1 inhibition using Affimers would promote A431 cell cycle progression. This was proven to be the case after VEGF-A stimulation, but this was not the situation when a PlGF, a specific ligand of VEGFR1 was used. From 24-48 h, there were noticeable differences in total cell count as well as the number of cells in the S phase, implying that there was increased cell cycling. Normally PlGF is specific to VEGFR1, so theoretically inhibition of the receptor would prevent binding and therefore reduce cell growth as mediated by VEGFR2, but the results of these experiments seem to oppose this theory. There could be a case, however, for the use of VEGFR1-specific Affimers to be also used to target cancer signalling, as this receptor may also have a role in cell metastasis, invasion and survival.

The upregulation of VEGFR1 expression is common in many types of malignancies including bladder and prostate cancer (Lee *et al.*, 2007;

Schmidt M *et al.*, 2008; Kopparapu PK *et al.*, 2013; Tsourlakis *et al.*, 2015). For instance, Tsourlakis *et al.,* (2015) identified a connection between overexpressed VEGFR1 on the prostate epithelium and the progression of aggressive prostate cancer cell lines post-prostatectomy. Immunohistochemistry showed increased VEGFR1 staining in the samples was significantly associated to the Gleason grade ($p=0.03$), tumour stage ($p<0.0001$), and PSA recurrence ($p=0.0005$) of the particularly aggressive cancers (Tsourlakis *et al.*, 2015). This could potentially highlight a link between VEGFR1 expression and the status of aggressive, metastatic cancers (Autiero et al., 2003). Studies on choriocarcinomas, which naturally express high levels of PlGF, also showed that adding VEGFR1 inhibitory antibodies seemed to increase tumour angiogenesis and growth in general. Although this study focused on choriocarcinoma tumours, it could still potentially be applicable to the results of this project as A431 cells also naturally express PlGF (Hedlund et al., 2013).

There is also an association with VEGFR1 and non-aggressive cancer sub-types, as seen by increased VEGFR1 mRNA expression in several breast cancer cell lines Schmidt *et al.* (2008) concluded that there could be the involvement of an autocrine signalling loop, where the binding of VEGF may increase VEGFR1 expression. There is usually a good prognosis for patients at the early stages of cancer, as indicated by the lack of tumour cells in the lymph nodes, so this led to the theory that the presence of VEGF and VEGFR1 would also predict a successful outcome using anti-angiogenic treatments (Schmidt M et al., 2008). The general set of results in this PhD could prove very useful, given that VEGFR1 has only been associated with pathological and not physiological angiogenesis, so inhibiting the receptor may be a good alternative to conventional therapies which are often associated with problematic side-effects seen from inhibiting VEGFR2 (Ceci et al., 2020).

7.6 Affimer-specific VEGFR2 inhibition modulates pro-angiogenic responses in endothelial cells

In Chapters 4-6, several results seemed to oppose the original hypothesis that anti-VEGFR2 Affimers would inhibit endothelial cell growth and their normal function. This could potentially be explained by some of the results in chapter 3 (Fig. 3.5), where VEGFR1 bands were apparently present in the pulldown assay even with the VEGFR2 Affimer shown. This could indicate slightly less specificity with regard to this particular Affimer. This discrepancy, however, could also be explained by the effect of the presence of the cysteine tag, as there was more protein present in this lane compared to the non-cysteine tagged version. This alteration in function has been seen with other tags for labelling and purification such as GST (Bell *et al.*, 2013). However, any changes in functional effects are usually avoided if the tags are attached to the C-terminus, which is the case for the Affimers.

VEGFR2-specific Affimers were also found to have specific implications on the A431 squamous cancer cell line. These Affimers seemed to decrease overall cell growth, even in the presence of VEGF-A and PlGF-1, which may be attributed to the cell cycle stages. The findings indicated a link between reduced cycling between the S-G2 phases, but this was often accompanied by a decrease in cells in G1. Current strategies like chemotherapy can have complications such as requiring high concentrations of drugs which may impact normal cells in the body which can also rapidly divide, such as those in the gastrointestinal tract. Considering the cancer cell cycle in more detail, current therapeutics which target the cancer, and protein synthesis, are often geared towards the G1 phase. However, this approach may affect normal cells as well as cancerous ones, and is often associated with nephro- or hepatotoxicity. It would appear, therefore, that drugs which specifically target the S (DNA synthesis) phase of the cycle would be more beneficial (Johnson and Wolberg, 1971). The FUCCI system, consequently, is a great aid in the understanding of the mechanism of action of conventional cancer drugs, such as chemoresistance being attributed to cells being in G2/M arrest (Miwa et al., 2015).

7.5 Concluding remarks and future research

The aims of this study were to identify how VEGFR1-specific Affimers inhibit VEGFR1 *in vitro*. One limitation of this work was a lack of time to profile the signalling pathways under conditions of Affimer-specific VEGFR modulation. There were several experiments carried out where the Affimers were incubated with HUVECs prior to stimulation with VEGF-A and other growth factors. Unforeseen issues, however, such as the best use of cysteine vs. non-cysteine tagged Affimers in cellular assays, made such work more complicated to analyse. Future studies, therefore, could elucidate more detail about the specific downstream signalling events influenced by VEGFR1 inhibition and the best Affimers to use in this context. This ideally would include immunoblotting to show the effects of the Affimers on all of the VEGFR1/VEGFR2 intracellular pathways in endothelial cells; these could be complemented by siRNA and CRISPR Cas9 knockdowns and knockouts of one or both of these receptors.

These studies could have also benefited from additional controls to further clarify some of the more unexpected findings. For instance, the tubulogenesis assays had comparisons between wells both with and without VEGF-A, which had an added benefit of identifying the effects of the VEGFR-specific Affimers on the HUVECs without an external ligand. This would have been an ideal set-up for the other cellular assays and would be strongly recommended for anyone wishing to try these in the future. VEGFR2-specific Affimers were often used as negative controls at the start of the project for studies on VEGFR1 alone, but it would have also been beneficial to carry out reciprocal studies to assess the effects of VEGFR1 on binding to VEGFR2. For example, further optimisation of the immunoprecipitation protocols could have possibly allowed an insight into whether VEGFR1-specific Affimers might have isolated VEGFR2 from HUVECs in order to identify any possible cross-reactivity. If there was any, this could have explained any unusual results in the previous experiments. It was also planned to use surface plasmon resonance (SPR) within the project, in order to get a numerical value for the affinities of all of the VEGFR

Affimers. It is hoped that it could be used in the future to further explain the results achieved within this research.

Additionally, it would also have been very beneficial, to have been able to carry out more ELISA experiments in order to further confirm the inhibition of VEGF binding to VEGFR1 and VEGFR2. Biotinylated VEGFR1 Affimers were added to ELISAs, as well as in the immunoblots mentioned previously, but needed further optimisation. This involved the addition of the different isolated domains of the VEGFR1 to streptavidin coated plates followed by the addition of biotinylated Affimers. The idea was to potentially identify where on the receptor the Affimers were actually binding, but this same ELISA set-up could have also been used to measure the inhibitory potential of these proteins. This could have been done with the addition of the soluble full-length VEGFR1 protein to streptavidin coated plates, followed by the addition of Affimers for 30 min prior to stimulation with VEGF-A (similar to the cellular assay protocols). ELISAs still remain an ideal technique for identifying protein binding whether it be naturally occurring antibodies or synthetic proteins.

The study of both cardiovascular disease and cancer is an important one. Whilst they may be thought of as separate entities, they are in fact often closely linked, an example being the ability of tumour cells to supplement themselves by hijacking physiological angiogenesis. They are also similar in terms of their major impact on the human body if disease occurs; the cardiovascular system supplies the entire body with blood and, therefore, is linked to a broad spectrum of disease, whilst cancer has an almost endless number of signal transduction pathways. The common ground for both of these possible mechanisms for disease, is angiogenesis. Angiogenesis is therefore, at the nexus of many medical troubles for people and thereby demonstrates that there is a great urgency to find very specific and effective therapies to target this process. This project shows the clear potential for these novel VEGFR-inhibitory Affimers, where they demonstrate almost opposing results on the cell pathways involved in angiogenesis, depending upon the receptor targeted. By targeting the VEGFR using specific probes to elicit positive or negative endothelial responses, better therapies could be

developed to meet the challenges presented by a range of disease states. If successful, Affimers could potentially be added to a roster of safe, cost-effective yet highly specific pharmaceuticals to target VEGFR signalling and thus treat cancer and cardiovascular disease.

REFERENCES

Abdel-Rahman, O. and ElHalawani, H. (2016) 'Risk of cardiovascular adverse events in patients with solid tumors treated with ramucirumab: A meta analysis and summary of other VEGF targeted agents', *Critical Reviews in Oncology/Hematology*. Elsevier Ireland Ltd, 102, pp. 89–100. doi: 10.1016/j.critrevonc.2016.04.003.

Adams VR, L. M. (2007) 'Sunitinib malate for the treatment of metastatic renal cell carcinoma and gastrointestinal stromal tumors', *Clinical Therapeutics*, 29(7), pp. 1338–1353.

Adler, R. . (2004) *Medical firsts: From Hippocrates to the human genome*. 1st edn. Hoboken, New Jersey: John Wiley and Sons Inc.

Agarwal, A. *et al.* (2015) 'Novel Therapies in Development for Diabetic Macular Edema', *Current Diabetes Reports*, 15(10). doi: 10.1007/s11892-015-0652-z.

Ahmadizar F, Onland-Moret NC, de Boer A, Liu G, M. der Z. A. (2015) 'Efficacy and Safety Assessment of the Addition of Bevacizumab to Adjuvant Therapy Agents in Cancer Patients: A Systematic Review and Meta-Analysis of Randomized Controlled Trials', *PLoS One*, 10(9), p. e0136324.

Aird, W. C. (2011) 'Discovery of the cardiovascular system: from Galen to William Harvey', *Journal of Thrombosis and Haemostasis*, 9(s1), pp. 118–129.

Akutsu N, Sasaki S, Takagi H, Motoya M, Shitani M, Igarashi M, Hirayama D, Wakasugi H, Yamamoto H, Kaneto H, Yonezawa K, Yawata A, Adachi T, Hamamoto Y, S. Y. (2015) 'Development of hypertension within 2 weeks of initiation of sorafenib for advanced hepatocellular carcinoma is a predictor of efficacy', *International Journal of Clinical Oncology*, 20(1), pp. 105–110.

Alfaleh, M. A. *et al.* (2020) 'Phage Display Derived Monoclonal Antibodies: From Bench to Bedside', *Frontiers in Immunology*. Frontiers Media S.A., 11, p. 1986. doi: 10.3389/FIMMU.2020.01986/BIBTEX.

Allen, J. E. *et al.* (2012) 'Targeting TRAIL death receptor 4 with trivalent DR4 Atrimer complexes.', *Molecular cancer therapeutics*. United States, 11(10), pp. 2087–2095. doi: 10.1158/1535-7163.MCT-12-0366.

Altunay, B. *et al.* (2021) 'HER2-directed antibodies, affibodies and nanobodies as drug-delivery vehicles in breast cancer with a specific focus on radioimmunotherapy and radioimmunoimaging.', *European journal of nuclear medicine and molecular imaging*, 48(5), pp. 1371–1389. doi: 10.1007/s00259-020-05094-1.

Aragon-Ching JB, Dahut WL. (2009). VEGF inhibitors and prostate cancer therapy. *Curr Mol Pharmacol*. 2 (2), p161-8.

Arbabi-Ghahroudi, M. (2017) 'Camelid single-domain antibodies: Historical perspective and future outlook', *Frontiers in Immunology*, 8(NOV), pp. 1–8. doi: 10.3389/fimmu.2017.01589.

Arrata, I. *et al.* (2017) 'Interfacing native and non-native peptides: using Affimers to recognise α-helix mimicking foldamers', *Chemical Communications*, 53(19), pp. 2834–2837. doi: 10.1039/c6cc09395g.

Autiero, M. *et al.* (2003) 'Role of PlGF in the intra- and intermolecular cross talk between the VEGF receptors Flt1 and Flk1.', *Nature medicine*, 9(7), pp. 936–943. doi: 10.1038/nm884.

Avacta (2020) *SARS-CoV-2 Rapid Antigen Test Update | Avacta Life Sciences Limited*, *2020*. Available at: https://avacta.com/sars-cov-2-rapid-antigen-test-update/ (Accessed: 22 January 2021).

Avacta Ships SARS-COV-2 Affimer Reagents to Cytiva and Adeptrix | Business Wire (2020). Available at: https://www.businesswire.com/news/home/20200511005754/en/Avacta-Ships-SARS-COV-2-Affimer-Reagents-Cytiva- (Accessed: 22 January 2021).

Azad, N. S. *et al.* (2008) 'Combination targeted therapy with sorafenib and bevacizumab results in enhanced toxicity and antitumor activity', *Journal of Clinical Oncology*, 26(22), pp. 3709–3714. doi: 10.1200/JCO.2007.10.8332.

Baghban Kohnehrouz, B. *et al.* (2018) 'Novel Recombinant Traceable c-Met Antagonist-Avimer Antibody Mimetic Obtained by Bacterial Expression Analysis.', *Avicenna journal of medical biotechnology*, 10(1), pp. 9–14.

Barozzi, A. *et al.* (2020) 'Affibody-Binding Ligands.', *International journal of molecular sciences*, 21(11). doi: 10.3390/ijms21113769.

Barr, J. (2014) 'Vascular medicine and surgery in ancient Egypt', *Journal of Vascular Surgery*. Society for Vascular Surgery, 60(1), pp. 260–263. doi: 10.1016/j.jvs.2014.04.056.

Bazan, J., Całkosiński, I. and Gamian, A. (2012) 'Phage display - A powerful technique for immunotherapy: 2. Vaccine delivery', *Human Vaccines and Immunotherapeutics*, pp. 1829–1835. doi: 10.4161/hv.21704.

Béhar, G. *et al.* (2014) 'Switching an anti-IgG binding site between archaeal extremophilic proteins results in Affitins with enhanced pH stability.', *Journal of biotechnology*. Netherlands, 192 Pt A, pp. 123–129. doi: 10.1016/j.jbiotec.2014.10.006.

Bell MR, Engleka MJ, Malik A, Strickler JE. (2013). To fuse or not to fuse: what is your purpose? *Protein Sci*. 22 (11), p1466-77.

Bendre, A. D., Ramasamy, S. and Suresh, C. G. (2018) 'Analysis of Kunitz inhibitors from plants for comprehensive structural and functional insights.', *International journal of biological macromolecules*. Netherlands, 113, pp. 933–943. doi: 10.1016/j.ijbiomac.2018.02.148.

Bennett, N. J. and Rakonjac, J. (2006) 'Unlocking of the filamentous bacteriophage virion during infection is mediated by the C domain of pIII', *Journal of Molecular Biology*, 356(2), pp. 266–273. doi: 10.1016/j.jmb.2005.11.069.

Bergler W, Petroianu G, Schadel A. (1993). Feasibility of proliferation studies using the BrdU and MTT assays with a head and neck carcinoma cell line. *ORL J Otorhinolaryngol Relat Spec*. 55 (4), p230-5.

De Boer, E. *et al.* (2003) 'Efficient biotinylation and single-step purification of tagged transcription factors in mammalian cells and transgenic mice', *Proceedings of the National Academy of Sciences*. National Academy of Sciences, 100(13), pp. 7480–7485. doi: 10.1073/PNAS.1332608100.

Boettcher M, McManus MT. (2015). Choosing the Right Tool for the Job: RNAi, TALEN, or CRISPR. *Mol Cell*. 58 (4), p575-85.

Bolli, R. (2019) 'William Harvey and the Discovery of the Circulation of the Blood - Part II', *Circulation Research*, 124, pp. 1300–1302.

Boyden, S. (1962). The chemotactic effect of mixtures of antibody and antigen on polymorphonuclear leucocytes. *J Exp Med*. 115 (3), p453-66.

Braile M, Marcella S, Cristinziano L, Galdiero MR, Modestino L, Ferrara AL, Varricchi G, Marone G, Loffredo S. (2020). VEGF-A in Cardiomyocytes and Heart Diseases. *Int J Mol Sci*. 21 (15), p5294.

Bruns, A. F. *et al.* (2010) 'Ligand-Stimulated VEGFR2 Signaling is Regulated by Co-Ordinated Trafficking and Proteolysis', *Traffic*. John Wiley & Sons, Ltd, 11(1), pp. 161–174. doi: 10.1111/J.1600-0854.2009.01001.X.

Bussolati B, Dunk C, Grohman M, Kontos CD, Mason J, Ahmed A. (2001). Vascular endothelial growth factor receptor-1 modulates vascular endothelial growth factor-mediated angiogenesis via nitric oxide. *Am J Pathol*. 159 (3), p993-1008.

Care, S., Health, P. and Porton, E. (2020) 'Preliminary report from the Joint PHE Porton Down & University of Oxford SARS-CoV-2 test development and validation cell : Rapid evaluation of Lateral Flow Viral Antigen detection devices (LFDs) for mass community testing ':, (November), pp. 2–7.

Carmeliet P, Moons L, Luttun A, Vincenti V, Compernolle V, De Mol M, Wu Y, Bono F, Devy L, Beck H, Scholz D, Acker T, DiPalma T, Dewerchin M, Noel A, Stalmans I, Barra A, Blacher S, VandenDriessche T, (2001). Synergism between vascular endothelial growth factor and placental growth factor contributes to angiogenesis and plasma extravasation in pathological conditions. *Nat Med*. 7 (5), p575-83.

Carmeliet, P. and Jain, R. K. (2011) 'Molecular mechanisms and clinical applications of angiogenesis', *Nature*. Nature Publishing Group, pp. 298–307. doi: 10.1038/nature10144.

Carpenter G, Liao HJ. (2009). Trafficking of receptor tyrosine kinases to the nucleus. *Exp Cell Res*. 315 (9), p1556-66.

Carrington, G., Tomlinson, D. and Peckham, M. (2019) 'Exploiting nanobodies and Affimers for superresolution imaging in light microscopy', *Molecular Biology of the Cell*, 30(22), pp. 2737–2740. doi: 10.1091/mbc.E18-11-0694.

Ceci C, Atzori MG, Lacal PM, Graziani G. (2020). Role of VEGFs/VEGFR-1 Signaling and its Inhibition in Modulating Tumor Invasion: Experimental Evidence in Different Metastatic Cancer Models. *Int J Mol Sci*. 21 (4), p1388.

Channathodiyil P, Houseley J. (2021). Glyoxal fixation facilitates transcriptome analysis after antigen staining and cell sorting by flow cytometry. *PLoS One*. 16 (1), e0240769.

Chappell JC, Cluceru JG, Nesmith JE, Mouillesseaux KP, Bradley VB, Hartland CM, Hashambhoy-Ramsay YL, Walpole J, Peirce SM, Mac Gabhann F, Bautch VL. (2016). Flt-1 (VEGFR-1) coordinates discrete stages of blood vessel formation. *Cardiovasc Res*. 111 (1), p84-93.

Chasteen, L. *et al.* (2006) 'Eliminating helper phage from phage display', *Nucleic Acids Research*, 34(21), pp. 1–11. doi: 10.1093/nar/gkl772.

Chen HC. (2005). Boyden chamber assay. *Methods Mol Biol*. 294, p15-22.

Cheng MHY, Maruani A, Savoie H, Chudasama V, Boyle RW. (2018). Synthesis of a novel HER2 targeted aza-BODIPY-antibody conjugate: synthesis, photophysical characterisation and in vitro evaluation. *Org Biomol Chem*. 16 (7), p1144-1149.

Cheng R, Zhang F, Li M, Wo X, Su YW, Wang W. (2019). Influence of Fixation and Permeabilization on the Mass Density of Single Cells: A Surface Plasmon Resonance Imaging Study. *Front Chem*. 7, p588.

Choi WY, Gemberling M, Wang J, Holdway JE, Shen MC, Karlstrom RO, Poss KD. (2013). In vivo monitoring of cardiomyocyte proliferation to identify chemical modifiers of heart regeneration. *Development*. 140 (1), p660-6.

Clifford, C. J. and Downes, S. (1996) 'A comparative study of the use of colorimetric assays in the assessment of biocompatibility', *Journal of Materials Science: Materials in Medicine*, 7(10), pp. 637–643. doi: 10.1007/BF00058204.

Cortez-Retamozo, V. *et al.* (2004) 'Efficient Cancer Therapy with a Nanobody-Based Conjugate', *Cancer Research*, 64(8), pp. 2853–2857. doi: 10.1158/0008-5472.CAN-03-3935.

Cursiefen, C. *et al.* (2004) 'VEGF-A stimulates lymphangiogenesis and hemangiogenesis in inflammatory neovascularization via macrophage recruitment', *Journal of Clinical Investigation*. The American Society for Clinical Investigation, 113(7), pp. 1040–1050. doi: 10.1172/JCI20465.

Dammicco, S. *et al.* (2017) 'Regiospecific radiolabelling of Nanofitin on Ni magnetic beads with [(18)F]FBEM and in vivo PET studies.', *Nuclear medicine and biology*. United States, 51, pp. 33–39. doi: 10.1016/j.nucmedbio.2017.04.006.

Di Benedetto M, Starzec A, Vassy R, Perret GY, Crépin M, Kraemer M. (2003). Inhibition of epidermoid carcinoma A431 cell growth and angiogenesis in nude mice by early and late treatment with a novel dextran derivative. *Br J Cancer*. 88 (12), p1987-94.

Debeljak N, Feldman L, Davis KL, Komel R, Sytkowski AJ. (2006). Variability in the immunodetection of His-tagged recombinant proteins. *Anal Biochem*. 359 (2), p216-23.

Deeks, J. J. and Raffle, A. E. (2020) 'Lateral flow tests cannot rule out SARS-CoV-2 infection', *The BMJ*. BMJ Publishing Group. doi: 10.1136/bmj.m4787.

Desmet, J. *et al.* (2014) 'Structural basis of IL-23 antagonism by an Alphabody protein scaffold.', *Nature communications*, 5, p. 5237. doi: 10.1038/ncomms6237.

Ding, L. *et al.* (2015) 'A new Kunitz-type plasmin inhibitor from scorpion venom.', *Toxicon : official journal of the International Society on Toxinology*. England, 106, pp. 7–13. doi: 10.1016/j.toxicon.2015.09.004.

Domingues I, Rino J, Demmers JA, de Lanerolle P, Santos SC. (2011). VEGFR2 translocates to the nucleus to regulate its own transcription. *PLoS One*. 6 (9), e25668.

Donskov F, Michaelson MD, Puzanov I, Davis MP, Bjarnason GA, Motzer RJ, Goldstein D, Lin X, Cohen DP, Wiltshire R, R. B. (2015) 'Sunitinib-associated hypertension and neutropenia as efficacy biomarkers in metastatic renal cell carcinoma patients', *British Journal of Cancer*, 113(11), pp. 1571–1580.

Dreier B, P. A. (2012) 'Rapid Selection of High-Affinity Binders Using Ribosome Display', in Douthwaite J., J. R. (ed.) *Ribosome Display and Related Technologies.*

Methods in Molecular Biology (Methods and Protocols). New York: Springer, pp. 261–286. doi: 10.1007/978-1-61779-379-0_15.

Dugel, P. U. *et al.* (2020) 'HAWK and HARRIER: Phase 3, Multicenter, Randomized, Double-Masked Trials of Brolucizumab for Neovascular Age-Related Macular Degeneration', *Ophthalmology*. American Academy of Ophthalmology, 127(1), pp. 72–84. doi: 10.1016/j.ophtha.2019.04.017.

EA, M. *et al.* (2009) 'Affilin molecules selected against the human papillomavirus E7 protein inhibit the proliferation of target cells', *Journal of molecular biology*. J Mol Biol, 390(4), pp. 710–721. doi: 10.1016/J.JMB.2009.05.027.

Ebersbach, H. *et al.* (2007) 'Affilin-novel binding molecules based on human gamma-B-crystallin, an all beta-sheet protein.', *Journal of molecular biology*. England, 372(1), pp. 172–185. doi: 10.1016/j.jmb.2007.06.045.

El-Brolosy MA, Stainier DYR. (2017). Genetic compensation: A phenomenon in search of mechanisms. *PLoS Genet*. 13 (7), e1006780.

Eriksson A, Cao R, Pawliuk R, Berg SM, Tsang M, Zhou D, Fleet C, Tritsaris K, Dissing S, Leboulch P, Cao Y. (2002). Placenta growth factor-1 antagonizes VEGF-induced angiogenesis and tumor growth by the formation of functionally inactive PlGF-1/VEGF heterodimers. *Cancer Cell.* 1 (1), p99-108.

Ewan, L. C. *et al.* (2006) 'Intrinsic Tyrosine Kinase Activity is Required for Vascular Endothelial Growth Factor Receptor 2 Ubiquitination, Sorting and Degradation in Endothelial Cells', *The Authors Journal compilation* #, 7, pp. 1270–1282. doi: 10.1111/j.1600-0854.2006.00462.x.

Ferrara, N. (1999) 'Role of vascular endothelial growth factor in the regulation of angiogenesis', *Kidney International*, 56(3), pp. 794–814. doi: 10.1046/j.1523-1755.1999.00610.x.

Galley, H. F. and Webster, N. R. (2004) 'Physiology of the endothelium', *British Journal of Anaesthesia*. Oxford University Press, 93(1), pp. 105–113. doi: 10.1093/bja/aeh163.

Gebauer, M. and Skerra, A. (2012) 'Anticalins small engineered binding proteins based on the lipocalin scaffold.', *Methods in enzymology*. United States, 503, pp. 157–188. doi: 10.1016/B978-0-12-396962-0.00007-0.

Gellman, S. H. (1998) *Foldamers: A Manifesto*. Available at: https://pubs.acs.org/sharingguidelines (Accessed: 25 January 2021).

Gold Bio (2019) *Gold Biotechnology Guide to E. coli Genotype and Genetic Marker Nomenclature*, *Gold Biotechnology*.

Goodman, V. L. *et al.* (2007) 'Approval summary: Sunitinib for the treatment of imatinib refractory or intolerant gastrointestinal stromal tumors and advanced renal

cell carcinoma', *Clinical Cancer Research*, 13(5), pp. 1367–1373. doi: 10.1158/1078-0432.CCR-06-2328.

Goux, M. *et al.* (2017) 'Nanofitin as a New Molecular-Imaging Agent for the Diagnosis of Epidermal Growth Factor Receptor Over-Expressing Tumors.', *Bioconjugate chemistry*. United States, 28(9), pp. 2361–2371. doi: 10.1021/acs.bioconjchem.7b00374.

Gunnoo, S. B. and Madder, A. (2016) 'Chemical Protein Modification through Cysteine', *ChemBioChem*. John Wiley & Sons, Ltd, 17(7), pp. 529–553. doi: 10.1002/CBIC.201500667.

Gregory CW, He B, Johnson RT, Ford OH, Mohler JL, French FS, Wilson EM. (2001). A mechanism for androgen receptor-mediated prostate cancer recurrence after androgen deprivation therapy. *Cancer Res*. 61 (11), p4315-9.

Han KY, Chang JH, Lee H, Azar DT. (2016). Proangiogenic Interactions of Vascular Endothelial MMP14 With VEGF Receptor 1 in VEGFA-Mediated Corneal Angiogenesis. *Invest Ophthalmol Vis Sci*. 57 (7), p3313-22.

Hamer-Casterman, Atarchouch, T, C. *et al.* (1993) 'Naturally occurring antibodies devoid of light chains', *Nature*, 363(June), pp. 446–448. Available at: https://www.nature.com/articles/363446a0.pdf.

Hanlon, A. and Metjian, A. (2020) 'Caplacizumab in adult patients with acquired thrombotic thrombocytopenic purpura', *Therapeutic Advances in Hematology*. SAGE Publications, 11, p. 204062072090290. doi: 10.1177/2040620720902904.

Hansen, S. *et al.* (2018) 'Curvature of designed armadillo repeat proteins allows modular peptide binding.', *Journal of structural biology*. United States, 201(2), pp. 108–117. doi: 10.1016/j.jsb.2017.08.009.

Hashimoto H, Yuasa S, Tabata H, Tohyama S, Hayashiji N, Hattori F, Muraoka N, Egashira T, Okata S, Yae K, Seki T, Nishiyama T, Nakajima K, Sakaue-Sawano A, Miyawaki A, Fukuda K. (2014). Time-lapse imaging of cell cycle dynamics during development in living cardiomyocyte. *J Mol Cell Cardiol*. 72 (1), p241-9.

Haussecker D. (2016). Stacking up CRISPR against RNAi for therapeutic gene inhibition. *FEBS J*. 283 (17), p3249-60.

He, Y. *et al.* (2002) 'Suppression of tumor lymphangiogenesis and lymph node metastasis by blocking vascular endothelial growth factor receptor 3 signaling', *Journal of the National Cancer Institute*. Oxford University Press, 94(11), pp. 819–825. doi: 10.1093/jnci/94.11.819.

Hedlund EM, Yang X, Zhang Y, Yang Y, Shibuya M, Zhong W, Sun B, Liu Y, Hosaka K, Cao Y. (2013). Tumor cell-derived placental growth factor sensitizes antiangiogenic and antitumor effects of anti-VEGF drugs. *Proc Natl Acad Sci U S A*. 110 (2), p654-9.

Hiratsuka S, Minowa O, Kuno J, Noda T, Shibuya M. (1998). Flt-1 lacking the tyrosine kinase domain is sufficient for normal development and angiogenesis in mice. *Proc Natl Acad Sci U S A*. 95 (16), p9349-54.

Hjerpe, R. *et al.* (2009) 'Efficient protection and isolation of ubiquitylated proteins using tandem ubiquitin-binding entities.', *EMBO reports*. Nature Publishing Group, 10(11), pp. 1250–1258. doi: 10.1038/embor.2009.192.

Holmes, D. I. R. and Zachary, I. (2005) 'The vascular endothelial growth factor (VEGF) family: Angiogenic factors in health and disease', *Genome Biology*, 6(2), p. 209. doi: 10.1186/gb-2005-6-2-209.

Hong, Y. *et al.* (2004) 'VEGF-A promotes tissue repair-associated lymphatic vessel formation via VEGFR-2 and the α1β1 and α2β1 integrins', *The FASEB Journal*. Wiley, 18(10), pp. 1111–1113. doi: 10.1096/fj.03-1179fje.

Horowitz, A. and Seerapu, H. R. (2012) 'Regulation of VEGF signaling by membrane traffic', *Cellular Signalling*, 24(9), pp. 1810–1820. doi: 10.1016/j.cellsig.2012.05.007.

Hosse, R. J. (2006) 'A new generation of protein display scaffolds for molecular recognition', *Protein Science*, 15(1), pp. 14–27. doi: 10.1110/ps.051817606.

Hsieh, P. C. H. *et al.* (2006) 'ENDOTHELIAL-CARDIOMYOCYTE INTERACTIONS IN CARDIAC DEVELOPMENT AND REPAIR', *Annu. Rev. Physiol*, 68, pp. 51–66. doi: 10.1146/annurev.physiol.68.040104.124629.

Hsu, J. Y. and Wakelee, H. A. (2009) 'Monoclonal Antibodies Targeting Vascular Endothelial Growth Factor Current Status and Future Challenges in Cancer Therapy', 23(5), pp. 289–304. doi: 10.2165/11317600-000000000-00000.

Hughes, D. J. *et al.* (2017) 'Generation of specific inhibitors of SUMO-1- and SUMO-2/3-mediated protein-protein interactions using Affimer (Adhiron) technology', *Science Signaling*. American Association for the Advancement of Science, 10(505). doi: 10.1126/scisignal.aaj2005.

Huppertz, B. and Peeters, L. L. H. (2005) 'Vascular biology in implantation and placentation', *Angiogenesis*, pp. 157–167. doi: 10.1007/s10456-005-9007-8

Im K, Mareninov S, Diaz MFP, Yong WH. (2019). An Introduction to Performing Immunofluorescence Staining. *Methods Mol Biol*. 1897 (1), p299-311.

Iyer, S. and Acharya, K. R. (2011) 'Tying the knot: The cystine signature and molecular-recognition processes of the vascular endothelial growth factor family of angiogenic cytokines', *FEBS Journal*, 278(22), pp. 4304–4322. doi: 10.1111/j.1742-4658.2011.08350.x.

Jain, R. K. (2005) 'Normalization of tumor vasculature: An emerging concept in antiangiogenic therapy', *Science*. American Association for the Advancement of Science, pp. 58–62. doi: 10.1126/science.1104819.

Johnson RO, Wolberg WH. (1971). Cellular kinetics and their implications for chemotherapy of solid tumors, especially cancer of the colon. *Cancer*. 28 (1), p208-12.

Jopling HM, Odell AF, Pellet-Many C, Latham AM, Frankel P, Sivaprasadarao A, Walker JH, Zachary IC, Ponnambalam S. (2014). Endosome-to-Plasma Membrane Recycling of VEGFR2 Receptor Tyrosine Kinase Regulates Endothelial Function and Blood Vessel Formation. *Cells*. 3 (2), p363-85.

Kalichuk, V. *et al.* (2020) 'Affitins: Ribosome Display for Selection of Aho7c-Based Affinity Proteins.', *Methods in molecular biology (Clifton, N.J.)*. United States, 2070, pp. 19–41. doi: 10.1007/978-1-4939-9853-1_2.

Karpov, O. A. *et al.* (2015) 'Receptor tyrosine kinase structure and function in health and disease', *AIMS Biophysics*, 2(4), pp. 476–502. doi: 10.3934/biophy.2015.4.476.

Kearney, K. J. *et al.* (2019) *Affimer proteins as a tool to modulate fibrinolysis, stabilize the blood clot, and reduce bleeding complications*, *Blood*. Available at: http://ashpublications.org/blood/article-df/133/11/1233/1552695/blood856195.pdf.

Kemp, A. *et al.* (2013) 'Myocardial infarction after intravitreal vascular endothelial growth factor inhibitors: a whole population study.', *Retina (Philadelphia, Pa.)*, 33(5), pp. 920–7. doi: 10.1097/IAE.0b013e318276e07b.

Kerbel RS. (1991). Inhibition of tumor angiogenesis as a strategy to circumvent acquired resistance to anti-cancer therapeutic agents. *Bioessays*. 13 (1), p31-6.

Kim D, Bae S, Park J, Kim E, Kim S, Yu HR, Hwang J, Kim JI, Kim JS. (2015). Digenome-seq: genome-wide profiling of CRISPR-Cas9 off-target effects in human cells. *Nat Methods*. 12 (3), p237-43.

Kimple ME, Brill AL, Pasker RL. (2013). Overview of affinity tags for protein purification. *Curr Protoc Protein Sci*. 73 (9), p9.1-9.9.23.

Kisand K, Kerna I, Kumm J, Jonsson H, Tamm A. (2011). Impact of cryopreservation on serum concentration of matrix metalloproteinases (MMP)-7, TIMP-1, vascular growth factors (VEGF) and VEGF-R2 in Biobank samples. *Clin Chem Lab Med*. 49 (2), p229-35.

Kivelä R, Hemanthakumar KA, Vaparanta K, Robciuc M, Izumiya Y, Kidoya H, Takakura N, Peng X, Sawyer DB, Elenius K, Walsh K, Alitalo K. (2019). Endothelial Cells Regulate Physiological Cardiomyocyte

Growth via VEGFR2-Mediated Paracrine Signaling. *Circulation*. 139 (22), p2570-2584.

Klont, F. *et al.* (2018) 'Affimers as an Alternative to Antibodies in an Affinity LC−MS Assay for Quantification of the Soluble Receptor of Advanced Glycation End-Products (sRAGE) in Human Serum'. doi: 10.1021/acs.jproteome.8b00414.

Koch, S. *et al.* (2011) 'Signal transduction by vascular endothelial growth factor receptors', *Biochemical Journal*. Portland Press, pp. 169–183. doi: 10.1042/BJ20110301.

Kopparapu PK, Boorjian SA, Robinson BD, Downes M, Gudas LJ, Mongan NP, Persson JL. (2013). Expression of VEGF and its receptors VEGFR1/VEGFR2 is associated with invasiveness of bladder cancer. *Anticancer Res*. 33 (6), p2381-90.

Kondo, T. *et al.* (2020) 'Antibody-like proteins that capture and neutralize SARS-CoV-2.', *Science advances*, 6(42). doi: 10.1126/sciadv.abd3916.

Koutsoumpeli, E. *et al.* (2017) 'Antibody Mimetics for the Detection of Small Organic Compounds Using a Quartz Crystal Microbalance', *Analytical Chemistry*, 89(5), pp. 3051–3058. doi: 10.1021/acs.analchem.6b04790.

Kumar, A. *et al.* (2017) 'Antibody-Drug Conjugates', *Annual Reports in Medicinal Chemistry*. Academic Press, 50, pp. 441–480. doi: 10.1016/BS.ARMC.2017.08.002.

Kurt, L. *et al.* (2011) 'Structure-function studies of an engineered scaffold protein derived from Stefin A. II: Development and applications of the SQT variant', *Protein Engineering, Design & Selection*, 24(9), pp. 751–763. doi: 10.1093/protein/gzr019.

Lange PH, Lightner DJ, Medini E, Reddy PK, Vessella RL. (1990). The effect of radiation therapy after radical prostatectomy in patients with elevated prostate specific antigen levels. *J Urol*. 144 (4), p927-32.

Lavine KJ, Pinto AR, Epelman S, Kopecky BJ, Clemente-Casares X, Godwin J, Rosenthal N, Kovacic JC. (2018). The Macrophage in Cardiac Homeostasis and Disease: JACC Macrophage in CVD Series (Part 4). *J Am Coll Cardiol*. 72 (18), p2213-2230.

Le Tourneau C, Raymond E, Faivre S. (2007). Sunitinib: a novel tyrosine kinase inhibitor. A brief review of its therapeutic potential in the treatment of renal carcinoma and gastrointestinal stromal tumors (GIST). *Ther Clin Risk Manag*. 3 (2), p341-8.

Lee TH, Seng S, Sekine M, Hinton C, Fu Y, Avraham HK, Avraham S. (2007). Vascular endothelial growth factor mediates intracrine survival in human breast carcinoma cells through internally expressed VEGFR1/FLT1. *PLoS Med*. 4 (6), e186.

Lee JE, Kim SY, Shin SY. (2015). Effect of Repeated Freezing and Thawing on Biomarker Stability in Plasma and Serum Samples. *Osong Public Health Res Perspect*. 6 (6), p357-62.

Lee, A. W. *et al.* (2019) 'A knottin scaffold directs the CXC-chemokine-binding specificity of tick evasins.', *The Journal of biological chemistry*, 294(29), pp. 11199–11212. doi: 10.1074/jbc.RA119.008817.

Leestemaker, Y. and Ovaa, H. (2017) 'Tools to investigate the ubiquitin proteasome system', *Drug Discovery Today: Technologies*. Elsevier, 26, pp. 25–31. doi: 10.1016/J.DDTEC.2017.11.006.

Lehmann, A. (2008) 'Ecallantide (DX-88), a plasma kallikrein inhibitor for the treatment of hereditary angioedema and the prevention of blood loss in on-pump cardiothoracic surgery', *Expert Opinion on Biological Therapy*. Taylor & Francis, 8(8), pp. 1187–1199. doi: 10.1517/14712598.8.8.1187.

Lemmon, M. A. and Schlessinger, J. (2010) 'Cell signaling by receptor tyrosine kinases', *Cell*, 141(7), pp. 1117–1134. doi: 10.1016/j.cell.2010.06.011.

Leonard F, Devaux Y, Vausort M, Ernens I, Rolland-Turner M, Wagner DR. (2011). Adenosine modifies the balance between membrane and soluble forms of Flt-1. *J Leukoc Biol*. 90 (1), p199-204.

Leung, D. W. *et al.* (1989) 'Vascular endothelial growth factor is a secreted angiogenic mitogen', *Science*. American Association for the Advancement of Science, 246(4935), pp. 1306–1309. doi: 10.1126/science.2479986.

Levine B, Kalman J, Mayer L, Fillit HM, P. M. (1990) 'Elevated circulating levels of tumor necrosis factor in severe chronic heart failure', *New England Journal of Medicine*, 323(4), pp. 236–241.

Lipovšek, D. *et al.* (2018) 'Adnectin-drug conjugates for Glypican-3-specific delivery of a cytotoxic payload to tumors.', *Protein engineering, design & selection : PEDS*, 31(5), pp. 159–171. doi: 10.1093/protein/gzy013.

Liu, Y. *et al.* (2017) 'Reversible retinal vessel closure from VEGF-induced leukocyte plugging', *JCI insight*. NLM (Medline), 2(18). doi: 10.1172/jci.insight.95530.

Löfblom, J. *et al.* (2010) 'Affibody molecules: Engineered proteins for therapeutic, diagnostic and biotechnological applications', *FEBS Letters*. Federation of European Biochemical Societies, 584(12), pp. 2670–2680. doi: 10.1016/j.febslet.2010.04.014.

Lopata, A., Hughes, R., Tiede, C. et al. (2018). Affimer proteins for F-actin: novel affinity reagents that label F-actin in live and fixed cells. *Sci Rep*. 8 (6572)

Loussouarn, A. *et al.* (2020) 'Characterization of Affitin proteolytic digestion in

biorelevant media and improvement of their stabilities via protein engineering.', *Scientific reports*, 10(1), p. 19703. doi: 10.1038/s41598-020-76855-z.

Lugano, R., Huang, H. and Dimberg, A. (2018) 'Vascular Endothelial Growth Factor Receptor (VEGFR)', *Encyclopedia of Signaling Molecules*. Springer, Cham, pp. 5884–5892. doi: 10.1007/978-3-319-67199-4_101914.

MacGinnitie AJ, Campion M, Stolz LE, P. W. (2012) 'Ecallantide for treatment of acute hereditary angioedema attacks: analysis of efficacy by patient characteristics', *Allery and Asthma Proceedings*, 33(2), pp. 178–185.

Maghsoudlou, A. *et al.* (2016) 'RNF121 Inhibits Angiogenic Growth Factor Signaling by Restricting Cell Surface Expression of VEGFR-2', *Traffic*, 17(3), pp. 289–300. doi: 10.1111/tra.12353.

Mahapatra, S. and Chandra, P. (2020) 'Clinically practiced and commercially viable nanobio engineered analytical methods for COVID-19 diagnosis', *Biosensors and Bioelectronics*. Elsevier Ltd, 165, p. 112361. doi: 10.1016/j.bios.2020.112361.

Malik, Y. S. *et al.* (2021) 'SARS-CoV-2 Spike Protein Extrapolation for COVID Diagnosis and Vaccine Development', *Frontiers in Molecular Biosciences*. Frontiers Media S.A., 8, p. 315. doi: 10.3389/FMOLB.2021.607886/BIBTEX.

Mamluk, R. *et al.* (2010) 'Anti-tumor effect of CT-322 as an adnectin inhibitor of vascular endothelial growth factor receptor-2', *mAbs*. Taylor & Francis, 2(2), pp. 199–208. doi: 10.4161/mabs.2.2.11304.

Marcion, G. *et al.* (2021) 'Nanofitins targeting heat shock protein 110: An innovative immunotherapeutic modality in cancer.', *International journal of cancer*. United States, 148(12), pp. 3019–3031. doi: 10.1002/ijc.33485.

Markovic-Mueller S, Stuttfeld E, Asthana M, Weinert T, Bliven S, Goldie KN, Kisko K, Capitani G, Ballmer-Hofer K. (2017). Structure of the Full-length VEGFR-1 Extracellular Domain in Complex with VEGF-A. *Structure*. 25 (2), p341-352.

Martins, A. H. and Ulrich, H. (2007) 'Development of the anti-VEGF aptamer to a therapeutic agent for clinical ophthalmology', 1(4), pp. 393–402.

Matson JP, Cook JG. (2017). Cell cycle proliferation decisions: the impact of single cell analyses. *FEBS J*. 284 (3), p362-375.

Mattila, M. M. T. *et al.* (2002) 'VEGF-C induced lymphangiogenesis is associated with lymph node metastasis in orthotopic MCF-7 tumors', *International Journal of Cancer*. Wiley, 98(6), pp. 946–951. doi: 10.1002/ijc.10283.

McGivern, J. G. (2007) 'Ziconotide: A review of its pharmacology and use in the treatment of pain', *Neuropsychiatric Disease and Treatment*, 3(1), pp. 69–85. doi: 10.2147/nedt.2007.3.1.69.

Mentzer SJ, Konerding MA. (2014). Intussusceptive angiogenesis: expansion and remodeling of microvascular networks. *Angiogenesis*. 17 (3), p499-509.

Mesquita, E. T., de Souza, C. V. and Ferreira, T. R. (2015) 'Andreas Vesalius 500 years - A Renaissance that revolutionized cardiovascular knowledge', *Brazilian Journal of Cardiovascular Surgery*, 30(2), pp. 260–265. doi: 10.5935/1678-9741.20150024.

Michel Burnier, Sverre Kjeldsen, Anthony Heagerty, and B. W. (2020) 'Drug treatment of hypertension', in Camm, A. J. et al. (eds) *ESC CardioMed*. 3rd edn. Oxford University Press: Oxford University Press, pp. 1–7. doi: 10.1093/MED/9780198784906.003.0569_UPDATE_001.

Michmerhuizen AR, Spratt DE, Pierce LJ, Speers CW. (2020). ARe we there yet? Understanding androgen receptor signaling in breast cancer. *NPJ Breast Cancer*. 6, p47.

Miles, J. A. *et al.* (2021) 'Selective Affimers Recognise the BCL-2 Family Proteins BCL-xL and MCL-1 through Noncanonical Structural Motifs**', *ChemBioChem*, 22(1), pp. 232–240. doi: 10.1002/cbic.202000585.

Miller, K. *et al.* (2007) 'Paclitaxel plus bevacizumab versus paclitaxel alone for metastatic breast cancer.', *The New England journal of medicine*, 357(26), pp. 2666–76. doi: 10.1056/NEJMoa072113.

Mishra, M. (2020) 'Evolutionary Aspects of the Structural Convergence and Functional Diversification of Kunitz-Domain Inhibitors.', *Journal of molecular evolution*. Germany, 88(7), pp. 537–548. doi: 10.1007/s00239-020-09959-9.

Miwa S, Yano S, Kimura H, Yamamoto M, Toneri M, Matsumoto Y, Uehara F, Hiroshima Y, Murakami T, Hayashi K, Yamamoto N, Bouvet M, Fujiwara T, Tsuchiya H, Hoffman RM. (2015). Cell-cycle fate-monitoring distinguishes individual chemosensitive and chemoresistant cancer cells in drug-treated heterogeneous populations demonstrated by real-time FUCCI imaging. *Cell Cycle*. 14 (4), p621-9.

Moisseiev, E. and Loewenstein, A. (2020) 'Abicipar pegol—a novel anti-VEGF therapy with a long duration of action', *Eye (Basingstoke)*. Springer Nature, pp. 605–606. doi: 10.1038/s41433-019-0584-y.

Moore, S J. R. C. (2012) 'Engineering Knottins as Novel Binding Agents', in *Methods in Enzymology*. 503rd edn. Academic Press, pp. 223–251. doi: https://doi.org/10.1016/B978-0-12-396962-0.00009-4.

Moradi, Mohammadreza & Solgi, Reza & Najafi, Rezvan & Tanzadehpanah, Hamid & Saidijam, Massoud. (2018). Determining Optimal Cell Density and Culture Medium Volume simultaneously in MTT Cell Proliferation Assay for Adherent Cancer Cell Lines. *HELIX*. 8, 10.29042/2018-3274-3280.

Mourad, J. J. *et al.* (2008) 'Blood pressure rise following angiogenesis inhibition by bevacizumab. A crucial role for microcirculation', *Annals of Oncology*, 19(5), pp. 927–934. doi: 10.1093/annonc/mdm550.

Mross, K. *et al.* (2013) 'First-in-Human Phase I Study of PRS-050 (Angiocal), an Anticalin Targeting and Antagonizing VEGF-A, in Patients with Advanced Solid Tumors', *PLoS ONE*. Edited by M. Fernandez-Zapico. Public Library of Science, 8(12), p. e83232. doi: 10.1371/journal.pone.0083232.

Mullard A. (2021). FDA approves 100th monoclonal antibody product. *Nat Rev Drug Discov*. 20 (7), p491-495.

Münch, R. C. *et al.* (2011) 'DARPins: an efficient targeting domain for lentiviral vectors.', *Molecular therapy : the journal of the American Society of Gene Therapy*. Nature Publishing Group, 19(4), pp. 686–693. doi: 10.1038/mt.2010.298.

Muyldermans, S. (2013) 'Nanobodies: Natural single-domain antibodies', *Annual Review of Biochemistry*. Annu Rev Biochem, pp. 775–797. doi: 10.1146/annurev-biochem-063011-092449.

Nagaya, N. *et al.* (2004) 'Intravenous administration of mesenchymal stem cells improves cardiac function in rats with acute myocardial infarction through angiogenesis and myogenesis', *Am J Physiol Heart Circ Physiol*, 287, pp. 2670–2676. doi: 10.1152/ajpheart.01071.2003.-Mesenchymal.

Nagy, J. A. *et al.* (2002) 'Vascular permeability factor/vascular endothelial growth factor induces lymphangiogenesis as well as angiogenesis', *Journal of Experimental Medicine*. J Exp Med, 196(11), pp. 1497–1506. doi: 10.1084/jem.20021244.

Nakamura K, Yamamoto A, Kamishohara M, Takahashi K, Taguchi E, Miura T, Kubo K, Shibuya M, Isoe T. (2004). KRN633: A selective inhibitor of vascular endothelial growth factor receptor-2 tyrosine kinase that suppresses tumor angiogenesis and growth. *Mol Cancer Ther*. 3 (12), p1639-49.

Nalluri, S. R. *et al.* (2008) 'Risk of venous thromboembolism with the angiogenesis inhibitor bevacizumab in cancer patients: a meta-analysis.', *JAMA : the journal of the American Medical Association*, 300(19), pp. 2277–2285. doi: 10.1001/jama.2008.656.

Nanda, J. S. and Lorsch, J. R. (2014) 'Labeling of a Protein with Fluorophores Using Maleimide Derivitization', *Methods in Enzymology*. Academic Press, 536(1), pp. 79–86. doi: 10.1016/B978-0-12-420070-8.00007-6.

National Research Council (US) (1999) 'Large-Scale Production of Monoclonal Antibodies', in (US), N. A. P. (ed.) *Monoclonal Antibody Production*. Washington DC: National Academies Press (US), p. 5. Available at: https://www.ncbi.nlm.nih.gov/books/NBK100189/ (Accessed: 4 February 2022).

Newman AC, Nakatsu MN, Chou W, Gershon PD, Hughes CC. (2011). The requirement for fibroblasts in angiogenesis: fibroblast-derived matrix proteins are essential for endothelial cell lumen formation. *Mol Biol Cell*. 22 (20), p3791-800.

Newman HA, Meluh PB, Lu J, Vidal J, Carson C, Lagesse E, Gray JJ, Boeke JD, Matunis MJ. (2017). A high throughput mutagenic analysis of yeast sumo structure and function. *PLoS Genet*. 13 (2), e1006612.

Ng, E. W. M. *et al.* (2006) 'Pegaptanib, a targeted anti-VEGF aptamer for ocular vascular disease', *Nature Reviews Drug Discovery*. Nat Rev Drug Discov, pp. 123–132. doi: 10.1038/nrd1955.

Nian, M. *et al.* (2004) 'Inflammatory Cytokines and Postmyocardial Infarction Remodeling', *Circulation Research*, 94(12), pp. 1543–1553. doi: 10.1161/01.RES.0000130526.20854.fa.

Nicholes, N. *et al.* (2015) 'Modular protein switches derived from antibody mimetic proteins', *Protein Engineering, Design and Selection*, 29(2), pp. 77–85. doi: 10.1093/protein/gzv062.

Nimjee, S. M. *et al.* (2017) 'Aptamers as Therapeutics.', *Annual review of pharmacology and toxicology*, 57, pp. 61–79. doi: 10.1146/annurev-pharmtox-010716-104558.

Nishida N, Yano H, Nishida T, Kamura T, Kojiro M. (2006). Angiogenesis in cancer. *Vasc Health Risk Manag*. 2 (3), p213-9.

Nishigaki, K. *et al.* (1997) 'Plasma Fas ligand, an inducer of apoptosis, and plasma soluble Fas, an inhibitor of apoptosis, in patients with chronic congestive heart failure', *Journal of the American College of Cardiology*. Elsevier Masson SAS, 29(6), pp. 1214–1220. doi: 10.1016/S0735-1097(97)00055-7.

Odorisio T, Schietroma C, Zaccaria ML, Cianfarani F, Tiveron C, Tatangelo L, Failla CM, Zambruno G. (2002). Mice overexpressing placenta growth factor exhibit increased vascularization and vessel permeability. *J Cell Sci*. 115 (12), p2559-67.

Pannecoucke, E. *et al.* (2021) 'Cell-penetrating Alphabody protein scaffolds for intracellular drug targeting.', *Science advances*, 7(13). doi: 10.1126/sciadv.abe1682.

Park M, Lee ST. (1999). The fourth immunoglobulin-like loop in the extracellular domain of FLT-1, a VEGF receptor, includes a major heparin-binding site. *Biochem Biophys Res Commun*. 264 (3), p730-4.

Parmeggiani, F. *et al.* (2008) 'Designed armadillo repeat proteins as general peptide-binding scaffolds: consensus design and computational optimization of

the hydrophobic core.', *Journal of molecular biology*. England, 376(5), pp. 1282–1304. doi: 10.1016/j.jmb.2007.12.014.
Perren, T. J. *et al.* (2011) 'A Phase 3 Trial of Bevacizumab in Ovarian Cancer', *New England Journal of Medicine*, 365(26), pp. 2484–2496.

Peyvandi, F. *et al.* (2016) 'Caplacizumab for Acquired Thrombotic Thrombocytopenic Purpura', *New England Journal of Medicine*. New England Journal of Medicine (NEJM/MMS), 374(6), pp. 511–522. doi: 10.1056/nejmoa1505533.

Podgrabinska, S. *et al.* (2002) 'Molecular characterization of lymphatic endothelial cells', *Proceedings of the National Academy of Sciences of the United States of America*. National Academy of Sciences, 99(25), pp. 16069–16074. doi: 10.1073/pnas.242401399.

Pölcher, M. *et al.* (2010) 'Sorafenib in combination with carboplatin and paclitaxel as neoadjuvant chemotherapy in patients with advanced ovarian cancer', *Cancer Chemotherapy and Pharmacology*, 66(1), pp. 203–207. doi: 10.1007/s00280-010-1276-2.

Postic, G., Gracy, J., Périn, C., Chiche, L. and Gelly, J.-C. (2018) 'KNOTTIN: the database of inhibitor cystine knot scaffold after 10 years, toward a systematic structure modeling.', *Nucleic acids research*, 46(D1), pp. D454–D458. doi: 10.1093/nar/gkx1084.

Postic, G., Gracy, J., Périn, C., Chiche, L. and Gelly, J. C. (2018) 'KNOTTIN: The database of inhibitor cystine knot scaffold after 10 years, toward a systematic structure modeling', *Nucleic Acids Research*, 46(D1), pp. D454–D458. doi: 10.1093/nar/gkx1084.

Pulkki, K. J. (1997) 'Cytokines and Cardiomyocyte Death', *Annals of Medicine*, 29(4), pp. 339–343. doi: 10.3109/07853899708999358.

Rabellino A, Andreani C, Scaglioni PP. (2020). Roles of Ubiquitination and SUMOylation in the Regulation of Angiogenesis. *Curr Issues Mol Biol*. 35, p109-126.

Rahimi N. (2006). VEGFR-1 and VEGFR-2: two non-identical twins with a unique physiognomy. *Front Biosci*. 11, p818-29.

Rakonjac, J. *et al.* (2011) 'Filamentous bacteriophage: biology, phage display and nanotechnology applications.', *Current issues in molecular biology*, 13(2), pp. 51–76. doi: 10.1002/9780470015902.a0000777.

Raza, A., Franklin, M. J. and Dudek, A. Z. (2010) 'Pericytes and vessel maturation during tumor angiogenesis and metastasis', *American Journal of Hematology*. John Wiley & Sons, Ltd, 85(8), pp. 593–598. doi: 10.1002/AJH.21745.

Reichen, C. *et al.* (2016) ‘Structures of designed armadillo-repeat proteins show propagation of inter-repeat interface effects.’, *Acta crystallographica. Section D, Structural biology*, 72(Pt 1), pp. 168–175. doi: 10.1107/S2059798315023116.

Ribatti D, Nico B, Floris C, Mangieri D, Piras F, Ennas MG, Vacca A, Sirigu P. (2005). Microvascular density, vascular endothelial growth factor immunoreactivity in tumor cells, vessel diameter and intussusceptive microvascular growth in primary melanoma. *Oncol Rep*. 14 (1), p81-4.

Richter KN, Revelo NH, Seitz KJ, Helm MS, Sarkar D, Saleeb RS, D'Este E, Eberle J, Wagner E, Vogl C, Lazaro DF, Richter F, Coy-Vergara J, Coceano G, Boyden ES, Duncan RR, Hell SW, Lauterbach MA, Lehna. (2018). Glyoxal as an alternative fixative to formaldehyde in immunostaining and super-resolution microscopy. *EMBO J*. 37 (1), p139-159.

Risau, W. (1997) ‘Mechanisms of angiogenesis’, *Nature*, 386(April), pp. 671–674.

Roberts, N. *et al.* (2006) ‘Inhibition of VEGFR-3 activation with the antagonistic antibody more potently suppresses lymph node and distant metastases than inactivation of VEGFR-2’, *Cancer Research*. Cancer Res, 66(5), pp. 2650–2657. doi: 10.1158/0008-5472.CAN-05-1843.

Rosano, G. L. and Ceccarelli, E. A. (2009) ‘Rare codon content affects the solubility of recombinant proteins in a codon bias-adjusted Escherichia coli strain’, *Microbial Cell Factories*. BioMed Central, 8(1), pp. 1–9. doi: 10.1186/1475-2859-8-41/FIGURES/5.

Rosano, G. L. and Ceccarelli, E. A. (2014) ‘Recombinant protein expression in Escherichia coli: Advances and challenges’, *Frontiers in Microbiology*. Frontiers Research Foundation, 5(APR), p. 172. doi: 10.3389/FMICB.2014.00172/BIBTEX.

Rossi A, Kontarakis Z, Gerri C, Nolte H, Hölper S, Krüger M, Stainier DY. (2015). Genetic compensation induced by deleterious mutations but not gene knockdowns. *Nature*. 524 (7564), p230-3.

Roy I, Gupta MN. (2004). Freeze-drying of proteins: some emerging concerns. *Biotechnol Appl Biochem*. 39 (2), p165-77.

Ruch C, Skiniotis G, Steinmetz MO, Walz T, Ballmer-Hofer K. (2007). Structure of a VEGF-VEGF receptor complex determined by electron microscopy. *Nat Struct Mol Biol*. 14 (3), p249-50.

Sakaue-Sawano A, Kurokawa H, Morimura T, Hanyu A, Hama H, Osawa H, Kashiwagi S, Fukami K, Miyata T, Miyoshi H, Imamura T, Ogawa M, Masai H, Miyawaki A. (2008). Visualizing spatiotemporal dynamics of multicellular cell-cycle progression. *Cell*. 132 (3), p487-98.

Salven P, Lymboussaki A, Heikkilä P, Jääskela-Saari H, Enholm B, Aase K, von Euler G, Eriksson U, Alitalo K, Joensuu H. (1998). Vascular endothelial growth factors VEGF-B and VEGF-C are expressed in human tumors. *Am J Pathol*. 153 (1), p103-8.

Sawano A, Takahashi T, Yamaguchi S, Shibuya M. (1997). The phosphorylated 1169-tyrosine containing region of flt-1 kinase (VEGFR-1) is a major binding site for PLCgamma. *Biochem Biophys Res Commun*. 238 (2), p487-91.

Schamel WW. (2001). Biotinylation of protein complexes may lead to aggregation as well as to loss of subunits as revealed by Blue Native PAGE. *J Immunol Methods*. 252 (1-2), p171-4.

Schlatter, D. *et al.* (2012) 'Generation, characterization and structural data of chymase binding proteins based on the human Fyn kinase SH3 domain.', *mAbs*, 4(4), pp. 497–508. doi: 10.4161/mabs.20452.

Schlichthaerle, T. *et al.* (2018) 'Site-Specific Labeling of Affimers for DNA-PAINT Microscopy', *Angewandte Chemie - International Edition*, 57(34), pp. 11060–11063. doi: 10.1002/anie.201804020.

Schmidt M, Voelker HU, Kapp M, Dietl J, Kammerer U. (2008). Expression of VEGFR-1 (Flt-1) in breast cancer is associated with VEGF expression and with node-negative tumour stage. *Anticancer Res*. 28 (3A), P1719-24.

Schnitzbauer, J. *et al.* (2017) 'Super-resolution microscopy with DNA-PAINT', *Nature Publishing Group*, 12. doi: 10.1038/nprot.2017.024.

Schoppmann, S. F. *et al.* (2002) 'Tumor-associated macrophages express lymphatic endothelial growth factors and are related to peritumoral lymphangiogenesis', *American Journal of Pathology*. American Society for Investigative Pathology, 161(3), pp. 947–956. doi: 10.1016/S0002-9440(10)64255-1.

Schwarz, E. (2017) 'Cystine knot growth factors and their functionally versatile proregions', *Biological Chemistry*, 398(12), pp. 1295–1308. doi: 10.1515/hsz-2017-0163.

Scully, M. *et al.* (2019) 'Caplacizumab Treatment for Acquired Thrombotic Thrombocytopenic Purpura', *New England Journal of Medicine*. New England Journal of Medicine (NEJM/MMS), 380(4), pp. 335–346. doi: 10.1056/nejmoa1806311.

Settele, F. *et al.* (2018) 'Construction and Selection of Affilin(®) Phage Display Libraries.', *Methods in molecular biology (Clifton, N.J.)*. United States, 1701, pp. 205–238. doi: 10.1007/978-1-4939-7447-4_11.

Shaik F, Cuthbert GA, Homer-Vanniasinkam S, Muench SP, Ponnambalam S, Harrison MA. (2020). Structural Basis for Vascular Endothelial Growth Factor Receptor Activation and Implications for Disease Therapy. *Biomolecules*. 10 (12), p1673.

Shamsuddin, S. H. *et al.* (2021) 'Selection and characterisation of Affimers specific for CEA recognition', *Scientific Reports*, 11(11), p. 744. doi: 10.1038/s41598-020-80354-6.

Sharma A, Kumar N, Bandello F, Kuppermann BD, Loewenstein A, R. C. (2020) 'Brolucizumab: the road ahead', *British Journal of Ophthalmology*, 104(12), pp. 1631–1632.

Shi, M. M., Shi, C. H. and Xu, Y. M. (2017) 'Rab GTPases: The key players in the molecular pathway of Parkinson's disease', *Frontiers in Cellular Neuroscience*. Frontiers Media S.A., 11, p. 81. doi: 10.3389/FNCEL.2017.00081/BIBTEX.

Shibuya, M. (2011) 'Vascular Endothelial Growth Factor (VEGF) and Its Receptor (VEGFR) Signaling in Angiogenesis: A Crucial Target for Anti- and Pro-Angiogenic Therapies', *Genes and Cancer*, 2(12), pp. 1097–1105. doi: 10.1177/1947601911423031.

Shibuya, M. and Claesson-Welsh, L. (2006) 'Signal transduction by VEGF receptors in regulation of angiogenesis and lymphangiogenesis', *Experimental Cell Research*, 312(5), pp. 549–560. doi: 10.1016/j.yexcr.2005.11.012.

Silacci, M. *et al.* (2014) 'Linker length matters, fynomer-Fc fusion with an optimized linker displaying picomolar IL-17A inhibition potency.', *The Journal of biological chemistry*, 289(20), pp. 14392–14398. doi: 10.1074/jbc.M113.534578.

Silverman, J. *et al.* (2005) 'Multivalent avimer proteins evolved by exon shuffling of a family of human receptor domains.', *Nature biotechnology*. United States, 23(12), pp. 1556–1561. doi: 10.1038/nbt1166.

Simeon, R. and Chen, Z. (2018) 'In vitro-engineered non-antibody protein therapeutics', *Protein and Cell*. Higher Education Press, pp. 3–14. doi: 10.1007/s13238-017-0386-6.

Singh, S. R. *et al.* (2017) 'Intravitreal ziv-aflibercept: Clinical effects and economic impact', *Asia-Pacific Journal of Ophthalmology*. Asia-Pacific Academy of Ophthalmology, pp. 561–568. doi: 10.22608/APO.2017263.

Skerra, A. (2001) '"Anticalins": a new class of engineered ligand-binding proteins with antibody-like properties.', *Journal of biotechnology*. Netherlands, 74(4), pp. 257–275. doi: 10.1016/s1389-0352(01)00020-4.

Škrlec, K., Štrukelj, B. and Berlec, A. (2015) 'Non-immunoglobulin scaffolds: a focus on their targets.', *Trends in biotechnology*. England, 33(7), pp. 408–418. doi: 10.1016/j.tibtech.2015.03.012.

Smith, G. A. *et al.* (2015) 'The cellular response to vascular endothelial growth factors requires co-ordinated signal transduction, trafficking and proteolysis.', *Bioscience reports*, 35(5), p. e00253. doi: 10.1042/BSR20150171.

Smith, G. A. *et al.* (2017) 'Ubiquitination of basal VEGFR2 regulates signal transduction and endothelial function', *Biology Open*, 6(10), pp. 1404–1415. doi: 10.1242/bio.027896.

Smith, G. P. (1985) 'Filamentous fusion phage: novel expression vectors that display cloned antigens on the virion surface.', *Science (New York, N.Y.)*, 228(4705), pp. 1315–1317. doi: 10.1126/science.4001944.

Smith, R. *et al.* (2013) 'A novel approach to improve the function of FGF21.', *BioDrugs : clinical immunotherapeutics, biopharmaceuticals and gene therapy*. New Zealand, 27(2), pp. 159–166. doi: 10.1007/s40259-013-0013-x.

Soker, S. *et al.* (1998) 'Neuropilin-1 is expressed by endothelial and tumor cells as an isoform- specific receptor for vascular endothelial growth factor', *Cell*, 92(6), pp. 735–745. doi: 10.1016/S0092-8674(00)81402-6.

Sokolova, E. *et al.* (2016) 'Recombinant targeted toxin based on HER2-specific DARPin possesses a strong selective cytotoxic effect in vitro and a potent antitumor activity in vivo', *Journal of Controlled Release*. Elsevier B.V., 233, pp. 48–56. doi: 10.1016/j.jconrel.2016.05.020.

Spitzer MS, Wallenfels-Thilo B, Sierra A, Yoeruek E, Peters S, Henke-Fahle S, Bartz-Schmidt KU, Szurman P; Tuebingen Bevacizumab Study Group. (2006). Antiproliferative and cytotoxic properties of bevacizumab on different ocular cells. *Br J Ophthalmol*. 90 (10), p1316-21.

STACKER, S. A., BALDWIN, M. E. and ACHEN, M. G. (2002) 'The role of tumor lymphangiogenesis in metastatic spread', *The FASEB Journal*. Wiley, 16(9), pp. 922–934. doi: 10.1096/fj.01-0945rev.

Stahl, A. *et al.* (2013a) 'Highly potent VEGF-A-antagonistic DARPins as anti-angiogenic agents for topical and intravitreal applications', *Angiogenesis*. Springer, 16(1), pp. 101–111. doi: 10.1007/s10456-012-9302-0.

Stahl, A. *et al.* (2013b) 'Highly potent VEGF-A-antagonistic DARPins as anti-angiogenic agents for topical and intravitreal applications', *Angiogenesis*, 16(1), pp. 101–111. doi: 10.1007/s10456-012-9302-0.

Staton CA, Kumar I, Reed MW, B. N. (2007) 'Neuropilins in physiological and pathological angiogenesis', *Journal of Pathology*, 212(3), pp. 237–248.

Ta, A. N. and Mcnaughton, B. R. (2017) 'Antibody and antibody mimetic immunotherapeutics', *Future Medicinal Chemistry*. Future Medicine Ltd., pp. 1301–1304. doi: 10.4155/fmc-2017-0057.

Tammela, T. *et al.* (2005) 'The biology of vascular endothelial growth factors', *Cardiovascular Research*. Cardiovasc Res, pp. 550–563. doi: 10.1016/j.cardiores.2004.12.002.

Tchaikovski V, Fellbrich G, Waltenberger J. (2008). The molecular basis of VEGFR-1 signal transduction pathways in primary human monocytes. *Arterioscler Thromb Vasc Biol*. 28 (22), p322-8.

Teran M, Nugent MA. (2015). Synergistic Binding of Vascular Endothelial Growth Factor-A and Its Receptors to Heparin Selectively Modulates Complex Affinity. *J Biol Chem*. 290 (26), p16451-62.

Thangsunan, P. *et al.* (2021) 'Affimer-based impedimetric biosensors for fibroblast growth factor receptor 3 (FGFR3): a novel tool for detection and surveillance of recurrent bladder cancer', *Sensors and Actuators, B: Chemical*. Elsevier B.V., 326(July 2020), p. 128829. doi: 10.1016/j.snb.2020.128829.

ThermoFisher Scientific. (2015). *Overview of Protein Expression.* Available: https://www.thermofisher.com/uk/en/home/life-science/protein-biology/protein-biology-learning-center/protein-biology-resource-library/pierce-protein-methods/overview-protein-expression-systems.html. Last accessed 15/12/2021.

Thompson Coon, J. *et al.* (2010) 'Bevacizumab, sorafenib tosylate, sunitinib and temsirolimus for renal cell carcinoma: a systematic review and economic evaluation', *Health Technology Assessment*, 14(2), pp. 1–184. doi: 10.3310/hta14020.

Tiede, C. *et al.* (2014) 'Adhiron: A stable and versatile peptide display scaffold for molecular recognition applications', *Protein Engineering, Design and Selection*, 27(5), pp. 145–155. doi: 10.1093/protein/gzu007.

Tiede, C. *et al.* (2017) 'Affimer proteins are versatile and renewable affinity reagents', *eLife*, (c), pp. 1–35. doi: 10.7554/eLife.24903.

Tolcher, A. W. *et al.* (2011) 'Cancer Therapy: Clinical Phase I and Pharmacokinetic Study of CT-322 (BMS-844203), a Targeted Adnectin Inhibitor of VEGFR-2 Based on a Domain of Human Fibronectin'. doi: 10.1158/1078-0432.CCR-10-1411.

Tsoucalas, G. *et al.* (2014) 'Queen Cleopatra and the other "Cleopatras": Their medical legacy', *Journal of Medical Biography*, 22(2), pp. 115–121. doi: 10.1177/0967772013480602.

Tsourlakis MC, Khosrawi P, Weigand P, Kluth M, Hube-Magg C, Minner S, Koop C, Graefen M, Heinzer H, Wittmer C, Sauter G, Krech T, Wilczak W, Huland H, Simon R, Schlomm T, Steurer S. (2015). VEGFR-1 overexpression identifies a small subgroup of aggressive prostate cancers in patients treated by prostatectomy. *Int J Mol Sci*. 16 (4), p8591-606.

UniProt Consortium. (2021). UniProt: the universal protein knowledgebase in 2021. *Nucleic Acids Res*. 49 (D1), D480-D489.

US Food and Drug Administration (2011a) *Avastin (bevacizumab) Information*. Available at: https://www.fda.gov/drugs/postmarket-drug-safety-information-patients-and-providers/avastin-bevacizumab-information (Accessed: 14 December 2020).

US Food and Drug Administration (2011b) *Macugen*. Available at: https://www.accessdata.fda.gov/drugsatfda_docs/label/2011/021756s018lbl.pdf (Accessed: 14 December 2020).

US Food and Drug Administration (2011c) *Sutent*. Available at: https://www.accessdata.fda.gov/drugsatfda_docs/label/2011/021938s13s17s18lbl.pdf (Accessed: 14 December 2020).

US Food and Drug Administration (2011d) *Ziconotide*. Available at: https://www.accessdata.fda.gov/drugsatfda_docs/label/2011/021060s006lbl.pdf (Accessed: 14 December 2020).

US Food and Drug Administration (2012) *Zaltrap*. Available at: https://www.accessdata.fda.gov/drugsatfda_docs/label/2012/125418s000lbl.pdf (Accessed: 14 December 2020).

US Food and Drug Administration (2014) *Kalbitor*. Available at: https://www.accessdata.fda.gov/drugsatfda_docs/label/2014/125277s071lbl.pdf (Accessed: 14 December 2020).

US Food and Drug Administration (2018) *Nexavar*. Available at: https://www.accessdata.fda.gov/drugsatfda_docs/label/2018/021923s020lbl.pdf (Accessed: 14 December 2020).

US Food and Drug Administration (2019a) *Beovu*. Available at: https://www.accessdata.fda.gov/drugsatfda_docs/label/2019/761125s000lbl.pdf (Accessed: 14 December 2020).

US Food and Drug Administration (2019b) *Eylea*. Available at: https://www.accessdata.fda.gov/drugsatfda_docs/label/2019/125387s061lbl.pdf (Accessed: 14 December 2020).

US Food and Drug Administration (2019c) *FDA approved caplacizumab*. Available at: https://www.fda.gov/drugs/resources-information-approved-drugs/fda-approved-caplacizumab-yhdp (Accessed: 14 December 2020).

US Food and Drug Administration (2020) *Ramucirumab*. Available at: https://www.accessdata.fda.gov/drugsatfda_docs/label/2020/125477s034lbl.pdf (Accessed: 14 December 2020).

Wang, H. *et al.* (2019) ‘Genetic variants of VEGFR-1 gene promoter in acute myocardial infarction’, *Human Genomics*. BioMed Central Ltd., 13(1). doi: 10.1186/s40246-019-0243-1.

Wadsley JJ, Watt RM. (1987). The effect of pH on the aggregation of biotinylated antibodies and on the signal-to-noise observed in immunoassays utilizing biotinylated antibodies. *J Immunol Methods*. 103 (1), p1-7.

Weddell JC, Chen S, Imoukhuede PI. (2017). VEGFR1 promotes cell migration and proliferation through PLCγ and PI3K pathways. *NPJ Syst Biol Appl*. 4, p1.

Wehbe N, Slika H, Mesmar J, Nasser SA, Pintus G, Baydoun S, Badran A, Kobeissy F, Eid AH, Baydoun E. (2020). The Role of Epac in Cancer Progression. *Int J Mol Sci*. 21 (18), p6489.

Weidle, U. H. *et al.* (2013) ‘The emerging role of new protein scaffold-based agents for treatment of cancer’, *Cancer Genomics and Proteomics*, 10(4), pp. 155–168.

Wen, J., Chen, X. and Bowie, J. U. (1996) ‘Exploring the allowed sequence space of a membrane protein’, *Nature Structural Biology 1996 3:2*. Nature Publishing Group, 3(2), pp. 141–148. doi: 10.1038/nsb0296-141.

West, J. B. (2008) ‘Ibn al-Nafis, the pulmonary circulation, and the Islamic Golden Age’, *Journal of Applied Physiology*, 105(6), pp. 1877–1880.

Wojcik, J. *et al.* (2010) ‘A potent and highly specific FN3 monobody inhibitor of the Abl SH2 domain.’, *Nature structural & molecular biology*. NIH Public Access, 17(4), pp. 519–27. doi: 10.1038/nsmb.1793.

Wu, F. T. H. *et al.* (2010) ‘A systems biology perspective on sVEGFR1: its biological function, pathogenic role and therapeutic use’, *Journal of Cellular and Molecular Medicine*. John Wiley & Sons, Ltd, 14(3), pp. 528–552. doi: 10.1111/J.1582-4934.2009.00941.X.

Yapijakis, C. (2009) ‘Hippocrates of Kos, the father of clinical medicine, and asclepiades of Bithynia, the father of molecular medicine’, *In Vivo*, 23(4), pp. 507–514.

Young CL, Britton ZT, Robinson AS. (2012). Recombinant protein expression and purification: a comprehensive review of affinity tags and microbial applications. *Biotechnol J*. 7 (5), p620-34.

Yu X, Yang YP, Dikici E, Deo SK, Daunert S. (2017). Beyond Antibodies as Binding Partners: The Role of Antibody Mimetics in Bioanalysis. *Annu Rev Anal Chem (Palo Alto Calif)*. 10 (1), p293-320.

Zentilin L, Puligadda U, Lionetti V, Zacchigna S, Collesi C, Pattarini L, Ruozi G, Camporesi S, Sinagra G, Pepe M, Recchia FA, Giacca M. (2010). Cardiomyocyte VEGFR-1 activation by VEGF-B induces compensatory hypertrophy and preserves cardiac function after myocardial infarction. *FASEB J*. 24 (5), p1467-78.

Zhang, D. *et al.* (2010) 'Suppression of tumor growth and metastasis by simultaneously blocking vascular endothelial growth factor (VEGF)-A and VEGF-C with a receptor-immunoglobulin fusion protein', *Cancer Research*. Cancer Res, 70(6), pp. 2495–2503. doi: 10.1158/0008-5472.CAN-09-3488.

Zhao, M. *et al.* (2011) 'JAK2/STAT3 signaling pathway activation mediates tumor angiogenesis by upregulation of VEGF and bFGF in non-small-cell lung cancer', *Lung Cancer*. Elsevier Ireland Ltd, 73(3), pp. 366–374. doi: 10.1016/j.lungcan.2011.01.002.

Zhao Q, Zhang T, Xiao XR, Huang JF, Wang Y, Gonzalez FJ, L. F. (2019) 'Impaired clearance of sunitinib leads to metabolic disorders and hepatotoxicity', *British Journal of Pharmacology*, 176(13), pp. 2162–2178.

Zheng, X. L. (2015) 'ADAMTS13 and von willebrand factor in thrombotic thrombocytopenic purpura', *Annual Review of Medicine*. Annual Reviews Inc., 66, pp. 211–225. doi: 10.1146/annurev-med-061813-013241.

Zhou HJ, Xu Z, Wang Z, Zhang H, Zhuang ZW, Simons M, Min W. (2018). SUMOylation of VEGFR2 regulates its intracellular trafficking and pathological angiogenesis. *Nat Commun*. 9 (1), p3303.

Zhou, M. *et al.* (2019) 'The pro-angiogenic role of hypoxia inducible factor stabilizer FG-4592 and its application in an in vivo tissue engineering chamber model', *Scientific Reports 2019 9:1*. Nature Publishing Group, 9(1), pp. 1–12. doi: 10.1038/s41598-019-41924-5.

Zielke N, Edgar BA. (2015). FUCCI sensors: powerful new tools for analysis of cell proliferation. *Wiley Interdiscip Rev Dev Biol*. 4 (5), p469-87.

Zirlik, K. and Duyster, J. (2018) 'Anti-Angiogenics: Current Situation and Future Perspectives', *Oncology Research and Treatment*. S. Karger AG, 41(4), pp. 166–171. doi: 10.1159/000488087.

Zorba, A. *et al.* (2019) 'Allosteric modulation of a human protein kinase with monobodies.', *Proceedings of the National Academy of Sciences of the United States of America*, 116(28), pp. 13937–13942. doi: 10.1073/pnas.1906024116.

Zou J, Fei Q, Xiao H, Wang H, Liu K, Liu M, Zhang H, Xiao X, Wang K, Wang N. (2019). VEGF-A promotes angiogenesis after acute myocardial infarction through increasing ROS production and enhancing ER stress-mediated autophagy. *J Cell Physiol*. 234 (10), p17690-17703.